RHEOLOGICAL STUDIES OF FEEDSTOCK FOR THE HYDROCRACKING OF WASTE PLASTICS

A THESIS SUBMITTED TO THE UNIVERSITY OF MANCHESTER FOR THE DEGREE OF DOCTOR OF PHILOSOPHY IN THE FACULTY OF ENGINEERING AND PHYSICAL SCIENCES

2013

PETRUS CHIEMEKA NZEREM

SCHOOL OF CHEMICAL ENGINEERING AND ANALYTICAL SCIENCE

List of contents

Word count: 44,319

LIST OF TABLES

LIST OF FIGURES

NOMENCLATURE

List of abbreviations

CFCs	Chlorofluorocarbons
CH_4	Methane
CO_2	Carbon dioxide
C_{SF}	Shape factor
DTG	Derivative thermogravimetric analysis
H_2O	Water vapour
HDPE	High Density Polyethylene
HFCs	Hydrofluorocarbons
iC8	Iso-octane
k	Consistency factor (Pas^n)
k'	Shear rate conversion factor
M	Torque (Nm)
Mn	Number-average molecular weight (g/mol)
MSW	Municipal Solid waste
MW	Molecular weight (g/mol)
Mw	Weight-average molecular weight (g/mol)
MWD	Molecular weight distribution
N	Impeller rotational speed (rps)
N_2O	Nitrous oxide
nC10	Decane
nC14	Tetradecane
nC15	Pentadecane
nC16	Hexadecane
NF_3	Nitrogen trifluoride
NO_x	Nitogen oxides
Nu	Nusselt Number
PE	Polyethylene
PET	Polyethylene terephthalate
PFCs	Perfluorinated compounds
PI	Polydispersity Index
PMMA	Poly(methyl methacrylate)
Po	Power number
PP	Polypropylene
Pr	Prandtl number
PS	Polystyrene
PVC	Polyvinyl chloride
Re	Reynolds number
SF_6	Sulphur hexafluoride
Sh	Sherwood number
SO_2	Sulphur dioxide
T_g	Glass transition temperature
TGA	Thermogravimetric analysis
VOCs	Volatile organic compounds

Symbols

τ	Shear stress (Pa)
$\dot{\gamma}$	shear rate (s^{-1})
μ / η	viscosity (Pas)
μ_∞ / η_∞	infinite shear viscosity
μ_0 / η_0	zero shear viscosity
μ_a	apparent viscosity
ρ	density (kg/m^3)

Rheological Studies of Feedstock for the Hydrocracking of Waste Plastics, by Petrus Chiemeka Nzerem, submitted to THE UNIVERSITY OF MANCHESTER for the Degree of Doctor of Philosophy, 2013

ABSTRACT

Hydrocracking of plastic wastes offers the best value in terms of quality of its process oil product among other feedstock recycling methods capable of recycling mixed plastic waste; a paraffin-rich synthetic crude similar in composition to gasoline and diesel is produced. Additional benefits of the process include heteroatom removal, catalyst conservation as well as a lower process temperature. However PVC content in mixed plastics waste and the high viscosity of plastics are prominent issues in relation to subjecting plastics to petrochemical processes such as hydrocracking. A 5ppm chlorine limit and maximum feedstock viscosity of 0.5 Pas at 200^{o}C is tolerable in the petrochemical industry. Although dechlorination of mixed plastic waste has been studied exhaustively, viscosity studies in relation to process improvement or efficiency in the pyrolysis or hydrocracking of plastics haven't received as much attention. Viscosity has been identified as being inhibitive to heat and mass transfer, and transport into reactors, as well as being a major problem in relation to designing reactors for feedstock recycling.

In this research, four of the main polymer types; high-density polyethylene (HDPE), linear low-density polyethylene (LLDPE), Polypropylene (PP), Polystyrene (PS) and Polyethylene Terephthalate (PET) were rheological characterised to establish the extent to which they exceed the recommended viscosity in the petroleum industry. Viscosities 400 – 1200 times the feedstock viscosity in the petrochemical industry at a shear rate of 500s^{-1}, which is typical for pumping and atomisation operations, were obtained during the characterisation of the plastic samples in a conventional capillary rheometer.

Saturated chain hydrocarbon solvents (iso-octane, decane, tetradecane, pentadecane and hexadecane) were investigated for treating HDPE, in a range of HDPE-solvent mixtures, in order to reduce its viscosity. Preliminary results of differential scanning calorimetry tests carried out on the solvent-treated HDPE revealed a 12 – 16% drop in the melting peak temperature of the pure HDPE (129 ^{o}C) using tetradecane (108 ^{o}C), pentadecane (110 ^{o}C) and hexadecane (113 ^{o}C) for the 20:80 PE-solvent mixtures. iso-octane and decane however only produced a viscosity drop of 3% and 4% respectively for the same 20:80 PE-solvent mixtures. Thermal stability of HDPE was largely unaffected by the solvent treatment except in the case of pentadecane which showed a reducing trend on the decomposition onset temperature as solvent concentration in the starting mixtures was increased, albeit marginal (from 441^{o}C to 437^{o}C).

A custom built sealed-vessel impeller viscometer designed to facilitate the treatment of the HDPE via solvent refluxing and in situ viscosity measurement was calibrated by determining constants which enable the conversion of machine data to viscosity and shear rate using Newtonian and non-Newtonian calibration fluids. These constants, the shape factor and shear rate conversion factor, were determined to be 81.03 and 22.08, respectively, with corresponding 95% confidence limits of 79.21 and 86.26, and 21.47 and 24.00. Viscosity measurements of a 40:60 PE-nC15 mixture carried out in the sealed-vessel impeller viscometer at a shear rate of between 71s^{-1} and 80s^{-1} at 95% confidence level and 250^{o}C was 7 Pas representing approximately 200 fold reduction from the virgin HDPE measured in the conventional capillary rheometer

DECLARATION

No portion of the work referred to in the thesis has been submitted in support of an application for another degree or qualification of this or any other university or other institute of learning

Petrus Chiemeka Nzerem
2013

COPYRIGHT STATEMENT

i. The author of this thesis (including any appendices and/or schedules to this thesis) owns certain copyright or related rights in it (the "Copyright") and s/he has given The University of Manchester certain rights to use such Copyright, including for administrative purposes.

ii. Copies of this thesis, either in full or in extracts and whether in hard or electronic copy, may be made **only** in accordance with the Copyright, Designs and Patents Act 1988 (as amended) and regulations issued under it or, where appropriate, in accordance with licensing agreements which the University has from time to time. This page must form part of any such copies made.

iii. The ownership of certain Copyright, patents, designs, trademarks and other intellectual property (the "Intellectual Property") and any reproductions of copyright works in the thesis, for example graphs and tables ("Reproductions"), which may be described in this thesis, may not be owned by the author and may be owned by third parties. Such Intellectual Property and Reproductions cannot and must not be made available for use without the prior written permission of the owner(s) of the relevant Intellectual Property and/or Reproductions.

iv. Further information on the conditions under which disclosure, publication and commercialisation of this thesis, the Copyright and any Intellectual Property and/or Reproductions described in it may take place is available in the University IP Policy (see http://documents.manchester.ac.uk/DocuInfo.aspx?DocID=487), in any relevant Thesis restriction declarations deposited in the University Library, The University Library's regulations (see http://www.manchester.ac.uk/library/aboutus/regulations) and in The University's policy on Presentation of Theses

ACKNOWLEDGEMENT

First and foremost, I would like to thank my supervisor, Dr Alastair Martin, for offering me this opportunity to start with and for his guidance and support all through, especially the difficult times.

I would also like to thank all those who have made the challenge of the work leading up to this thesis less difficult, particularly Mrs Elizabeth Davenport, Mr John Riley, Mr Loris Doyle, Dr Andrew Campen, Dr Aaron Akah and Dr Michael Cooke; you all have been of immense help.

Last but not least, I would like to thank all my friends and colleagues whose moral support kept me going and, at one point or the other, provided a shoulder to lean on, or at times, cry on. Steve, Julia, Edidiong, Iniobong, Tania, Nuria, Ifeanyi, Fadhil, Rasha, Salam, Amer Cynthia, Nnamdi, Vesta, Kachi; there are no words to express my gratitude to you all.

DEDICATION

To my parents, whom I have put through so much.

1 INTRODUCTION

1.1 BACKGROUND

Arguably the most widely used engineering material, with applications spanning across different markets and fields, plastics have experienced a phenomenal growth in a short space of time (Waste Watch and Recoup, 2003). In just the latter half of the 20th century, the global consumption of plastics has increased by at least 1900% (Figure 1.1), replacing and surpassing more traditional manufacturing materials such as aluminium and steel (Rosato et al., 2001; Biron, 2007) in various applications. This phenomenal growth in consumption has largely been due to economic reasons (i.e. cost effectiveness) and the unique blend of chemical, thermal and electrical insulation, and optical properties inherent in different types of plastics (Aguado and Serrano, 1999). They also are easy to mould into a variety of shapes at high temperature and have a high strength-to-weight ratio (Aguado and Serrano, 1999). Thus plastics have evolved from such early precursors as Parkesine, Celluloid and Bakelite developed in the 19th century, to modern plastics such as Polyethylene (PE), Polypropylene (PP), Polystyrene (PS), Polyvinyl Chloride (PVC) and Polyethylene Terephthalate (PET), all of which became commodity plastics by the end of the 1950's and account for around 90% of the global plastics use (Aguado and Serrano, 1999; Andrady and Neal, 2009; Thompson et al., 2009; Plastics News Global Group, 2010; British Plastics Federation, ca 2011).

With its great benefits and extensive penetration into a diverse spectrum of sectors and applications, as shown in Table 1.1, the worldwide production of plastics has already hit

288 million tonnes and averages a year on year growth of around 5% since the late 1970's (Plastics Europe, 2013). This phenomenal growth has however come at a price.

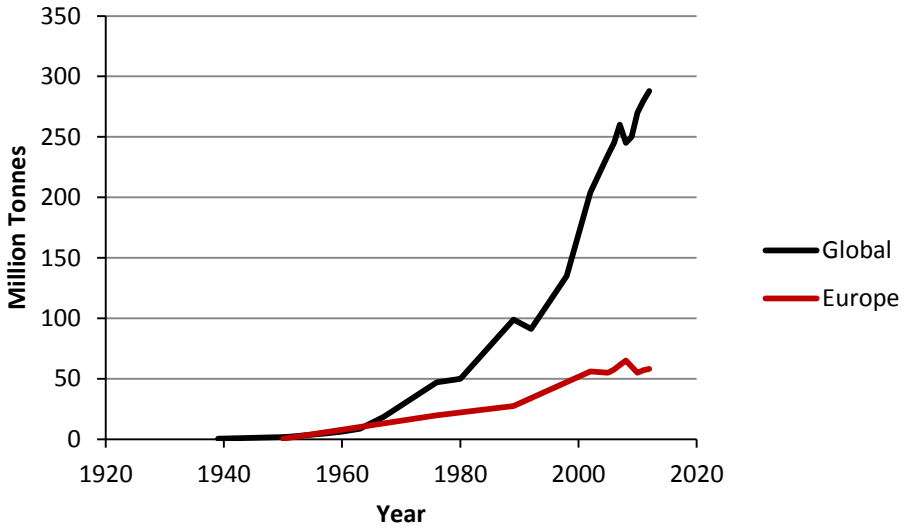

Figure 1.1: Production of Plastic resins from 1939 – 2010 (adapted from Bryson, 1999; PlasticsEurope, 2008a; 2008b; 2009; 2013)

1.2 PROBLEMS ASSOCIATED WITH PLASTICS

Problems associated with the production, use and disposal of plastics can be categorised under the following headings:

1.2.1 Environmental

Plastics are largely made from petroleum resources and account for approximately 8% of its use; 4% for the production of the raw-materials they are fabricated from, i.e. polymers, and another 4% consumed as fuel by the plastics industry (Waste Watch, 2006). As such, the production of plastics will contribute to harmful emissions into the atmosphere and, along with process waste, also leave behind waste from the used plastic products which

have to be managed. The issue of emissions, waste generation and waste management becomes even more pertinent considering the exponential trend in the consumption of plastics and concerns over global warming and climate change becoming more apparent.

Table 1.1: Applications of Plastics

Sectors	***Applications***
Packaging	Films, sacks, bottles, bubble wraps, blister packs, etc
Building and construction	Pipes, insulation, window and door profiles, etc
Transport	Bonnets, fuel tanks, seats and seat covers, air bags, train panels and luggage racks, helicopter rotor blades, aircraft wing skins, nacelles and flaps, etc
Electrical and electronics	Electrical appliance housing, circuit breakers, switches, cable/wire insulation, electric kettles, etc
Agriculture	Greenhouses, tunnel and silage films, drainage and irrigation pipes, etc
Medicine	Intravenous bags, hospital durables, plastic nets, artificial organs, orthopaedic implants, etc

Global warming refers to the increase in the earth's average atmospheric temperature due to an imbalance of the earth's natural composition of greenhouse gases and addition of aerosol particles into earth's atmosphere through anthropogenic activities such as fossil fuel combustion, deforestation and industrial processes (Casper, 2010; Hoffert, 2009; Daintith and Martin, 2010). This warming of the earth's atmosphere, in the order of $0.6^{o}C$ in the last century, has resulted in changing climatic conditions with adverse effects on the environment, ecosystem and human health (Casper, 2010; Daintith and Martin, 2010).

1 INTRODUCTION

Melting glaciers and ice caps, evaporation, warming oceans, increased precipitation, smog and changing weather patterns are some of the manifestations of global warming. Consequences of these manifestations include flooding, desertification, famines, droughts and hurricanes, wildfires, destruction and disruption of ecosystems, etc.

Greenhouse gases, both natural and anthropogenic, are atmospheric gases that largely allow the permeation of solar radiation (visible and ultraviolet radiation) but absorb infrared radiation emitted from the earth's surface (Marland, 2009; Daintith and Martin, 2010). The absorbed infrared is dissipated back into the atmosphere thus causing warming. The earth's natural stock of greenhouse gases, particularly CO_2 and H_2O, keeps it warm (greenhouse gas effect) and maintains surface temperatures at around 33^oC. Anthropogenic greenhouse gases have increased this natural stock significantly to cause what is regarded as enhanced greenhouse effect. For instance, CO_2 has risen from pre-industrial concentration of 280 ± 20 ppm (Indermuhle et al., 1999) to about 393 ppm according to the World Meteorological Organisation (WMO, 2013).

CO_2, CH_4, N_2O, SF_6, HFCs, PFCs are all greenhouse gases whose combined emissions were targeted for reduction by at least 5% of their 1990 levels by 2012 under the Kyoto protocol (UNFCCC, 1998). Nitrogen trifluoride (NF_3) has been added to the aforementioned group of greenhouse gases for reduction in the yet to be ratified 2nd commitment period of the Kyoto protocol, with an increased combined reduction target of 18% below 1990 levels by 2020 (UNFCCC, 2013). Global CO_2 emission has however increased by around 50% above the 1990 levels (22.7 billion Tonnes) although a reduction of 16% was achieved among countries with binding targets (Schiermeier, 2012). Emissions from other gases such as SO_2, NO_x and volatile organic compounds (VOCs) are also

regulated in most industrialised countries due to their environmental and health impacts (Andrady, 2003b). All these gases are emissions predominantly associated with the use of fossil fuels for energy and their synthesis into other products, or specific industrial processes.

More closely associated with the plastics industry, however, are CO_2, CH_4, SO_2, NO_x and VOCs; emissions from fossil fuel use (Andrady, 2003b). Petroleum, a fossil fuel resource, provides the feedstock (Stein and Wilcox, 1996; Waste Watch, 2006) and fuel (Waste Watch, 2006) used by the plastics industry, accounting for around 8% of its global consumption to the plastics. A study by Franklin Associates (1990) on emissions of CO, SO_x, NO_x, hydrocarbons and particulates estimated the contribution from the plastic industry as 1%. Hydrofluoroalkanes, used as auxiliary blowing agents, are greenhouse gases used to replace the more dangerous CFCs, which have higher greenhouse gas effects and are ozone depleting substances, in the production of foams (Andrady, 2003b). These are released with time in usage and when destroyed.

Other processes in the plastic industry also lead to emissions of VOCs and hazardous air pollutants (Andrady, 2003b). VOCs are organic compounds with boiling points of 250°C or lower measured at standard atmospheric pressure (The Volatile Organic Compounds in Paints, Varnishes and Vehicle Refinishing Products Regulations 2012) which contribute to the formation of photochemical smog. Eye irritation, breakdown in the molecular structure of rubber based materials, flora damage and fading in dyed fabrics are health and environmental problems attributed to photochemical smog (Rao and Rao, 1989). Pichtel (2005) also stated on page 76 that “VOCs are sometimes very toxic and may be carcinogenic, mutagenic or teratogenic”. HAPs on the hand, are compounds, most of which are also VOCs, specifically defined by the US Clean Air Act of 1990 as

carcinogenic, or potentially so; or as having adverse health, environmental or ecological effects (USEPA., 2009). Some VOCs and/or HAPs that have been associated with the Plastics industry include styrene from polystyrene synthesis and vinyl chloride from polyvinyl chloride synthesis (Andrady, 2003b; Hill, 2010).

Jansen et al. (1992) published a set of data which shows the contamination to air and water caused by the production of plastic products in comparison to tin, aluminium, recycled aluminium and glass. Although these figures show plastics as generally less polluting, they also indicate the level of contamination relative to European drinking water standards and upper air concentration limits. Andrady (2003b) however made a similar comparison but went further to include data on paper which showed higher levels of contamination to water. In both cases, the importance of recycling can be deduced by comparing the sets of data for energy use, and air and water emissions from both the processing of aluminium and the recycled aluminium which clearly shows virgin aluminium to be more polluting.

Plastics contribute to cadmium and lead found in MSW accounting for about 14% and 1% respectively of their contents in US MSW according to USEPA's (1989) projected 2000 figures. Cadmium and lead are both contained in pigments and stabilisers used in plastics (Brydson, 1999; Oswald et al., 2006; Peacock and Calhoun, 2006; Hill 2010). The use of lead stabilisers, particularly in PVC, is being phased out especially in food and water packaging due health concerns (Brydson, 1999; Oswald et al., 2006; Peacock and Calhoun, 2006). Health effects related to Lead include late psychological development of children, and neurological disorders in children and adults, anaemia, high blood pressure, kidney and infertility problems (Pinto and Salgado, 2004; Hill, 2010). Cadmium exposure on the other hand can lead to kidney problems, bronchitis, fibrosis, pulmonary oedema, lung and

prostate cancer, as well as birth defects (Pereira et al., 1999 as cited by Pinto and Salgado, 2004 p.439; Hill, 2010).

Another major concern elicited by plastics is that of litter. It is the most visible environmental effect of plastics waste possibly due to their lightweight and durability. This means wastes from end-of-life plastics, particularly from packaging, is easily airborne and can persist in the environment for a very long time (Barnes et al., 2009). This is very obvious in beaches where an estimated 60% of wastes arising are plastics (Waste Watch, 2006; Marine Conservation Society, ca. 2008). Beach plastic litter and plastic litter from other terrestrial sources are considered a major source of the plastics, up to 80%, found in oceans (Andrady, 2011). Other sources include dumped ship waste, accidental spillage of sea-freighted polymer resins and lost or abandoned fishing accessories (Andrady, 2003b). Some of the major effects of plastics litter include deterioration of the aesthetic quality of urban landscapes, trapping of marine animals in disposed plastics which may lead to death, as well as feeding on plastic litter which interfere with their growth (Andrady, 2003b; Hill, 2010).

1.2.2 Waste generation and management problem

Plastic waste is a major global concern. One major reason for this concern is the substantial quantity of post-consumer plastics currently believed to enter the waste stream annually. Plastic waste in Western Europe (European Union member states, Norway and Switzerland) was recently estimated at 25.2 million tonnes of which 38% was discarded in landfill (Figure 1.2) (Plastics Europe, 2013). These figures are much higher in the United Kingdom and United States, with disposal rates to landfill at around 69% (Figure 1.3) and 86% (Themelis et al., 2011), respectively. Landfill is the waste management option of last

resort in line with the waste management hierarchy principle set out in the European Union's (EU) Waste Framework Directive (Council Directive, 2008), and reinforced by other legislative instruments such as the Landfill Directive (Council Directive, 1999),

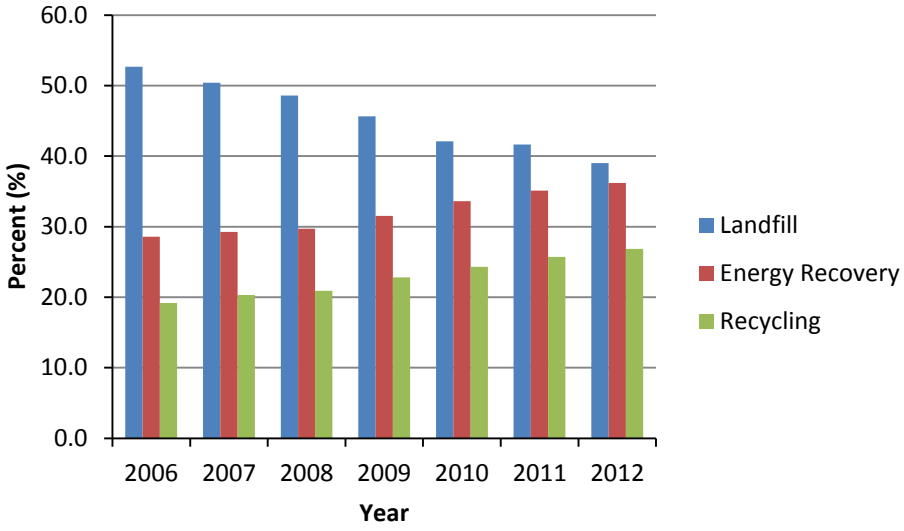

Figure 1.2: Waste Treatment of Post-consumer Plastics in Western Europe (adapted from Plastics Europe, 2008a; 2008b; 2009a; 2010; 2011; 2012; 2013)

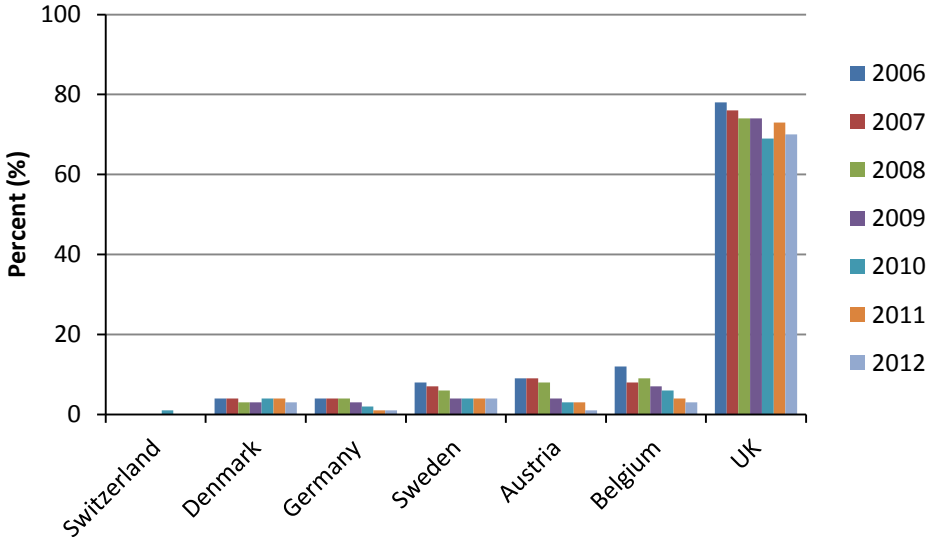

Figure 1.3: Landfilled (or incinerated without energy recovery) Plastic Waste in the UK and the top 5 performing countries in Europe (adapted from Plastics Europe, 2008a; 2008b; 2009a; 2010; 2011; 2012; 2013)

Waste Electrical and Electronic Equipment Directive (Council Directive, 2012) and the Packaging and Packaging Waste directive (Council Directive, 1994). It is discouraged due to its production of explosive greenhouse gas emissions, soil and groundwater pollution, limited capacity and lack of any valorisation potential; making it an unsustainable practice (Aguado and Serrano, 1999; Williams, 2005; Hopewell et al., 2009; Oehlmann et al., 2009; Teuten et al., 2009; Thompson et al., 2009). With a volume-to-weight ratio ranging between 2.4 and 3.9 (Andrady, 2003b), plastics are generally considered to take up space and create voids in landfills (Waste Watch, 2006), thus occupying up to 25% of landfill capacity (Aguado and Serrano, 1999). This would cause landfills to fill up quicker and contain less waste than it should. Andrady (2003b) however questioned the space generally attributed to plastics in landfill, suggesting that its volume fraction in MSW should reduce in a landfill under the weight above it. He also added that plastics would not yield considerable landfill space even if it were biodegradable, which reinforces the USEPA's (1990) position on the behaviour of plastics in landfill. Globally, the quantity of post-consumer plastics entering the waste stream yearly is believed to be as much as 50% of the yearly consumption of plastics (Hopewell et al., 2009; Butler et al., 2011) and about a tenth of total waste generated worldwide (Thompson et al., 2009). Furthermore, the year-on-year increase in the consumption of plastics (around 5%) which accounts for around 8% of the oil and gas, limited fossil natural resources, produced worldwide makes the current life cycle of plastics also unsustainable (Hopewell et al., 2009).

Incineration as a waste management method is only ranked above landfill in the waste management hierarchy. Naturally, it has a negative public perception due to concerns over the toxicity of its visible emissions (Williams, 2005). Particularly of concern is the disputed production of dioxins and furans associated with the combustion of chlorinated

waste, of which the presence of PVC and other chlorinated plastics, have been mooted as a possible source (Marklund et al., 1987; Probert et al., 1987; Rigo and Chandler, 1998; Aguado and Serrano, 1999; UNEP., 1999; Pichtel, 2005; Williams, 2005). Dioxins and furans are toxic compounds which are reported to cause cancer and other health problems.

1.2.3 Resource management/sustainability

Plastics are generally made from petroleum sources (Aguado and Serrano, 1999; Brydson, 1999) which are fossil fuels thus a finite resource. These fossil fuels are however the main source of primary energy delivering around 59% of the total (BP, 2009).

With the current abnormal increase in crude oil price and peak production period forecasted by Campbell (Bentley, 2002) for conventional oil subsistent, and that of conventional gas imminent, the need for resource management has never been more urgent. Furthermore, petroleum consumption is projected to rise worldwide, which can be put down to the transport sector as provided by the EIA (2009). The projection shows the progressive increase of the share of petroleum-fuelled transport based possibly on historical trends and current disposition to alternative energy sources and policy, as well as improved per capita income in developing countries. This assumption has been made based on the historical data of the UK where the portion of petroleum use by transport increased gradually (DFT., 2008; MacLeay et al., 2009), the US which has experienced consistent growth in petroleum consumption and the share occupied by the transport sector (EIA, 2009), and the steep rise in transport fuel consumption in developing countries (Birol, 2004).

Although seemingly insignificant, plastics account for 8% of global oil consumption. However, unlike some oil products such as transportation fuels, which are used exhaustively in service, plastics are not and have an energy value estimated at around 40MJ/Kg (Williams, 2005). This energy or calorific value is comparable with conventional solid and liquid fuels as highlighted in Table 1.2 below. This shows the potential of plastics as not only an energy source but also in contributing to effective resource management and sustainability when valorised, considering that most of it is landfilled.

Table 1.2: Calorific value comparison of different plastics to oil and coal

Materials	**Calorific value (MJ/kg)**
Polyethylene	46.5
Polypropylene	45.0
Polystyrene	41.6
Polyethylene Terephthalate	21.6
Polyvinyl chloride	19.0
Coal*	30.0
Fuel Oil*	42.0

Source: Environment & Plastics Industry Council (2004b) and *Williams (2005)

Recycling plastics is limited in its current application as it requires high quality single stream plastics. Another environmental problem associated with plastics is with the management of its waste. Landfill still remains the predominant waste treatment option for end-of-life plastics in Western Europe and the US as already highlighted. In Figure 1.2 , it singly accounts for close to 40% of current waste management routes employed in Western Europe, with recovery routes, which includes material recycling and energy recovery, accounting for the remaining management capacity. However, material recycling; primary recycling (re-extrusion), secondary (mechanical) recycling or chemical (tertiary) recycling (Mastellone, 1999); is preferred over energy recovery (quaternary/thermal recycling) (Mastellone, 1999; Plastics Waste Management Institute, 2009) but is the least utilised route for managing waste plastics.

Figure 1.4 and Figure 1.5 compares material recycling and energy recovery rates amongst the top 6 Western European countries with the best overall recovery performance and the UK between 2006 and 2012. As can be observed, material recycling seems to be limited at around 35% of plastic waste generated in contrast to the less desired incineration with energy recovery, which currently accounts for up to 75% in Switzerland. In contrast, total recovery rate in the UK is around 26%, 23% recycling and 3% energy recovery, of its

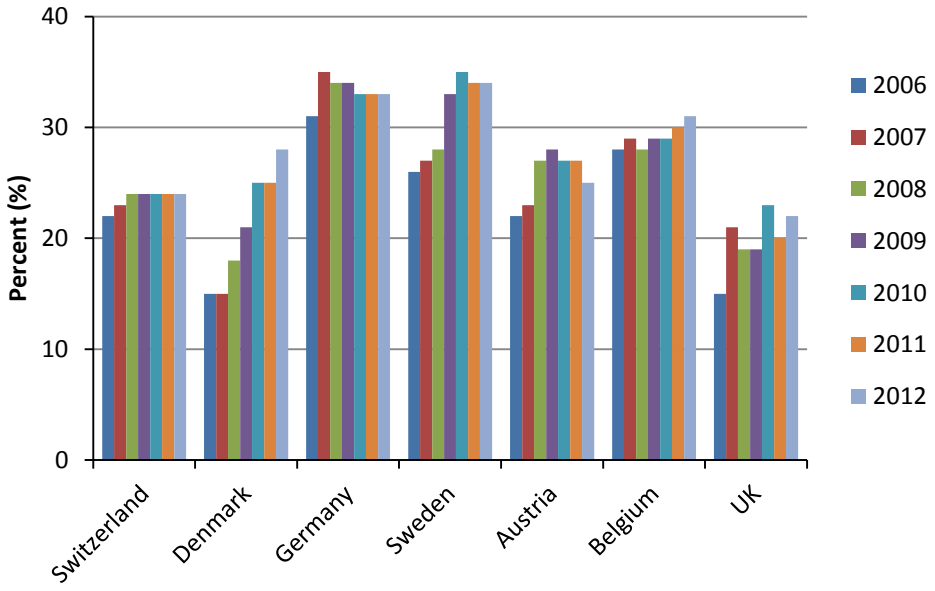

Figure 1.4: Recycled Plastic Waste in the UK and the top 6 performing countries in Europe (adapted from Plastics Europe, 2008a; 2008b; 2009a; 2010; 2011; 2012; 2013)

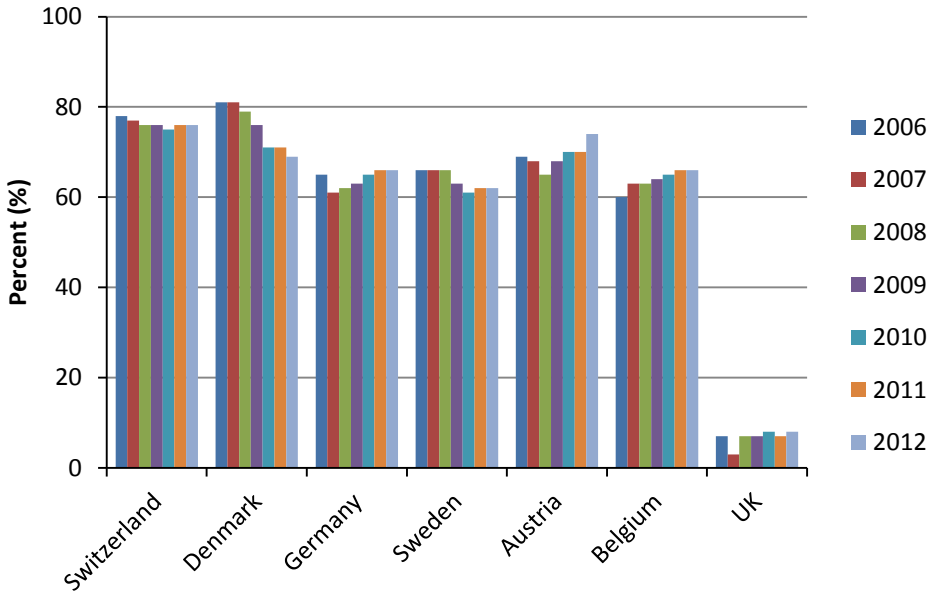

Figure 1.5: Energy recovery from plastic waste in the UK and the top 5 performing countries in Europe (adapted from Plastics Europe, 2008a; 2008b; 2009a; 2010; 2011; 2012; 2013)

estimated 3-6 million tonnes (Waste Watch and Recoup, 2003; DEFRA, 2007; Huang et al., 2007; Siddique et al., 2008; Waste Watch, 2006) of post-consumer plastics generated each year. Furthermore, material recycling in the UK involves reprocessing between 0.25 and 0.3 million tonnes of industry scraps (British Plastics Federation, ca 2010) and the remainder by mechanical recycling. Mechanical recycling also account for almost 99% of the recycling carried out in Western Europe with Austria, Germany and Poland (Plastics Europe, 2009a; Mudgal et al., 2011), accounting for most of the around 1.5% of recycling achieved via feedstock recycle.

1.3 PLASTICS AND POLYMERS

Although the terms plastics and polymers may be used indistinguishably, technically they are two different entities. It is pertinent to point out that polymers may be organic or inorganic (Cowie, 2008) and where mentioned henceforth refers to organic polymers.

Basically, polymers are the main raw-materials for plastics. Polymers refer to synthetic or naturally occurring long chain, high molecular weight compounds (Figure 1.6) constituted of chemically linked units of specific or different short, low molecular weight, carbon compounds (Aguado and Serrano, 1999; Brydson, 1999; Rosato et al., 2001; Osswald et al., 2006; Sperling, 2006; Cowie, 2008). Plastics on the other hand are modified polymers. They usually refer to synthetic polymers blended with specific chemical modifiers called additives to enhance targeted service use properties (Aguado and Serrano, 1999, Osswald et al., 2006, Rosato et al., 2001) and can be thermomechanically formed into end use products. These additives are listed in Table 1.3 (Aguado and Serrano, 1999; Brydson, 1999; Andrady, 2003a; Osswald et al., 2006).

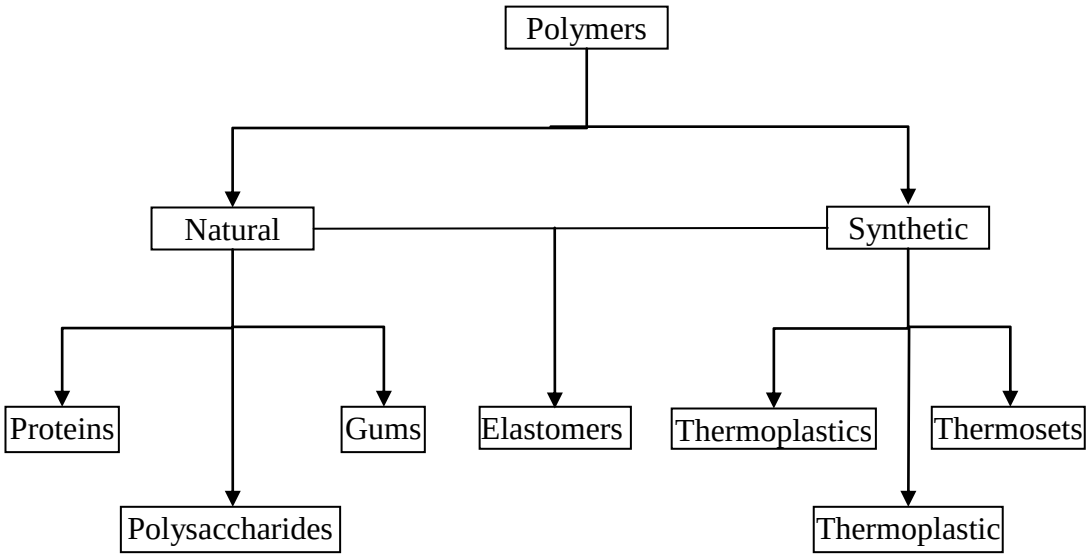

Figure 1.6: Classification of polymers

The number of constitutive units for a polymer molecule, otherwise known as monomers, must be large enough for it to maintain stable service properties with minor chain length alterations. The minimum chain length for a polymer is estimated to be equivalent to that with a molecular weight of around 25000 g/mol (Sperling, 2006).

Plastics are usually known by the type of polymer they are made from, i.e. Polyethylene, Polypropylene, etc; hence all plastics can be referred to as polymers. However not all polymers are plastics (Aguado and Serrano, 1999) and are indeed a subclass of polymers(Callister and Rethwisch, 2011). Further reference shall be made to plastics, i.e. modified polymers, unless when attention is being drawn to molecular structure or behaviour in response heat or stress, then the term polymer may be preferred.

Table 1.3: Polymer additives and functions

Additive	***Function***
Plasticizers	Rheological or mechanical modifiers that make polymers flow easier thus improving processability
Fillers	Natural supplements added to a polymer to reduce material cost, improve mechanical strength or, at times, electrical conductivity
Anti-ageing agents Stabilizers	Light, thermal and PVC stabilizer, flame retardants, antioxidants, added to polymers to slow down thermal and chemical decomposition
Colourants	Dyes and pigments used to impart colour into plastic products
Antistatic agents	Prevents or lessens the accumulation of static electrical charges on plastics
Blowing agents	Chemical compounds which decompose to produce polymer foams
Antiblocking agents	Reduces adhesion between plastics sheets and films to facilitate separation

1.3.1 Types of Plastics

Plastics may be categorised according to the formation mechanism of their polymers, i.e. mode of polymerisation, or their thermal behaviour; both of which are pertinent to recycling.

In terms of mode of polymerisation, there are addition polymers and condensation polymers (Aguado and Serrano, 1999; Brydson, 1999; Rosato et al., 2001; Peacock and Calhoun, 2006). Addition polymers are long chain products of a repeating unit formed by chemically linking a double-bonded, low molecular weight molecule, known as a monomer; e.g. polyethylene (Figure 1.7a). Condensation polymers, on the other hand, are long chain products of repeating units but produced along with a small molecule as by-products, by chemically linking one or more different monomers with different functional groups; Nylon-6,6 (Figure 1.7b).

In terms of thermal behaviour, there are thermosets and thermoplastics. Thermosets are plastics that set into an irreversible, hard, network structure once heated above a critical temperature (Cowie, 2008). This network structure is formed during fabrication through a chemical reaction known as curing which facilitates the cross-linking of the long chain molecules of the polymer with strong covalent bonds (Aguado and Serrano, 1999). Once fabricated, thermosets remain immobile even when reheated. This may be as a consequence of having high glass transition temperatures, T_g, which are more or less in the region of their degradation temperatures (Osswald et al., 2006). T_g is a molecular transition temperature through which a non-crystalline polymer moves between a glassy, rigid structure to a rubbery, flexible one. Above the T_g, the polymer molecules are able to slide past each other or “flow”. Thus thermosets are known for their excellent shape retention

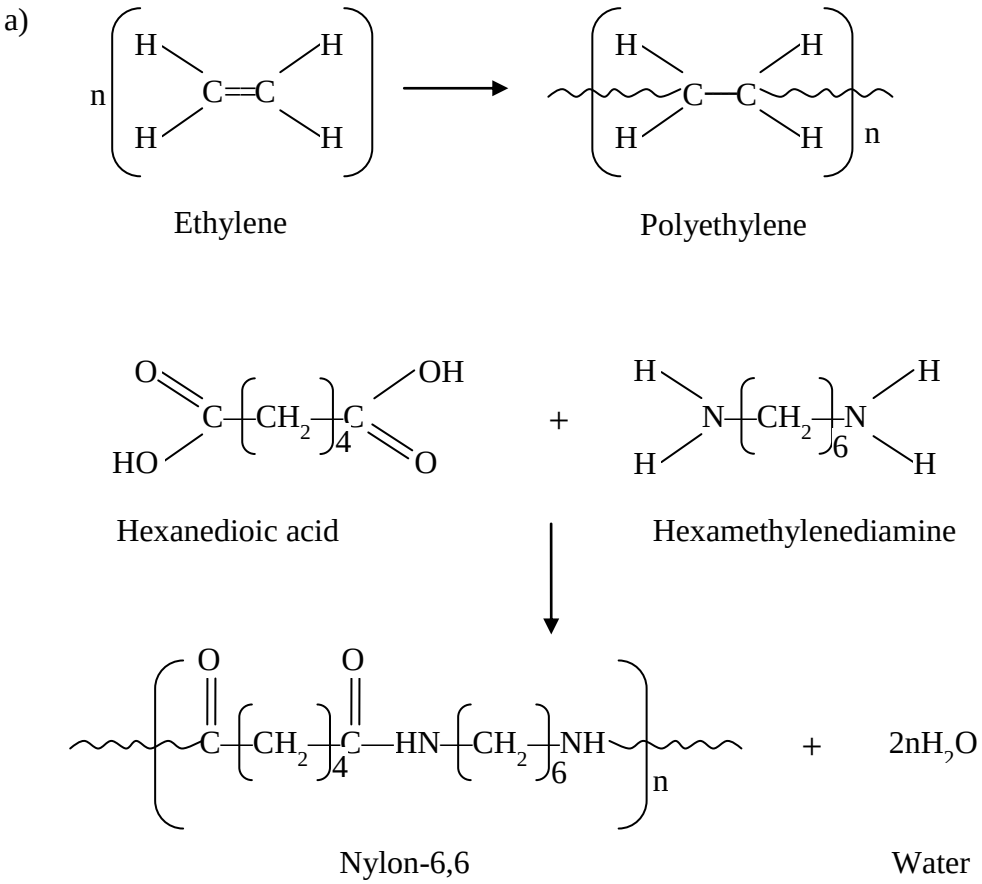

Figure 1.7: Synthesis of (a) Addition polymer; (b) Condensation polymer

attributes and resistance to frictional effects. Some examples include vulcanised rubber, epoxy resins, phenol formaldehyde, amino resins, etc (Cowie, 2008).

Thermoplastics, on the other hand, refer to plastics that can be reprocessed repeatedly, i.e., the heat-and-cool processing steps can be repeated. They soften when heated above their glass transition temperature (T_g) and set when cooled. Above the T_g, the polymer molecules are able to slide past each or "flow". Their ability to soften above the T_g is as a result of having chain molecules which, unlike thermosets, are loosely held together by weak electrostatic forces rather than covalent bonds (Aguado and Serrano, 1999).

There are two morphological forms of thermoplastics namely amorphous and semi-crystalline. Amorphous polymers are characterised by their random molecular structure as the polymer molecules solidify while still entangled or disordered. Semi-crystalline thermoplastics, however, have crystalline regions, i.e. ordered or aligned units of chain molecules, interspersed with the amorphous regions which form and solidify at different temperatures within the polymer molecule structure during cooling and solidification. The crystalline regions begin to develop and harden below a critical temperature which coincides with the melting temperature. The remaining amorphous regions retain mobility above the glass transition temperature where they solidify. The extent to which crystallization occurs however depends on the degree of branching as well as rate of cooling after polymerisation (Osswald et al., 2006).

Virtually all plastics are semi-crystalline (Osswald et al., 2006). There are 5 main types of plastics based on their share of the market (Biron, 2007). They include:

1.3.1.1 Polyethylene

As the name suggests, polyethylenes are polymers that consist of repeating units of ethylene formed by addition polymerisation. They are the most widely used type of polymer worldwide (Rosato et al., 2001) especially in packaging. They comprise different grades of varying densities, molecular weights and molecular weight distributions, and crystallinities (Andrady, 2003b), formulated using different methods (Brydson, 1999; Biron, 2007) and process conditions (Aguado and Serrano, 1999). They include linear low density polyethylene, low density polyethylene, medium high density polyethylene, high density polyethylene, ultra high density polyethylene, etc. There is also crosslinked polyethylene which is thermosetting (Rosato et al., 2001). The various polyethylene grades deliver a wide range of properties such as good electrical insulation, resistance to

chemicals and moisture, good processibility, toughness, flexibility, low coefficient of friction, impact resistance, low density, weldability, machinability for rigid grades, good resistance against high-energy radiation (Brydson, 1999; Rosato et al., 2001; Andrady, 2003a; Peacock and Calhoun, 2006; Biron, 2007).

There are however three major types of polyethylene based on bulk density but also on use. These include:

a) **Low density polyethylene** (LDPE) is a moderately crystalline polyethylene (40-60%) with significant short chain and long chain branching (around 60 per 1000 carbon atom) within its polymer structure (Rosato et al., 2001; Andrady, 2003b; Cowie, 2008). It thus has a low density of 0.92 g/cm^3(Cowie, 2008). It has a melting peak temperature range of 110 -115^{o}C (Andrady, 2003b). LDPE is produced at very high pressures of 100 - 300 MPa and at temperatures of about 100-275^{o}C (Osswald et al., 2006). LDPE is characterised by its good flexibility, impact resistance at ambient temperature and electrical insulation even in a wet medium (Biron, 2007). LDPE is extensively used in films for bags and food packaging, greenhouses, bottles, cable insulation, steel coating, pipes and injection moulded parts (Aguado and Serrano, 1999; Osswald et al., 2006).

b) **High density polyethylene** (HDPE) is a highly crystalline polyethylene (70-95%) (Andrady, 2003b) made up of long polymer chain molecules with little or no short chain branching- less than 7 per 1000 carbon atoms (Cowie, 2008). It thus has a linear structure and is densely packed with densities between 0.94 and 0.97 g/cm^3 (Aguado and Serrano, 1999). It has a melting temperature of 130 - 135^{o}C (Andrady, 2003b). It is produced at low to medium temperature (20 - 150 ^{o}C) and pressure (0.1 - 5 MPa) (Osswald et al., 2006). The main applications of HDPE are for films,

housewares, food and domestic containers, industrial drums, crates, toys, gas tanks, car fuel tanks, pipes, etc produced by blow moulding and injection moulding (Aguado and Serrano, 1999; Osswald et al., 2006).

c) **Linear low density polyethylene** (LLDPE) is also moderately crystalline (40-60%) (Andrady, 2003b; Biron, 2007) but with regularly located short chain branches (10 - 35 per 1000 carbon atom) between polymer long chain molecules giving it densities between those of LDPE and HDPE (0.92 - 0.94 g/cm^3) (Cowie, 2008). The short chain branches are co-monomers to ethylene such as but-1-ene, pent-1-ene, hex-1-ene or oct-1-ene used during LLDPE synthesis (Brydson, 1999; Rosato et al., 2001; Andrady, 2003a; Osswald et al., 2006; Peacock and Calhoun, 2006). The longer the ethylene co-monomer the higher the density of LLDPE produced, i.e. oct-1-ene co-monomer will yield a higher density LLDPE with ethylene compared to but-1-ene co-monomer. LLDPE has intermediate properties with respect to LDPE and HDPE. Main applications for LLDPE are films, injection moulded parts and wire insulation

1.3.1.2 Polypropylene

Polypropylene is a low density polyolefin (ca. 0.90 g/cm^3) polymerized from propylene monomers (Andrady, 2003a, Brydson, 1999, Cowie, 2008, Osswald et al., 2006, Peacock and Calhoun, 2006). It exists in 3 distinct structural configurations namely isotactic, syndiotactic and atactic defined by the relative spatial orientation of methyl pendant groups to one another and produced under different conditions. It is almost completely used in its isotactic form (usually less than 100% isotactic), commercially (Brydson, 1999; Andrady, 2003b; Giles et al., 2005; Peacock and Calhoun, 2006), where the methyl pendant groups are spatially located all one side of the carbon chain, or on the outside of the helix-shaped

chain (Osswald et al., 2006). Alternate and random spatial arrangement of the methyl pendant groups along the carbon chain characterise the syndiotactic and atactic polypropylene, respectively.

Isotactic polypropylene (iPP) is highly crystalline (80 - 85%) (Aguado and Serrano, 1999) due to its configuration which enables compact, close packing of the polymer chain molecules (Rosato et al., 2001). It is synthesized at temperatures and pressures of around 60 - 80^{o}C and 0.5 – 1.5 MPa, respectively (Andrady, 2003b). Properties are similar to that of HDPE but they are brittle at low temperatures (Osswald et al., 2006). It is more rigid and crack resistant than HDPE, having good electrical insulation properties. Moreover, i-PP has a higher crystalline melting temperature of 160 – 165^{o}C (Osswald et al., 2006) which enables its use in products that must be steam sterilized (Aguado and Serrano, 1999). The main commercial applications for iPP include the manufacture of injection moulded car parts such as dashboards, exterior light housings; white goods such as washing machines, dryers, dishwashers; and other products such as food containers, cups, pipes, sheets, carpet textile fibres, etc (Aguado and Serrano, 1999; Osswald et al., 2006). It is also available as a copolymer such as ethylene-propylene copolymer and ethylene-propylene copolymer diene copolymer (Osswald et al., 2006).

1.3.1.3 Polyvinyl Chloride

PVC belongs to the vinyl family of polymers which have a monomer repeat unit with all but one of the four pendant groups attached to its two carbon atoms hydrogen (Rosato et al., 2001). The fourth pendant group, in this case chlorine, is unique and imparts a characteristic property on the particular polymer; fire retardancy with respect to PVC (Biron, 2007).

General properties include flame retardancy, good clarity, colourability, strength, abrasion resistance and barrier protection properties against air (as well as N_2, O_2 and CO_2) (Rosato et al., 2001; Osswald et al., 2006). It however has poor thermal (and photo) stability (Andrady, 2003b) which accounts for its poor long-term, service temperature of not more than 60 - 65^{o}C (Rosato et al., 2001; Osswald et al., 2006). PVC is a low crystallinity plastic (7 - 20%) due to the syndiotactic arrangement of its chlorine molecule (Andrady, 2003b). It is prepared by polymerization of vinyl chloride at temperatures of about 50^{o}C (Aguado and Serrano, 1999; Andrady, 2003b).

There are two main grades of PVC; the rigid unplasticized PVC (uPVC) and the flexible plasticized PVC (pPVC) (Aguado and Serrano, 1999; Andrady, 2003b; Osswald et al., 2006). uPVC is produced directly from vinyl chloride polymerization and has a high elastic modulus but low impact strength (Aguado and Serrano, 1999; Osswald et al., 2006). pPVC, on the other hand, is soft and flexible due to incorporation of plasticizers which increases the intermolecular chain distance (Osswald et al., 2006). The increased intermolecular chain distance thus leads to a decrease in intermolecular chain bonding forces and Tg.

uPVC is used mainly in the building and construction sector to produce sheets, pipes, fittings, claddings, window profiles and rainwater products, while pPVC include wire/cable insulation, dolls, balls, floor coverings, packaging films, tubing conveyor belts, shoe soles and roofing membranes (Aguado and Serrano, 1999; Andrady, 2003b; Osswald et al., 2006).

1.3.1.4 Polystyrene

Polystyrene is the polymerization product of styrene monomer which, like in PVC, has a unique pendant group, phenyl in this case, that is different from the remaining three hydrogen pendant groups attached to the monomer. The phenyl group has an atactic arrangement in all commercial polystyrene (although isotactic and syndiotactic arrangements are possible) thus making them amorphous as crystallisation is hindered due to steric effects (Giles et al., 2005; Peacock and Calhoun, 2006). Polystyrene is produced in three main commercial grades namely general-purpose PS, high-impact PS and expanded PS (Aguado and Serrano, 1999; Brydson, 1999; Rosato et al., 2001; Andrady, 2003a; Osswald et al., 2006; Biron, 2007).

General-purpose polystyrene also known as crystal polystyrene is a polystyrene homopolymer and thus produced from just the polymerization of styrene units (Aguado and Serrano, 1999; Brydson, 1999; Rosato et al., 2001; Peacock and Calhoun, 2006). They are non-flexible polymers (at room temperature) that have a glassy transparency, low water permeation, resistance to some chemicals (alkalis, non-oxidizing acids, alcohols, aliphatic amines, foods, drinks, polyglycols, most household fluids and pharmaceuticals) good dimensional stability; and are excellent electrical insulators and easy to process and colour (Rosato et al., 2001; Osswald et al., 2006; Biron, 2007). It has a density of about 1.04-1.05 g/cm^{3}and a T_g of 100^{o}C (Aguado and Serrano, 1999; Andrady, 2003b; Osswald et al., 2006; Peacock and Calhoun, 2006; Biron, 2007). However they are very brittle and have a low service temperature maximum of around 90^{o}C which limits its industrial applications (Rosato et al., 2001; Osswald et al., 2006; Biron, 2007). Some products include radio and TV parts, electronic components, disposable cutlery and cups, toys, yogurt containers, and clamshell packs (Aguado and Serrano, 1999; Peacock and Calhoun, 2006).

Expanded polystyrene (EPS) is basically commercial PS beads injected with a blowing agent, such as butane, pentane or carbon dioxide and fabricated into beads or foams (Aguado and Serrano, 1999; Andrady, 2003b; Osswald et al., 2006; Peacock and Calhoun, 2006). Their properties include low density (0.016-0.16 g/cm^3 for beads and 0.027-0.16 g/cm^3 for foams) , thermal and acoustic insulation, shock absorption, low water and water vapour absorption (Peacock and Calhoun, 2006; Biron, 2007). They have widespread use in packaging and insulation. Products include disposable cups, plates and bowls, egg cartons, meat trays, coolers, thermal, shock and sound insulation, packaging, transport palettes, safety helmets and seats, surf board cores, and model airplanes (Osswald et al., 2006; Peacock and Calhoun, 2006).

High impact polystyrene (HIPS) is synthesized by copolymerizing styrene and styrene-butadiene. As the name suggests, they have better impact resistance even at low temperature and also higher flexibility and environmental stress cracking resistance (ESCR) (Biron, 2007). The improved impact strength makes HIPS suitable for use in the manufacture of sheets, food containers, window frames, and household goods.

Other PS copolymers include styrene maleic anhydride, styrene acrylonitrile, acrylonitrile butadiene styrene, etc.

1.3.1.5 Polyethylene Terephthalate (PET)

PET is a polyester produced by the polymerisation of bis 2-hydroxyethyl terephthalate; a reaction product of terephthalic acid (a dicaboxylic acid), or its diester product of dimethyl terephthalate from methanol esterification, and ethylene glycol (a dialcohol) (Klein, 1996; Andrady, 2003a; Osswald et al., 2006; Peacock and Calhoun, 2006).

PET is produced in amorphous, crystalline and copolymer grades (Rosato et al., 2001; Osswald et al., 2006). General properties include good mechanical properties (high tensile strength and modulus of elasticity, good creep behaviour), fatigue resistance, excellent electrical insulation, low moisture and gas permeation (of CO_2 and O_2), inertness to organic solvents at room temperature and weak acid and alkaline solutions and a broad service temperature range (-60 up to 140^{o}C) (Osswald et al., 2006; Peacock and Calhoun, 2006; Biron, 2007). The different grades deliver additional properties such as high transparency and low shrinkage for Amorphous PET; and higher dimensional stability, stiffness and strength below 80^{o}C, and increased maximum service temperature in Crystalline PET (Rosato et al., 2001; Osswald et al., 2006; Peacock and Calhoun, 2006). PET copolymers are generally amorphous as a result of increased irregularity of repeat units synthesized from more than one glycol and/or more than one dicarboxylic acid which reduces crystallization and provide different properties (Rosato et al., 2001).

PET is mainly used in the manufacture of bottles, textile fibres and films (Aguado and Serrano, 1999; Brydson, 1999; Osswald et al., 2006; Peacock and Calhoun, 2006).

1.4 Recycling

Once post-consumer wastes exist, in which case waste reduction and reuse no longer applies, value or resource recovery is favoured to disposal in line with the waste management hierarchy under article 4 of the EU Waste Framework Directive (Council Directive, 2008). Value or resource recovery can be accomplished through recycling and energy recovery.

Recycling refers to those processes which enable waste, i.e. any substance or item that requires disposal by choice or statute by the holder, to be transformed back into its pre-waste or alternative existence or form with the exception of being used as fuel or backfilling material (Council Directive, 2008).

1.4.1 Plastics Recycling

Plastics recycling is ambiguous to define (Tukker, 2002; Hopewell et al., 2009) but generally refers to the conversion of post-production (pre- or post-consumer), discarded plastics into similar or alternative products with commercial and economic value.

There are four basic types of recycling, namely primary, secondary, tertiary and quaternary recycling (Michaeli and Breyer, 1998; Lettieri and Al-Salem, 2011). However, quaternary recycling (also known as energy recovery) is not regarded as recycling in the Europe Union (Council Directive, 2008; Mudgal et al., 2011) so will not be discussed further. Figure 1.8 below shows the different types of recycling.

1.4.1.1 Primary recycling

Primary recycling is otherwise known as re-extrusion as it involves reprocessing production discards or off-cuts through the same production line; or post-consumer, single stream, discards reprocessed into the same products e.g. reprocessing discarded PET bottles into new ones (Hopewell et al., 2009; Lettieri and Al-Salem, 2011). Waste plastics for primary recycling have a high purity requirement and narrow property specification with each other and the original product (Waste Watch, 2006; Al-Salem, 2009; Hopewell et al., 2009). This type of recycling is also known as closed-loop recycling, as it involves like-to-like conversion, for instance bottle-to-bottle or film-to-film recycling (Buekens,

2006; British Plastics Federation, ca 2010); and is a common practice in the industry with their process scraps.

1.4.1.2 Secondary recycling

Otherwise known as mechanical recycling, open-loop recycling or downgrading (Hopewell et al., 2009; Lettieri and Al-Salem, 2011)- involves using physically pre-processed (melted, shredded or granulated), single stream waste plastics (recyclates), together with fillers and/or virgin polymer resins to fabricate new products (Kartalis et al., 2000). In this case, the single stream waste plastic do not meet the requirements for primary recycling and are used to fabricate materials for which virgin polymer resins would be unsuitable (Hopewell et al., 2009). For instance, PET fibres for spinning fleece jackets and other clothing produced from waste PET bottle (Recoup, ca. 2002) or fabricating garden fencing from waste plastic films (British Plastics Federation, ca 2010). Secondary recycling also relies on good quality waste plastics as inhomogeneity and contamination of products compromises its application (Aznar et al., 2006; Zia et al., 2007). Degradation during service life, which causes a loss in mechanical property and hence performance of the waste plastics, also limits it application (Aguado and Serrano, 1999; Peacock and Calhoun, 2006).

1.4.1.3 Tertiary recycling

Tertiary recycling refers to the conversion of plastics back to its monomers to produce new polymers, or petrochemicals and other chemicals for use as chemical feedstock or fuel, through thermal and chemical processes (Aguado and Serrano, 1999; Mastellone, 1999; Buekens, 2006; Hopewell et al., 2009). It is also known as chemical or feedstock recycling. This can be achieved via the following methods

a) Chemical depolymerisation: Otherwise known as solvolysis or chemolysis (Yoshioka and Grause, 2006; Sinha et al., 2010), these are processes that reverse the polymerisation process through end-chain scission or unzipping of the polymer chain to yield its reactant monomer(s) (Aguado and Serrano, 1999; Arena and Mastellone, 2006) using a solvent. Unlike other tertiary recycling methods, they can only be used on high purity, single stream plastics (Bontoux, 1996), much like primary and secondary recycling, but mainly of condensation polymer types, for which processes are well established (Tukker, 2002; Aguado et al., 2007). It is a purely thermal process known as thermolysis in some plastics of particular polymer types (Pielichowski and Njuguna, 2005; Yoshioka and Grause, 2006).

   Solvolysis processes include (Bauer, 1996; Bontoux, 1996; Klein, 1996; Kopietz and Seeliger, 1996; ISOPA, 2001; Nikles and Farahat, 2005; Yoshioka and Grause, 2006; Aguado et al., 2007; Sinha et al., 2010)

   i. Acidolysis- Polyamide (Nylon 6, Nylon 6,6), PET, Polyoxymethylene

   ii. Alkalinolysis- Polyamide (Nylon 6, Nylon 6,6)

   iii. Aminolysis- PET

   iv. Ammonolysis- Polyamide- (Nylon 6, Nylon 6,6), PET

   v. Glycolysis- PET, Polyurethane (PU)

   vi. Hydrolysis- PET, Polyamide (Nylon 6, Nylon 6,6), PU

   vii. Methanolysis- PET, PU

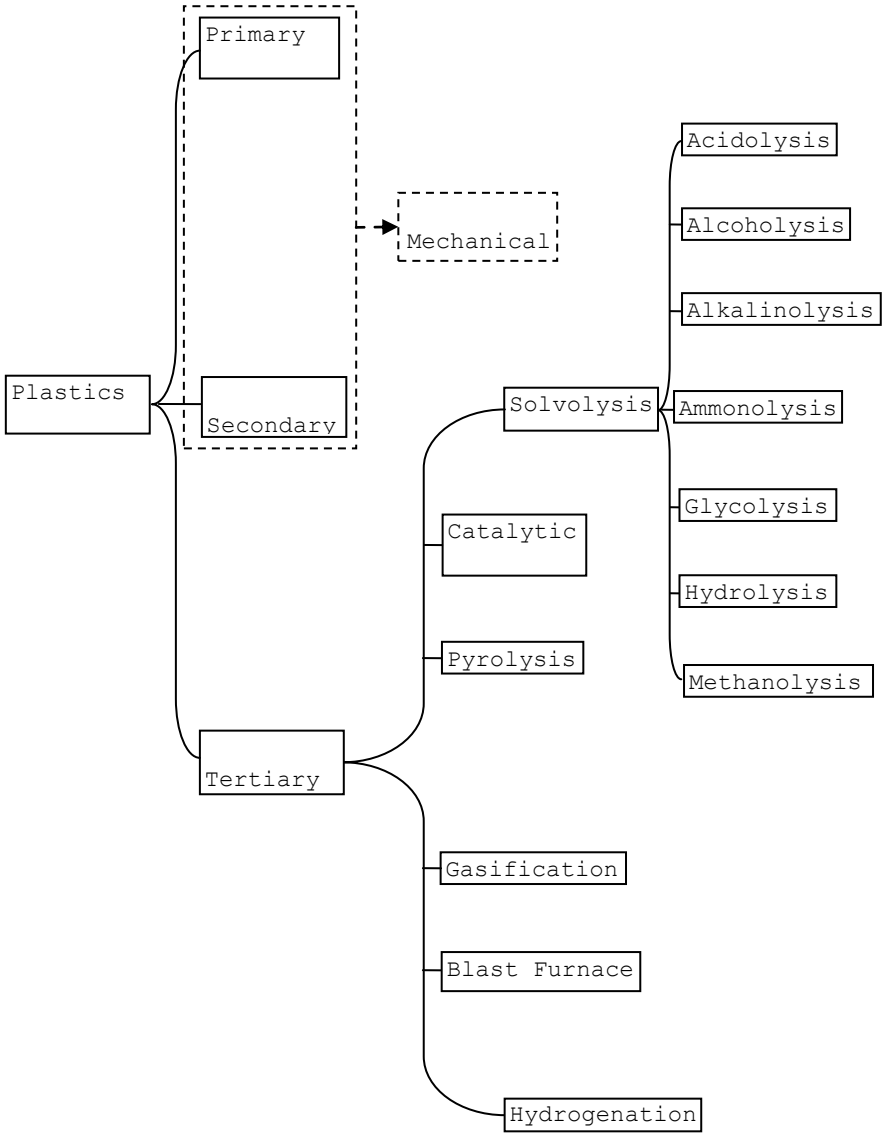

Figure 1.8: Plastic Recycling Technologies

Solvolysis is limited as a recycling process due to its restriction to mainly single stream, condensation polymers and not the more abundant polyolefins, and its sensitivity to impurities.

b) Thermal decomposition: Unlike the chemical depolymerisation process, these processes are adapted to handle mixed waste plastics consisting mainly of the more prevalent thermoplastic polyalkanes. They include.

i. Pyrolysis is the thermal anaerobic decomposition of organic materials in medium range temperature heat (400 – 800^{o}C) into a combination of char, oil and gas products (Williams, 2005). The distribution of these primary products, however, depend on its process conditions, especially temperature (Williams, 2005; Scheirs, 2006). Generally, as the process temperature increases, the gas products also increase at the expense of the liquid products.

The char can be used as fuel, carbon black or activated carbon (Williams, 2005); the oil as a fuel oil substitute in heat and power applications or as a feedstock for a variety of chemicals, while the gas can be used to provide process heat (Lettieri and Al-Salem, 2011). Process heat value of pyrolysis gas varies between 22 and 30MJ/m^3, or higher, depending on the process feedstock (Lettieri and Al-Salem, 2011).

The pyrolytic oil comprises C_7 – C_{20} hydrocarbons which, includes alkanes, alkenes, naphthenes, and aromatics in its oil fraction (Demirbas, 2004). Similar oil products described as naphtha-like by Meszaros (1996), which also contains substantial quantities of highly hydrogenated linear hydrocarbons and aromatics rich in benzene, toluene and xylene, are produced when a high liquid yield is targeted (liquefaction). However the value or composition of the pyrolysis oil is also temperature dependent; the proportion of straight chain compounds, the main oil constituent at lower temperatures, reduces with increasing temperature with aromatic compounds increasing simultaneously to become the main constituent at

high temperatures (Scheirs, 2006). Compositional differences are also influenced by the makeup of the waste plastics with polyolefins yielding an oil constituted of mainly alkanes and alkenes, while vinyl polymers such as PS and PVC contain aromatics in their oil's constitution (Williams and Williams, 1997; Williams, 2005). High value liquid products, such as contained in diesel, are low process temperature yields (390-425^{o}C) for mixed waste plastics (Scheirs, 2006). Pyrolysis produces 80-95% less gas compared to incineration and thus saves on the volume of emission to be treated for pollutants (Kaminsky and Sinn, 1995; Jung and Fontana, 2006). Pollutants associated with incineration are trapped within the char in the case of pyrolysis (Kaminsky and Sinn, 1995).

Though the importance of pyrolysis lies in its ability to recover hydrocarbon fuels and chemicals from mixed waste plastics, it can also be applied on a few single-stream plastics for monomer recovery (Pielichowski and Njuguna, 2005; Yoshioka and Grause, 2006). These include PMMA (Kaminsky and Franck, 1991; Smolders and Baeyens, 2004), PS (Kaminsky and Sinn, 1995; Zhang et al., 1995) and Polyamide (Nylon 6) (Kopietz and Seeliger, 1996; Shimasaki et al., 1997).

Fluidised-bed pyrolysis and rotary kiln pyrolysis technologies are well established processes for plastics recycling. Up to 90% monomer yield have been achieved with PMMA using rotary kiln pyrolysis while fluidised-bed have been successful for PMMA and PS (Kaminsky and Sinn, 1995). Mixed plastics waste has also been processed in fluidised-bed reactors.

Pyrolysis is an attractive process for plastics recycling as it can treat all plastics irrespective of their contamination by food, paper, aluminium foil or plastics of other resin types (Meszaros, 1996; Scheirs, 2006). Treatment for gas emission into

atmosphere is not required due to treatment carried out on pyrolysis process gas fuel product before it is used (Achilias et al., 2012).

However problems have been encountered pertaining to toxic emission and particle agglomeration due to the composition of mixed plastics feed stream for pyrolysis, especially those containing PVC, polyamide and polycarbonate (Kaminsky and Sinn, 1995) and sand as well. This results in corrosion and clogging issues in pyrolysis reactors due to formation of HCl and $CaCl_2$, respectively (Buekens, 2006). Other problems associated with plastics pyrolysis include batch processing nature of pioneer/earlier technologies, the poor heat conductivity associated with carbon/coke residue fouling of reaction vessel and high viscosity associated with plastic melts which makes it difficult to pump, poor fuel quality, and undesirable sulphur content (Leidner, 1981). Handling of char produced, i.e. finding suitable use, is difficult despite its high calorific value and thus usually landfilled (Okuwaki et al., 2006). The reaction mechanism is also not well understood thus inhibiting tailoring accurate product selectivity (Al-Salem et al., 2009).

Although plastics pyrolysis has been worked on extensively (Di Blasi, 1997; Fink and Fink, 1997; Kim et al., 1997; Bockhorn et al., 1998; Buekens and Huang, 1998; Kiran et al., 2000; Faravelli et al., 2001; Vasile et al., 2001; Bagri and Williams, 2002; Aguado et al., 2003) it has been beleaguered by the problems mentioned above in addition to oil still being more economically viable, making pyrolysis less attractive (Demirbas, 2004). The chlorine content of plastics pyrolytic oils is also an issue with respect to limits prescribed for petrochemical feedstock which should not exceed 10ppm (Kaminsky and Sinn, 1995). Pyrolytic oils from mixed plastics have an estimated chlorine content of 50 – 200ppm (Kaminsky and Sinn, 1995).

In general pyrolysis is yet to achieve commercial status as noted by Rada et al. (2009). However some technologies such as ROYCO, Hitachi and Chiyoda processes have been developed (Scheirs, 2006). With the exception of ROYCO which claims to have 6 operational plants in South and North Korea (ROYCO., ca. 2013), the commercial operation of the other technologies could not be readily confirmed. Technologies such as CYNAR (formerly Thermofuel), operational in the Republic of Ireland, Smuda process, Nanofuel process, Reentech process, Blowdec process, Conrad process, Likun process and Fuji process regarded as pyrolysis technologies involve the use of catalyst so could be considered catalytic cracking. Higher oil prices coupled with environmental awareness and incentives as tighter regulation of incineration emissions and landfilling could however make pyrolysis a viable commercial alternative.

ii. Catalytic cracking: This involves thermal decomposition of polymer waste in the presence of a catalyst, in other words, catalysed pyrolysis. In contrast to thermal cracking (pyrolysis), catalytic cracking offers some advantages, which include (Aguado and Serrano, 1999; Aguado et al., 2007):

- lower process temperature (~200^{o}C as opposed to ~400^{o}C for pyrolysis)
- lower process activation energy thus shorter reaction time at a given process temperature
- Product selectivity and distribution are controlled by catalyst activity thus higher quality products are produced
- Catalyst activity has also been known to prevent formation of undesirable species such as chlorinated hydrocarbon

Catalytic cracking however experiences the following problems

- Catalyst deactivation as a result of deposition of carbonaceous residues and heteroatom poisoning e.g. chlorine and nitrogen (Aguado and Serrano, 1999)
- Inorganic compounds associated with waste plastics collect on the catalysts preventing recovery and reuse (Aguado and Serrano, 1999).
- Requires relatively clean waste polyolefinic plastics thus may involve expensive pre-treatment steps (Aguado and Serrano, 1999).
- The presence of bulky polymer molecules limits cracking in the case of acid catalysts (Aguado et al., 2007)
- Efficiency of catalytic cracking is affected by plastic service use or history (Aguado et al., 2007).

A number of commercial catalytic cracking technologies (Scheirs, 2006) have been developed as mentioned earlier under pyrolysis.

iii. Gasification is the high temperature (up to 1600^{o}C) decomposition process through partial oxidation of organic materials to produce combustible gases, composed mainly of CO and H_2 otherwise known as synthesis gas (Lettieri and Al-Salem, 2011). In addition other gases such as CO_2, CH_4, nitrogen gas and water vapour, as well as tar and ash are also produced as by-products in smaller fractions (Williams, 2005; Jung and Fontana, 2006; Lettieri and Al-Salem, 2011). The constitution of the combustible gases depend on the oxidising reactant (Meszaros, 1996) and the reaction environment (Gebauer and Stannard, 1996). Possible oxidising reactants include O_2, air, $H_2O_{(g)}$, and CO_2 used independently or as mixtures (Gebauer and Stannard, 1996) with different pros and cons (Jung and Fontana, 2006; Al-Salem et al., 2009). For instance, gasification with air is cheap and simple but delivers a low energy value gas fuel of around of 4-6 MJ/m^3 versus 8-14 MJ/m^3 from O_2

gasification and 18 MJ/m^3 steam gasification (Jung and Fontana, 2006). Steam is usually used stoichiometrically as a co-oxidant with air and oxygen, to improve fuel quality by neutralising air's N_2 content and to deliver a more thermally stable endothermic process, respectively (Jung and Fontana, 2006).

Gasification is a good method for recycling plastics due to its suitability to handle a heterogeneous feedstock. It is also a very adaptable process as the composition of its gas product can be manipulated by the composition of oxidising reactants to deliver a wide range of applications (Gebauer and Stannard, 1996). These include uses as a fuel/combustion gas, reducing gas in pig iron production and as feedstock for chemical synthesis, particularly methanol, OXO-alcohols, ammonia, etc (Gebauer and Stannard, 1996; Buekens, 2006). It is also a good source of ethylene and propylene via steam cracking (Meszaros, 1996). Dioxin and furan production is inhibited in the gasification process due to the very high temperatures involved, which destroys any dioxin and furan or their precursors in the feed, and the reducing environment of sub-stoichiometric oxygen, which prevents the formation of free chlorine and thus its reaction with precursor organic compounds in the product gas (EPIC, 2004a).

Plastic gasification technologies are well established; they are all based on the gasification of natural organic materials, particularly coal (Gebauer and Stannard, 1996; Aguado and Serrano, 1999; Borgianni et al., 2002). Examples of established technologies include: Texaco Gasification Process, SVZ Gasification Process, Akzo Nobel Steam Gasification Process, Linde Gasification Process (Tukker, 2002; Jung and Fontana, 2006) and EBARA-UBE's high-pressure gasification (Buekens, 2006). The sole operational plant, the Japanese Ube Industries, which uses the

EBARA-UBE high-pressure gasification process, shut down in June 2010 due to lack of supply of waste plastics (UBE Industries Ltd, 2010)

Certain factors have however inhibited the growth of the technology for plastics recycling such as operational problems relating to plant capacity sustenance with adequate supply of required plastic waste volume and uncompetitive gate or dump fees (Buekens, 2006). Gasification plants need to have large processing capacity, between 0.4 and 0.5 million tonnes per year, to be economically viable (Hofmann and Gebauer, 1993 cited in Aguado and Serrano, 1999; Aguado et al., 2006a). In addition, melting behaviour and agglomeration issues associated with plastics processing have resulted in the common practice of plastics gasification with other materials (Gebauer and Stannard, 1996).

iv. Blast furnace: This treatment method makes use of mixed plastics waste as a reducing agent in steel production, where iron ore (Fe_2O_3) is required to be reduced to iron metal (Fe), as replacement for coke, coal and/or heavy oil in pig iron manufacture.

Plastics can be used mainly as reducing agents, alongside coke, in place of coal or heavy oil due to their comparable C:H ratio (Niemoller, 1996) while providing some of the process heat in the blast furnace through recovery of some of the plastics' energy content.

In the blast furnace, iron ore and coke are introduced from its top while the mixed plastics is blasted in through nozzles called tuyeres at the bottom with the aid of the oxygen-deficient hot air (ICPE, 2006; Plastics Europe, 2009b). The plastic waste is

broken down into CO and H_2 which reduces the iron ore as it descends down the blast furnace.

Advantages of blast furnace feedstock recycling of waste plastics include:

- Its capacity to treat large quantities of mixed plastics waste; a large plant can use more than 150,000 tonnes per annum (Heo and Yim, 1998; cited by Kim et al., 2002 and; Al-Salem et al., 2009)
- It is up to 80% more energy efficient compared to traditional reducing agents (Heo et al., 2000a and; 2000b; cited inKim et al., 2002 and; Al-Salem et al., 2009)
- Dioxin production is inhibited due to the high temperature (2100 ºC) and reducing environment in the furnace (Tukker, 2002; Everaert and Baeyens, 2004).
- The low sulphur content of waste plastics in contrast to coal and heavy oil makes it a desirable feedstock as sulphur contamination causes brittleness in pig and cast iron and the unpleasant odour of hydrogen sulphide produced during slag granulation (Niemoller, 1996; Kaushish, 2010)

This technology is well established but high cost due to operational instability, related to lower combustibility in contrast to coal (Pohang Iron and Steel Making Company, 1996 cited in Kim et al., 2002; Al-Salem et al., 2010), at pilot phase has hindered the expansion of the use of waste plastics as reducing agents in blast furnaces (Tukker, 2002). Insufficient availability of oxygen for waste plastics combustion in the blast furnace as a result of inadequate supply or distribution of oxygen through the blast furnace is also a major issue (Al-Salem et al., 2010).

Chlorine content is also restricted to a maximum of around 1.5%, i.e. around 3% PVC content in mixed plastics (Tukker, 2002).

v. Hydrogenation (Hydrocracking): Hydrocracking converts macromolecular hydrocarbons, through a catalyst assisted thermal breakdown, to unsaturated intermediate radicals, which are concurrently or subsequently hydrogenated into smaller saturated products (Scherzer and Gruia, 1996; Aguado and Serrano, 1999). It is a hydroprocessing or hydrogenation process that takes place at hydrogen partial pressures of between 85 and 250 bar, and temperatures between 300 and 480^{o}C (Niemann, 1996; Scherzer and Gruia, 1996; Aguado and Serrano, 1999).

Originally applied for upgrading heavy residues of the oil refining process, hydrocracking has been adapted for processing other materials such as coal and plastics due to their ability to remove heteroatoms associated with them (Niemann, 1996; Scherzer and Gruia, 1996; Aguado and Serrano, 1999). Heteroatoms, which lead to catalyst degeneration, are removed through hydrotreating reactions such as hydrodesulphurization, hydrodechlorination and dehydrochlorination, hydrodenitrogenation, and hydrodeoxygenation prior to hydrocracking (Scherzer and Gruia, 1996).

In addition to heteroatom removal and catalyst conservation which is an advantage over catalytic cracking, hydrocracking is an attractive process due to its lower process temperature and the quality of its liquid product, a synthetic crude oil of gasoline/diesel specification/grade, requires no further treatment or upgrading in contrast to pyrolysis oil (Walendziewski and Steininger, 2001; Garforth et al., 2004; Butler et al., 2011). This synthetic crude also has a higher value compared to

that from catalytic cracking due to the negligible content of alkene hydrocarbons (White, 2006).

An essential element in the hydrocracking process is the hydrocracking catalyst. These are bifunctional in activity due to the presence of two reactive sites; a metal site which accomplishes a hydrogenation-dehydrogenation function, and an acidic site which propagates a cracking function (Scherzer and Gruia, 1996; Aguado and Serrano, 1999). The catalyst's bifunctional activity can be manipulated to influence its activity and the range and distribution of products (Scherzer and Gruia, 1996).

Limitations to hydrocracking of plastics are mainly to do with economics of the raw-materials and equipments involved, i.e. high costs of hydrogen, catalyst and high pressure parts and machinery required for the process (Walendziewski, 2006).

1.5 SUMMARY ON RECYCLING METHODS

From the foregoing, mechanical recycling, which includes primary and secondary recycling is limited to clean, high quality, single stream, plastics. For this reason, mechanical recycling is reliant on pre-consumer industrial waste plastics (Hopewell et al., 2009) for its feed stream, with only about half of the significantly more abundant post-consumer waste plastics collected for recycling suitable (Butler et al., 2011). Despite mechanical recycling accounting for almost 99% of the material recycling already taking place in Western Europe, 42% of the post-consumer plastic waste generated is still sent to landfill, not to mention the 34% currently being incinerated with energy recovery (Plastics Europe, 2009a). This shows the potential for expanding feedstock recycling which only accounts for around 1% of the waste plastics recycled (Plastics Europe, 2009a). This

expansion is however limited to the thermal degradation processes since solvolysis, a monomer recovery method, is restricted to mainly condensation polymer plastics which are quantitatively less significant to their addition counterpart, containing the more prevalent polyolefins (Panda et al., 2010). Much like mechanical recycling solvolysis can only be used for single stream polymer plastics and process contamination is a problem (Aguado and Serrano, 1999; Grause et al., 2011).

Among the feedstock recycling methods capable of treating mixed waste plastics, hydrogenation offers the best value in terms of quality of its process oil product; it produces a paraffin-rich synthetic crude similar in composition to gasoline and diesel (Aguado and Serrano, 1999; White, 2006). Blast furnace was not considered as an independent feedstock recycling method as it is not widely recognised in literature as a feedstock recycling method. Moreover, it only qualifies as a feedstock recycling method when plastics are gasified to produce reducing gas, CO and H_2, for refining iron ore, and thus can be considered as gasification. Hydrocracking is an established refinery process, thus hydrocracking of plastics would be best incorporated into a refinery to take advantage of its existing installations and the improved fuel quality benefits of co-processing (Butler et al., 2011). Waste plastics would have to conform to the feed stream characteristics of processes in the refinery industry (Michaeli and Lackner, 1995). However viscosity problems experienced with conventional refinery equipment places limitation on the quantity of plastics, not more than 10% of feed composition, which can be mixed with refinery fractions (Lovett et al., 1997; Aguado et al., 2006a; Ali and Siddiqui, 2006; Aguado et al., 2008). Furthermore, the generation of waste plastics, though a major concern due to its rapid rate of growth, is trans-boundary, making it logistically difficult to be treated using petrochemical installations (Butler et al., 2011) except in areas where one

is in close proximity. This would require an elaborate collection, separation and transportation operation, which would not make economic or indeed environmental sense. Moreover, if an optimistic scenario of the current UK annual plastic consumption of around 41 kg per capita is assumed to enter the waste stream and yields an overestimated 41 L/person/yr of petrol or diesel, this will only account for about 5% of the around 880 L/person of diesel and petrol consumed in the UK in 2011 (Directgov, 2012; MacLeay et al., 2012). Hence, municipal hydrocracking plants, perhaps at a materials recovery facility (MRF), may provide the most viable opportunity to treat municipal mixed plastic waste for production of local fuelling needs (Stelmachowski, 2010)

Two major subjects are prominent in relation to subjecting plastics to petrochemical processes; its PVC content and viscosity (Michaeli and Lackner, 1995). Chlorine and viscosity feedstock specification limits for the petrochemical industry are 5 ppm (Ali and Siddiqui, 2006; Buekens, 2006) and 0.5 Pas at 200^{o}C (Menges and Lackner, 1996), respectively.

Under thermal degradation, PVC evolves hydrochloric acid, which is corrosive to the reaction environment. Chloro-organic compounds- or halogen organic compounds, if other halogen containing plastics such as brominated high impact polystyrene (HIPS-Br) are involved- also form in pyrolysis oil products, where they can lead to the toxic polychlorinated dibenzodioxins (PCDDs), dibenzofurans (PCDFs) and polychlorobiphenyls (PCBs) formation and release when burnt as fuel (Iida et al., 1974; Christmann et al., 1989; Bhaskar et al., 2002). For these reasons, as well as catalyst poisoning which is also an issue, dechlorination/dehalogenation pretreatment processes are imperative to make them acceptable refinery feedstock for fuel production.

While dechlorination of mixed plastic waste has been studied exhaustively, with research interest focused on chemical recycling of waste plastics dehalogenation, catalyst performance, i.e. product distribution and selectivity, viscosity studies in relation to process improvement or efficiency in the pyrolysis or hydrocracking plastics have scarcely been undertaken despite acknowledgements of its importance. Arandes et al. (1997), Serrano et al. (2003), Ali and Siddiqui (2006), Walendziewski (2006), and Butler et al. (2011) have all commented on the transport difficulty the high viscosity of plastics creates especially in relation to pumping into conventional reactors, such as the fixed-bed reactors traditionally used for hydrocracking in the oil industry (Scherzer and Gruia, 1996). Aguado (2006a) also identified the high viscosity of plastics as a major problem in relation to designing reactors for catalytic cracking and as a vital research area to develop. The high viscosity of polymer melts is known to inhibit heat and mass transfer (Bremner et al., 1990; Sato et al., 1990; Murakata et al., 1993; Shyichuk, 1996) between molten polymer and catalyst. This mass transfer limitation inhibits diffusion and promotes secondary reactions (oligomerization, cyclization and aromatization) during cracking (Aguado et al., 2006a; Yanik and Karayildirim, 2006; Grause et al., 2011). Secondary reactions may lead to undesired constituents in the composition profile of the final product (White, 2006; Grause et al., 2011) and the formation of coke (Buekens, 2006). Fluidized bed reactors have however fared better in catalytic cracking operation of plastics due to their enhanced heat and mass transfer characteristics and facilitation of contact between catalyst and plastic (Garforth et al., 1998; Aguado et al., 2006a; Buekens, 2006). A laboratory extruder-type reactor, the screw kiln reactor, has also been developed and used for thermal and catalytic pyrolysis of plastics, showing good heat and mass transfer characteristics (Serrano et al., 2001; Aguado et al., 2002; Serrano et al., 2003).

Several methods have been employed as solution with limited success to solve this high viscosity problem. Degradative extrusion, which involves the use of a twin-screw extruder system and degradation agents such as steam, air, oxygen, or catalyst, at around 400^{o}C, has been used to achieve viscosity reductions to 2 - 0.2 Pas at 200^{o}C (Michaeli and Lackner, 1995). The system also involves an initial dehydrochlorination phase, either on a single extruder unit or a cascaded unit, where HCl is vented off and collected at around 300^{o}C. Scale-up potential for this process is, as yet, unknown as it has been mainly used in research, pilot, or small industrial scale applications (Al-Salem et al., 2009) and no commercial examples were found. An alternative method to reduce the viscosity of plastics that has gained a lot of interest is co-processing plastics with petroleum fractions or product chemicals as solvents. Examples of petrochemical solvents used include vacuum gas oil (VGO) (Ng, 1995), Arabian light petroleum residues (Siddiqui et al., 2002), light cycle oil (LCO) (Arandes et al., 1997), lube oils (Serrano et al., 2003) or even raw chemicals such as benzene (De La Puente and Sedran, 1998). Hydrogen donating solvents such as 9,10-dihydroanthracene, 1-methylnaphthalene, tetralin, decalin, have also been used to improve the selectivity towards valuable paraffin hydrocarbon within the product yield (Sato et al., 1990; Murakata et al., 1993; Aguado et al., 2006b; Serrano et al., 2007). However, processing of mixtures with more than 10% plastic content tends to be counterproductive as viscosity begins to rise beyond tolerable refinery level (Lovett et al., 1997; Aguado et al., 2006a; Ali and Siddiqui, 2006; Aguado et al., 2008). Serrano et al. (2003) however successfully catalytically cracked mixtures of lubrication oil and 40-70% LDPE in the screw kiln reactor. Other than the work of Marcilla et al. (2008) which investigated the influence of LDPE/VGO mixing proportions on the viscosity behaviour over a range of shear rates and temperature, all other studies are however lacking in quantitative insight into viscosity reduction with respect to requirements of industry.

2 LITERATURE REVIEW

2.1 INTRODUCTION

The application of hydrocracking to mixed waste plastics as a recycling method has attracted some interest due to the quality of its gasoline/diesel range product oil; it has a richer content of paraffin hydrocarbons as opposed to olefin, in contrast to both thermal and catalytic pyrolysis (White, 2006). It is also more robust in dealing with heteroatom containing mixed plastic waste owing to the high pressure hydrogen atmosphere of the hydrocracking process which facilitates the removal of the undesirable heteroatoms.

Plastics hydrocracking, and feedstock recycling in general, has been studied and demonstrated on a laboratory scale but have focused primarily on improving products yield and compositional distribution therein. Hence studies have focused on catalysts and the influence of catalysts activity, as well as, co-processing with coal, petroleum fractions and hydrocarbon solvents, on products yields and quality for both single and mixed stream plastics hydrocracking. Studies have also been carried out on dechlorination of PVC containing mixed plastic waste stream. A cross section of these studies are shown in table 2.1 below.

Table 2.1: A cross-section of research focus in plastics feedstock recycling studies

Study	*Authors*
Coliquefaction of waste plastics with coal	(Taghiei et al., 1994)
Direct liquefaction of plastics and coliquefaction of waste plastic with coal	(Huffman et al., 1995)
Direct liquefaction of waste plastics and coliquefaction of coal-plastic mixtures	(Feng et al., 1996)
Liquefaction of commingled waste plastics containing PVC	(Huffman et al., 1996)
Catalytic coprocessing of plastics with coal and petroleum resid using $NiMo/Al_2O_3$	(Joo and Curtis, 1996)
Catalytic reactions in waste plastics, hdpe and coal studied by high-pressure thermogravimetry with on-line gc/ms	(Liu and Meuzelaar, 1996)
Effect of reaction parameters and catalyst type on waste plastics liquefaction and coprocessing with coal	(Luo and Curtis, 1996)
Catalytic degradation of medium density polyethylene over silica - alumina supports	(Ochoa et al., 1996)
Hydrocracking and hydroisomerization of long-chain alkanes and polyolefins over metal-promoted anion-modified zirconium oxides	(Venkatesh et al., 1996)

Study	*Authors*
Depolymerization-liquefaction of plastics and rubbers. 2. Polystyrenes and styrene-butadiene copolymers	(Zmierczak et al., 1996)
Depolymerization of waste plastics with coal over metal-loaded silica-alumina catalysts	(Ding et al., 1996)
Hydrocracking of waste plastics to clean liquid fuels	(Ding et al., 1997a)
Hydrocracking and hydroisomerization of high-density polyethylene and waste plastic over zeolite and silica-alumina-supported Ni and Ni-Mo sulfides	(Ding et al., 1997b)
Sulfur-promoted degradation of polyethylene/polypropylene detected by electron spin resonance spectroscopy	(Ibrahim and Seehra, 1997)
Hydrocracking of a plastics pyrolysis gas oil to naphtha	(Joo and Guin, 1997)
Investigation of first-stage liquefaction of coal with model plastic waste mixtures	(Rothenberger et al., 1997)
Depolymerization-liquefaction of plastics and rubbers. 1. Polyethylene, polypropylene, and polybutadiene	(Shabtai et al., 1997)
Catalytic coprocessing of LDPE with coal and petroleum resid using different catalysts	(Joo and Curtis, 1998)

Study	*Authors*
Conversion of waste plastic to oil: Direct liquefaction versus pyrolysis and hydroprocessing	(Shah et al., 1999)
Gas phase catalytic dehydrochlorination and hydrodechlorination of aliphatic and aromatic systems	(Tavoularis and Keane, 1999)
Liquefaction of municipal waste plastics in VGO over acidic and non-acidic catalysts	(KarayIldIrIm et al., 2001)
Catalytic dehydrochlorination of chloro-organic compounds from PVC containing waste plastics derived fuel oil over FeCl2/SiO2 catalyst	(Lingaiah et al., 2001)
Thermal and catalytic conversion of waste polyolefines	(Walendziewski and Steininger, 2001)
The catalytic effect of Red Mud on the degradation of poly (vinyl chloride) containing polymer mixture into fuel oil	(Yanik et al., 2001)
Conversion of polymers to fuels in a refinery stream	(Uçar et al., 2002)
Liquefaction of mixed plastics containing PVC and dechlorination by calcium-based sorbent	(Bhaskar et al., 2003)
Liquefaction of municipal waste plastics in VGO over acidic and non-acidic catalysts	(Karagoz et al., 2003a)
Catalytic and thermal degradation of high-density polyethylene in vacuum gas oil over non-acidic and acidic catalysts	(Karagoz et al., 2003b)

Study	***Authors***
Study on the conversion of waste plastics/petroleum resid mixtures to transportation fuels	(Ali et al., 2004)
Catalytic and thermal degradation of high-density polyethylene in vacuum gas oil over non-acidic and acidic catalysts	(Zhou et al., 2004)
Thermal and catalytic decomposition behavior of PVC mixed plastic waste with petroleum residue	(Ali and Siddiqui, 2005)
Influence of Iron Chloride on Hydrocracking of Waste Plastics Using Coal Tar	(Kakuta et al., 2006)
Catalytic conversion of waste plastics: Focus on waste PVC	(Keane, 2007)
Catalytic coprocessing of waste plastics and petroleum residue into liquid fuel oils	(Siddiqui and Redhwi, 2009)
Catalytic coprocessing of coal and petroleum residues with waste plastics to produce transportation fuels	(Ali et al., 2011)
Dechlorination of fuels in pyrolysis of PVC containing plastic wastes	(Lopez-Urionabarrenechea et al., 2011)
Catalytic stepwise pyrolysis of packaging plastic waste	(Lopez-Urionabarrenechea et al., 2012)
Thermal decomposition of poly(vinyl chloride) in organic solvents under high pressure	(Kamo, 2013)

One important parameter that has however received little attention is viscosity despite its militating effects on, and delayed commercialisation (Murakata et al., 1993) of plastics hydrocracking. Plastics have very high viscosities which make them difficult to pump through pipes and into conventional reactors (Arandes et al., 1997; Serrano et al., 2003; Walendziewski, 2006; Butler et al., 2011). Their high viscosity also inhibits heat and mass transfer and promotes secondary reactions which may produce undesirable products such as coke (Bremner et al., 1990; Sato et al., 1990; Murakata et al., 1993; Shyichuk, 1996; Buekens, 2006). These few points underline the importance of viscosity in advancing the processing of mixed waste plastic by pyrolysis, catalytic cracking, or hydrocracking.

From a general point of view, viscosity is one of the controlling parameters of both mass and heat transfer. Mass transfer is usually expressed in terms of mass transfer coefficients (or the dimensionless form, Sherwood number) in empirical correlations (Levec and Goto, 1986; Thoenes, 1994; Ranade et al., 2011). Heat transfer is expressed in terms of heat transfer coefficients (or the dimensionless form, Nusselt number) in similar correlations and effective bed thermal conductivities (Thoenes, 1994; Ranade et al., 2011). The liquid viscosity term is contained in the Reynolds number (*Re*) a dimensionless power function of the Sherwood (*Sh*) and Nusselt (*Nu*) numbers; and the Schmidt (*Sc*) and Prandtl (*Pr*) numbers, which are power functions of the Sherwood and Nusselt numbers, respectively.

$$Sh = A.Re_L^b.Sc_L^c \qquad 2.1$$

$$Nu = A.Re_L^b.Pr_L^c \qquad 2.2$$

$$where\ Sh = \frac{k_F.d}{D_m}; Nu = \frac{hd}{\lambda}; Re = \frac{du\rho}{\mu}; Sc = \frac{\mu}{D_m.\rho}; Pr = \frac{C_p\mu}{\lambda}$$

C_p = specific heat; d =characteristic length (e.g. particle diameter); Dm = fluid molecular diffusivity; h = heat transfer coefficient; λ = thermal conductivity; k_F = gas-liquid or liquid-solid mass transfer coefficient; ρ = liquid density; u = liquid velocity; μ = liquid viscosity

In a three-phase reaction such as hydrocracking, involving gas (hydrogen), liquid (molten plastic), and solid (catalyst) phases; inter-phase transport of the reacting species, i.e. gas-liquid mass transfer, liquid-solid transfer, and intra-particle diffusion, are required for chemical reaction to take place (Levec and Goto, 1986). Hydrocracking is also an exothermic reaction thus heat removal from the reaction is important to avoid loss of activity in the catalyst and maintain temperature uniformity in the reactor (Ranade et al., 2011). Heat transfer inside the catalyst (reaction site), from particle to fluid (gas and liquid phases), from catalyst to catalyst (in a packed bed), and from bed to wall (bulk reactor content to reactor wall) are thus essential parameters that need to be optimized (Ranade et al., 2011). Viscosity, which is high for plastics, generally has a negative effect on mass transfer (Lee et al., 1993) and heat transfer (Fan, 1989; Kim and Laurent, 1991) as is indicated by the relatively higher power which the Reynolds number is raised to in such correlations (Buekens, 2006). The low thermal conductivity of plastics also hinders heat transfer (Buekens, 2006).

Viscosity is also a source of inhomogeneity in chemical reactions (Coulson et al., 1999). The attainment of homogeneity is achieved by mixing, which primarily aims to induce interphase migration of reactant molecules. For reactions involving gas and liquid phases, penetration of the liquid phase by the gaseous to create a high surface contact area is very

important as gas-liquid mixtures are characteristically unstable and require agitation to maintain intermolecular contact (Coulson et al., 1999).

Information on how the viscosity of plastic melts affect the hydrocracking process in view of the technical and operational challenges highlighted (transport and heat and mass transfer) so far in the context of conventional processing equipment is not readily available. Given the nature of plastic melts as non-Newtonian, viscoelastic materials with high viscosities, knowledge of their precise deformational flow behaviour in response to induced stress (rheology) would also benefit process design and instrumentation. It will also be useful to compare the viscosity behaviour of plastics with those of crude oil or petroleum fractions which the hydrocracking process is traditionally used for. The energy implications of inducing mixing and pumping reactants and products/residues, in and out of vessels, respectively, is affected to large extent by viscosity, especially as it relates to equipment selection and design (Coulson et al., 1999). Pumpable viscosity specification for oil, petrochemical feedstock is 0.2 – 0.5 Pas (Brandrup, 1996)

2.2 Rheology and viscosity measurement of polymer melts

2.2.1 Introduction

In rheology, the deformation behaviour and properties of materials are studied under different conditions of an externally applied force (stress). Thus rheological classification of materials is based on two major factors; a material's response to deformation and whether it can be considered as a solid or fluid. However, for fluids, two major

classifications exist namely, Newtonian and Non-Newtonian fluids. While Newtonian fluids show a directly proportional relationship between shear stress (τ) and shear rate ($\dot{\gamma}$) (see figure 2.1 and equation 2.3), Non-Newtonian fluids exhibit a shear stress related shear rate response which deviates from proportionality (fig 2.2). Thus viscosity (μ), which is the proportionality constant, is characteristically constant in Newtonian fluids, but is a function of shear rate in non-Newtonian fluids.

$$\boldsymbol{\tau = \mu\dot{\gamma}} \qquad \textbf{2.3}$$

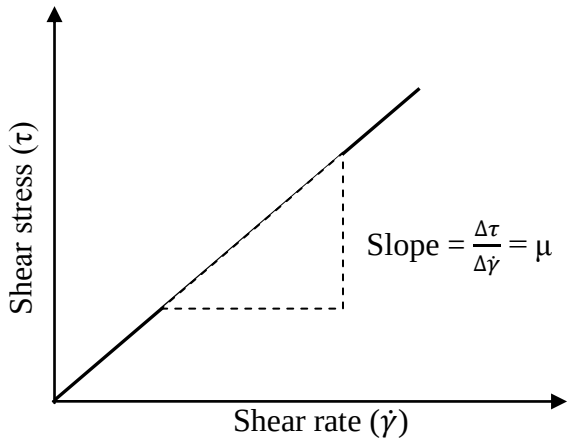

Figure 2.1: Newtonian shear stress-shear rate relationship

The major Non-Newtonian sub-classes include (Brydson, 1981):

1. Time-independent fluids: Also known as viscous fluids, these fluids show a distinct shear stress relationship to shear-rate at any given point, i.e. shear rate is a function of the shear stress. The viscosity thus either increases or decreases with shear rate. They are made up of the following subtypes of fluids based on their shear stress-shear rate relationships:

a. Shear thinning fluids: These are fluids (also known as pseudoplastic) for which their viscosities characteristically decrease as shear rate is increased (Figure 2.2). This means that as shear rate increases, the shear stress falls at a less than linear rate.

b. Shear thickening fluids: Otherwise referred to as dilatants, these fluids on the other hand experience a rise in viscosity as shear rate is increased (Figure 2.2). This means that as shear rate increases, the shear stress increases at a more than linear rate.

The shear-thinning and shear-thickening behaviour of Non-Newtonian fluids have normally been accounted for by the Power Law Model (Equation 2.4a and 2.4b)

$$\tau = k\dot{\gamma}^{n} \tag{2.4a}$$

or

$$\mu = k\dot{\gamma}^{n-1} \tag{2.4b}$$

Where: k is the consistency coefficient and n is known as power-law or flow index. k is considered to approximate to the numerical value of the shear stress (or viscosity depending on which equation is being used) at $1s^{-1}$. The value of n describes the behaviour of the fluid and thus depicts Newtonian behaviour (n = 1), shear-thinning (n < 1) or shear-thickening (n > 1).

c. Bingham fluids: Bingham fluids are idealised fluids which only flow once a critical shear stress (yield stress, τ_y) has been surpassed. In other words, their shear stress difference above the yield stress is directly proportional to shear rate (Equation 2.5) with the proportionality constant referred to as plastic viscosity (μ_p).

$$\tau - \tau_y = \mu_p\dot{\gamma} \tag{2.5}$$

Where $\tau > \tau_y$; $\mu_p =$ plastic viscosity

A modified or more generalised form of this model which depicts a non-linear relationship above the yield stress is the Herschel-Bulkley model

$$\tau - \tau_y = k\dot{\gamma}^n \tag{2.6}$$

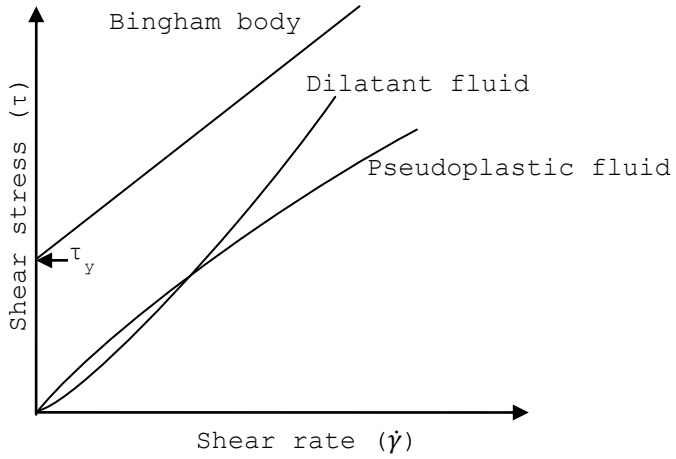

Figure 2.2: Non-Newtonian shear flow curves

2. Time-dependent fluids: This group of fluids has shear stress as a function of both shear rate and time, i.e. shearing time interval at a particular shear rate. In other words, their shear stress not only increases (or decreases) as shear rate is increased, but also shows a similar shear stress response with time interval at a constant shear rate. As a result, their viscosity changes, usually reversibly, with shear rate and time interval. The shear history of time-dependent fluids also influences their shear behaviour. This group consist of:

a. Thixotropic fluids which exhibit a decreasing viscosity (shear-thinning) behaviour, with increasing time duration of a constant shear rate until an equilibrium shear stress value, and hence viscosity, is reached (Barnes, 1997).
b. Anti-thixotropic fluids where viscosity increases (shear-thickenning) with increasing time duration of constant shear rate until an equilibrium shear stress value, and hence viscosity, is reached (Barnes, 1997).

3. Elasticoviscous fluids: More commonly (but inappropriately) known as viscoelastic fluids, is a group of fluids in-between the solid and liquid phase and possess properties of both elastic (Hookean) solids and viscous (Newtonian) fluids (Ferry, 1980). Thus, like viscous liquids, shear stress is a function of shear rate, however only part of the induced shear stress propagates deformation, i.e. flow, while the rest is elastically stored representing a delayed deformation much like elastic solids (Brydson, 1981; Chhabra and Richardson, 1999; Schramm, 2000). They only manifest some of the delayed deformation due to the stored stress once the induced stress is removed unlike pure elastic solids (Brydson, 1981). This behaviour has been linked to the internal structure of fluids in this group which could be described as being made up of aggregates such as in polymer melts or in emulsions of two Newtonian liquids (Collyer, 1973a, Brydson, 1981). In the case of polymer melts, which are made of a network of interlocking long-chain molecules able to rotate about each other, the application of stress aligns these chains in the direction of stress. These molecules randomly reorganise back to their original network structure once stress is removed. Manifestation of elasticoviscous behaviour

include die swell, Weissenberg effect, self-siphoning and spinnability (Collyer, 1973a).

Polymer melts, despite displaying elasticoviscous behaviour when stress is discontinued, do exhibit a shear-thinning behaviour when in flow, i.e. when being sheared (Collyer, 1973b; Brydson, 1999), except at very low and high shear rates. At these extreme shear rate regions, i.e. less than 0.01 s^{-1} and greater than 100000 s^{-1}, most shear-thinning fluids exhibit Newtonian behaviour characterised by a high constant viscosity (zero shear viscosity) and a low constant viscosity (infinite shear viscosity) at the low and high shear rate regions, respectively (Chhabra and Richardson, 1999). However, since we are concerned with the higher end of shear rates employed in pumping (1 – 1000 s^{-1}) and mixing (10 – 1000 s^{-1}) operations (Chhabra and Richardson, 1999), which is the region intervening these extreme shear rate regions, polymer melts will be treated as shear thinning. It is also pertinent to mention that shear thinning behaviour of polymer melts which is classically modelled using the power law equation (equation 2.4 above) only holds over a narrow shear rate range not greater than 20 s^{-1} as revealed by (Brydson, 1981). He indicated that the power law index (n) in equation 2.4 above decreases as shear increases over larger shear rate ranges.

2.2.2 Viscosity of polymer melts

Viscosity in liquids is as a result of inter-molecular forces restricting flow as molecules slide past each other. Common liquids such as water are Newtonian. In polymer melts however, the molecules are unable to slide past each other in flow due to molecular

entanglement which unwinds into aligned chains when sheared. When shear is discontinued, these molecules are predisposed to returning to their initial natural state of entanglement due to strong intermolecular forces which accounts for the elastic behaviour of elasticoviscous fluids like polymer melts (Brydson, 1999).

Effects of polymer melt elasticity are strongly linked to molecular weight, molecular weight distribution and generally, predisposition to a molecular state of entanglement (Cogswell, 1981; Brydson, 1999). Prominent among these effects which are manifested in post polymer extrusion are die swell and melt fracture (Cogswell, 1981; Brydson, 1999).

Factors that affect polymer melt viscosity are mainly molecular weight, molecular weight distribution (MWD) and chain branching (Cogswell, 1981; Brydson, 1999; Giles et al., 2005), in order of their degree of influence. For instance an increase in molecular weight results in more than a proportionate increase in viscosity when just doubled (Cogswell, 1981). Cogswell (1981) illustrated this viscosity-molecular weight relationship using Poly(methyl methacrylate) (PMMA) which is shown below in Table 2.2. This relationship

Table 2.2: Viscosity - Molecular weight correlation for PMMA at 210^{o}C

M_w	G_o (Pa)	η_o (Pas)	$\sigma_{\frac{1}{2}}$ KPa
34000	-	600	300
75000	2 x 10^4	16000	80
160000	-	400000	30
360000	-	8000000	20

M_w = weight average molecular weight; G_o = modulus at 1000 Pa shear stress; η_o = viscosity at 1000 Pa shear stress; $\sigma_{\frac{1}{2}}$ = shear stress at which the viscosity of the polymer, η is half the viscosity value η_o

between viscosity and molecular weight is represented in the empirical formula given in equation 2.7 (Cross, 1970; Ferry, 1980; Brydson, 1981; Chhabra and Richardson, 1999). Equation 2.7 only holds for a limited range of molecular

$$\eta_0 = kM_w{}^a \tag{2.7}$$

Where: η_0 is zero shear rate viscosity; a = 3.4 – 3.5

weights and above a critical molecular weight value below which molecular weight is low and contains virtually no entanglement resulting in viscosity increasing proportionally with molecular weight, i.e. a = 1 (Ferry, 1980; Brydson, 1981; Chhabra and Richardson, 1999). In general, high molecular weight polymers exhibit a more discernible non-Newtonian flow in response to low average shear rates due to a higher probability of encountering a region of dense entanglement as the average sites of entanglement per chain increases (Cogswell, 1981).

The concept of molecular weight in commercial grade polymers differs from simple molecules. While simple molecules have an absolute molecular weight value, polymers have a Molecular Weight Distribution (MWD); polymers are made up of a network of molecules of different chain lengths as a result of different rates of chain end termination and growth, during addition and condensation polymerisation, respectively (Brydson, 1999; Peacock and Calhoun, 2006). Thus, rather than an absolute molecular weight, polymers are characterised in terms of molecular weight averages, usually Weight-Average Molecular Weight (M_w) and Number-Average Molecular Weight (M_n) (Brydson, 1999; Giles et al., 2005; Peacock and Calhoun, 2006). M_w, as the name suggests, is a weighted

average which calculates the average molecular weight based on the contribution of each individual molecular weight species or molecular chains of a particular weight that make up the polymer (equation 2.8). M_n is a simple arithmetic mean average of the molecular weights of the molecular chains that make up the polymer (equation 2.9). MWD is quantitatively represented by the dimensionless Polydispersity Index (*PI*) and is the ratio between two molecular weight averages, Weight-Average Molecular Weight (M_w) and Number-Average Molecular Weight (M_n) as shown in equation 2.10. Polydispersity for commercial polymers vary between 1.5 and 8 (Giles et al., 2005).

$$M_w = \frac{\sum n_i {M_i}^2}{\sum n_i M_i} \tag{2.8}$$

$$M_n = \frac{\sum n_i M_i}{\sum n_i} \tag{2.9}$$

Where: M_i is molecular weight of chain i; n_i is number of polymer chains of with a given molecular weight, M_i.

$$PI = \frac{M_w}{M_n} \tag{2.10}$$

The viscosity of a polymer with a broad MWD is reported to have a higher initial viscosity, i.e. at very low shear stress, and lower viscosity in high shear regions, in contrast to a polymer of similar average molecular weight, but of narrower MWD (Cogwell, 1981). The viscosity of narrower MWD is more temperature sensitive and less shear sensitive (more Newtonian) compared to broad MWD polymer of similar molecular weight (Brydson, 1981; Giles et al., 2005).

The effect of chain branching on viscosity is mostly an inverse linear relationship for polymers with the same weight average molecular weight (Barnes, 2000; Brydson, 1999).

In other words, linear polymer with little or no branching within its structure will have a higher viscosity, at a given shear rate, compared to a regularly branched polymer that has the same average molecular weight. Exceptions to this rule of thumb may occur when a polymer molecule is abundantly branched, or has regular long chain branching which would normally show a broad MWD, thus resulting in a high, initial, low shear rate viscosity in both cases. These two contrasting effects of chain branching are illustrated by polyethylene and poly(vinyl acetate), in which viscosity decreases and increases, respectively, with increasing branching (Brydson, 1999).

The shear rate-shear stress behaviour of polymer melts vary over different ranges of shear rate (Barnes, 2000). Polymers normally exhibit a Newtonian behaviour at very low shear rates, or zero shear rate, and very high shear rates, or infinite shear rate, but exhibit a non-Newtonian, shear-thinning behaviour between these extreme shear rate regions (Barnes, 2000). Thus below and above critical values within these zero and infinite shear rate regions, respectively, polymer melt viscosity begin to "plateau off" towards constant viscosities. These constant viscosities are known as zero-shear-rate viscosity (μ_0) and infinite-shear-rate viscosity (μ_∞) (Coulson et al., 1999). The shear thinning region is bound by these limiting viscosity regions and is normally captured on log-log plot of viscosity against shear rate or shear stress (Barnes, 2000).

Different empirical models have been formulated to depict the behaviour of shear thinning fluids. The most popular of these models is the Power Law model already mentioned above (equations 2.4a & 2.4b). However, this only depicts the shear-thinning region of the viscosity flow curve. The Cross Model (see Figure 2.3 and Equation 2.11) has been known

to approximate the complete flow curve (Barnes, 2000). Another model which has also found practical application in predicting the flow behaviour of shear-thinning fluids between the shear-thinning and infinite shear rate regions is the Sisko Model (Figure 2.3 and Equation 2.12). The Sisko model is basically the Power Law with a constant,

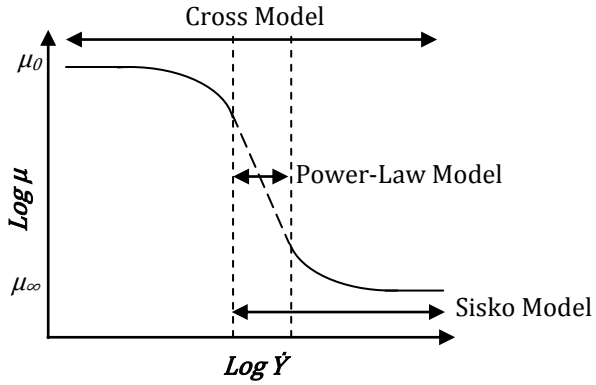

Figure 2.3: Flow curve description using mathematical models

$$\frac{\mu-\mu_\infty}{\mu_0-\mu_\infty} = \frac{1}{1+(K.\dot{\gamma})^m} \qquad 2.11$$

$$\mu = \mu_\infty + k.\dot{\gamma}^{n-1} \qquad 2.12$$

μ_∞ (infinite viscosity), added to it to incorporate the asymptotic viscosity value, at high shear rates, the Power law section of the curve in Figure 2.3 transitions into.

In the Cross equation (equation 2.11), K is a time constant (with time units) and m is a dimensionless rate constant (Barnes, 2000; Rheology School, no date). The reciprocal of the time constant, K, represents a critical shear rate at which shear thinning commences (Rheology School, no date) while m measures the degree of shear-thinning on a scale of 0 to 1 (Barnes, 2000). μ is viscosity at any shear rate $(\dot{\gamma})$, μ_0 is the zero shear rate viscosity at very low shear rates and $\mu_\infty$is the infinite viscosity at very high shear rates. When the

value of m is 0, the fluid behaviour is Newtonian, and as m departs from 0 and approaches 1, the fluid behaviour becomes increasingly shear thinning (Barnes, 2000). In the Sisko equation μ and μ_0 are same as in the Cross equation (equation 2.11), while k and n are same as in the Power law equation (equation 2.4).

Barnes (2000) suggested an approach to analyse a set of shear stress-shear rate data for a particular shear thinning fluid in order to determine which model best fits its flow behaviour. This involves plotting the data in log scales and employing the appropriate model depending on the data's curve fit to the model curve identity as shown in Figure 2.3.

2.3 VISCOSITY MEASUREMENT

Viscosity measurements are carried out using either a viscometer or rheometer. Although both terms may be used interchangeably, a viscometer is used purely for viscosity measurements in fluids, while a rheometer also measures viscoelastic properties of material (Steffe, 1996; Schramm, 2000). Since the research focus is purely on viscosity measurement, further reference will be made only to viscometers.

2.3.1 Types of viscometers

2.3.1.1 Conventional viscometers

These refer to the commercial type, precision made, viscometers, otherwise known as absolute viscometers (Schramm, 2000). Absolute viscometers have well defined design characteristics and test boundary conditions, which enable them to be calibrated to directly

calculate viscosity in standard units using mathematical formula, whose components- force, deformation (displacement) and time scale- are measured (Schramm, 2000). Design characteristics define ideal, standard, geometries between which samples are deformed in the viscometer (Schramm, 2000, pp.13-14). The boundary conditions specify the test requirements which include (Schramm, 2000, pp.30-33):

- Deformation must be steady state,
- Deformation must be within the laminar flow regime,
- Test sample must be homogeneous and
- No slipping between measuring geometries and test sample

a) Rotational viscometer

There are 3 types of rotational viscometers, characterised by the relative geometry of the shearing members. They include:

i) coaxial or concentric cylinder (cup-and-bob) viscometers,

ii) cone and plate viscometers, and

iii) parallel or flat plate viscometers

In the above geometries, the outer cylinder, in the case of the coaxial viscometer, and lower plates, for the cone and plate and parallel plate viscometer, are usually fixed while their complementary inner cylinder and top plates are rotated by a motor about a fixed axis.

These may be operated either in controlled stress mode or controlled rate mode (Steffe, 1996; Barnes, 2000; Schramm, 2000). In the controlled stress mode, the shear stress (converted from torque) is defined and the resultant shear rate

(converted from angular velocity) measured. It has the benefit of being able to measure very small shear rates, in the order of 10^{-8} rad/s or approximately 1 revolution in 2 years (Barnes, 2000), and thus useful for creep and yield stress measurements (Steffe, 1996). In the controlled rate mode, shear stress (torque) is measured instead by defining shear rate (angular velocity).

An important design requirement for these groups of viscometers is a narrow shearing gap between geometries to enable them maintain and extract a constant shear rate between shearing surfaces (Chhabra and Richardson, 1999). Thus they require small sample volumes to carry out measurements and have a compact design which are benefits of these types of viscometers (Fisher et al., 2007). Other benefits include operation simplicity and availability of inherent analytical tools (Fisher et al., 2007).

However, they are unsuitable for most non-Newtonian fluids, which unlike Newtonian fluids usually contain particles with diameters larger than the recommended one-tenth of the gap size (Chhabra and Richardson, 1999). They are also expensive.

As suggested above, shear stress (τ) and shear rate ($\dot{Y}$) values are determined from the directly measurable machine quantities of torque (M) and angular velocity (ω) using a pair of conversion factors, z_1 (shear stress conversion factor) and z_2 (shear rate conversion factor). Conversion equations are shown in equations 2.13 and 2.14, and the shear stress and shear rate conversion geometries are shown in Table 2.3 below.

$$\tau = M * z_1 \qquad 2.13$$

$$\dot{\gamma} = \omega * z_2 \qquad 2.14$$

Table 2.3: Conventional viscometer geometries and their conversion factors

Geometry	z_1 (shear stress conversion factor)	z_2 (shear rate conversion factor)
Coaxial cylinder	$\frac{1}{2.\pi.R^2.H.(CF)}$	$\frac{2.R_i^2.R_o^2}{R^2(R_o^2 - R_i^2)}$
Cone and plate	$\frac{3}{2.\pi.R_c^3.}$	$\frac{1}{\alpha}$
Flat plate	$\frac{2}{\pi.R_p^3}$	$\frac{R_p}{d}$

Where: Coaxial cylinder

$R = \frac{R_i + R_o}{2}$; $R_i = radius\ of\ outer\ cylinder$; $R_o = radius\ of\ inner\ cylinder$;

$H = inner\ cylinder\ height$; $CF = torque\ correction\ factor$

Cone and plate

$R_c = cone\ radius$; $\alpha = cone\ angle$

Flat plate

$R_p^3 = plate\ radius$; $d = gap\ height$

Shear stress values must be corrected for shear thinning or shear thickening fluids ($n \neq 1$) by applying Weissenberg's correction factor as follows:

$$\tau_c = \tau.\left(\frac{3+n}{4}\right)$$

Where τ_c = corrected shear stress

b) Vane viscometers

As the name suggests, these viscometers make use of vane impellers as internal members in the coaxial cylinder geometric configuration for rotational viscometers. For this reason, they are comparable to the bob-and-cup viscometer and its formulas given in equations 2.15 – 2.17. However, in contrast to the bob impeller,

vane impellers are preferred for use with complex liquids or solutions such as suspensions and emulsions characterised by the presence of a yield stress (Barnes and Carnali, 1990; Fisher et al., 2007). Minimum structural alteration resulting in less time-dependent shear thinning (thixotropy) during the introduction of the impeller into the medium to be sheared, reduction in measurement error due to large particle sizes in liquid medium and slip reduction between the impeller and medium interface are benefits of the vane over bob impellers (Barnes and Carnali, 1990; Fisher et al., 2007).

Vane viscometers may be of two types; the vane-in-cup viscometer or the bucket viscometer. The vane-in-cup viscometer was studied by (Barnes and Carnali, 1990) to evaluate their use for carrying out rheological measurements on Newtonian fluids and non-Newtonian fluids with power law characteristics in comparison to the bob-and-cup. They found that the integrity of viscosity measurements obtained from the vane improved as the power law index, n, fell and became comparable to viscosity measurements performed using the bob-in-cup at $n < 0.5$. Viscosity measurements carried out on a 4.8 Pas Newtonian fluid using the vane returned a value of 2.9 Pas. This error was attributed to the development of non-circular fluid streamlines within the vane thus leading to fluid interaction between the sample volumes on either side of the circumference defined by the vane radius. This produced fluctuations in the stress measurements around the vane blade edges which yielded a lower viscosity when averaged. In the case of power law fluids with $n < 0.5$, the vane geometry approximates a bob of identical radius and height as it rotates as a solid cylinder with the fluid within the circumference defined by

the vane radius. This was conversely attributed to the formation of circular streamlines within the circumscribed fluid volume. They however found the vane was better suited for determining the flow curve of non-Newtonian fluids that exhibit yield stress characteristics in which a rapid complete decay in viscosity was observed eventually resulting in a permanent state of slip between the impeller and sample. In the vane, the viscosity decay is delayed for the same fluid and shear condition, occurring at a higher stress value.

Shear stress formula

$$\tau = \frac{M}{2\pi R_i^2 H} \tag{2.15}$$

Shear rate formula (Newtonian)

$$\dot{\gamma} = \frac{2\Omega}{1-\varepsilon^2} \tag{2.16}$$

Shear rate formula (non-Newtonian)

$$\dot{\gamma} = \frac{2\Omega}{n(1-\varepsilon^{\frac{2}{n}})} \tag{2.17}$$

Correction factor, C.F., applied to Newtonian shear rate formula to obtain non-Newtonian shear rate formula

$$C.F. = \frac{1-\varepsilon^2}{n(1-\varepsilon^{\frac{2}{n}})}$$

Note: $\varepsilon = \frac{R_i}{R_o}$

Furthermore, the stress profile in the annular gap is more consistent with the vane compared to the bob, which shows a marginal but constant decline in the stress values between its surface and that of the cup. They however found the vane produced a more complete flow curve in the low shear rate region, thus highlighting the transition from the zero-shear viscosity region to the shear thinning region. In the bob-and-cup, an abrupt termination of the flow curve was reported within the zero-shear viscosity region, which coincides with low shear rates, and was re-established in the shear thinning phase at higher shear rates. The flow curve not only revealed a missing transition region but also a shear thinning region with a lower than expected slope. They ascribed this observation to the breakdown of the layer at the immediate vicinity of the bob, resulting in a rapid decay in viscosity before the transition region was reached. This low shear rate viscosity decay continued in tandem with increasing shear rate but also showed time dependency and eventually resulted in complete viscosity decay and a permanent state of slip between the bob and sample. The vane also showed the same decay in viscosity leading to the permanent state of slip experienced with the bob but occurred at higher shear rate as indicated earlier.

The vane-in-bucket viscometer, otherwise known as the vane in an infinite medium, was also proposed, by (Fisher et al., 2007), for determining the flow curves for of complex liquids or solutions that appear to exhibit yield stress characteristics and have large particles, which can lead to erroneous results in conventional rotational viscometers. It is characterised by the shearing container having a radius that sufficiently exceeds the radius that coincides with the yield stress of the sample (R_y)

and demarcates a sheared region from an unsheared region. Thus the boundary condition is given by equation 2.18 and R_y can be determined by substituting the yield stress value of the sample into the shear stress equation (equation 2.15), and is related to the yield stress as shown in equation 2.19. The shear rate of the vane impeller can be determined using equation 2.20 derived by (Krieger and Maron, 1952). Like its precursor, the vane-in-cup rheometer discussed above, it replaces the bob impeller (the inner solid cylinder) with a vane impeller. Unlike the vane-in-cup, however, it is not restricted to shear thinning fluids that have a power-law or flow index, n, which is not more than 0.5. Its low-to-medium shear rate, flow curves were shown to complement flow curves obtained from the medium to high shear rate capillary rheometer. Wall slip effects were also not experienced, unlike in the vane-in-cup rheometer, and yield stress calculation easily carried out.

$$\tau_1 > \tau_y > \tau_2 \qquad 2.18$$

$$\frac{\tau_1}{\tau_y} = \frac{R_y^2}{R^2} \qquad 2.19$$

$$\dot{\gamma} = \frac{2\Omega}{n} \qquad 2.20$$

Where: τ_1= shear stress at the vane boundary; τ_2 = shear stress at the container wall; τ_y = yield stress; R_y = yield stress radius; R = vane radius; Ω = angular velocity; $n\ (power\ law\ index) = \frac{d(log\Omega)}{d(logM)}$

c) Capillary (Tube) viscometer

Also referred to as pipe viscometers, these refer to the high pressure viscometers comprising of a fixed barrel (reservoir) with a high length-to-diameter ratio slit or

capillary die, at least 30 (Schramm, 2000), at the end through which a loaded test sample is pushed out of by an overhead variable speed piston. Capillary viscometers can be operated in a controlled stress mode or controlled rate mode (Steffe, 1996; Barnes, 2000; Schramm, 2000).

Shear stress in capillary viscometers is determined by measuring the pressure drop (ΔP) that occurs between the die entry and exit, as a result of the flow resistance of the test sample, with the aid of pressure transducers as shown in in equation 2.21. Shear rate is determined using equation 2.22 from the flow rate (Q) which is a function of speed of piston through the barrel.

They are widely used in the process industry, particularly the polymer industry where high shear rates (up to 10^8 s^{-1}) are required (Chhabra and Richardson, 1999; Schramm, 2000; Malvern Instruments, 2006). Examples of processes that require high shear rates include extrusion, pumping, brushing, roller coating, reverse gravure and spraying (Malvern Instruments, 2006).

For capillary dies

$$\tau_w = \frac{\Delta P.R}{2.L} \qquad 2.21$$

$$\dot{\gamma}_{w,c} = \frac{4.Q}{\pi.R^3} * \frac{(3.n+1)}{4.n} \qquad 2.22$$

$$\mu_c = \frac{\tau_w}{\dot{\gamma}_{w,c}} \qquad 2.23$$

For slit dies

$$\tau_w = \frac{\Delta P h}{2L} \quad 2.24$$

$$\dot{\gamma}_{w,c} = \frac{6.Q}{w.h^2} . \frac{(2n+1)}{3n} \quad 2.25$$

Where: τ_w = shear stress at pipe wall; ΔP = Pressure drop across capillary die; $\dot{\gamma}_{w,c}$ = corrected shear rate; R = die radius; L = length of long die; μ_c = corrected shear viscosity; n = power law index (n =1 for Newtonian fluids); h = slit thickness; w = slit width.

A limitation to the use of capillary viscometers is that they are ideally suitable for measuring time-independent, Newtonian behaviour. This is because non-Newtonian liquids experience a nonlinear decrease in shear rate between the capillary wall and centre while the corresponding shear stress is time dependent as the sample volume decreases (Macosko, 1994). In their use with high molecular weight polymers, particularly polyethylene, with narrow molecular weight distributions an anomaly known as the stick-slip effect is also experienced at critical shear stress (τ_c) which results in a discontinuity in the flow curve in the form of a shear rate jump and a corresponding sudden drop in viscosity (Bagley et al., 1958; Metzger et al., 1963; Blyler and Hart, 1970; Kataoka and Ueda, 1971; Rudin and Chang, 1978; Drda and Wang, 1995; Wang and Drda, 1996b). This sudden drop in viscosity has been attributed to the unravelling of entanglement of polymer chains at the capillary wall/polymer melt interface relative to the bulk polymer melt and show dependencies on molecular weight and temperature (Brochard and Degennes, 1992; Drda and Wang, 1995; Wang and Drda, 1996b). In terms of temperature, this sudden drop in viscosity, which is otherwise quantified as extrapolated length (ℓ_e),

is quantitatively independent but qualitatively dependent (Wang and Drda, 1996b). That is to say the magnitude of ℓ_e remains the same but occurs at a higher critical stress as temperature increases. Below a certain critical temperature, however, the ℓ_e was observed to decrease as temperature increased up to this critical temperature albeit for lower molecular weight (Wang and Drda, 1996a). Molecular weight on the other hand, was shown to have an increasing effect on ℓ_e while having a reducing effect on τ_c (Wang and Drda, 1996a; b).

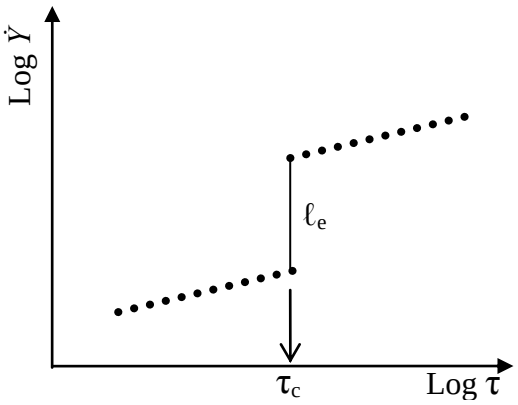

Figure 2.4: Stick-slip effect in a polymer flow curve

Heat runaway is also a problem as some of the energy applied in shearing is converted to heat energy making temperature control difficult (Steffe, 1996; Schramm, 2000). End effect artefacts are also experienced with non-Newtonian liquids as can be observed from the equations above (2.22 and 2.25), which have to be corrected due to viscoelastic properties associated with these fluids. It is wasteful as samples, which are significantly large in volume compared to the rotational methods discussed above, are used exhaustively per run (Schramm, 2000; Fisher et al., 2007).

2.3.1.2 Mixer viscometers

Mixer viscometers are suitable when time dependency, slip, particle size and particle settling may otherwise be a problem (Steffe, 1996). They involve basic mixing configurations of an impeller and a vessel, calibrated to extract viscosity data during mixing. Mixing refers to homogenisation of a mixture of two or more different materials through agitation. The degree of mixing is a balance between inertial forces imparted on the mixture by the impeller and the mixture's viscous forces. The impeller type used is determined by the viscosity of the fluid; axial and radial type impellers for low viscosity fluids, close clearance, anchor type impellers for viscous fluids, and screw or helical ribbon impellers for very viscous fluids (Holland and Chapman, 1966; Shah, 1991; Steffe, 1996).

A technique for calibrating mixer viscometers was developed by Metzner and Otto (1957). The Metzner-Otto calibration method (Metzner and Otto, 1957), makes use of Newtonian and non-Newtonian, power law calibration fluids of known viscosity characteristics and densities, and Reynolds number values of not more than 10 (Holland and Bragg, 1995; Steffe, 1996). It relies on established dimensionless numbers, Reynolds number and Power number correlation (equations 2.26 – 2.28) that link power input by an impeller in generating a mixing torque, to rotational speed and viscosity. This correlation describes the geometry of the mixing system.

$$Re.Po = C_{SF} \qquad 2.26$$

$$Re = \frac{\rho N D_i^2}{\mu} \qquad 2.27$$

$$Po = \frac{P}{\rho N^3 D_i^5} = \frac{2\pi MN}{\rho N^3 D_i^5} \qquad 2.28$$

Where: Re is Reynolds number for stirred tanks; Po is Power number; C_{SF} is shape factor of mixing system; ρ is density of calibration fluid (kg/m^3); N is impeller rotational speed (rps); D_i is impeller diameter (m); μ is viscosity of calibration fluid (Pas); P is Power (W); M is torque (Nm)

The calibration process fundamentally involves determining two geometric constants for a mixing system; the shape factor using the Newtonian calibration fluid and a dimensionless shear rate conversion factor using the non-Newtonian calibration fluid. These two constants can enable the direct conversion of torque and rotational speed readings to viscosity and shear rate values. The following steps were prescribed by Metzner and Otto (1957).

1. Torque readings from a mixing system charged with the Newtonian calibration fluid is recorded at pre-defined rotational speeds, calculating Po and Re accordingly using equations 2.27 and 2.28 above
2. A log-log plot of the Po and Re values determined above is produced

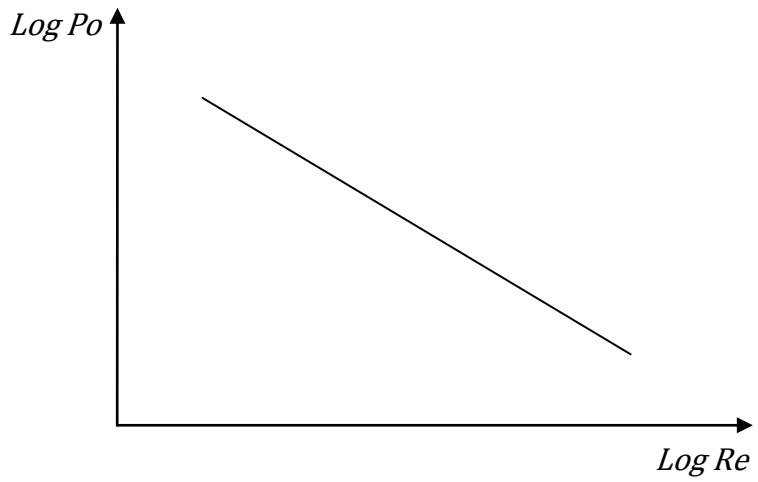

Figure 2.5: Power curve from Newtonian calibration fluid

3. Next, the non-Newtonian calibration fluid is used to generate another set of Po values in the mixer system, at the pre-defined rotational speeds used in step 1 for the Newtonian calibration fluid, and their corresponding Re values determined from the power curve developed above (Figure 2.5).
4. Using equation 2.27 and Re values obtained in step 3, the apparent viscosities of the power law calibration fluid of known density is determined at each of the predefined rotational speeds.
5. The shear rate functions of the apparent viscosities determined above for the non-Newtonian power-law calibration fluid of known characteristics (k and n), at the various rotational speeds, is found graphically or by using equation 2.4b.
6. A plot of shear rate against rotational speed at each viscosity point is produced (Figure 2.6) and a dimensionless shear rate conversion factor, k' determined from the slope.

$$\dot{\gamma} = k'N \qquad 2.29$$

The shape factor of the mixing system, C_{SP}, can be determined from the power curve. C_{SF} is the antilog value of $log\ Po$ when $log\ Re$ is 1 according the logarithmic form of equation 2.20 given below.

$$logPo = (-1)logRe + logC_{SF} \qquad 2.30$$

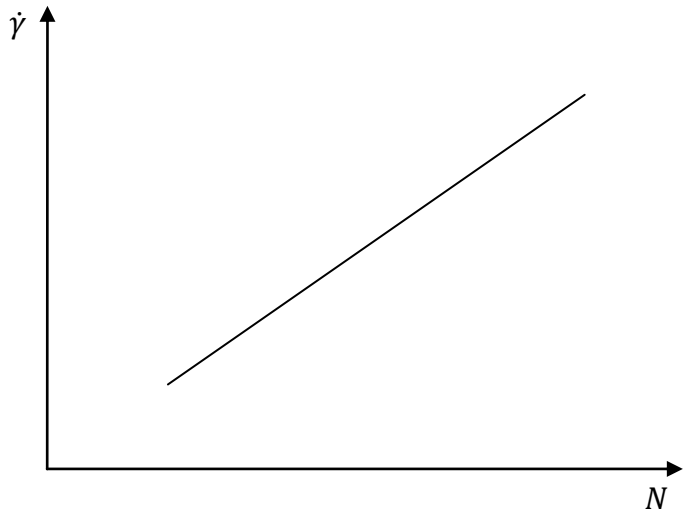

Figure 2.6: Plot of shear rate against rotational speed

2.4 VELOCITY PROFILE CALCULATION AND ITS IMPLICATIONS ON GAS-LIQUID PHASE CONTACTING/MIXING

Fluid flow behaviour through a channel or over a surface is characterised by the fluid properties, the geometry of the surface which it is flowing over, and the velocity of flow (Douglas et al., 2005). This fluid flow behaviour is normally represented by a velocity profile which is a plot of the radial velocity of the fluid elements along a profile.

Velocity profiles are normally classified as either laminar flow or turbulent flow (Coulson et al., 1999). Laminar flow is generally characterised by parallel streams or layers of fluid elements that are devoid of lateral interaction with each other. Thus the perpendicular component of the axial velocity is absent and normally takes place at low flow rates. With turbulent flow, which occurs at high flow rates, oscillation of the streams or layers of the

fluid elements are present and disintegrate into eddies (as the layers become obstacles to each other) causing dispersions across the cross-section of the channel.

Velocity profiles are made up of two major sections; the bulk or main flow and the boundary layer (Coulson et al., 1999; Douglas et al., 2005; Hauke, 2008). In bulk flow, the fluid elements flow at a uniform velocity and as a result, velocity gradient can be considered not to exist. In the boundary layer, which is the region next to the channel surface, a diminishing velocity gradient develops perpendicular to the direction of flow, from the surface to the channel axis. Hence, the velocity changes from zero at the surface to the free stream value away from the surface. However as flow continues across the channel surface, the boundary layer grows until it reaches maximum thickness which is limited in the case of a circular channel by its radius. Thus, in a fully developed pipe flow, the boundary layer thickness encompasses the pipe cross-section to form the dominant flow. The boundary layer, which always starts off as laminar can remain the same through development or transform into turbulent boundary layer (Figure 2.7). This however depends on the Reynolds number at the end of the entry length, given in equation 2.31, with the transition Reynolds number believed to be between 2000 and 4000 (Coulson et al., 1999). Reynolds number can also be calculated using equation 2.32, the Metzner and Reeds Reynolds number, otherwise known as the generalised Reynolds number (Coulson et al., 1999) which incorporates a correction for non-Newtonian fluids and reduces to

$$Re = \frac{Du\rho}{\mu} \qquad 2.31$$

Where: Re = Entry length Reynolds number; D = Pipe diameter; u= Mean velocity; ρ = Density; μ = Fluid viscosity.

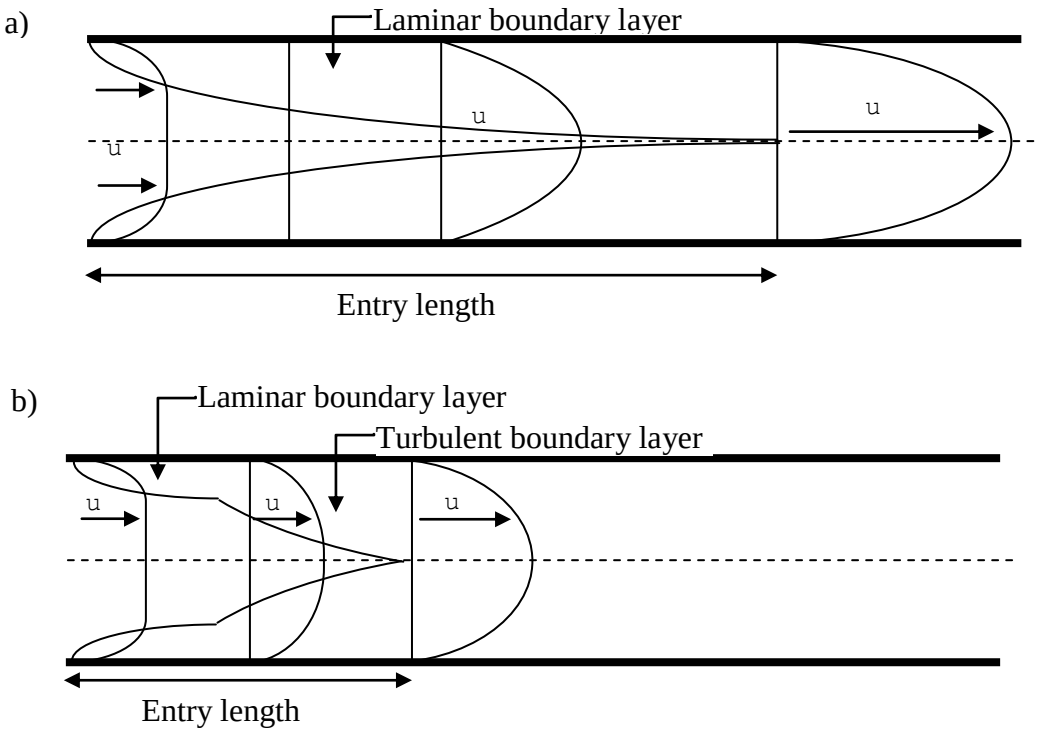

Figure 2.7: Development of a fully developed: a) laminar boundary layer; b) turbulent boundary layer (adapted from Douglas et al., 2005)

equation 2.31 when n = 1 for Newtonian fluids.

$$Re_{MR} = \frac{4n}{3n+1} . \frac{Du\rho}{\mu_a} \qquad 2.32$$

Where: n = flow behaviour index

The velocity profile, particularly the boundary layer, is important in flow kinematics as it affects heat and mass transfer, and is required in estimating power requirement from a pump (Holland and Bragg, 1995; Chhabra and Richardson, 1999; Coulson et al., 1999; Hauke, 2008). For polymer melts, laminar flow is expected being non-Newtonian fluids which generally have very high viscosities (Chhabra and Richardson, 1999).

The velocity profile of polymer melts flowing through a circular channel can be estimated with the equations 2.33 and 2.34 below (Agassant, 1991; Coulson et al., 1999; Bird et al., 2007):

$$u_x \approx u_{CL}\left[1-\left(\frac{s}{r}\right)^{\frac{n+1}{n}}\right] \quad 2.33$$

and

$$u_{CL} \approx u\left[\frac{1+3n}{1+n}\right] \quad 2.34$$

Where: u_x = Velocity of polymer melt at radial positions, s; u_{CL} = Velocity of polymer melt at pipe axis; u = Mean velocity of polymer melt; r = Radius of circular channel; n = characteristic flow index of polymer melt.

The effect of viscosity on velocity profile can be illustrated by comparing the velocity profiles of a power law fluid model which is dictated by the variation of n. As viscosity falls, velocity profile transposes to a parabolic flow from a plug-like one as illustrated by Brydson (1999), and Holland and Bragg (1995) and shown in Figure 2.8 below.

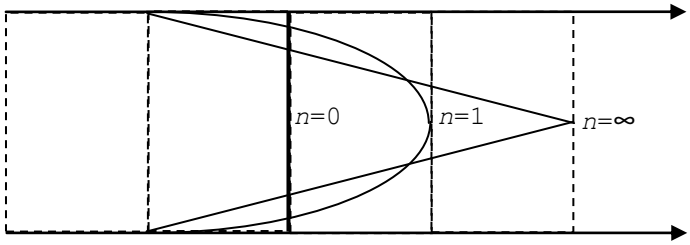

Figure 2.8: Effect of viscosity on velocity profile

2.5 COMPARISON WITH PETROLEUM HYDROCRACKING FEEDS

Comparable viscosities for heavy petroleum feedstocks are scarce as most measurements in the petroleum industry are done at reservoir temperature and normally given in kinematic viscosity units, usually centistokes. In situ process viscosity measurement is considered expensive and thus predicted using correlations (Miadonye et al., 1994). Viscosity measurements thus rarely exist for temperatures above 100^{o}C and vary quite widely due to variation in composition and their multiphase nature as noted by Bazyleva et al. (2010) in their review of literature. Moreover characteristics are strongly influenced by the origin of the petroleum fraction, its geological background, pre-production treatment and the method used (Bazyleva et al., 2010). However, Brandrup (1996) indicated pumpable viscosities for petroleum feedstocks to be between 0.2 and 0.5 Pas at ~200^{o}C.

Viscosities of heavy oils range between 0.01 and 10000 Pas (Hinkle and Batzle, 2006; Ancheyta and Speight, 2007) and in this case includes bituminous sands (also known as tar or oil sands) which are not recoverable in their natural form by conventional oil production methods. Athabasca oil sands viscosity has been quoted to be greater than 10^3 Pas at around 15^{o}C (Dusseault, 2001) and is one of the heaviest naturally occurring petroleum resource. Bazyleva et al. (2010) showed the effect of temperature on the viscosity of Athabasca bitumen at various shear rates using different methods of viscosity measurement from a compilation of studies. The viscosity of Athabasca bitumen reduced to around 0.001 - 0.01 Pas, at around 200^{o}C and shear rates of up to 2300s^{-1}, from 10,000 – 1,000,000 Pas. Miadonye et al. (1994) had earlier studied the effect of temperature on

viscosity of different Alberta bitumen. Their analysis of various Alberta bitumens revealed viscosity reduced to values in the order of 10^{-1} Pas at temperatures below 100^{o}C by 2 orders of magnitude from 30 ^{o}C. Aminu et al. (2004) also reported viscosities of 30 – 50 Pas for Athabasca Vacuum residue between 400 and 530^{o}C. This however increased from extrapolated, unreacted value of between 0.001 – 0.002 Pas and was attributed to volatisation of light ends and polymerisation of liquid components leading to coke formation during thermal cracking. Brauch et al. (1996) determined the viscosities of samples of vacuum residue feeds for visbreaking, the mild thermal cracking of vacuum or atmospheric residue feeds into lighter products (Fahim et al, 2010), which ranged between 0.19 Pas and 2.36 Pas at 100^{o}C. This yielded distillates with reduced viscosities, 0.05 – 0.27 Pas, at 100^{o}C. In another study by Fainberg et al. (1996), a tar residue product of a visbroken vacuum residue sample of viscosity of about 0.3 Pas at 100^{o}C, was subjected to further visbreaking which reduced its viscosity from approximately 3.15 Pas to 0.35 Pas. In both studies by Aminu et al (2004) and Bazyleva et al. (2010) studies, viscosity values of unreacted, preproduction samples are below the recommended maximum viscosity specification specified by Brandrup (1996)

2.6 CO-PROCESSING OF PLASTICS WITH SOLVENTS AND PETROLEUM FRACTION

Co-processing plastics with liquid co-feeds in thermal-, catalysed-, and hydro- cracking processes have been undertaken typically with the aim of influencing or investigating the mixture’s product yield or their composition selectivity (Karaduman et al., 2002; Serrano

et al., 2007). Two options are involved; either by altering the decomposition pathway of polymers, or through the interaction or synergy of the decomposition intermediates.

The first option involves using mainly organic hydrogen-donor solvents, such as 9,10-dihydroanthracene, tetralin, diphenylamine, decalin and 1-methylnaphthalene (in descending order of hydrogen donating potential), as well as phenol, 2-naphtol, n-pentane, cyclohexane and toluene, to aid the saturation of olefin primary decomposition products in the case of PS and styrene derivative polymers (Sato et al., 1990; Murakata et al., 1993; Matsumoto, 2001; Karaduman et al., 2002). Hydrogen donor solvents have also been used in the solvent co-pyrolysis of HDPE to increase the yields of C_5–C_{32} α-olefins (Serrano et al., 2007). In a preceding study carried out by this group (Aguado et al., 2006b), involving the co-pyrolysis of HDPE and decalin (solvent), they observed substantial improvements in the yield of the target $C_5 - C_{20}$ hydrocarbon group as solvent mass fraction was increased (solvent mass fractions used; 0.59, 0.67, 0.77 and 0.91). General improvement in the yields of the $C_1 - C_4$ and $C_{21} - C_{32}$ hydrocarbon groups was also observed in the pyrolysis of the different mixtures of HDPE and decalin with reference to solvent-free pyrolysis of HDPE. This was attributed to the mitigation of the heat and mass transfer limitations experienced in the chemical recycling of plastics, which also had an influence improving selectivity for the $C_5 - C_{20}$ hydrocarbon group.

The ability to achieve saturation in the case of the primary olefinic decomposition products of polystyrene into saturated products was observed to increase with hydrogen donor capacity, in contrast to conversion (Sato et al., 1990; Murakata et al., 1993). Thus in the paper by Sato et al. (1990), 2-naphthol achieved the highest conversion followed by

phenol, with 9, l0-Dihydroanthracene achieving the least conversion. A similar observation was made with the $C_5 - C_{32}$ α-olefins products of HDPE/solvent co-pyrolysis, which increased in decreasing order of solvent hydrogen donating ability (Serrano et al., 2007). In both cases however, the improved heat and mass transfer effect from solvent co-processing of the polymers concerned, in contrast to processing without solvent, was observed in the higher liquid and overall yield, as in Karaduman et al. (2002), and higher gas yields with HDPE in the work by Serrano et al. (2007). Karaduman et al. (2002) co-pyrolysed polystyrene with 3 distinct types of hydrocarbon solvents, viz.: n-pentane (aliphatic), cyclohexane (cyclic) and toluene (aromatic). They observed between 76 and 91% increase in liquid yields, compared to the pyrolysis of the pure PS, which corresponded with considerable reductions to the solid residue, from ~30% to less than 5%, to give an overall increase in conversion (gas and liquid products only) of around 40%.

The second option has involved using refinery feeds in catalysed and non-catalysed thermal co-processing of plastics. Ng (1995) for instance catalytically cracked VGO with 5% and 10% HDPE content and observed an increase in overall conversion with decreasing HDPE content, although product distribution was different. While only hydrocarbon gases and coke was the product in the VGO containing 5% HDPE, at 10% HDPE content, the yield of gasoline range hydrocarbons increased substantially to more than 50%. This was attributed to an increase in the quantity of HDPE in relation to catalyst which curtailed the excessive cracking of gasoline formed in the 5% blend. Ng (1995) also noted that the amount of plastic incorporated in the VGO FCC feed could cause flow problems if “too much” due to associated viscosity increases. Arandes et al. (2003a) in their work undertook the catalytic cracking of a blends of PP-LCO (5% PP) and LDPE-

LCO (10% LDPE) over a mesoporous silica catalyst to alleviate the heat transfer limitations and defluidisation problem associated with treating plastics in fluidised bed reactors. They observed benefits in co-pyrolysis of both blends over the individual types of materials. The quality of gasoline stock produced from the blends was of higher quality compared to the LCO; it contained substantially less aromatic hydrocarbons and improved naphthalene, olefins, paraffins and isoparaffins content due to the high reactivity of the radicals from PP and LDPE cracking and their hydrogenation in the process. On the other hand, gasoline (C_5 - C_{12}) range hydrocarbons produced from the catalytic pyrolysis of blends improved compared to the individual plastics and was attributed to improved heat transfer and thus lower cracking activation energy for the blends. Arandes et al. (2003b) also undertook a similar study using PS and polystyrene-butadiene (PS-BD) instead and also alluded to the improvement of heat and mass transfer and thus product selectivity. They reported higher conversions and yields of C_5 - C_{12} range of hydrocarbons as a direct result of the presence of PS and PS-BD in the mixture, relative to LCO in their respective catalytic cracking products. High contents of aromatics however characterised the gasoline range liquid products of both mixtures, mainly composed of styrene. They compared the amount of styrene yield in the PS/LCO mixture at 550 ^{o}C to the yield from the direct pyrolysis of PS, which was similar but the coke, benzene and methane, which are all undesirable, were lower in PS/LCO mixture making it amenable to monomer recovery.

Marcilla et al. (2007) also used VGO with blends of 5, 25 and 75 wt% LDPE, thermally cracked in a fluidised bed reactor at 500 ^{o}C, alluding to the heat transfer problems associated with chemical recycling of plastics. Overall conversion improved from 80 to 99% as the fraction of LDPE in the blend fell from 100 to 5%, which could be indicative of

the influence of the VGO on the heat transfer limitation of plastics. They reported increasing gas products (both dry gas and LPG) yield as the LDPE fraction increased, with a corresponding decrease in liquid and solid product yields. The content of aromatics fell with LDPE addition while a-olefins dominated in the 3 LDPE/VGO blends, with C_{10} - C_{31} n-paraffins showing varying amounts.

Serrano et al. (2003) carried out the catalytic and thermal cracking of LDPE and lubricating oil base mixtures (40/60 - 70/30 wt%) in a screw kiln reactor (with two operating temperature zones, T_1/T_2). The screw kiln reactor and lubricating oil were respectively being tested as an alternative continuous reactor and a viscosity reducing solvent, due to limitations in the recycling of the high viscosity plastics. Catalytic cracking was carried out on just the 70/30 wt % blend. They revealed a significant reduction in the viscosity of the plastic was achieved citing the influence of the lubricating oil base admixture. This was reflected in an increase in throughput up to 244.4 g/h, from ~40 g/h achieved in both thermal and catalytic cracking, as the proportion of lubricating base oil in the mixture increased. They noted the effect of the lubricating oil on the thermal cracking intensity on LDPE, suggesting its reduction and a corresponding reduction in residence time with increasing lubricating oil ratio. This was evidenced by its higher selectivity for the heavier end of lubricating base oil range hydrocarbons (C_{30} - C_{40}) in the product (carbon number) distribution for the 40/60 wt% LDPE/lubrication base oil blend in contrast to the 70/30 wt% LDPE/lubricating base oil blend and pure LDPE. They however did experience a drawback in the use of lubricating base oil as a solvent in catalylic cracking. The presence of lubricating oil resulted in low conversion rates (29.6 and 1.3%) for the catalysts used (Al-MCM-41(1) and Al-MCM-41(3)) at T_1/T_2 temperatures of

400/450 ^{o}C in contrast to the conversions, 40.7 and 80.4%, respectively, achieved for pure LDPE by the same catalysts. Conversion did however improve to 85% or more at higher T_1/T_2 temperatures of 450/500 ^{o}C in blends, which led them to suggest catalyst poisoning by the organic sulphur and nitrogen and weak acid site activity in the first instance, both alleviated by increase in the reactor operating temperature.

The work done by Marcilla et al. (2008) looked at the viscosity characteristics of LDPE and VGO blends, containing 0, 2.5, 5, 7.5 and 10% LDPE, between 60 and 160 ^{o}C. The test temperatures represent operational temperatures in a Fluid Catalytic Cracking unit as regards operations such as fluid transport through pipes and atomization, and choice of associated equipment such as pumps and mixers. In all the blends tested, they observed a Newtonian shear response to shear rate at higher temperature (100-160 ^{o}C) but a non-Newtonian, shear thinning response at the lower temperatures of 60 and 80 ^{o}C, which became more and more pronounced at lower shear rates and as the blend concentration of LDPE increased. They also showed the effects of temperature and LDPE content, at constant LDPE concentration and shear rate, respectively, on viscosity. While viscosity decreased with increase in temperature at constant LDPE concentration, it increased exponentially as the LDPE content in the LDPE-VGO blend increased at constant shear rate (500 s^{-1}). The decrease in viscosity observed as temperature was increased became more significant in the blends containing higher LDPE concentrations. A departure from non-Newtonian, shear thinning behaviour towards Newtonian flow was also observed to accompany the decrease in viscosity as temperature was increased in viscosity-shear rate curves for individual blend (e.g. 2.5/97.5 wt% LDPE/VGO). The constant shear rate of 500 s^{-1} used during the analysis of the effect of LDPE content of the blend on the viscosity

behaviour is significant because it is a characteristic shear rate at which pipe flow and fuel atomisation is achieved . In the same work by Marcilla et al. (2008), the integration of the VGO into the LDPE matrix through blending had a plasticising effect on LDPE, with the plasticising effect increasing with proportion of VGO in the blend. The plasticising effect manifested in reductions in DSC melting peak temperatures and areas, from the values for 100% LDPE towards 100% VGO values, as the blend content of VGO increased from 90% to 97.5%. They attributed these manifestations to the unravelling of the polymer molecular entanglements and a shift of the relaxation time spectrum (shortening of the average elastic recovery time for the chain molecules).

3 RESEARCH AIMS AND OBJECTIVES

Having reviewed the current state of waste management with respect to waste plastics, an attempt has been made to highlight the importance of feedstock recycling methods. Hydrocracking has however been shown to have clear benefits over other feedstock recycling methods for mixed waste plastics. It possesses heteroatom removal capability due to the presence of hydrogen which improves the quality of its fuel and ameliorates equipment corrosion compared to pyrolysis and catalytic cracking (Aguado and Serrano, 1999; Buekens, 2006; Butler et al., 2011; Garforth et al. 2004; Scherzer and Gruia, 1996; Walendziewski and Steininger, 2001; Xingzhong, 2006; Yanik and Karayildirim, 2006; Zadgaonkar, 2006). Catalyst conservation is also enhanced as a result in contrast to catalytic cracking (Scherzer and Gruia, 1996). Hydrocracking also has a lower process temperature in relation to the other feedstock recycling methods (Walendziewski and Steininger, 2001; Garforth et al., 2004; Butler et al., 2011). Hydrocracking of mixed waste plastics offers the best feedstock recycling option for producing a syncrude rich in gasoline range hydrocarbons for producing transportation fuel and feedstock chemicals. However several limitations present themselves.

The hydrocracking process involves reactants which exist in three different phases; gas phase hydrogen, liquid phase polymer melts and solid phase catalysts; and requires contact at a molecular level between these three phases. In other words, hydrogen mass transfer into the polymer melt has to take place, both of which have to migrate to the catalyst active sites for hydrocracking to take place.

Mass transfer has however been acknowledged to be viscosity dependent and reduces with increasing viscosity in the various works cited in the literature review (Aguado et al., 2006b; Arandes et al., 2003a; Arandes et al., 2003b; Marcilla et al., 2007; Ng, 1995; Sato et al., 1990; Serrano et al., 2003; Serrano et al., 2007). As a consequence, secondary reactions that may produce undesirable products such as coke are promoted (Grause et al., 2011; Yanik and Karayildirim, 2006). In a similar manner, the high viscosity of plastics has a deleterious effect on heat transfer (Arandes et al., 2003a; Arandes et al., 2003b; Bremner et al., 1990; Murakata et al., 1993; Sato et al., 1990; Shyichuk, 1996) and thus makes viscosity an important parameter in the hydrocracking process.

Viscosity of plastics is characteristically high and has been highlighted to cause problems in the transportation of plastic melts within the refinery, especially in their introduction into refinery units or rectors (Ali and Siddiqui, 2006; Arandes et al., 1997; Butler et al., 2011; Marcilla et al., 2008; Serrano et al., 2003; Walendziewski, 2006), and in designing catalytic cracking units (Aguado et al., 2006a). However their absolute values at the hydrocracking process temperature are unknown.

The main aim of this research is to carry out a rheological characterisation of individual and mixed commodity plastics (PE, PP, PS and PET) as a step towards the conceptual design of a continuous process for the hydrocracking of mixed-plastics waste to produce liquid fuels.

The specific objectives were as follows:

I. Determination of the rheological properties and behaviour of polymer melts which include shear viscosity and velocity profile behaviour

II. Investigate methods to reduce the expected high viscosities for polymer melts. Treatment using volatile products of mixed plastics hydrocracking as sacrificial solvents will be the main focus but other solvents will be considered

III. Coupling and calibrating a sealed, agitated, reaction vessel for larger scale solvent treatment and in situ viscosity estimation

4 EXPERIMENTS AND METHODS

4.1 Experimental procedure

Five plastic types were acquired for testing: high-density polyethylene (HDPE), linear low-density polyethylene (LLDPE), polypropylene (PP), polystyrene (PS) and polyethylene terephthalate (PET). All the plastic types were commercial grade polymer pellets except PET which was prepared from post-consumer plastic bottles. The polymer resins were provided as follows:

- HDPE (BL2571), LLDPE (Borstar FB2230) and PP (Borclean HC300BF) were sourced from Borealis.
- PS (PS1540) was sourced from TOTAL Petrochemicals.
- PET was sourced from a PET bottle recycling bin situated by the Jackson Mill building at the University of Manchester.

4.2 Preparation of samples

The HDPE, LLDPE, PP and PS pellets were used as sourced; they were 4-5mm in diameter and 3mm thick. The PET was chipped in an industrial grinder to approximately 5mm particle size and then heated in a vacuum oven for 18hrs at 120^{o}C to eliminate moisture absorbed during service use.

4.3 Experiments

4.3.1 Viscosity measurement

A Rosand RH7 twin-bore rheometer was used to carry out tests on the plastics/polymer samples. A cross-section of the rheometer is shown in figure 4.1. The twin-bore rheometer, as the name implies, comprises two 15mm diameter bores in a 280mm long barrel with dies situated at the bottom of the bores. Situated above the dies are pressure transducers which measure the pressure drop along the dies. The bore in the right hand-side of the barrel enables the determination of corrected shear viscosity measurements by the use of a die of zero length (orifice die), relative to the die of the left hand-side bore (capillary die). The zero-length die accounts for pressure induced by die entry and exit pressure drop (P_0) contained within the pressure reading from the transducer in left hand-side (P_L). This correction is known as Bagley's correction on apparent shear stress (Brydson, 1981; Cogswell, 1981) as shown in equation 4.1.

$$\tau_c = \frac{(P_L - P_0)r}{2L} \tag{4.1}$$

$$\mu_c = \frac{\tau_c}{\dot{\gamma}} \tag{4.2}$$

Where: $\tau_c =$ corrected shear stress; $P_L =$ Pressure drop across capillary die; $P_0 =$ Pressure drop across orifice die; $\dot{\gamma} =$ shear rate; $r =$ die radius; $L =$ length of long die; $\mu_c =$ corrected shear viscosity.

The rheometer was setup by attaching the pistons and the appropriate die to both bores and defining the test shear rates and temperature parameters. For the shear rate, minimum and maximum values of 20 and 5000 s^{-1} were chosen with a sequential, stepwise, logarithmic

increases and decreases between them. This was preceded by 2 pre-sequence compression steps to achieve thermal and density consistency. The temperature was set to be uniform across all the heating zones, i.e. A, B and C shown in Figure 4.1. Once the rheometer attained set temperature, the bores were charged with plastics/polymer test samples. As the test samples were pellets, the bore was filled piecemeal with intermittent tamping using a tamping device provided to expel as much air as possible within the pellets. Further compression of the test sample is achieved to ensure complete expulsion of air during the

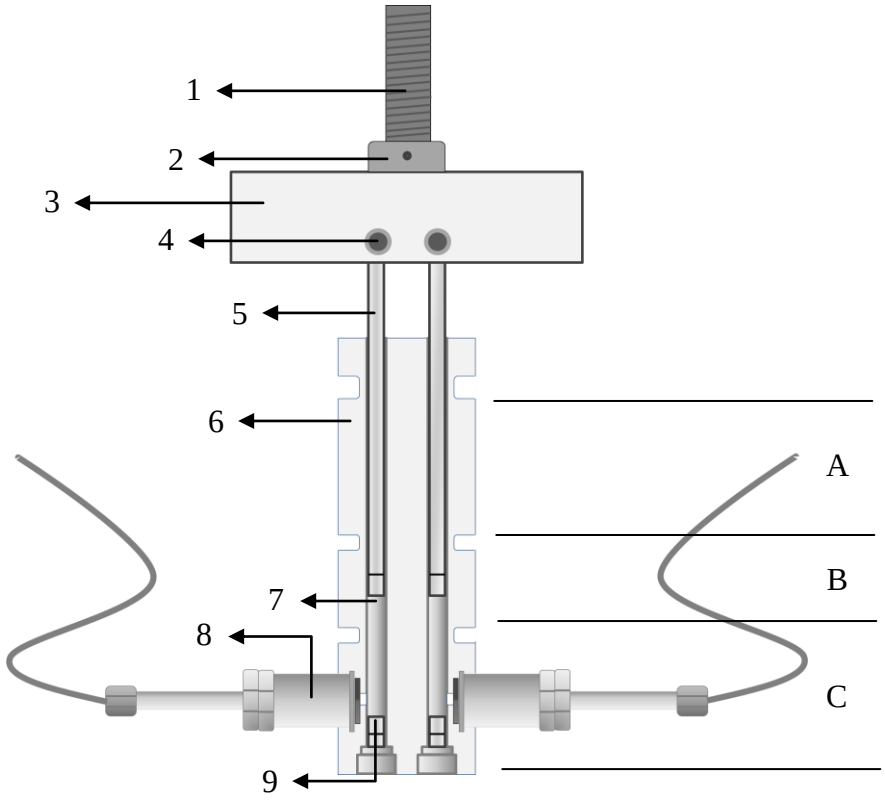

Figure 4.1: Rosand RH-7 barrel parts

Where: 1. Lead screw; 2. Force transducer; 3. Crosshead; 4. Piston retention pin; 5. Piston; 6. Barrel; 7. Bores; 8. Pressure Transducers; 9. Die. A. Top heating zone; B. Mid heating zone; C. die heating zone;

run by reattaching the pistons to the crosshead and driving it down slowly until contact is made with the top of the polymer and a pressure reading of about 1MPa was registered (Malvern Instruments, 2006)

Tests were run at 200 and 250^{o}C for HDPE, LLDPE, PP and PS; and at 300^{o}C for PET. Rheological data including corrected shear stress, corrected viscosity and power-law index were measured and logged real time.

4.4 SOLVENT TREATMENT

A 12-station reaction carousel, comprising a heated base and a water-cooled top half (Figure 4.2), was used to reflux 5 volatile hydrocarbon solvents namely iso-octane (iC_8), n-decane (nC_{10}), n-tetradecane(nC_{14}), n-pentadecane (nC_{15}) and n-hexadecane (nC_{16}) in 24mm-diameter test-tubes containing HDPE pellets. This was done to investigate these hydrocarbon solvents, constituents of the product slate of mixed-plastics hydrocracking, as possible sacrificial solvents for reducing the high viscosity of plastics/polymer melts.

Sample mixtures of HDPE resins (0.5g) and hydrocarbon solvents were prepared in the following ratios- 20:80, 30:70, 40:60, 50:50, 60:40, 70:30 and 80:20; and heated, under reflux, to temperatures around the boiling point of the solvents (Perry et al., 2008) for 24 hrs. The solvent boiling temperatures are as follows:

Iso-octane – 99.3^{o}C

n-decane - 174^{o}C

n-tetradecane – 252.5°C

n-pentadecane – 270.5°C

n-hexadecane – 287.5°C

a)

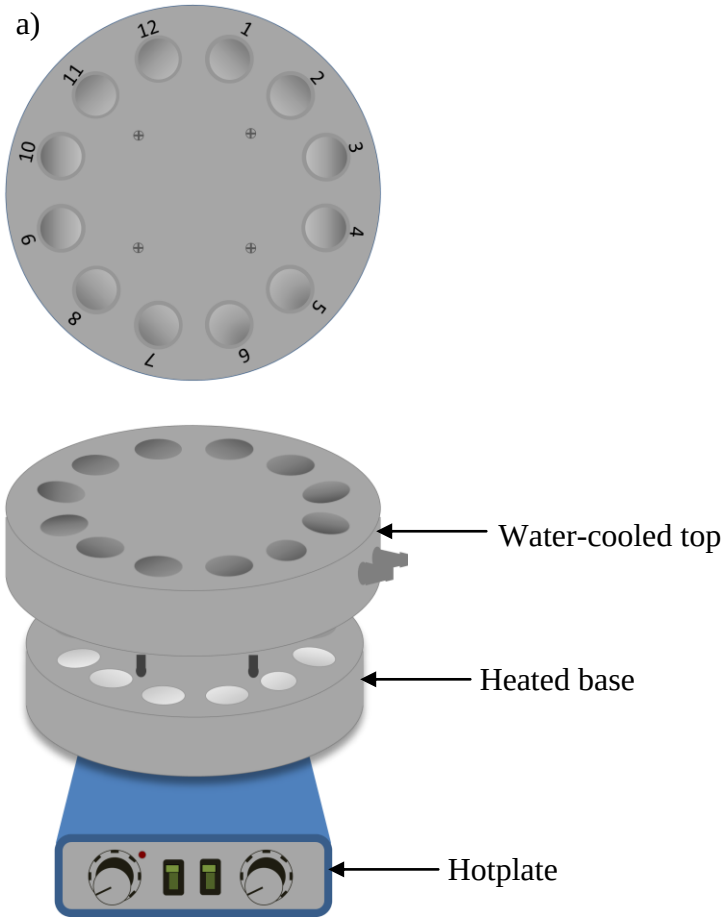

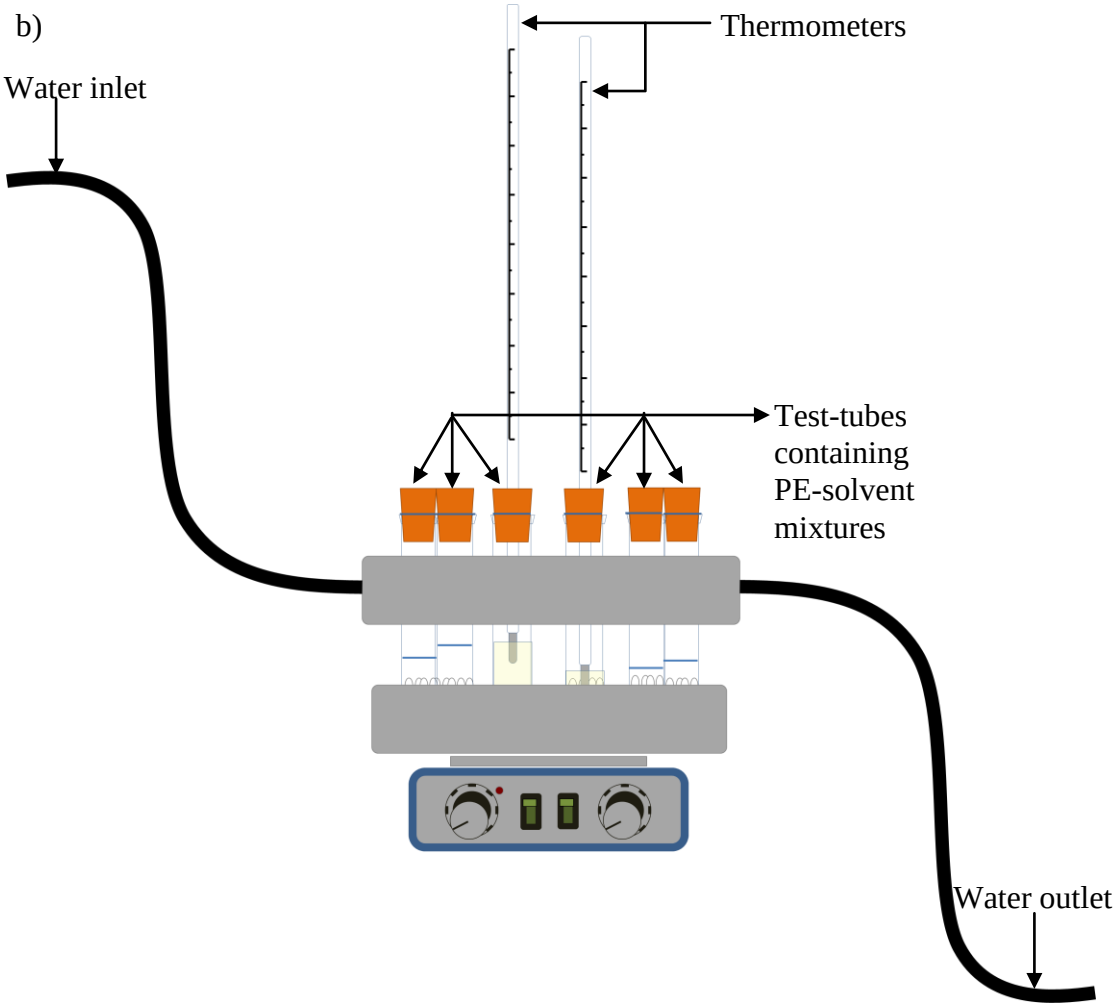

Figure 4.2: 12-station reaction carousel: a) Apparatus; b) Experimental setup

The weight of HDPE used was carefully chosen to maximize thermal contact and heat transfer between the hollow test-tube slots in heated base of the reaction carousel and the samples. In other words, the equivalent height of the HDPE in the test-tube was below the brim of the heated slots.

A thermal analysis of the product at the end was carried out using a differential scanning calorimeter (DSC) and thermogravimetric analyser (TGA)

4.4.1 Differential scanning calorimetry (DSC) measurements and results analysis

Differential scanning calorimetry (DSC) was used to measure the melting temperatures; extrapolated onset temperature (T_e) and the peak maximum temperature (T_m), for the PE-solvent mixtures as illustrated in Figure 4.3.

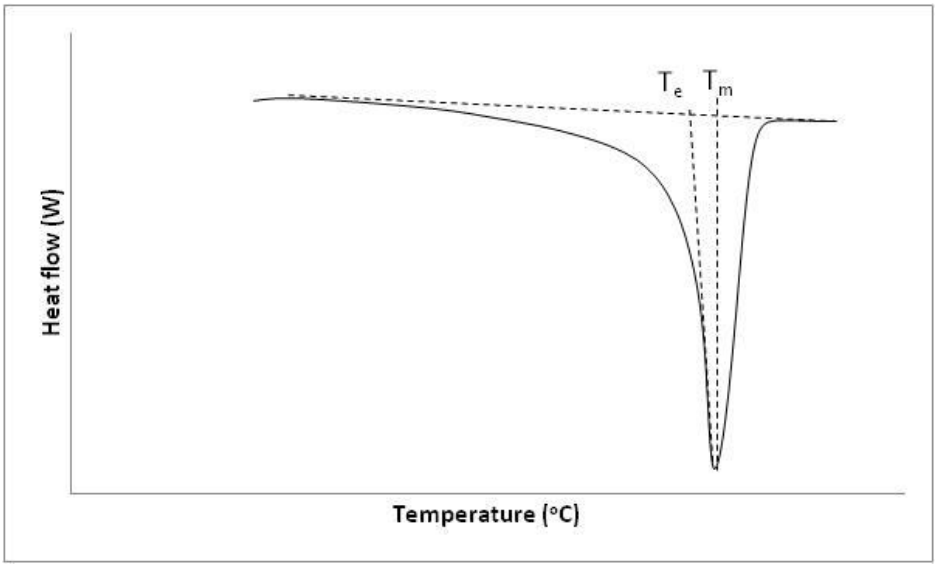

Figure 4.3: Melting peak (endotherm) showing extrapolated onset and peak maximum temperatures

DSC is a thermal analysis technique that measures the difference between the change of the rate of heating of a sample and a reference substance which occur during thermal transitions with respect to temperature (or time) during a defined temperature programme (Crompton, 1993; Laye, 2002; Hohne et al., 2003; Menczel et al., 2009). During melting, an endothermic process, the energy absorbed during this first order phase transition results in a deviation from the otherwise steady state heat flow rate differential between the sample and the reference. The heat flow rate signal thus produces a peak as shown in Figure 4.3 above. The extrapolated onset temperature is the point of intersection between

tangents drawn between the steady state heat flow rate signals on either sides of the peak (baseline) and the steepest edge of the of the descending peak (Laye, 2002; Hohne et al., 2003). The peak maximum temperature refers to the temperature signal that corresponds with point at which the difference between peak heat flow rate signals and the baseline is highest (Hohne et al., 2003).

A TA Instruments, DSC-Q100 and a Mettler DSC 30 were used to perform the melting temperatures measurement. The temperature programme used is summarised in Table 4.1.

Table 4.1: DSC temperature programme

	Programme segment	**Segment details**
1	Equilibrate at 40^{o}C	Sample heated to and stabilised at 40^{o}C before next segment is started
2	Ramp at 10^{o}C/min to 60^{o}C	Sample heated from 40^{o}C to 60^{o}C at 10^{o}C/min
3	Isothermal at 60^{o}C for 60 mins	Sample held at 60^{o}C for 60 mins to evaporate loosely bound surface solvent
4	Ramp at 5^{o}C/min to 150^{o}C	Heating resumed from 60^{o}C to 150^{o}C at 5^{o}C/min
5	Isothermal at 150^{o}C for 30 mins	Sample held at 150^{o}C for 30 mins
6	Ramp 5^{o}C/min to 25^{o}C	Sample cooled from 150^{o}C to 25^{o}C at 5^{o}C/min

Test results were subjected to F-statistic test, at 95% confidence ($\alpha = 0.05$), to validate any observed solvent effect on T_e and T_m by proposing a null hypothesis that the data points have no significant linear trend with a slope of zero. Test equation is shown in equation 4.3 below.

$$F = \frac{variance\ in\ data\ points\ explained\ by\ linear\ model}{variance\ in\ data\ unexplained\ by\ linear\ model}$$

$$= \frac{regression\ sum\ of\ squares}{residual\ sum\ of\ squares} * \frac{denominator\ degrees\ of\ freedom}{numerator\ degrees\ of\ freedom}$$

$$= \frac{\left(\sum_{i=1}^{n}(\hat{y}_i - \bar{y})^2\right)}{\left(\sum_{i=1}^{n}(y_i - \hat{y}_i)^2\right)} * \frac{df_2}{df_1} \qquad 4.3$$

Where: y_i are the experimental dependent variable values; $\hat{y}_i$ are the fitted or estimated dependent variable determined from model parameters (slope and intercept); $\bar{y}$ is the average of dependent variable values; df_1 = K-1 (K is the total number of variables) and df_2 = n-K (n is the number of data points)

4.4.2 Thermogravimetric analysis (TGA) measurements and results analysis

TGA is a quantitative thermal analysis technique that measures the mass change of a sample with respect to temperature (or time) during a defined temperature programme and in an inert, oxidising or reducing atmosphere (Earnest, 1988; Crompton, 1993; Heal, 2002; Prime et al., 2009). The TGA of a sample produces a step change, where mass loss occurs, between plateaus of thermal stability, with the step changes indicating decomposition products of the starting material as shown in Figure 4.4, or the reaction product between starting material and its reaction atmosphere. Thus, it is used for compositional analysis among other analysis such as thermal and oxidative stability, and decomposition kinetics (De, 2010). Thermogravimetry has also been used for vapour pressure determination using standards of known vapour pressures (Elder, 1997; Price and Hawkins, 1998; Phang and Dollimore, 2001; Price, 2001; Chatterjee et al., 2002). The rate of mass loss with respect to temperature (or time), otherwise known as derivative thermogravimetry, is an additional

signal that produces reaction peaks representing the various mass loss regions of a decomposing sample as depicted in Figure 4.5. Thus it reveals the compositional makeup of the decomposing sample, and in addition also helps to distinguish two or more reactions not separated by plateaus in the TG plot during a step change (Heal, 2002; Prime et al., 2009; De, 2010).

The extrapolated onset temperature of decomposition (T_e) for each weight loss region of the various polymer-solvent mixtures as well as the peak maximum temperature (T_m) of their corresponding DTG peaks were measured and analysed. T_e was measured as the point of intersection between tangents on the constant mass plateau and the steepest edge of the of the step change separating two adjacent plateaus (Heal, 2002). The peak maximum

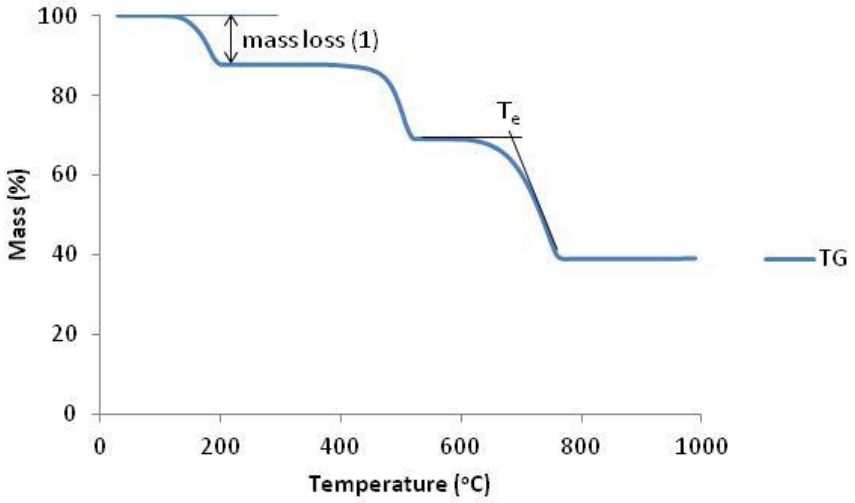

Figure 4.4: TGA curve showing mass loss regions and extrapolated onset temperature (T_e)

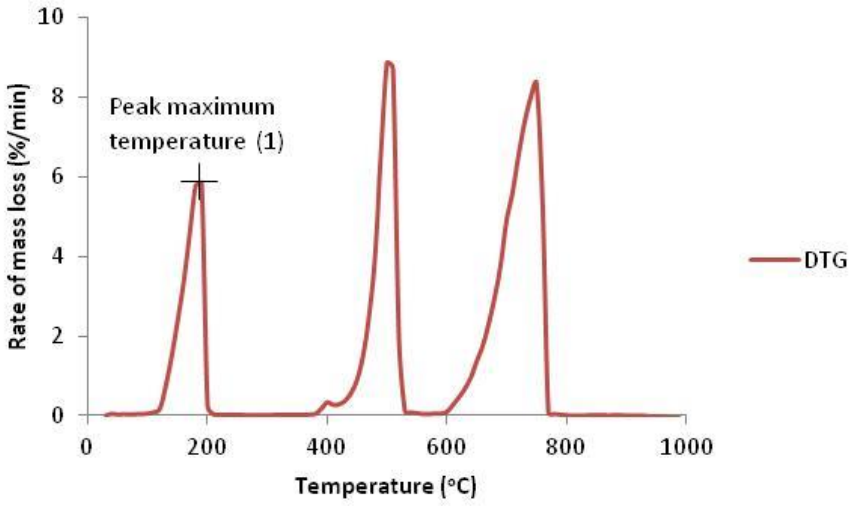

Figure 4.5: DTG peaks

temperature was measured in the same way as the DSC peak, i.e. the temperature signal that corresponds with point at which the difference between DTG peak signals and the baseline is highest.

A TA Instruments, TGA Q5000 was used to perform thermogravimetric analysis using the temperature programme presented in Table 4.2.

Test results were subjected to F-statistic test, at 95% confidence ($\alpha = 0.05$), to validate any observed solvent effect on T_e by proposing a null hypothesis that the data points have no significant linear trend with a slope of zero.

The DTG results of the thermogravimetric analysis were also used to determine vapour pressure from the decomposing samples. This was used as a means of testing for interaction between polymer and solvent by comparing the vapour of the solvents with those of the polymer-solvent samples.

Table 4.2: TGA temperature programme

	Programme segment	**Segment details**
1	Select gas 1	Gas 1, nitrogen, is selected as inert furnace atmosphere at a flow rate of 50mL/min for sample pyrolysis
2	Ramp at 10^{o}C/min to 60^{o}C	Sample heated from ambient temperature to 60^{o}C at 10^{o}C/min
3	Isothermal at 60^{o}C for 60 mins	Sample held at 60^{o}C for 60 mins to evaporate loosely bound surface solvent
4	Ramp at 5^{o}C/min to 500^{o}C	Heating resumed from 60^{o}C to 500^{o}C at 5^{o}C/min
5	Isothermal at 500^{o}C for 60 mins	Sample held at 500^{o}C for 60 mins to complete pyrolysis
6	Select gas 2	Gas 2, air, is selected as furnace atmosphere at a flow rate of 50mL/min to burn-off residue
7	Ramp 10^{o}C/min to 600^{o}C	Sample cooled from 150^{o}C to 25^{o}C at 5^{o}C/min
8	Isothermal at 600^{o}C for 30 mins	Sample held at 150^{o}C for 30 mins to complete residue combustion

Vapour pressures of evaporating or subliming species of known molar masses can be determined using a modified Langmuir equation (Price and Hawkins, 1998) for vaporisation taking place in a thermogravimetric analyser under the influence of a purge gas. The modified Langmuir equation is given below:

$$p = k_{vap} * v \qquad 4.4$$

Where: p = the vapour pressure, $k_{vap} = \frac{\sqrt{2\pi R}}{\alpha}$ and is the calibration constant for the TGA used, while $v = \frac{\delta m}{\delta t}\sqrt{\frac{T}{M}}$ and is the rate of volatilisation. For k_{vap}, R is the universal gas constant (8.314 J mol^{-1} K^{-1}) and α is the volatilisation coefficient; while for v, $\frac{\delta m}{\delta t}$ is the rate of mass loss per unit area (kg s^{-1} m^{-2}), T is absolute temperature (K) and M is molar mass (kg mol^{-1}).

Before k_{vap} for the thermogravimetric analyser can be derived, $\frac{\delta m}{\delta t}$ for calibration solvents of known vapour pressures (and Antoine equation parameters) and molar masses need to be obtained from their DTG data plots in order to generate p and v values. k_{vap} can then be determined by converting equation 4.4 into its log form as shown in equation 4.5 below (identical to the straight line equation, $y = mx + c$), and plotting $\log p$ against $\log v$ values of the calibration solvents and finding the antilog of $\log k_{vap}$, the intercept.

$$\log p = \log k_{vap} + \log v \qquad 4.5$$

Calibration solvents used to calibrate the Q5000 thermogravimetric analyser include tetradecane, pentadecane and hexadecane. Their vapour pressures were calculated using Antoine equation and coefficients given in equation 4.6 and Table 4.3, respectively:

$$P = 10^{\left(A-\left(\frac{B}{C+T}\right)\right)} \qquad 4.6$$

Where: P = vapour pressure in mmHg; T = temperature in Celsius; A, B, and C are the Antoine coefficients

Table 4.3: Antoine coefficients and application temperature range

Solvents	**A**	**B**	**C**	**T_{min} (^{o}C)**	**T_{max} (^{o}C)**
Tetradecane	7.26165	1914.86	183.519	5.86	419.25
Pentadecane	7.29987	1985.73	178.677	9.96	433.65
Hexadecane	7.36235	2094.08	180.407	18.19	447.45

4.5 COUPLING AND CALIBRATION OF THE CUSTOMISED SEALED-VESSEL IMPELLER VISCOMETER

A low budget sealed-vessel impeller viscometer comprising of a round-bottom flask, with a 5-socket, flat flanged lid and an overhead stirrer (Figure 4.6 and Figure 4.7) to be used in a heating mantle was assembled as shown in Figure 4.8 below.

The overhead stirrer was a Heidolph RZR 2102 control Z model with 2 operational rotational speed ranges; 4 - 106 rpm and 17 - 540 rpm, and torque display suitable for viscosities up to 350 Pas (Heidolph UK., 2010). The stirrer impeller was an 80mm, stainless steel VISCO JET® designed for low to high viscosity fluids.

Calibration was carried out using the Metzner-Otto calibration method described on pages 91 – 92 above. Silicone oils with viscosities of 9.1 Pas at 15^{o}C, 8.2 Pas at 20^{o}C, 5.9 and 7.3 Pas at 25^{o}C, and 4.9 Pas at 30^{o}C were used as Newtonian calibration liquids while 2% and 2.25% Carboxymethylcellulose (CMC) solutions were prepared for use as non-Newtonian calibration liquids. Viscosity and density characterisation of the calibration liquids were carried out using a Bohlin CVOR-200 rheometer and an Anton Paar DMA 45 density-meter, respectively. Calibration runs were also carried out with empty vessels to account for extraneous torque readings from the PTFE stirrer shaft guide and RODAVISS® connector fittings used to align the stirrer shaft with the central lid socket and create a sealed environment.

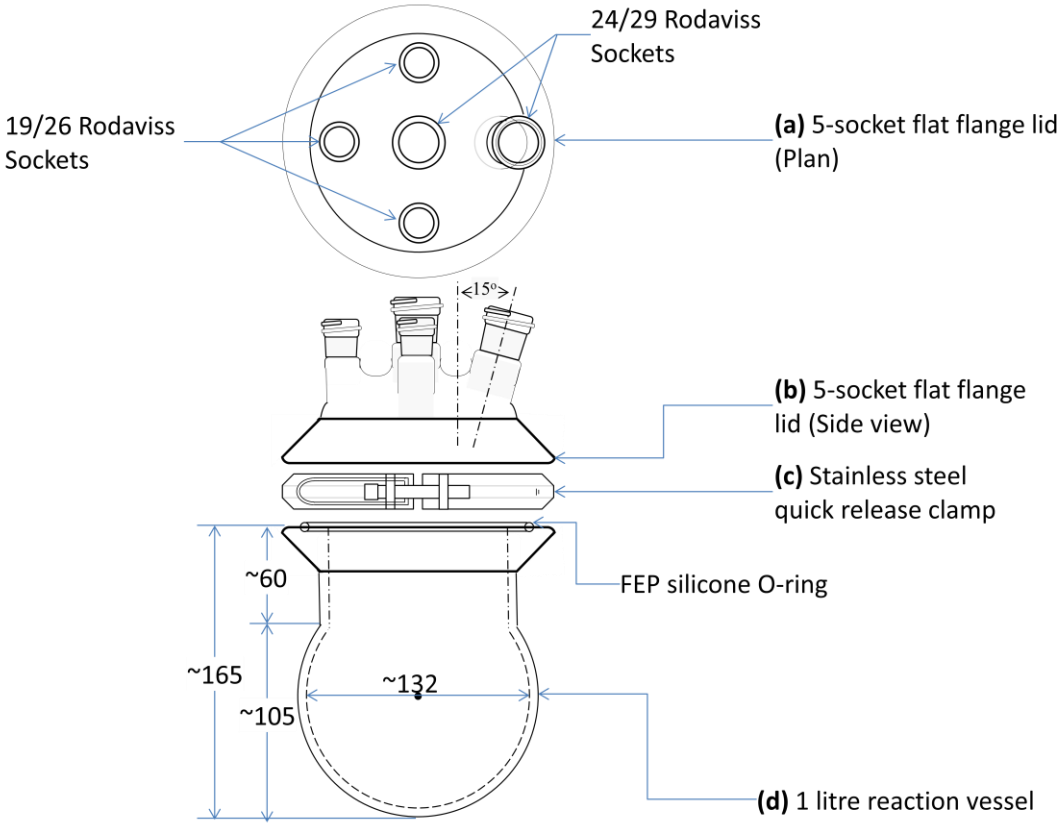

Figure 4.6: Reaction vessel (dimensions in mm)

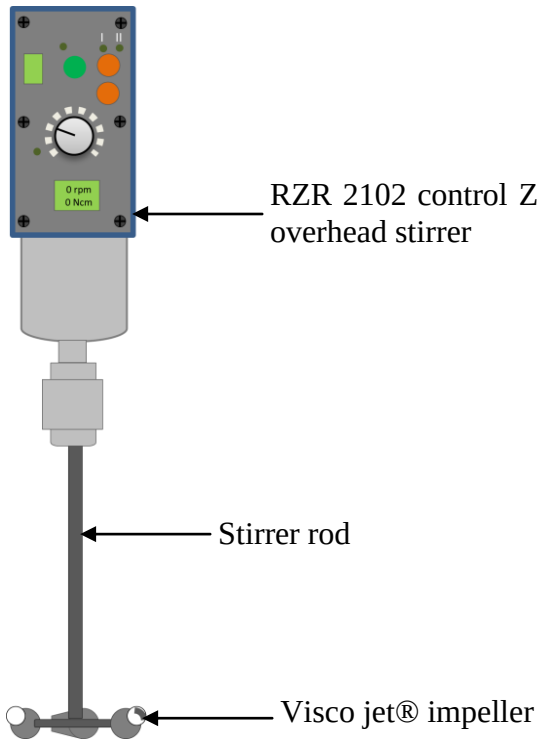

Figure 4.7: Overhead stirrer assembly

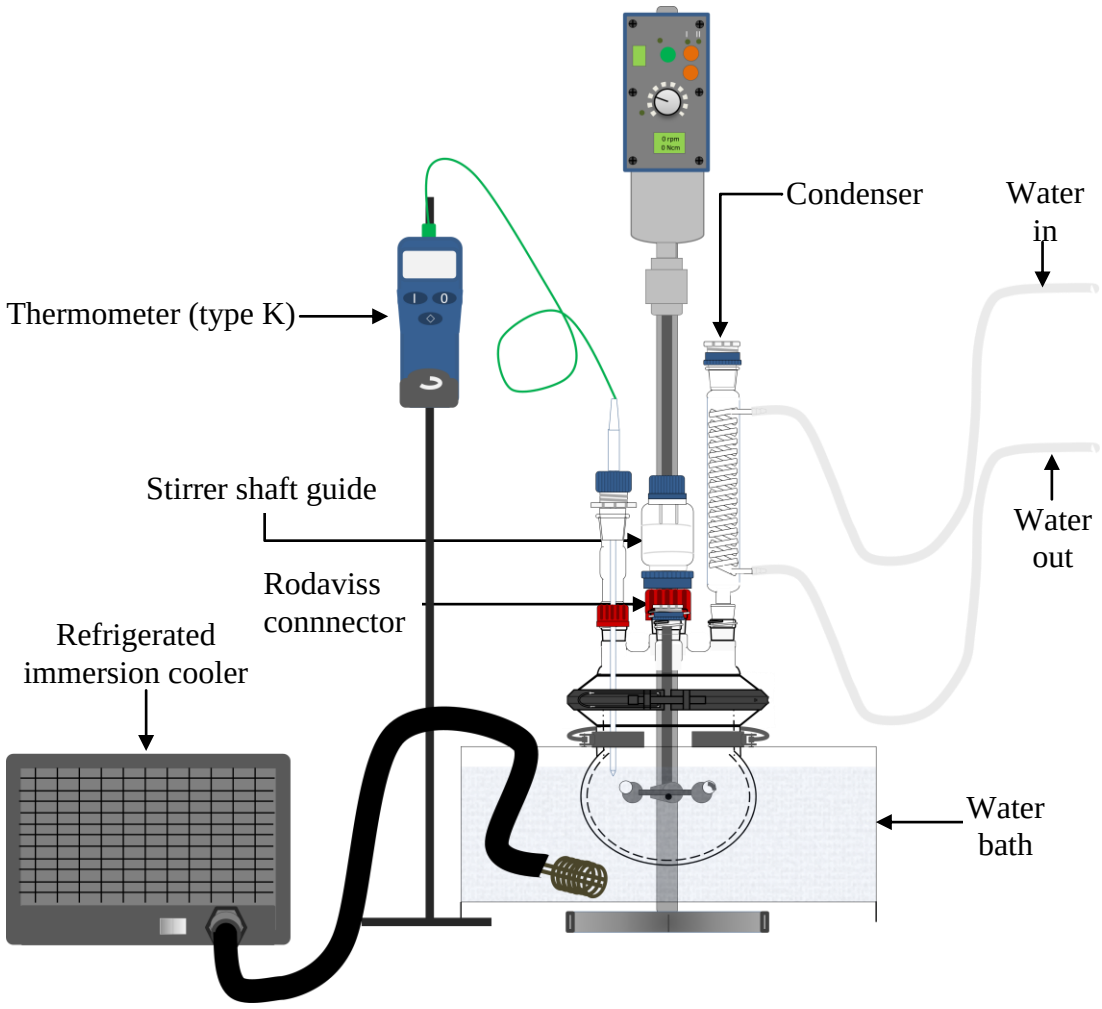

Figure 4.8: Customised sealed-vessel impeller viscometer

5 RESULTS AND DISCUSSION

5.1 VISCOSITY TESTS

Figure 5.1 (a, b and c) shows plots of the variation of shear stress with applied shear rate, otherwise known as the flow curve, of the HDPE, LLDPE, PP, PS and PET polymer melts. A clear distinction can be seen between HDPE and LLDPE on one hand, and PP and PS on the other hand. Polyethylene (HDPE and LLDPE) exhibited a considerably higher stress response to the induced shear rate in relation to the other resins. This shear response segregration can be largely attributed to the moleclar weights of the respective polymers which dictate polymer melt viscosity as earlier mentioned (page 74 - 75).

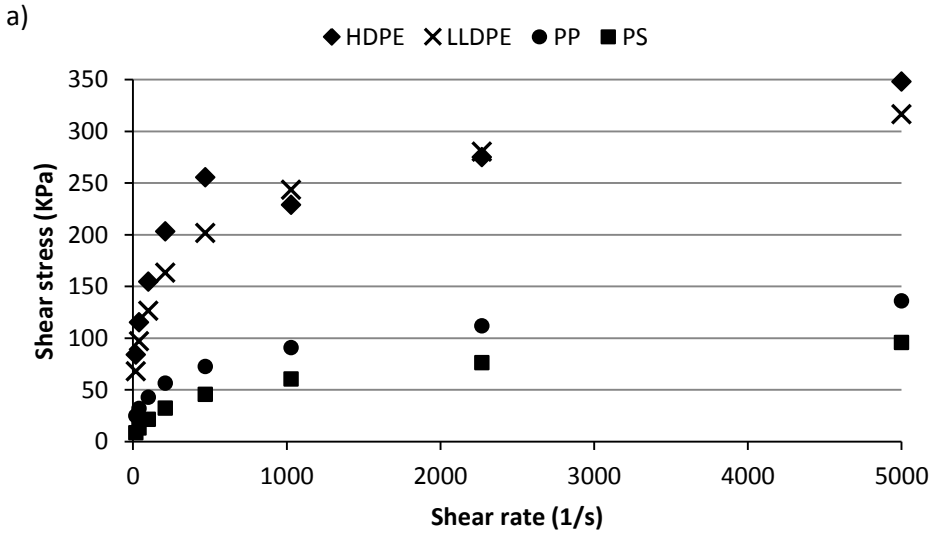

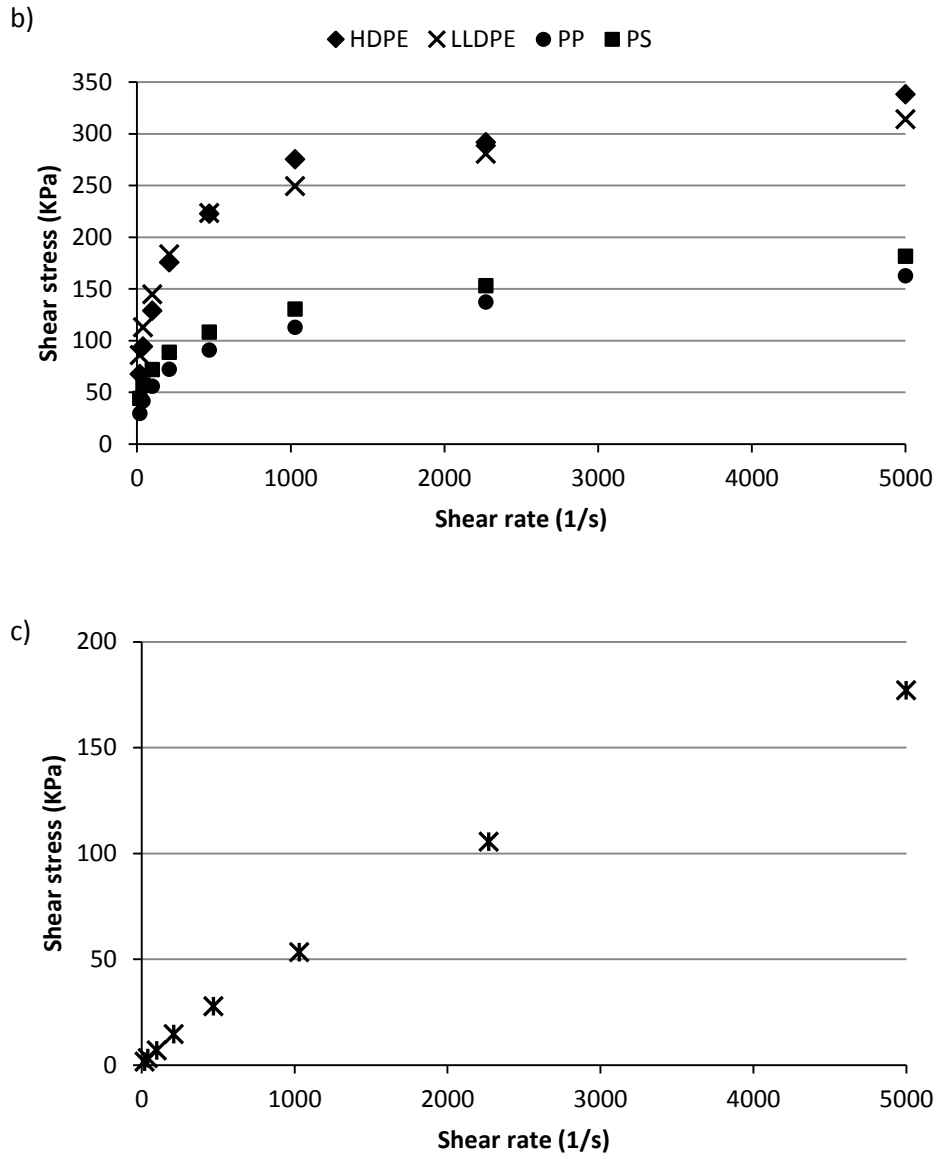

Figure 5.1: Shear stress vs shear rate curves HDPE, LLDPE, PP and PS: at- a) 200^{o}C and b) 250^{o}C; and c) PET at 300^{o}C

It can be observed from figure 5.1(a and b) that HDPE and LLDPE both have a steep flow curve, which levels off at higher shear rates compared to the other polymers. The kink observed in the HDPE flow curve at both 200 ^{o}C and 250 ^{o}C is a manifestation of the stick-slip effect common in high molecular weight polymers, particularly polyethylene (Bagley

et al., 1958; Metzger et al., 1963; Blyler and Hart, 1970; Kataoka and Ueda, 1971; Rudin and Chang, 1978; Drda and Wang, 1995; Wang and Drda, 1996b). This stick-slip effect results in a shear rate jump (or a sudden dip in viscosity) at a critical shear stress, as illustrated in Figure 2.4, is depicted for HDPE at 200 ^{o}C and 250 ^{o}C in Figure 5.2 below. This shear rate jump has been attributed to the unravelling of the chain entanglement of the polymer melt layer next to capillary surface relative to the polymer melt in the bulk flow (Brochard and Degennes, 1992; Drda and Wang, 1995; Wang and Drda, 1996b). It can also be seen that the difference between the flow curves at 200 and 250^{o}C for HDPE and LLDPE was marginal relative to the other polymers, especially at high shear rates(See Figure A.1 in appendices). This is because HDPE, LLDPE and PP are more sensitive to shear than temperature in contrast to PET, which is temperature sensitive, and PS which is both temperature and shear sensitive (Giles et al. 2005). PP did however show more sensitivity to temperature than the other shear sensitve polymers, as can be seen from Figure A.1c in the appendices. It appeared to be the least shear sensitive of the shear sensitive polymers judging by the shape of its flow curve which is more gentle in contrast

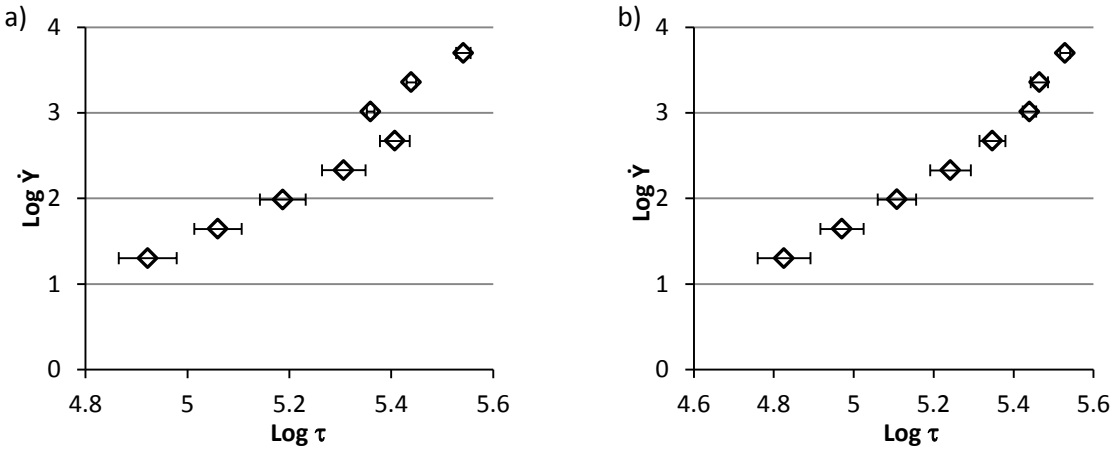

Figure 5.2: Stick-slip effect in HDPE at a) 200 ^{o}C and b) 250 ^{o}C

to HDPE and LLDPE (Figure A.1a and A.1b in the appendices).

From Figure 5.1, and as illustrated in Figure 2.2, the shear thinning behaviour of the polymers is evident within the range of shear rate employed as it can be clearly observed that the rate at which shear stress increases with shear rate decreased. This was confirmed by performing log-log plots of the shear rate-viscosity data as proposed by Barnes (2000) which showed a better fit to a quadratic model compared to a linear model according to both coefficient of determination and standard error of estimate (a measure of how well the model predicts the experimental data). This quadratic model highlights a deviation from the ideal shear-thinning behaviour (or power law model) which is akin to polymer melt behaviour over a wide range of shear rate (>20) as suggested by (Brydson, 1981) resulting in a power law index (n in equation 2.4) that decreases with shear rate. The deviation from linearity of logarithmic shear rate-viscosity data plots (Figure 5.3) also suggests a transition phase between the limiting zero shear rate region and the power law region as (Barnes, 2000) hinted. PET which was tested at 300^{o}C however could not be repeated due to the risk of equipment damage as PET quickly “caked” over the surfaces of the rheometer barrels and die making it difficult to clean.

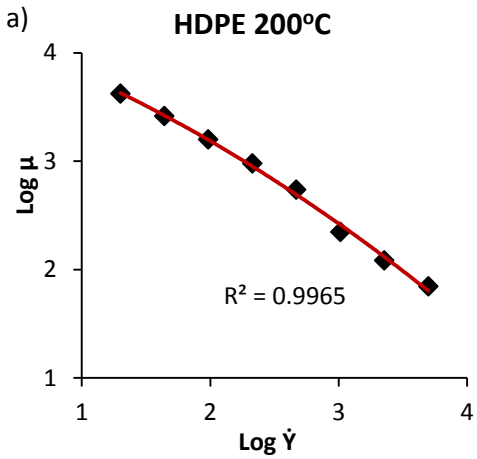
a)
HDPE 200ºC
Log μ
Log Ẏ
R² = 0.9965
1
2
3
4

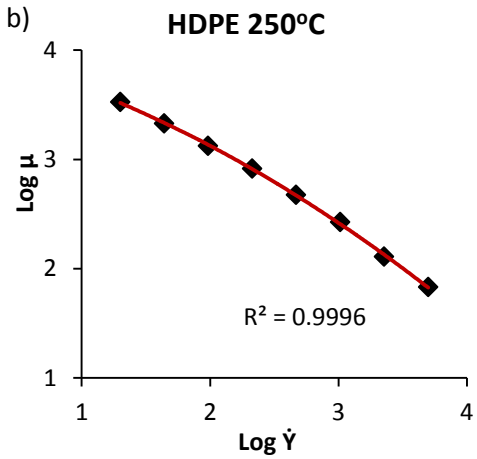
b)
HDPE 250ºC
Log μ
Log Ẏ
R² = 0.9996
1
2
3
4

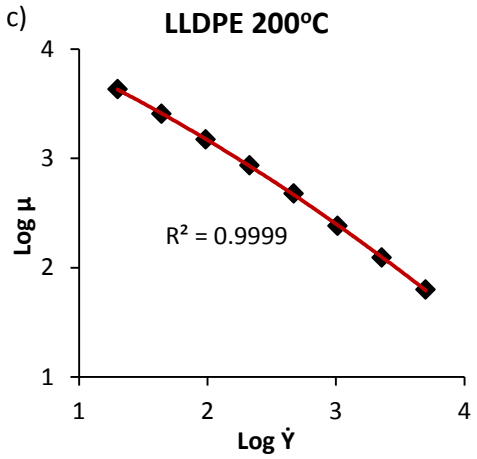
c)
LLDPE 200ºC
Log μ
Log Ẏ
R² = 0.9999
1
2
3
4

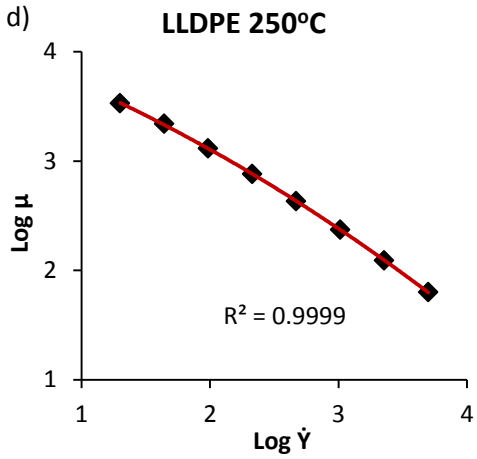
d)
LLDPE 250ºC
Log μ
Log Ẏ
R² = 0.9999
1
2
3
4

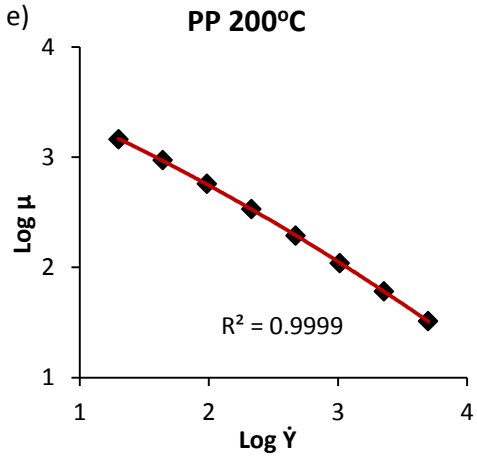
e)
PP 200ºC
Log μ
Log Ẏ
R² = 0.9999
1
2
3
4

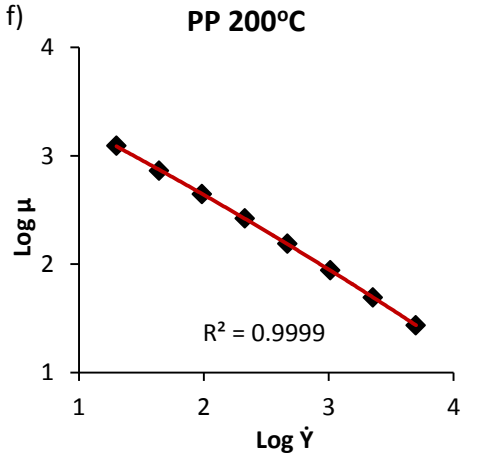
f)
PP 200ºC
Log μ
Log Ẏ
R² = 0.9999
1
2
3
4

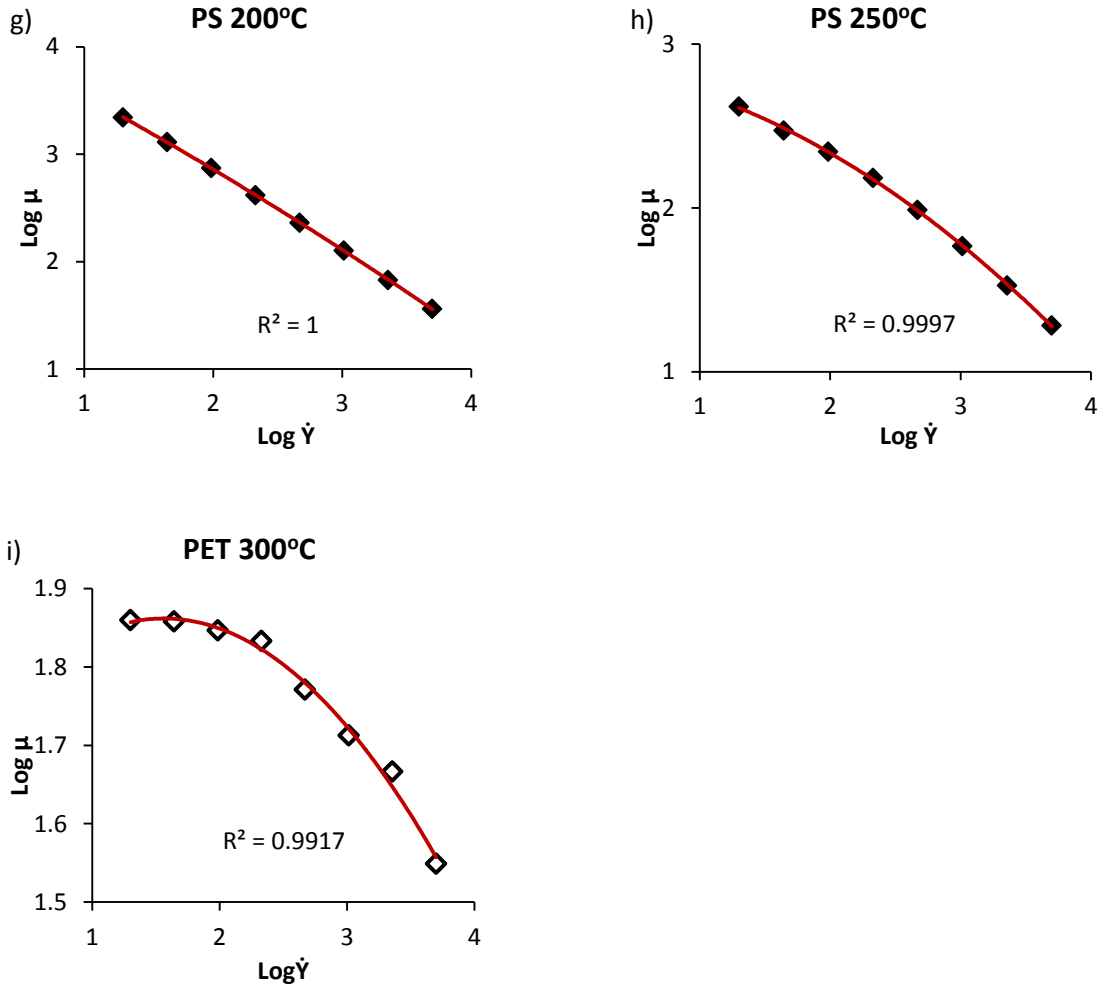

Figure 5.3: Shear rate–viscosity log-log plots (quadratic correlations).

The mean viscosities values for the various polymers in response to a shear rate variation at different temperatures are shown in Table 5.1 below. See appendices (Tables A.1 – A.9) for individual runs for each polymer. As may be observed from the table, the viscosity values are significantly high compared to 0.5 Pas specified for feedstock in the petrochemical industry (Brandrup, 1996) and viscosity data for heavy oils. As discussed earlier, Bazyleva et al., (2010) reported viscosities of between 0.001 and 0.01 Pas at around 200^{o}C and shear rate of up to 2300s^{-1}. Aminu et al. (2004), Brauch et al. (1996) and Fainberg et al. (1996) obtained significantly lower viscosities for different vacuum residue

Table 5.1: Shear rate-viscosity relationship

Shear rate (s^{-1})	Shear viscosity (Pa.s)								
	HDPE 200°C	HDPE 250 °C	LLDPE 200 °C	LLDPE 250 °C	PP 200 °C	PP 250 °C	PS 200 °C	PS 250 °C	PET 300 °C
20	4200	3370	4290	3390	1480	1240	2200	410	70
44	2620	2140	2560	2200	940	730	1300	300	70
97	1590	1330	1490	1310	580	440	740	220	70
210	950	820	860	760	340	260	420	150	70
470	550	480	480	430	190	150	230	100	60
1030	220	270	240	240	110	90	130	60	50
2270	120	130	120	120	60	50	70	30	50
5000	70	70	60	60	30	30	40	20	40

tar samples at even lower temperatures as have already been discussed above.

Large pressure drops were experienced as a result (Table 5.2). This will have significant transport implications of the polymer melts and power requirement for pumping.

Table 5.2: Pressure drop (bar) change with shear rate (s^{-1})

Polymer	T (°C)	-ΔP (bar)							
		20 s^{-1}	44 s^{-1}	97 s^{-1}	210 s^{-1}	470 s^{-1}	1030 s^{-1}	2270 s^{-1}	5000 s^{-1}
HDPE	**200**	56	76	102	134	168	144	177	227
	250	45	60	81	108	141	175	195	222
LLDPE	**200**	55	72	93	117	143	160	180	201
	250	38	53	72	93	119	146	171	194
PP	**200**	23	31	40	50	62	75	90	107
	250	16	21	28	36	47	58	72	87
PS	**200**	28	37	46	57	69	83	98	116
	250	5	8	14	21	29	38	49	61
PET	**300**	1	2	4	9	18	34	67	113

5.1.1 Velocity profile calculation

Figure 5.4 – Figure 5.8 show the velocity profiles of the polymer melts through the capillary die. The velocity profiles of the polymer melts were calculated and plotted using equations 2.27.

The velocity profiles of all the polymer samples tested, with the exception of PET, revealed a plug-like velocity profile, a characteristic of classical Bingham plastic materials and suggest the existence of yield or critical stress (King, 2002), and showed some response to the range of shear rate they were subjected to. Their velocity profiles broadened or flattened out as shear rate increased which is consistent with Brydson's (1981) prediction. The relationship between velocity profile and shear rate is dictated by the flow region captured by the shear rate range employed which exceeded the limit of the shear-thinning region characterised by the Power law model to include the transition phase between the Newtonian, zero-shear viscosity and shear-thinning regions (see Figure 5.3). The velocity profiles of the polymers at $500s^{-1}$, which was revealed in the article by Marcilla et al. (2008) as the typical shear rate for pumping and atomisation operations in the petroleum industry, and $1000s^{-1}$, the shear rate range maximum for pumping and mixing processes were compared. The difference between the two profiles appeared to be only marginal as can be observed in Figure 5.4 – Figure 5.8 but will be quantitatively analysed during the boundary layer thickness calculation in the next sub-section.

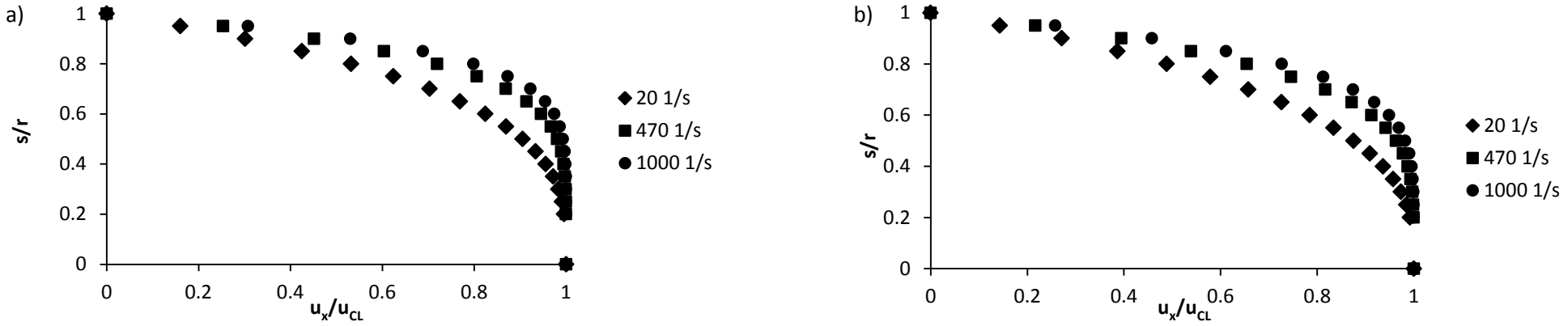

Figure 5.4: Effect of shear rate on the velocity profile of HDPE at a) 200°C and b) 250°C

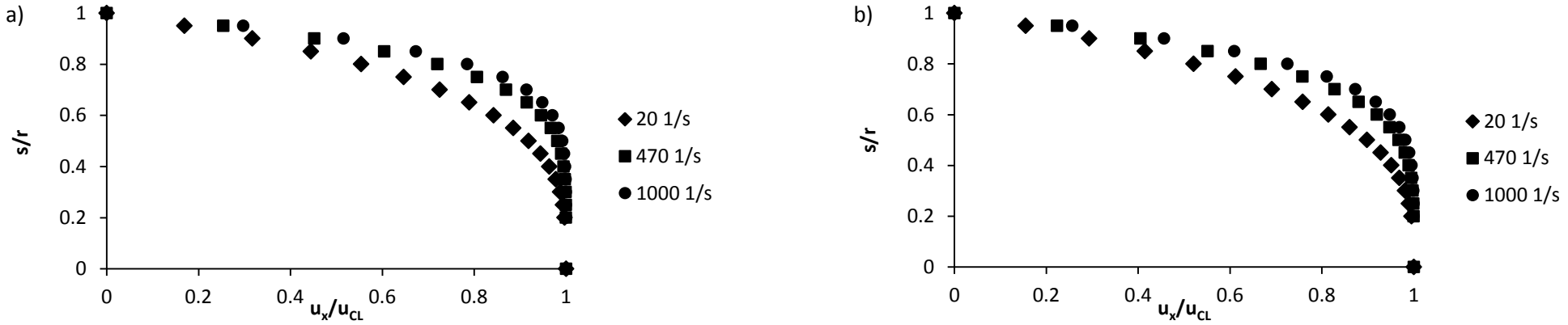

Figure 5.5: Effect of shear rate on the velocity profile of LLDPE at a) 200°C and b) 250°C

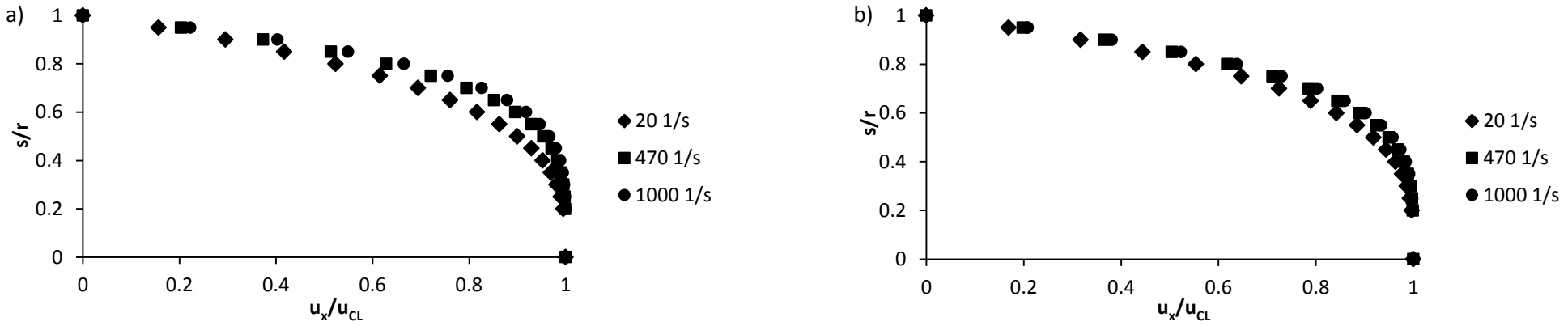

Figure 5.6: Effect of shear rate on the velocity profile of PP at: a) 200°C and b) 250°C

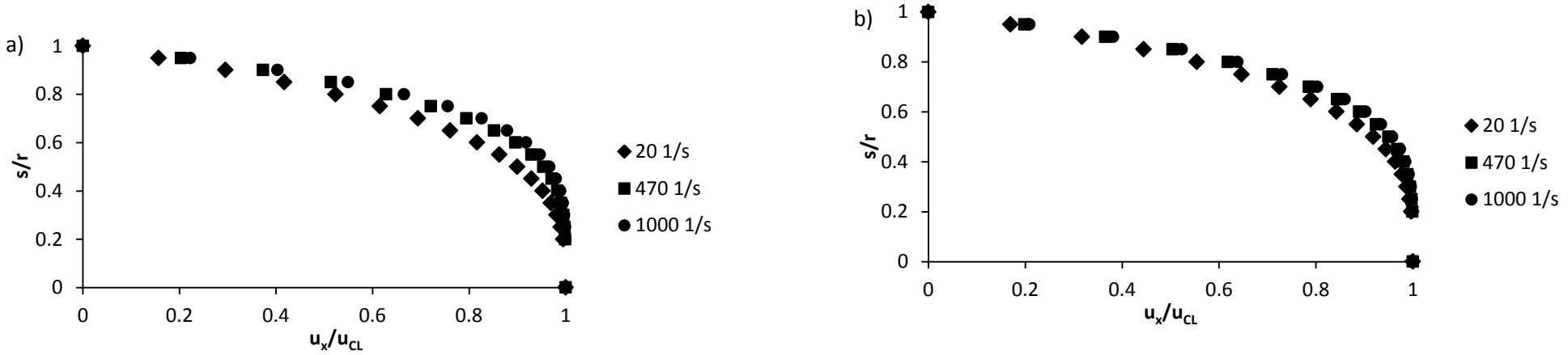

Figure 5.7: Effect of shear rate on the velocity profile of PS at: a) 200°C and b) 250°C

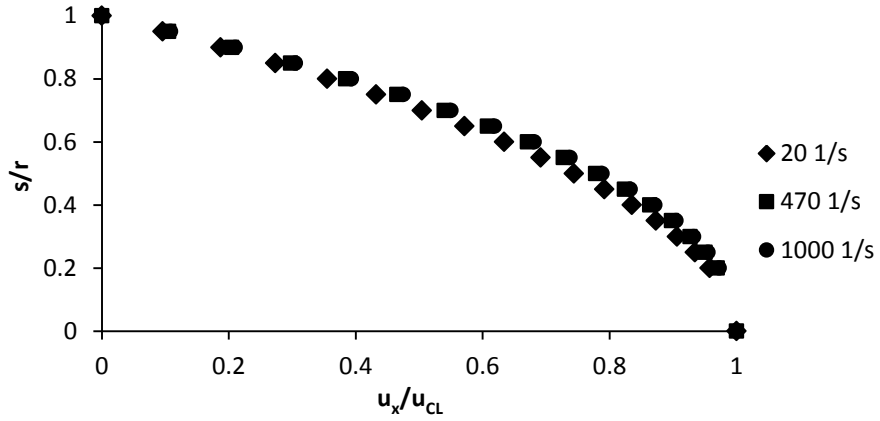

Figure 5.8: Effect of shear rates on the velocity Profile of PET

Temperature on the other hand generally resulted in a less plug-like velocity profile (see Figure 5.9). This sensitivity of velocity profile to temperature mirrors the effect of temperature on the polymer flow curves observed earlier where PS showed significant change in shear stress (or viscosity) at each shear rate between 200^{o}C and 250^{o}C. In contrast, HDPE, LLDPE and PP which are not temperature sensitive, as opposed to PS which is both temperature and shear sensitive (Giles et al., 2005), did not show any significant change in velocity profile between 200^{o}C and 250^{o}C.

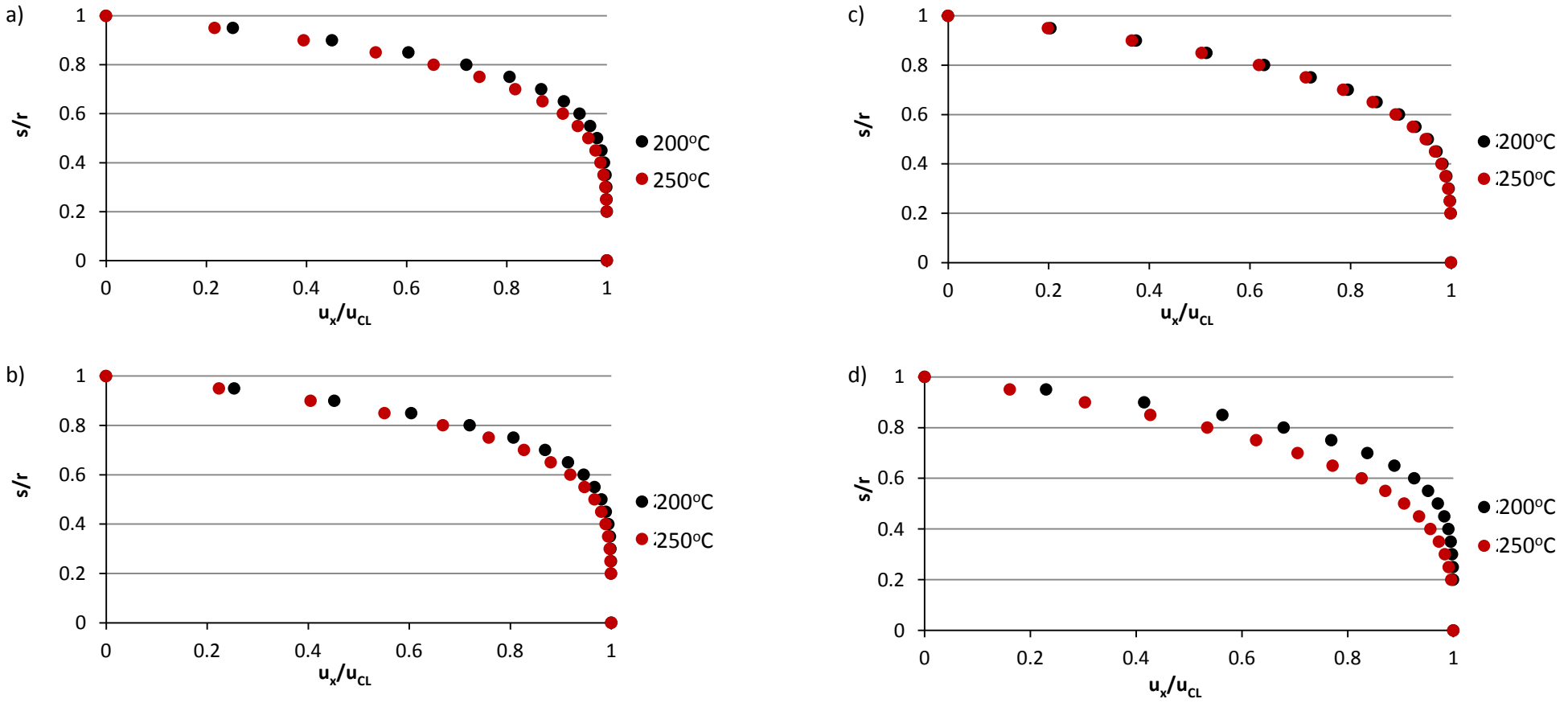

Figure 5.9: Effect of temperature on the velocity profiles (at ~500s^{-1}) of: a) HDPE; b) LLDPE; c) PP and d) PS

5.1.2 Boundary layer thickness and Reynolds number calculation

The velocity profiles of polymer melts flow are of significance since it defines the boundary layer thickness which has mass transfer implications with respect to mixing with the other phases and is required in estimating power requirement from a pump as mentioned earlier (Holland and Bragg, 1995; Chhabra and Richardson, 1999; Coulson et al., 1999; Hauke, 2008). The boundary layer thickness at each shear rate was estimated using the equation below, derived from the velocity profile equation (equations 2.27).

$$\delta = r - s_{0.99U_{CL}} \tag{5.1}$$

$$s_{0.99u_{CL}} = \left[r^{\frac{n+1}{n}} - \left(\frac{0.99\,u_{CL}}{u} \cdot \frac{n+1}{3n+1}\right)\right]^{\frac{n}{n+1}} \tag{5.2}$$

Where: r = die radius; s = radial position from axis; u_{CL} = Velocity at die axis; u = average velocity; n = power law index

Table 5.3:Boundary layer thickness (x10^{-4}m) change with shear rate

Polymer	T (^{o}C)	$\delta_{20s^{-1}}$	$\delta_{44s^{-1}}$	$\delta_{97s^{-1}}$	$\delta_{213s^{-1}}$	$\delta_{470s^{-1}}$	$\delta_{1030s^{-1}}$
HDPE	**200**	3.7	3.5	3.3	3.1	2.8	2.4
	250	3.9	3.8	3.6	3.4	3.1	2.7
LLDPE	**200**	3.6	3.4	3.3	3.0	2.8	2.4
	250	3.8	3.6	3.5	3.3	3.0	2.7
PP	**200**	3.7	3.6	3.5	3.4	3.2	3.0
	250	3.6	3.5	3.5	3.4	3.3	3.2
PS	**200**	3.4	3.3	3.2	3.1	3.0	2.8
	250	4.2	4.1	4.0	3.9	3.7	3.5
PET	**300**	4.5	4.5	4.5	4.5	4.4	4.4

As was observed with the velocity profile diagrams, boundary layer thickness generally decreased as shear rate was increased at both 200 and 250^{o}C as can be observed in Table

5.3. As was done qualitatively with the velocity profile diagrams, the change in boundary layer thickness between $500s^{-1}$ and $1000s^{-1}$ for each polymer at both 200 and 250^{o}C, with the exception of PET which was only run at 300^{o}C, were analysed. While the boundary layer for HDPE and LLDPE decreased by 14.3% and 14.2%, respectively at 200^{o}C, and 12.9% and 10%, respectively at 250^{o}C; PP and PS experienced a less shear-sensitive decrease in boundary layer thickness. While the boundary layer for PP only decreased by 6.3% and 3% at 200^{o}C and 250^{o}C, respectively, PS decreased by 6.7% and 5.4% at 200^{o}C and 250^{o}C, respectively. The change in the PP boundary layer thickness appears to suggest it is less shear-sensitive compared to the other shear-sensitive polymers (HDPE and LLDPE). PET, a temperature sensitive polymer (Giles et al., 2005), did not experience any change in boundary thickness between $500s^{-1}$ and $1000s^{-1}$ as shown in Table 5.3.

Temperature on the other hand generally increased the boundary layer thickness with PS showing the most significant change, 23.3% and 25% increase at $500s^{-1}$ and $1000s^{-1}$, respectively, between 200^{o}C and 250^{o}C. In contrast, the boundary layer thicknesses for HDPE, LLDPE and PP increased by 10.7% and 12.5%, 7.1% and 12.5%, and 3.1% and 6.7%, at $500s^{-1}$ and $1000s^{-1}$, respectively, between 200^{o}C and 250^{o}C.

The flow regime at each shear rate was also determined by calculating their Reynolds number values. This is shown in Table 5.4 below and shows that it is very much laminar. While a turbulent boundary layer promotes rapid mixing and therefore high heat and mass transfer rates, laminar boundary are devoid of mixing due to absence of lateral interaction between the streams of fluid layers (Coulson et al., 1999, Holland and Bragg, 1995). The

type of flow taking place, whether laminar or turbulent, is dictated by the dimensionless quantity, Reynolds number (Re).

Table 5.4: Reynolds number (Re x10^{-6}) at different shear rates and temperature

Polymer	T (^oC)	Re							
		20 s^{-1}	44 s^{-1}	97 s^{-1}	210 s^{-1}	470 s^{-1}	1030 s^{-1}	2270 s^{-1}	5000 s^{-1}
HDPE	200	0.4	1.4	4.7	15.8	53.5	243.1	749.2	1756.2
	250	0.6	1.9	6.2	20.3	69.9	237.0	873.6	2533.7
LLDPE	200	0.4	1.3	4.7	16.5	59.0	222.3	783.7	2493.7
	250	0.5	1.7	5.8	20.3	72.6	260.2	932.7	3185.8
PP	200	1.2	3.8	13.2	47.1	171.1	621.6	2274.9	8330.4
	250	1.4	4.9	17.3	61.5	222.0	820.4	3051.2	11400.1
PS	200	0.8	2.8	10.5	39.7	150.1	575.0	2244.4	8600.0
	250	5.6	16.8	47.7	144.1	466.9	1576.4	5416.7	17964.0
PET	300	48.76	106.4	237.7	531.42	1330.0	3303.61	7951.82	22501.6

5.2 SOLVENT TREATMENT

Results of the rheological characterisation undertaken above have revealed the extent by which viscosity of plastics supersedes the recommended feedstock viscosity for petroleum industry operations such as hydrocracking, the plug-like flow behaviour in pipes and the high pressure drop values. Solvent treatment using high yield alkane products of mixed plastics hydrocracking as sacrificial solvent was investigated as a means of viscosity reduction as described under section 4.4, using the 12-station reaction carousel shown in Figure 4.2. Iso-octane (iC_8), n-decane (nC_{10}), n-tetradecane (nC_{14}), n-pentadecane (nC_{15}) and n-hexadecane (nC_{16}) were investigated.

At the end of the solvent treatment experiment, the PE-solvent mixtures (PE-iC_8, PE-nC_{10}, PE-nC_{12}, PE-nC_{14}, PE-nC_{15} and PE-nC_{16}) were allowed to cool down and then separation carried out where possible. This was however only attempted for PE-iC_8 mixtures as a

result of the small quantities involved and the difficulty experienced during separation. A summary of this result is shown in Table 5.5 and appeared to show some phase interaction in the mixtures. Samples A – D had a distinct slurry phase and a solid phase residue of the resin (residue resin in Table 5.5). Samples E - G however showed a negligible slurry phase which was difficult to measure given the small quantities involved. The solid residue in these samples in contrast to samples A – D, which were still in distinguishable pellets, appeared melted and fused together.

Table 5.5: HDPE solvent treatment- Sample preparation and result

Sample (PE/iC8 ratio)	Reactants (g)		Products (g)		
	Polymer	Solvent	Slurry	Solid residue	
				1	2
A (20:80)	0.51	2.04	1.68	0.55	-
B (30:70)	0.51	1.19	0.86	0.58	-
C (40:60)	0.51	0.71	0.37	0.53	-
D (50:50)	0.51	0.51	0.27	0.57	-
E (60:40)	0.51	0.34	0.08	-	0.64
F (70:30)	0.51	0.22	0.13	-	0.58
G (80:20)	0.51	0.13	0.04	-	0.56
1. residue resin					
2. Fused melted & unmelted resin					

Differential Scanning Calorimetry (DSC) and Thermogravimery analysis (TGA) were carried out on the solid residues of the PE-solvent mixtures to assess the effect of the solvent treatment on the thermal behaviour of the polymers

5.2.1 Differential Scanning Calorimetry (DSC)

DSC was carried out on the solid residues of the solvent treated HDPE samples to establish the temperature at which melting endotherms develop relative to pure HDPE samples as an indication of viscosity reduction via molecular weight breakdown. Figures 5.9 and 5.10

show the results of the DSC while the melting peak for each PE-solvent 50:50 mixture showing the determination of the extrapolated onset and peak maximum temperatures are shown in the appendices (Figure A.2 – A.7).

As can be observed, iC8 and nC10 didn't show any significant effect on the onset and maximum peak temperatures of the melting endotherm. nC14, nC15 and nC16 on the other hand have a discernible reducing effect on the temperature of the melting endotherm. These observations were confirmed by performing the F-statistics test under the null hypothesis that regard the data points for each sample set of PE-solvent mixture as showing an insignificant linear trend with the slope being zero. This null hypothesis statement is accepted when F-statistic value (F_{stat}) calculated for the data set is less than the F-critical value (F_{crit}) that corresponds to the degrees of freedom for the data set. Test results are shown in Table 5.6

Some of the endotherms of the PE-solvent, 20:80 mixtures had shoulders or were bimodal in nature as shown in the example in Figures 5.11 - 5.13. Thus, 2 sets of data points, as well as trendlines, were used to capture the respective peak temperatures for each solvent in the graph. The shoulders or bimodal nature of these peaks may point to the formation of extended chain and folded chain crystals (Webber, 2009).

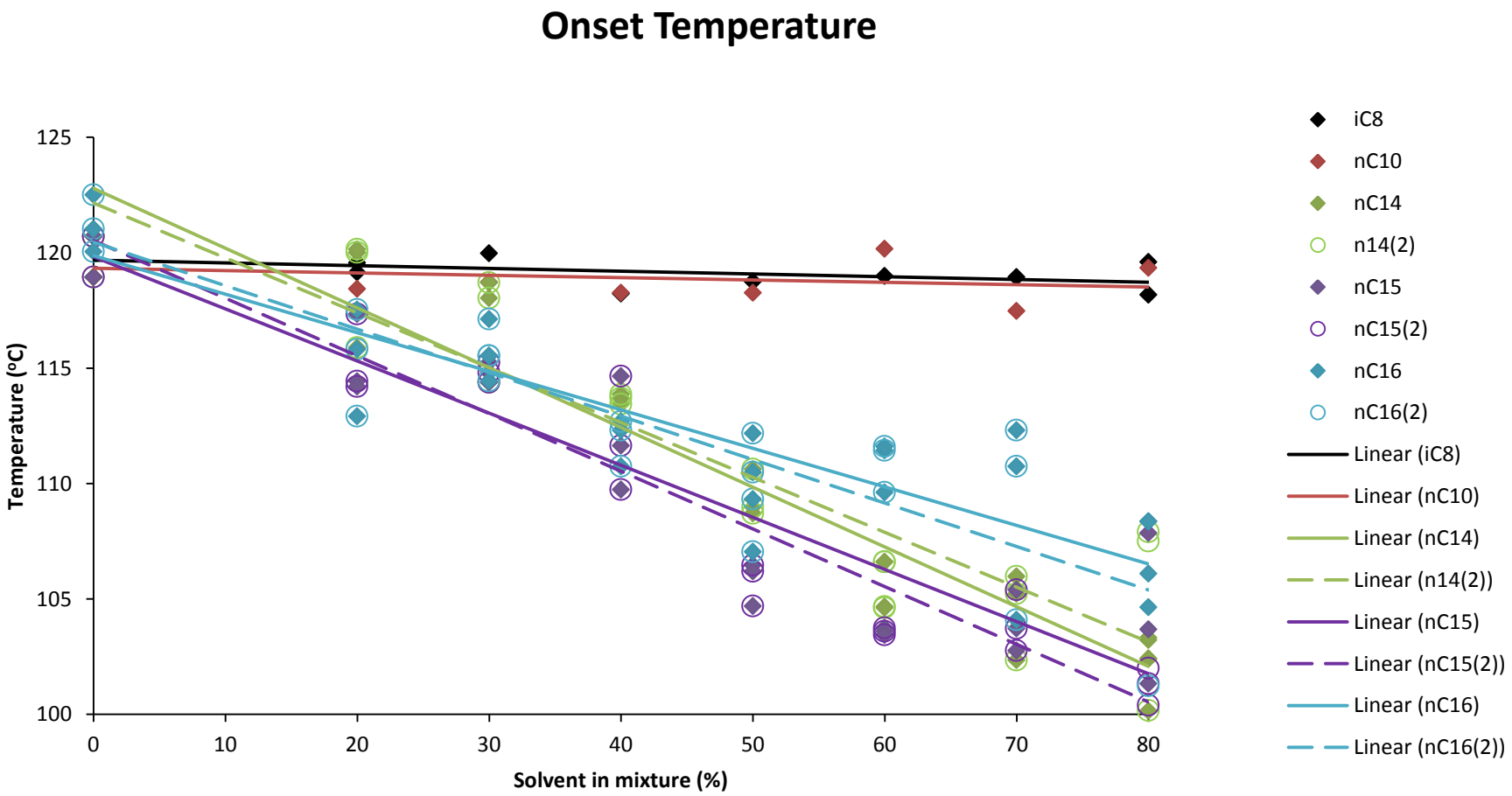

Figure 5.10: Effect of solvent treatment on onset temperature

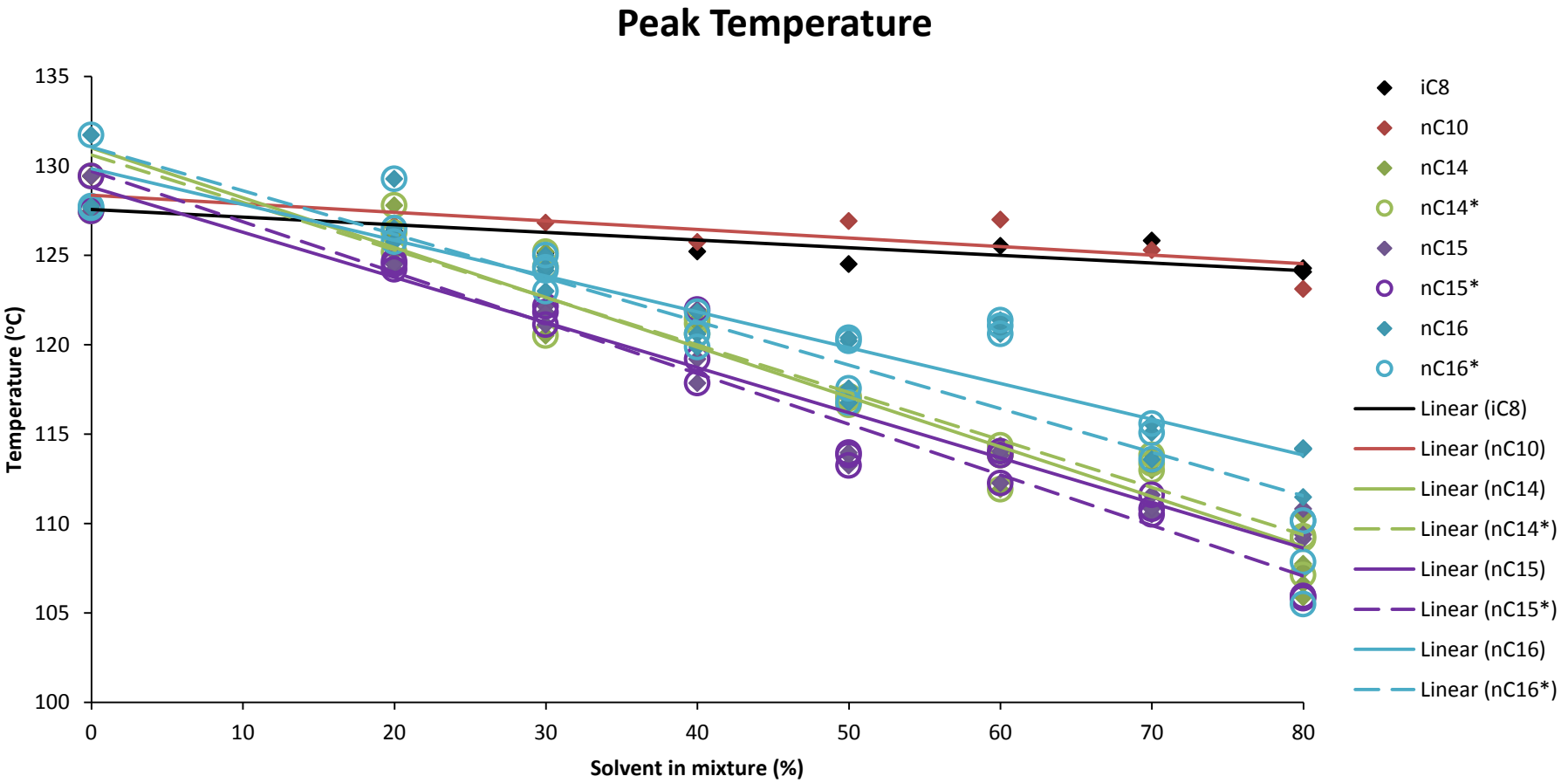

Figure 5.11: Effect of solvent treatment on peak temperature

Table 5.6: F-statistics test under null hypothesis for DSC endotherms

Solvent	Temperature	Slope	F_{stat}	F_{crit}	H_0: $F_{stat} < F_{crit}$
iC8	**Onset**	-0.0121 ± 0.0074	2.66	5.12	Accepted
	Maximum	-0.0427 ± 0.0104	17.00	5.12	Rejected
nC10	**Onset**	-0.0102 ± 0.0126	0.66	5.59	Accepted
	Maximum	-0.0480 ± 0.0133	13.10	5.59	Rejected
nC14 (main)	**Onset**	-0.2588 ± 0.0160	262.93	4.26	Rejected
	Maximum	-0.2784 ± 0.0143	376.75	4.26	Rejected
nC14 (minor)	**Onset**	-0.2377 ± 0.0224	113.04	4.30	Rejected
	Maximum	-0.2657 ± 0.0140	358.07	4.30	Rejected
nC15 (main)	**Onset**	-0.2258 ± 0.0214	111.11	4.32	Rejected
	Maximum	-0.2522 ± 0.0127	391.37	4.32	Rejected
nC15 (minor)	**Onset**	-0.2500 ± 0.0166	227.56	4.32	Rejected
	Maximum	-0.2830 ± 0.0125	508.62	4.32	Rejected
nC16 (main)	**Onset**	-0.1669 ± 0.0170	96.36	4.24	Rejected
	Maximum	-0.2002 ± 0.0148	183.18	4.24	Rejected
nC16 (minor)	**Onset**	-0.1884 ± 0.0218	74.46	4.30	Rejected
	Maximum	-0.2436 ± 0.0203	143.82	4.24	Rejected

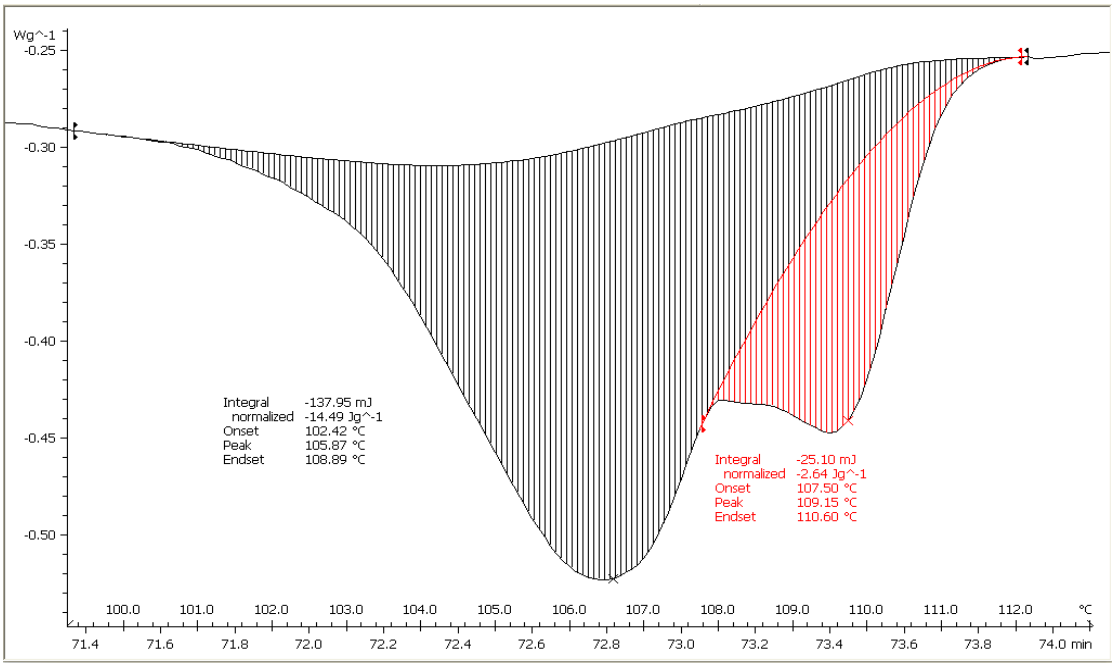

Figure 5.12: PE-nC14 (20:80) melting endotherm

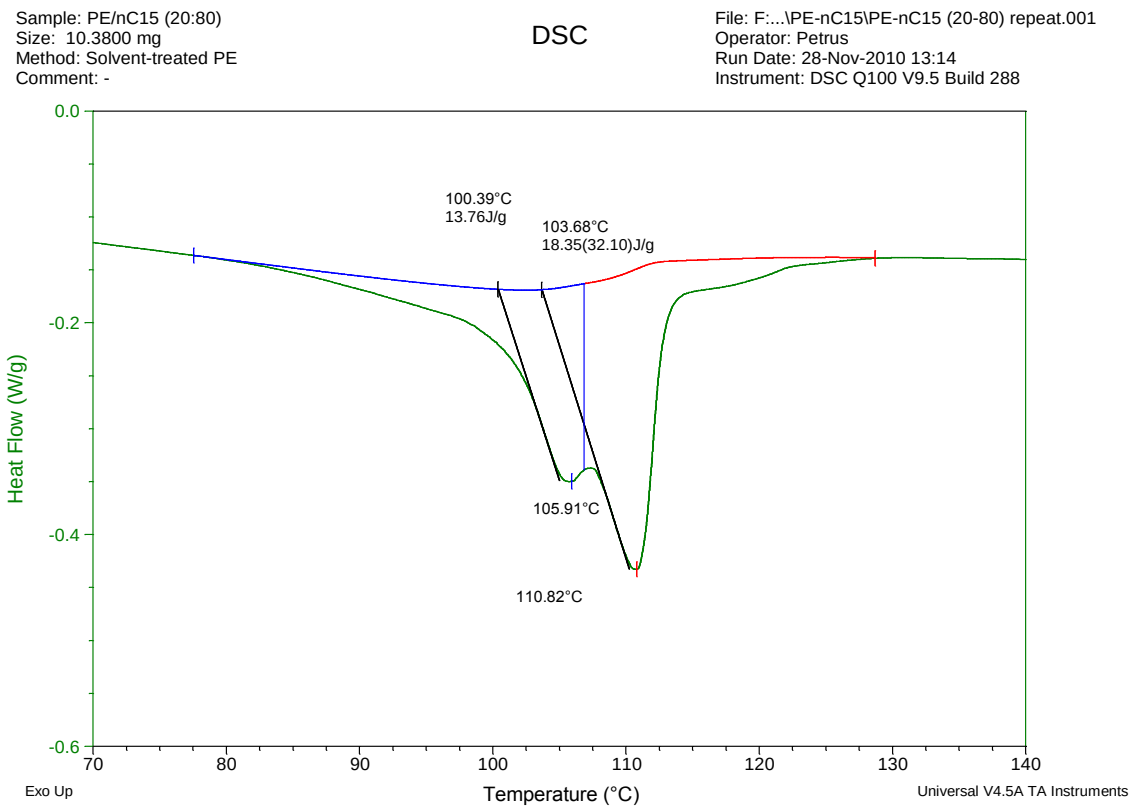

Figure 5.13: PE-nC15 (20:80) melting endotherm

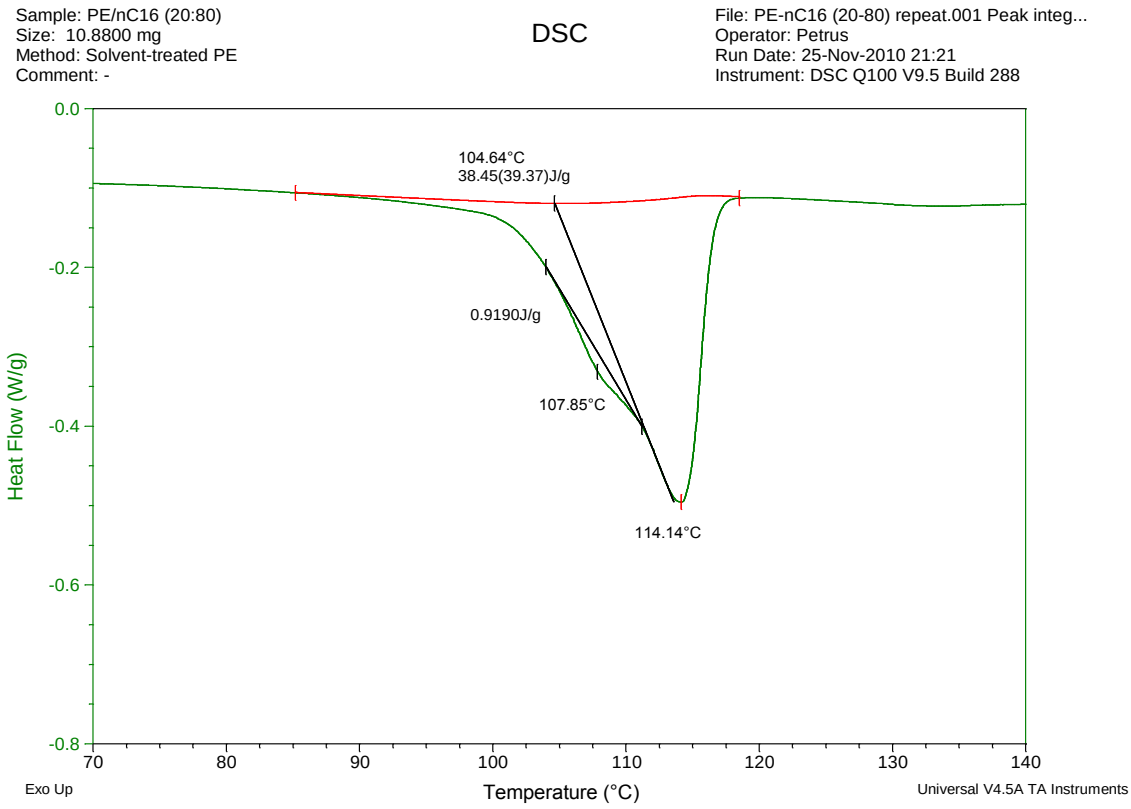

Figure 5.14: PE-nC16 (20:80) melting endotherm

5.2.2 Thermogravimetric analysis (TGA)

Thermogravimetric analysis of the untreated HDPE and solid residues of the solvent treated HDPE samples was undertaken (under nitrogen environment) to assess the effect of the solvent treatment. Hence the interaction between HDPE and the different proportions of the solvents used for treatment was investigated by analysing the decomposition steps, i.e. the decomposition weight loss regions, and the effect of the sample mixing ratios on their relative composition. The PE-solvent mixtures were observed to generally decompose in 2 weight loss regions, unlike their pure components, especially for the PE-solvent mixtures with high solvent content (Figure 5.15). The first, lower temperature, weight loss

region is referred to as phase 1 (P1) while the second, higher temperature, weight loss region is referred to as phase 2 (P2). Extrapolated onset temperatures for decomposition was measured and compared with those of the virgin polymer pellets and pure solvents.

As can the observed in Figure 5.16 and Figure 5.17, no discernible trend was established on the effect of iC8 and nC10 on the phase compositions of the PE-solvent mixtures. The reverse was however the case for nC14, nC15 and nC16 treated HDPE pellets which clearly revealed an increasing trend in the composition of phase 1 and a decreasing trend for phase 2 in the decomposition of the sample mixtures. These observations were further reinforced by the results of F-statistics test which assessed a null hypothesis of non-linearity of the data points. The null hypothesis was accepted for iC8 and nC10 treated PE and rejected for nC_{14}, nC_{15} and nC_{16} treated PE. It is important to point out that the PE-nC10 (30-70) data point, i.e. 70% solvent mixture ratio, exhibited 3 weight loss regions, the first occurring before the end of the 60^{o}C isothermal phase at the beginning of the temperature programme meant to drive off loosely bound surface solvent. This initial weight loss (11.5%) was combined with the second weight loss region.

The extrapolated onset temperatures of phases 1 and 2 of the different mixing ratios of solvent treated PE samples were compared with those of their corresponding pure solvents and virgin HDPE, respectively, as shown in Figure 5.18 and Figure 5.19. Phase 1 temperatures were thus compared with the temperatures of the solvents and phase 2 was compared to the onset temperatures of HDPE used. This comparison was made because the extrapolated onset temperatures of decomposition for the solvents corresponded with the

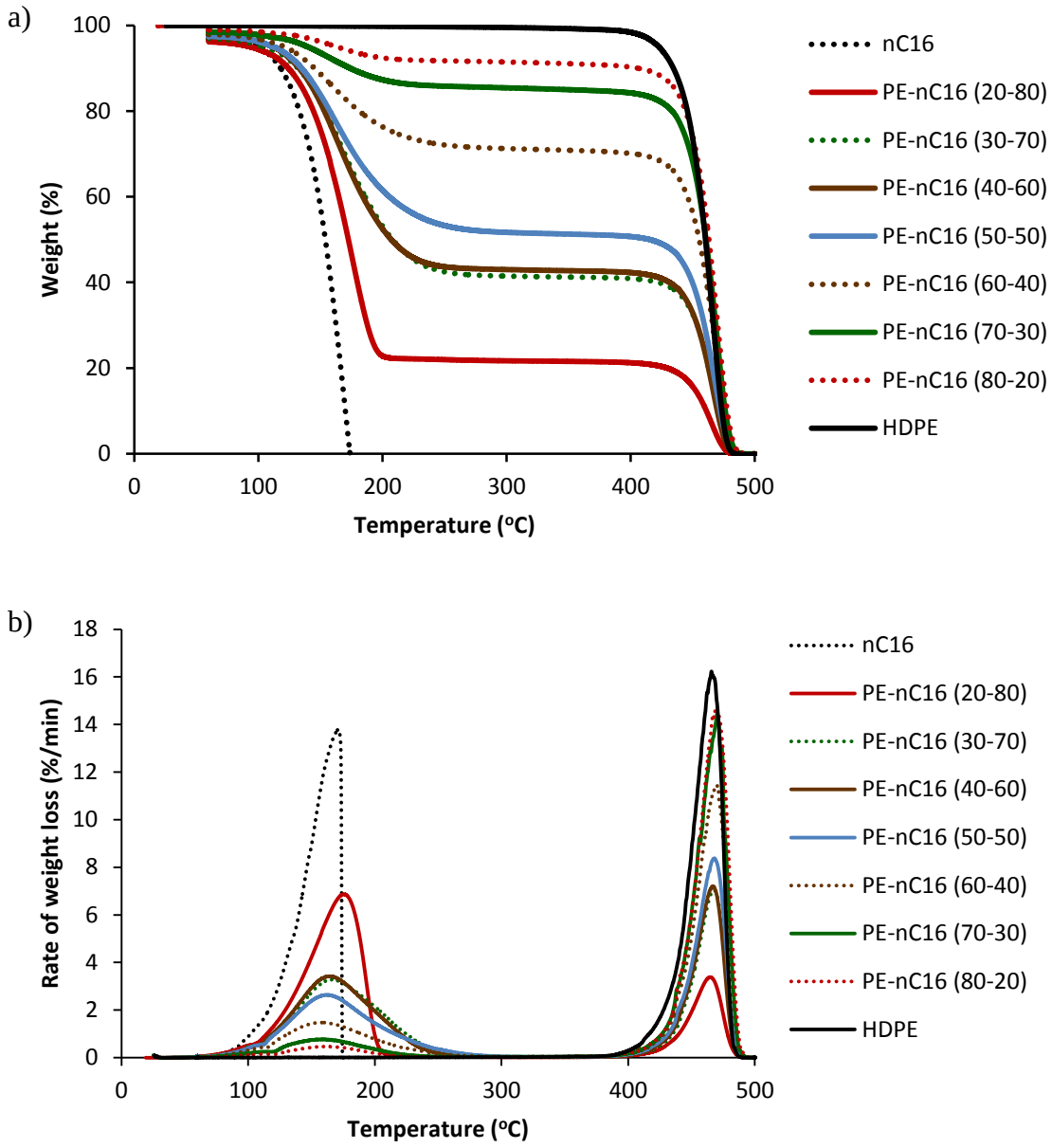

Figure 5.15: Thermogravimetric analysis curve- a) Weight loss curve (TG). b) Rate of weight loss curve (DTG).

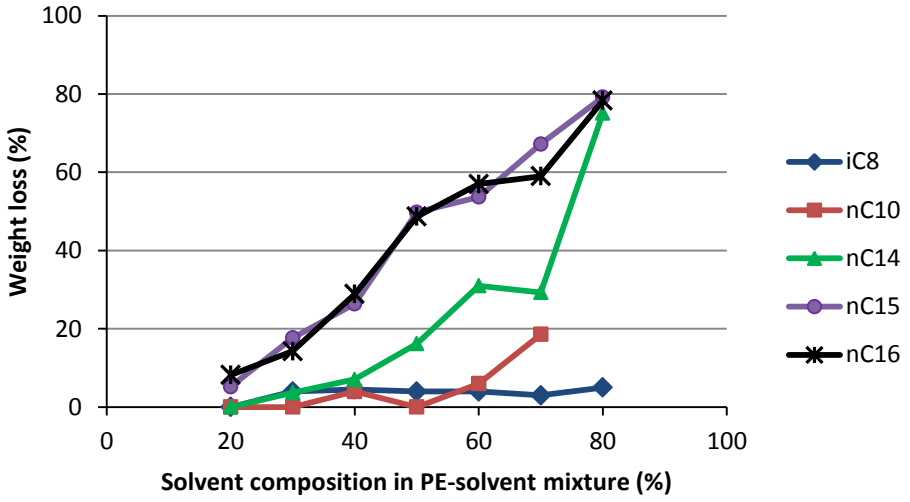

Figure 5.16: Solvent effect on phase 1 composition

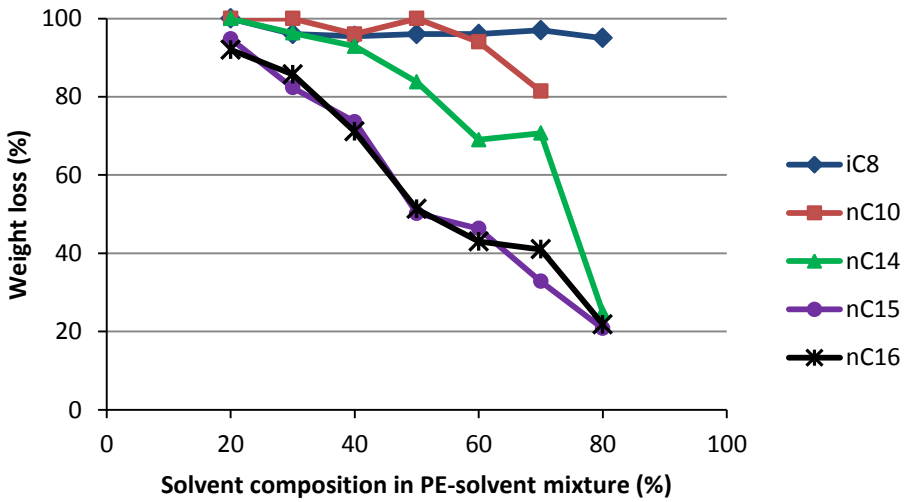

Figure 5.17: Solvent effect on phase 2 composition

lower extrapolated onset temperatures of decomposition of phase 1 as did the extrapolated onset temperatures of decomposition for the HDPE correspond to the higher extrapolated onset temperatures of decomposition for phase 2. The data points for the extrapolated onset temperature of decomposition for each set of PE-solvent mixture were subjected F-

statistics test also to test a null hypothesis of non-linearity which is summarised in Table 5.8. The null hypothesis in the case of the solvent effect on phase 1 onset temperatures of decomposition was accepted in each data set except nC_{15} and nC_{16} treated HDPE. These results corroborates deductions that can be made from Figure 5.18 which appears to

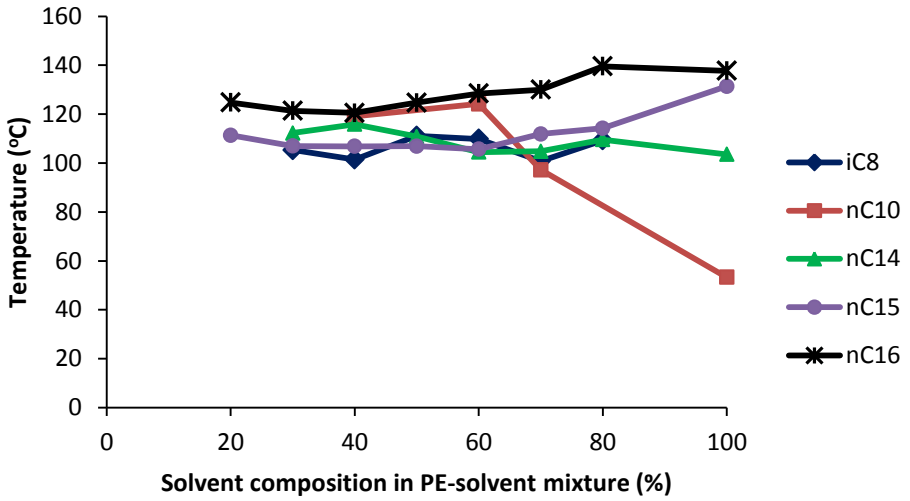

Figure 5.18: Solvent effect on phase 1 onset temperature

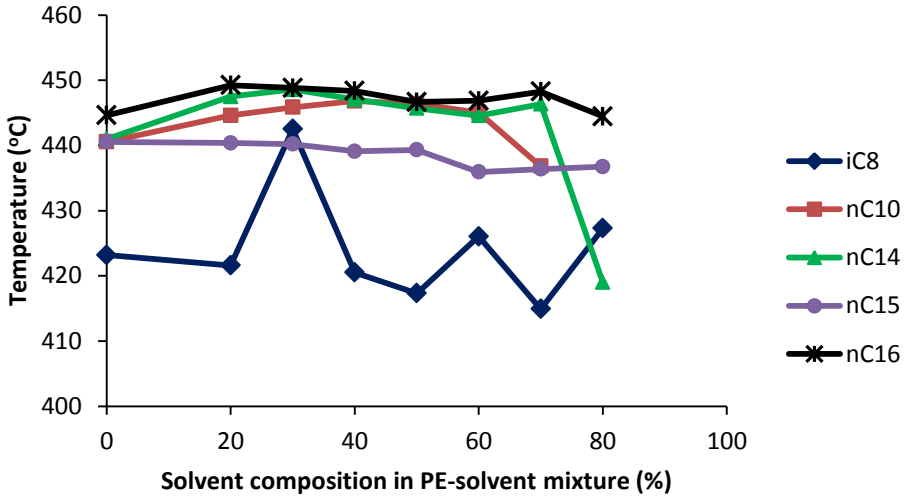

Figure 5.19: Solvent effect on phase 2 onset temperature

indicate a slight increase in the extrapolated onset temperature of decomposition as the solvent mixture ratio is increased in PE-solvent mixture increases. A similar but opposite observation was also made for the higher extrapolated onset temperature of decomposition for phase 2 (Figure 5.19). However only nC_{15} treated HDPE showed any statistical evidence of solvent effect on the extrapolated onset temperature of decomposition in this higher temperature weight loss region according to the F-statistic test result in Table 5.8.

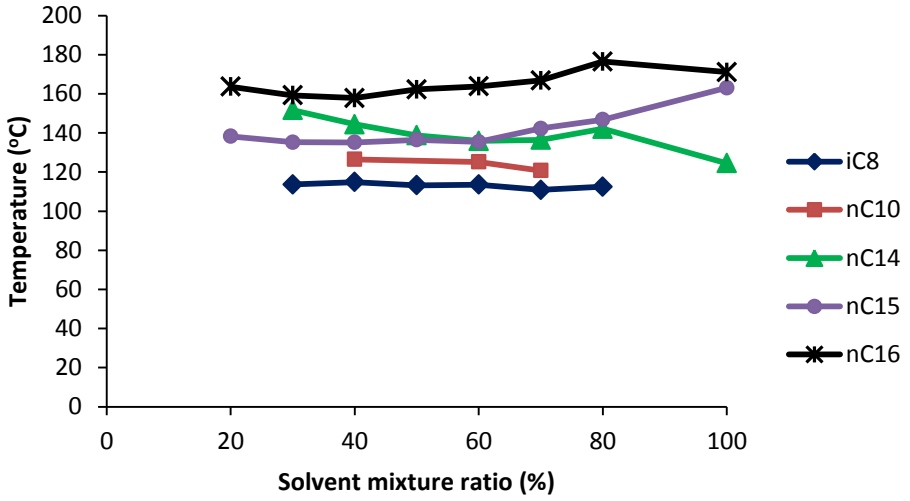

Figure 5.20: Solvent effect on phase 1 DTG peak maximum temperature

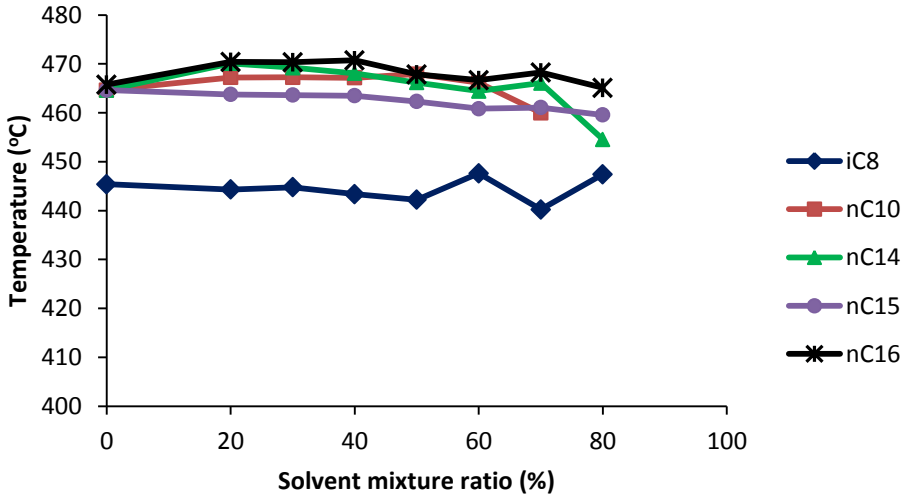

Figure 5.21: Solvent effect on phase 2 DTG peak maximum temperature

Table 5.7: F-statistics test under null hypothesis for solvent effect on phase composition

Solvent	Weight loss region	F_{stat}	F_{crit}	H_0: $F_{stat} < F_{crit}$
iC8	**P1**	2.56	6.61	Accepted
	P2	2.56	6.61	Accepted
nC10	**P1**	6.67	7.71	Accepted
	P2	6.67	7.71	Accepted
nC14	**P1**	20.34	6.61	Rejected
	P2	20.34	6.61	Rejected
nC15	**P1**	317.48	6.61	Rejected
	P2	317.48	6.61	Rejected
nC16	**P1**	159.51	6.61	Rejected
	P2	160.73	6.61	Rejected

Table 5.8: F-statistics test under null hypothesis for solvent effect on phase onset and DTG maximum peak temperatures

Solvent	Temperature	F_{stat}	F_{crit}	H_0: $F_{stat} < F_{crit}$
iC8	**P1 onset**	0.16	7.71	Accepted
	P1 DTG max peak	3.71	7.71	Accepted
	P2 onset	0.19	5.99	Accepted
	P2 DTG max peak	0.0004	5.99	Accepted
nC10	**P1 onset**	11.19	18.51	Accepted
	P1 DTG max peak	3.43	161.45	Accepted
	P2 onset	0.08	6.61	Accepted
	P2 DTG max peak	0.73	6.61	Accepted
nC14	**P1 onset**	6.27	6.61	Accepted
	P1 DTG max peak	12.54	6.61	Rejected
	P2 onset	1.67	5.99	Accepted
	P2 DTG max peak	3.07	5.99	Accepted
nC15	**P1 onset**	6.73	5.99	Rejected
	P1 DTG max peak	12.36	5.99	Rejected
	P2 onset	20.68	5.99	Rejected
	P2 DTG max peak	61.39	5.99	Rejected
nC16	**P1 onset**	19.98	5.99	Rejected
	P1 DTG max peak	9.03	5.99	Rejected
	P2 onset	0.10	5.99	Accepted
	P2 DTG max peak	0.60	5.99	Accepted

It can be deduced from the evidence in the results above that there was interaction between polymer and solvent in the HDPE solvent treatment involving nC14, nC15 and nC16 for which the composition of the phase 1 and phase 2 weight loss regions increased and decreased respectively with increasing solvent ratio in PE-solvent mixtures. In other words, the increase in solvent mixture (concentration) induces a change in the percentage composition of the phases, increasing the portion of the modified product decomposing in lower temperature (phase 1) while counteracting higher temperature weight loss region. Analysis of the solvent effect on the onset temperature of decomposition did not show any change that can be considered significant except in the case of nC15 where it is clearly observed to have a reducing effect in phase 2 as the solvent composition was increased.

5.2.2.1 Vapour pressure estimation by thermogravimetry

Vapour pressures due to evaporation occurring during the first weight loss region (phase 1), around the extrapolated onset temperatures of the solvents used for polymer treatment were estimated to compare with those of the pure solvents. Firstly, the calibration constant, k_{vap}, for the Q5000 thermogravimetric analyser was determined, as described in chapter 4 using pure hydrocarbon solvents and shown below in Figure 5.22.

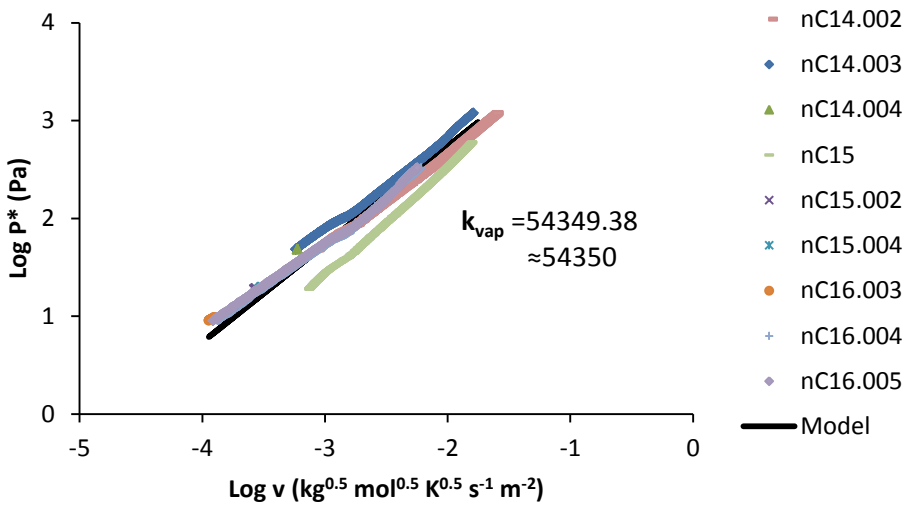

Figure 5.22: Calibration constant (k_{vap}) curve using nC14, nC15 and nC16

The derived k_{vap} was then used to calculate vapour pressures of 3 replicates of the calibration solvents using Equation 4.4 at 70, 80, 90, 100 and 110 ^{o}C and the mean vapour pressure mean values at each temperature compared with those derived from their Antoine constants (considered as the true mean) stated in Table 4.3. A plot of the mean vapour pressures of the calibration solvents at the aforementioned temperatures and their Antoine analogues is shown below (Figure 5.23) and the difference between them was found to be statistically insignificant using the one-sample t-test with the exception of hexadecane data points at 100 and 110^{o}C. The statistical significance of the difference between the two mean values was determined by comparing the t-statistic for the data, or the p-value associated with it, at significance level of 0.05.

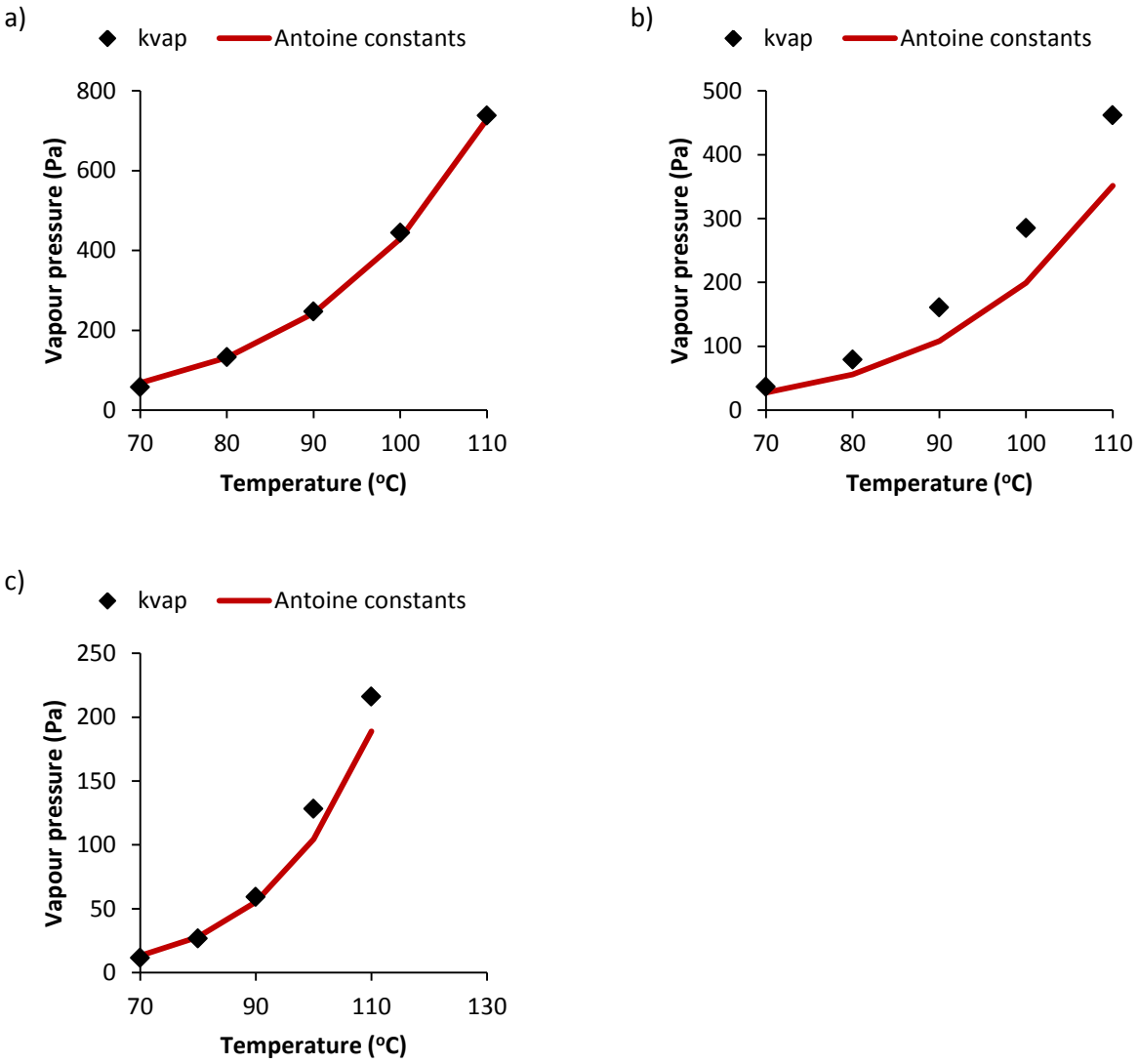

Figure 5.23: Comparison between vapour pressures derived using vaporisation calibration constant and Antoine constants for a) nC14 b) nC15 c) nC16

Table 5.9: P values at α = 0.05 for nC14, nC15 and nC16

T (°C)	P values at α = 0.05		
	nC14	**nC15**	**nC16**
70	0.24	0.52	0.09
80	0.96	0.43	0.49
90	0.88	0.26	0.21
100	0.77	0.24	0.003
110	0.91	0.32	0.008

The vapour pressures for the pure solvents derived using k_{vap} was compared with vapour pressure produced during the first weight loss region of the PE-solvent mixtures which was assumed to be solvent being vaporised. However the results of the vapour pressures for the PE-solvent mixtures obtained under this assumption was shown to differ from those of the pure solvents as shown in Figure 5.24 to Figure 5.26 below. The same observation is made using the A coefficient of the Antoine equation which is directly proportional to the logarithmic value of the vapour pressure but independent of temperature. This may indicate the evolution of a gas other than the solvent vapour and thus interaction between the solvent and polymer. This hypothesis was however considered unlikely as the extrapolated onset temperatures for both the P1 PE-solvent mixtures and the pure solvents showed little or no difference (Figure 5.18). Consequently, 2 models were proposed to explain the difference in vapour pressures between the pure solvents and the solvent concentrations of the PE-solvent mixtures, which showed an overall decrease in vapour pressure with solvent concentration. Raoult's law was considered to account for the apparent concentration dependent vapour pressure observed. Alternatively, a drying effect observed in porous materials was also considered due to what appears to be a suppressed, more or less constant, vapour pressure phase in relation to pure solvent at high solvent concentrations. Drying of saturated porous materials are characterised by the manifestation of 2 distinct evaporation rate phases; a constant rate phase and a declining rate phase (Van Brakel, 1980; Kaviany and Mittal, 1987; Peishi and Pei, 1989; Scherer, 1990; Schultz, 1991; Salvucci, 1997; Coussot, 2000; Yiotis et al., 2006; Lehmann et al., 2008; Shokri et al., 2009; Shokri and Or, 2013). The preceding constant rate phase is defined by a relatively high and consistent evaporation rate in contrast to the following declining rate

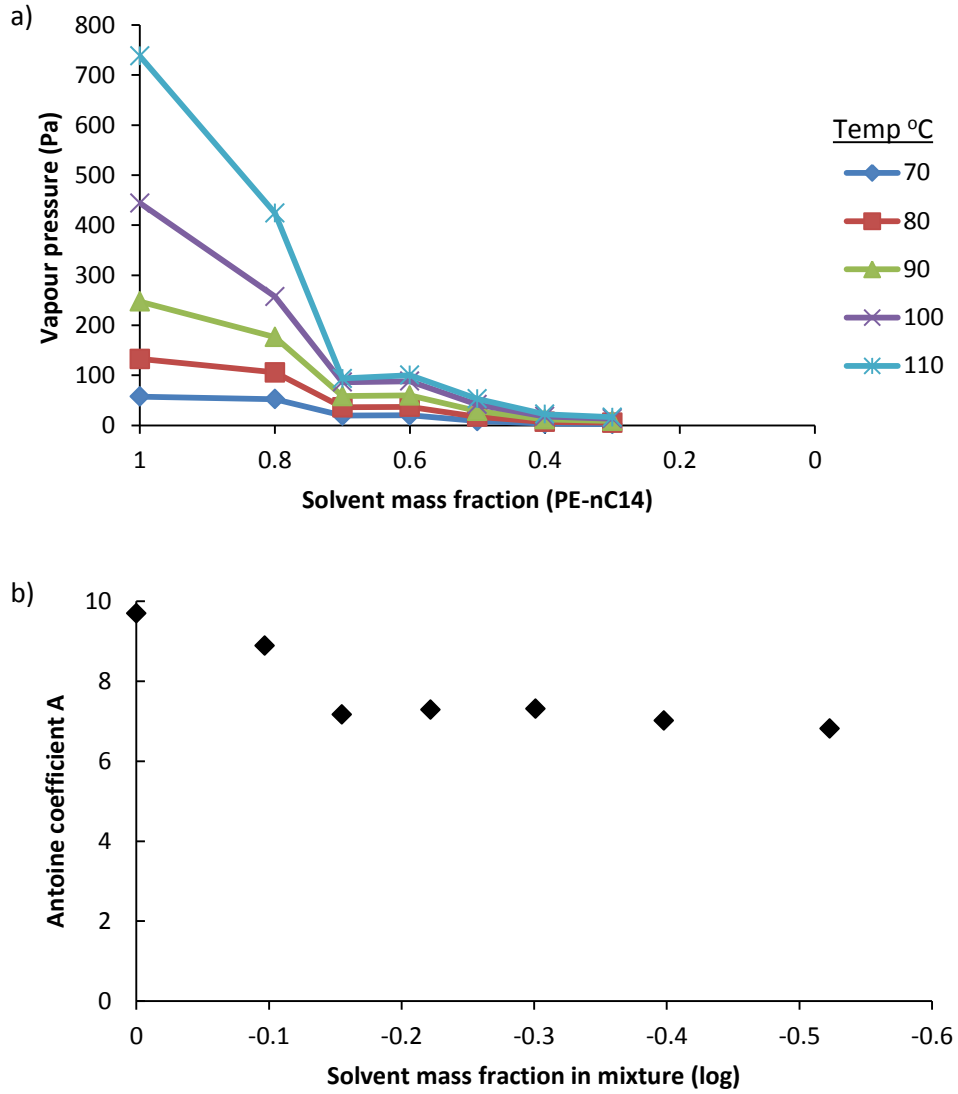

Figure 5.24: PE-nC14 solvent mass fraction relationship with a) vapour pressure and b) Antoine coefficient A

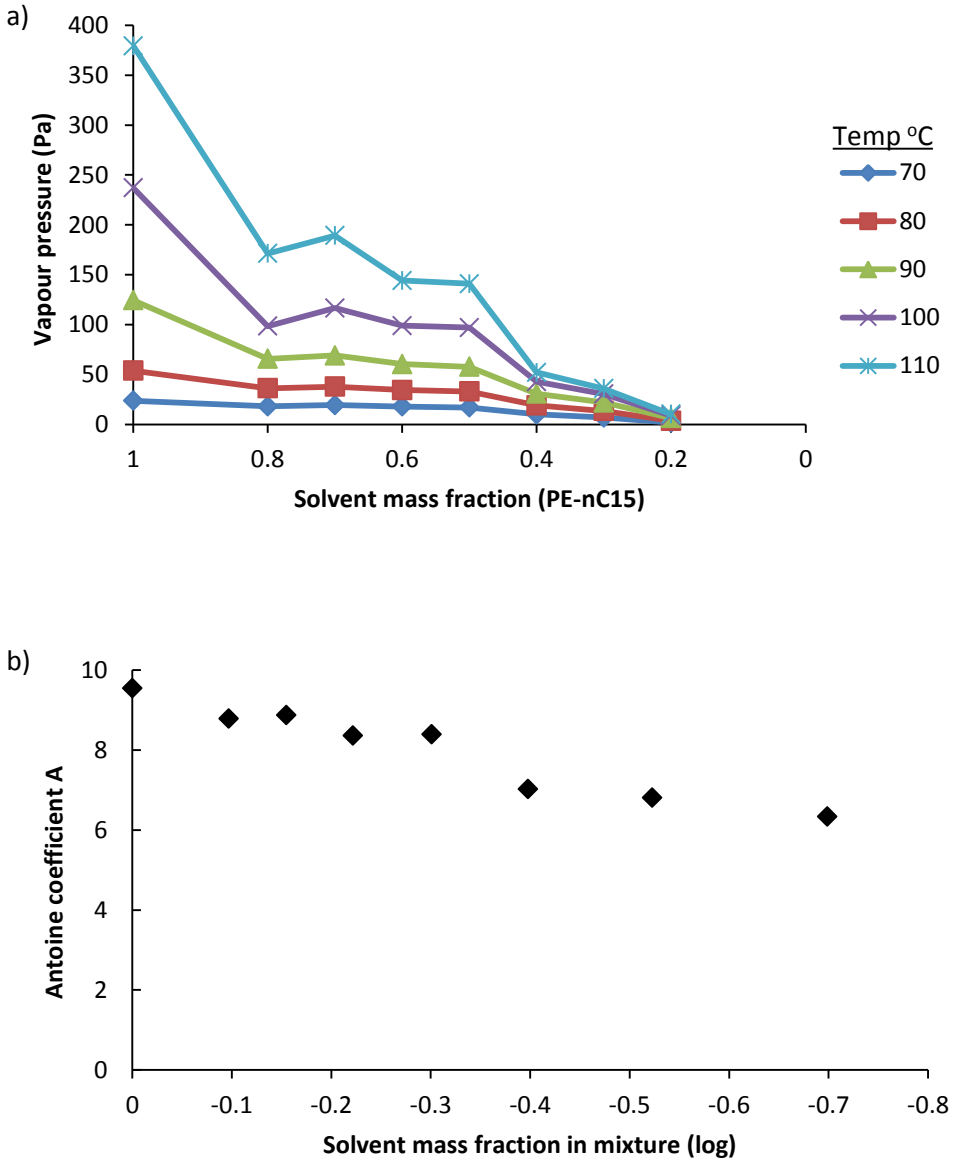

Figure 5.25: PE-nC15 solvent mass fraction relationship with a) vapour pressure and b) Antoine coefficient A

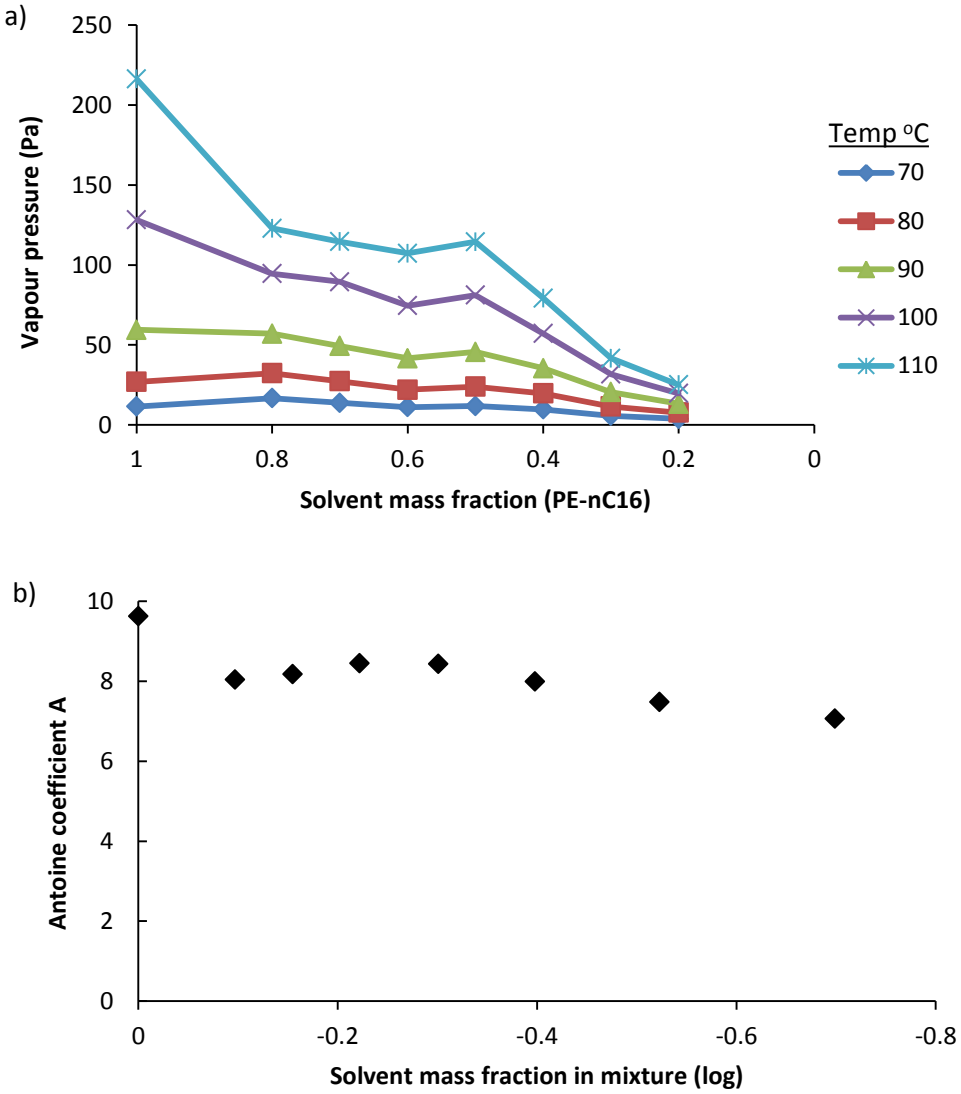

Figure 5.26: PE-nC16 solvent mass fraction relationship with a) vapour pressure and b) Antoine coefficient A

period. The constant rate phase relies on the development of a capillary pressure gradient between the unsaturated pore sites at the evaporation surface of the porous material and its internal, large, saturated pore spaces (Shokri and Or, 2013). This capillary pressure gradient develops as a drying front, an interface between saturated and partially saturated regions (Lehmann et al., 2008; Shokri and Or, 2013), is established and advances deeper

into the material. The transition from the constant rate phase to the declining rate phase occurs when the capillary pressure no longer dominates gravitational and viscous forces (Lehmann et al., 2008), which coincides with the drying front approaching a critical length referred to as characteristic length, or at a critical amount of surface liquid (Keey, 1972). The declining rate phase is thus characterised by diffusion mass transfer as the controlling transport mechanism due to the gravitational and viscous forces overcoming capillary pressure of the preceding phase.

It is being opined that during melt crystallisation following HDPE solvent treatment, parcels or pockets of the solvent phase were encapsulated in the polymer phase particularly in the amorphous region forming a clathrate structure. As the solvent treated HDPE samples were heated, a high but constant rate of volatilisation of solvent at the sample surface, through capillary fluid transport from internal solvent pockets, is sustained over a constant rate period denoting the first stage of evaporation. This constant rate period is swiftly followed by the second stage of evaporation in porous material termed falling rate period which is diffusion controlled.

The two hypothetical models were tested to establish the appropriate one using Microsoft Excel Solver optimisation tool to minimise their sum of squared residuals and then calculating their respective standard error of estimates (S_ε) for each sample. Accordingly, model 2 representing Raoult's law (equation 5.4) appears to be more plausible compared to model 1 representing drying of a porous material (equation 5.4), as can be seen from Figure 5.27(a – c) and indicated by their S_ε shown therein.

$$A_c = MIN[M(Log\mathrm{X}_{solv}) + C_1, C_2] \quad 5.3$$

$$A_c = M(Log\mathrm{X}_{solv}) + C \quad 5.4$$

Where: A_c = Antoine coefficient A; M = Slope; X_{solv} = mole fraction of solvent in solvent-treated HDPE; C_1 = intercept for declining rate phase for model 1; C_2 = intercept for constant rate phase for model 1; C = intercept for model 2.

Model 1 can be seen to have an insignificant or very short constant evaporation rate phase and appears to reduce to model 2 with the exception of PE-nC16 in which it is significant and returns a lower S_ε.

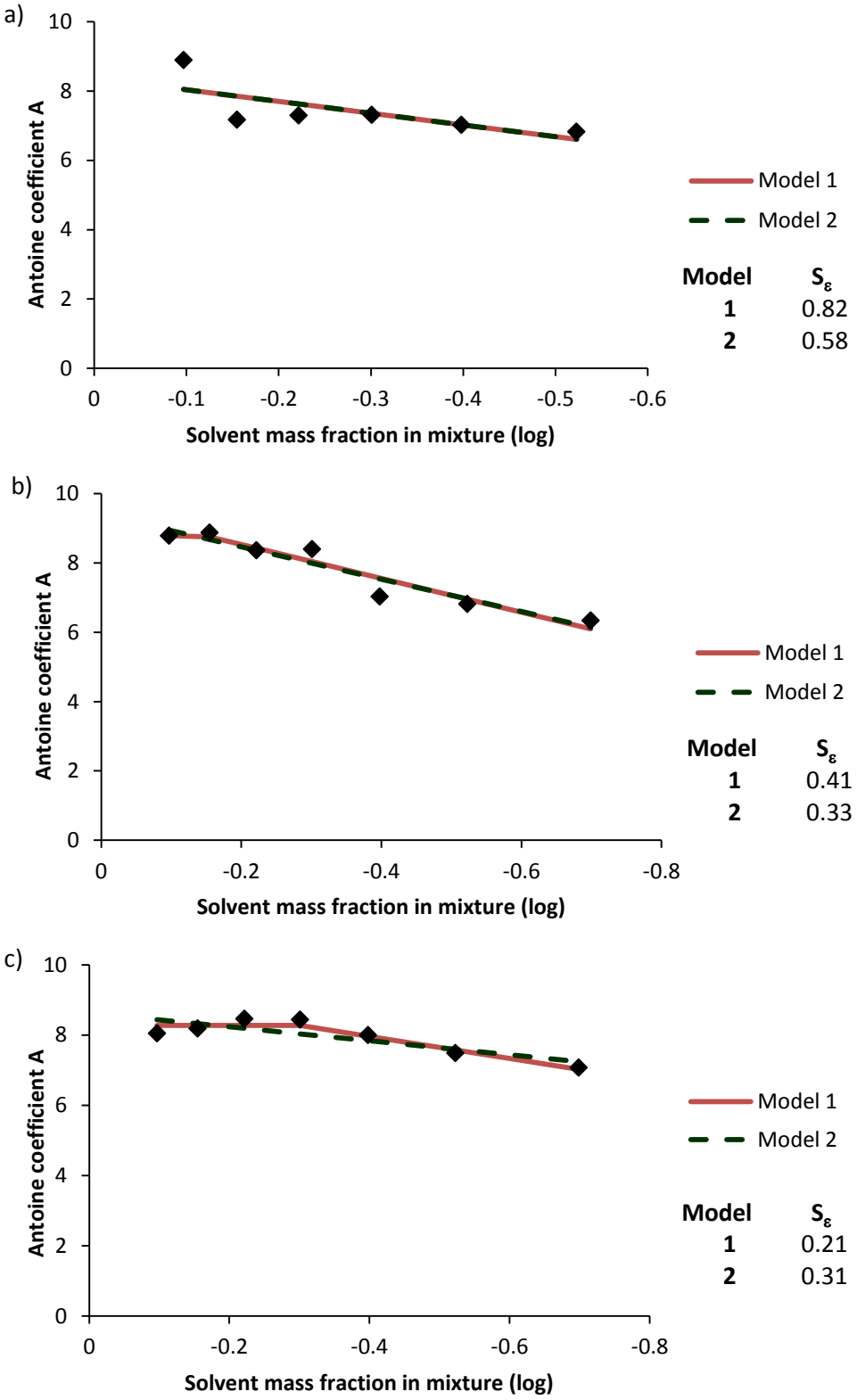

Figure 5.27: Standard Error of Estimates for a) PE-nC14; b) PE-nC15 and c) PE-nC16

5.3 COUPLING AND CALIBRATION OF THE CUSTOMISED SEALED-VESSEL IMPELLER VISCOMETER

The sealed-vessel impeller viscometer was coupled as shown in Figure 4.8 and calibrated as prescribed by Metzner and Otto (1957) and summarised on page 91 - 92 of chapter 4. The sealed-vessel impeller was designed to facilitate the safe use and refluxing of the sacrificial volatile saturated hydrocarbon solvent due to the preliminary results on the effects of the solvent treatment of the HDPE which revealed a lowering of the melting peak temperature. This observed solvent effect is similar to the effect of VGO on LDPE reported by Marcilla et al. (2008) which was accompanied by viscosity reductions with increasing VGO concentration. The customised impeller viscometer is also designed to function as a combination reaction vessel and viscometer to enable in situ measurement of viscosity for which expensive conventional viscometers are not suitable for risk of misuse and damage.

The design of customised impeller viscometer was undertaken due to the limitations of conventional viscometers or rheometers, nature of the experimental process and materials. The HDPE modification via solvent treatment was carried out using volatile solvents which required refluxing conditions and sealed environment. The very high viscosities of plastics also made it risky using an expensive viscometer or rheometer.

Torque readings were taken at predefined impeller speeds (0.8, 1.7, 2.5, 3.3, 4.2, 5.0 rps) in the empty vessel to account for any extraneous torque reading from bearings and glands on the device. During torque measurement, torque was observed to increase to an initial peak value (M_i), as the impeller accelerated to its set speed, and subsequently decline to a

"horizontal" asymptote (M_a) as shown in Figure 5.28 below. Consequently, torque measurements (M_t) were taken over a time duration of about 5 minutes and fitted to an

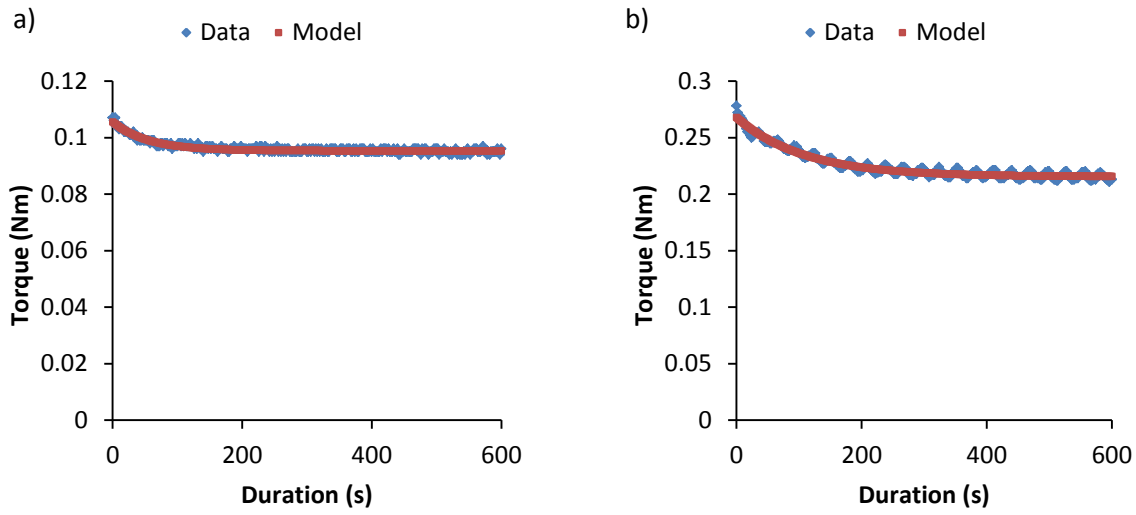

Figure 5.28: Torque measurement over time at a) 0.8 rps and b) 5 rps for 5.9 Pas Silicone oil at 25^{o}C

exponential decay equation (equation 5.5) using MS Excel Solver optimisation tool.

$$M_t = M_i e^{kt} + M_a \qquad 5.5$$

Where: M_t is torque reading from overhead stirrer at time, t; M_i is initial torque; M_a is asymptotic torque; k is the rate of torque decay.

M_a was used as the torque value in further calculations to generate the power curve data and determine the shape factor (C_{SF}) for the impeller viscometer.

The M_a readings from a blank vessel were first obtained and subjected to F-statistics test under a null hypothesis that the observed torque readings did not show any linear trend (i.e. neither increased nor decreased) as impeller speed was varied from 0.8 to 5.0 rps. As before, the null hypothesis statement is accepted if the F-statistic value (F_{stat}) calculated for

the observed values is less than the F-critical (F_{crit}) value that corresponds to the degrees of freedom (df) for the data set. The observations from the blank vessel calibration and the F-statistic parameters (F_{stat}, F_{crit}, df_1 and df_2) for the data set are presented in Figure 5.29 below. The null hypothesis, H_0: $F_{stat} < F_{crit}$, was accepted and the mean value of the

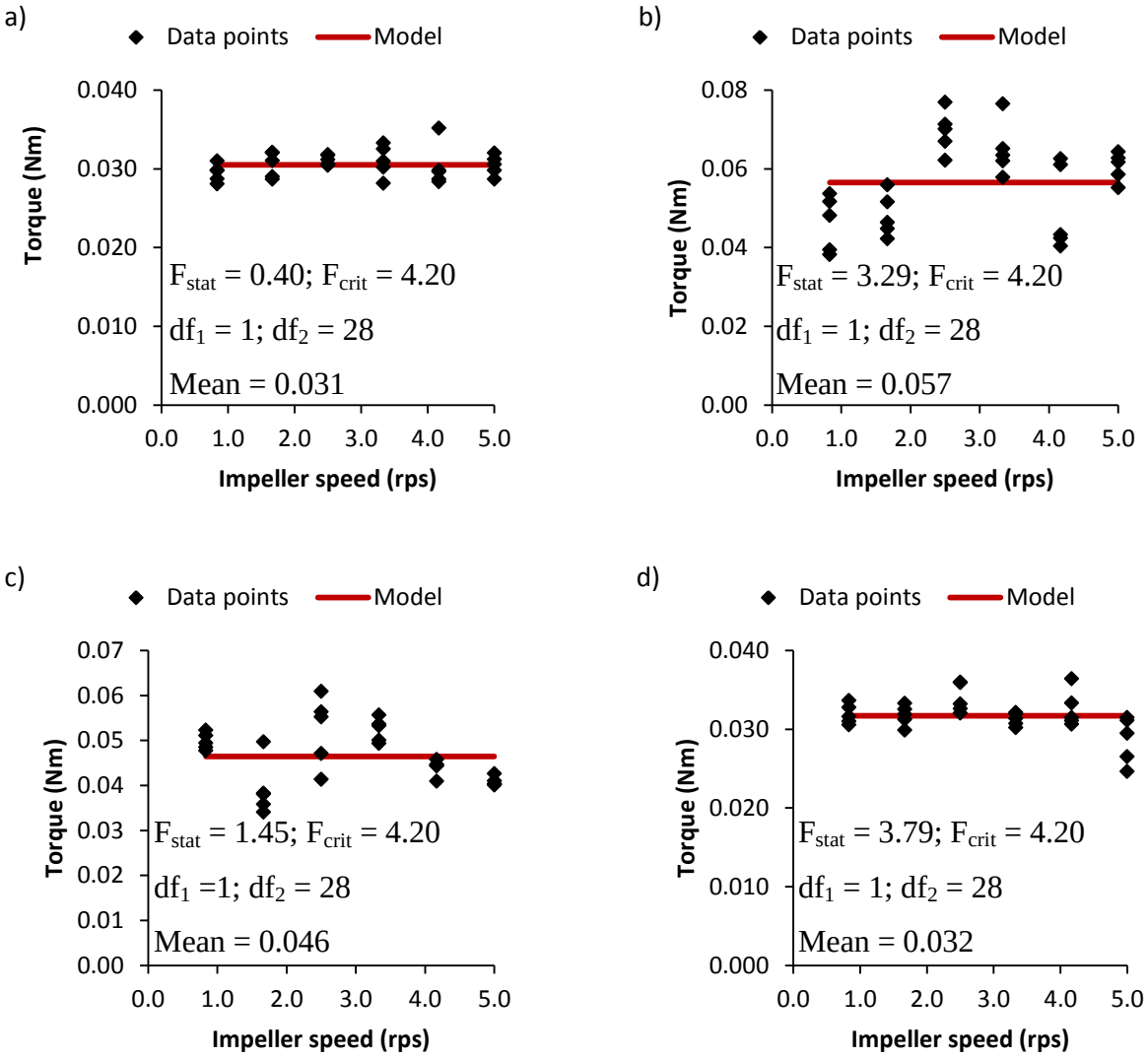

Figure 5.29: Sealed-vessel impeller viscometer blank calibration runs at a) 15°C, b) 20°C, c) 25°C and d) 35°C

observed data points was taken as the torque value due to restrictions from the device bearings and glands. These blank run, constant torque, values were deducted from torque

calibration values from charged vessel to yield residual torque values used for further calculations.

The Newtonian and non-Newtonian calibration fluids, silicone oil and Carboxymethylcellulose (CMC) were characterised as shown in Table 5.10 below.

Table 5.10: Characterisation results of calibration fluids

T	Silicone oils		CMC 2%			CMC 2.25%		
(^{o}C)	μ (Pa.s)	ρ (kg/m^3)	K (Pa.s^n)	n	ρ (kg/m^3)	K (Pa.s^n)	n	ρ (kg/m^3)
30	4.9	965						
25	5.9	970	58	0.25	1007	112	0.23	1008
	7.3	970						
20	8.2	975	65	0.24	1008			
15	9.1	980						

Residual torque values from calibration runs with the vessel charged with the silicone oils were deduced and Reynolds numbers (Re) and Power numbers (Po) derived accordingly (equation 2.27 and 2.28) as shown in Table 5.11. C_{SF} was subsequently determined according to equation 2.30 and shown graphically as the intercept of the power curves in Figure 5.30 (a-e). C_{SF} determination was carried out using MS Excel Solver tool, with the slope constrained to equate to -1. From the results of the calibration carried out using silicone oils of different viscosities, the C_{SF} values determined were found to have a somewhat linear trend with the silicone oils as it increased with viscosity. It is pertinent to note that the calibration runs carried out to determine C_{SF} were initially done at 25^{o}C with 5.9 Pas and 7.3 Pas viscosity silicone oils and then repeated at other temperatures (and viscosities) to authenticate the C_{SF} value, which should remain approximately constant, and ensure robustness of the calibration.

Please note that a row of data was removed from Table 5.13, for each impeller speed to prevent the table spilling over into the next page. Removed data can be found in Table A.10 in appendices.

Table 5.11: Torque calibration and power curve data

N (rps)	Residual Torque					Re					Po				
	9.1 Pas (15°C)	8.2 Pas (20°C)	5.9 Pas (25°C)	7.3 Pas (25°C)	4.9 Pas (35°C)	9.1 Pas (15°C)	8.2 Pas (20°C)	5.9 Pas (25°C)	7.3 Pas (25°C)	4.9 Pas (35°C)	9.1 Pas (15°C)	8.2 Pas (20°C)	5.9 Pas (25°C)	7.3 Pas (25°C)	4.9 Pas (35°C)
0.8	0.056	0.025	0.049	0.047	0.049	0.5744	0.6341	0.8768	0.7087	1.0503	156.6167	70.2227	139.3656	134.9743	139.6388
0.8	0.051	0.030	0.049	0.050	0.050	0.5744	0.6341	0.8768	0.7087	1.0503	143.8021	84.3371	139.2634	143.4153	144.3639
0.8	0.054	0.032	0.051	0.050	0.053	0.5744	0.6341	0.8768	0.7087	1.0503	152.9380	90.4892	145.3594	142.0023	151.9857
0.8	0.055	0.030	0.052	0.050	0.043	0.5744	0.6341	0.8768	0.7087	1.0503	155.3998	85.9589	148.3113	143.4043	122.4931
1.7	0.103	0.070	0.084	0.087	0.080	1.1487	1.2683	1.7537	1.4174	2.1007	72.8508	49.2874	59.9680	61.9556	56.8850
1.7	0.098	0.064	0.087	0.092	0.080	1.1487	1.2683	1.7537	1.4174	2.1007	69.1879	45.5392	62.0930	65.6549	57.5802
1.7	0.099	0.069	0.089	0.095	0.082	1.1487	1.2683	1.7537	1.4174	2.1007	69.5369	48.8978	63.0301	67.7992	58.3159
1.7	0.105	0.079	0.088	0.096	0.084	1.1487	1.2683	1.7537	1.4174	2.1007	74.2523	56.1623	62.3018	68.2462	60.1326
2.5	0.161	0.101	0.109	0.122	0.108	1.7231	1.9024	2.6305	2.1260	3.1510	50.5569	31.7009	34.5245	38.7238	34.3198
2.5	0.159	0.110	0.107	0.129	0.113	1.7231	1.9024	2.6305	2.1260	3.1510	49.9286	34.6222	33.7831	40.7496	35.8481
2.5	0.160	0.117	0.105	0.128	0.108	1.7231	1.9024	2.6305	2.1260	3.1510	49.9876	36.8238	33.1500	40.6415	34.4920
2.5	0.150	0.122	0.105	0.124	0.113	1.7231	1.9024	2.6305	2.1260	3.1510	46.8891	38.4559	33.2064	39.1870	35.9261
3.3	0.198	0.143	0.125	0.151	0.141	2.2974	2.5366	3.5073	2.8347	4.2014	34.8936	25.3589	22.1948	26.8406	25.1423
3.3	0.196	0.170	0.127	0.151	0.138	2.2974	2.5366	3.5073	2.8347	4.2014	34.5825	30.0316	22.5566	26.9160	24.6296
3.3	0.197	0.153	0.128	0.148	0.139	2.2974	2.5366	3.5073	2.8347	4.2014	34.7481	27.0819	22.8416	26.2804	24.8949
3.3	0.205	0.161	0.131	0.152	0.135	2.2974	2.5366	3.5073	2.8347	4.2014	36.0175	28.4593	23.3689	27.0441	24.2031
4.2	0.228	0.204	0.152	0.192	0.180	2.8718	3.1707	4.3842	3.5434	5.2517	25.7158	23.0726	17.3040	21.8096	20.5619
4.2	0.234	0.206	0.159	0.194	0.163	2.8718	3.1707	4.3842	3.5434	5.2517	26.4172	23.3567	18.0592	22.1281	18.6749
4.2	0.235	0.207	0.157	0.198	0.170	2.8718	3.1707	4.3842	3.5434	5.2517	26.4324	23.4876	17.8594	22.5611	19.5012
4.2	0.239	0.196	0.160	0.190	0.164	2.8718	3.1707	4.3842	3.5434	5.2517	26.8831	22.1971	18.1943	21.6207	18.8024
5.0	0.289	0.265	0.169	0.215	0.187	3.4462	3.8049	5.2610	4.2521	6.3020	22.6211	20.8290	13.3758	16.9798	14.8351
5.0	0.289	0.219	0.174	0.213	0.193	3.4462	3.8049	5.2610	4.2521	6.3020	22.6554	17.2546	13.7833	16.8070	15.3613
5.0	0.285	0.244	0.170	0.213	0.197	3.4462	3.8049	5.2610	4.2521	6.3020	22.3291	19.2027	13.4610	16.8447	15.6200
5.0	0.230	0.219	0.171	0.214	0.194	3.4462	3.8049	5.2610	4.2521	6.3020	18.0263	17.2276	13.4884	16.9598	15.4198

a)

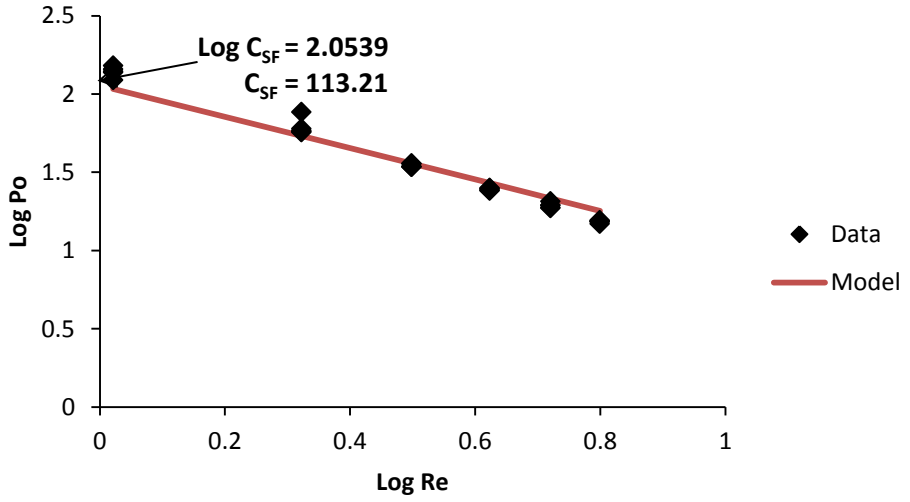
Log C_{SF} = 2.0539
C_{SF} = 113.21
Log Po
Log Re
Data
Model

b)

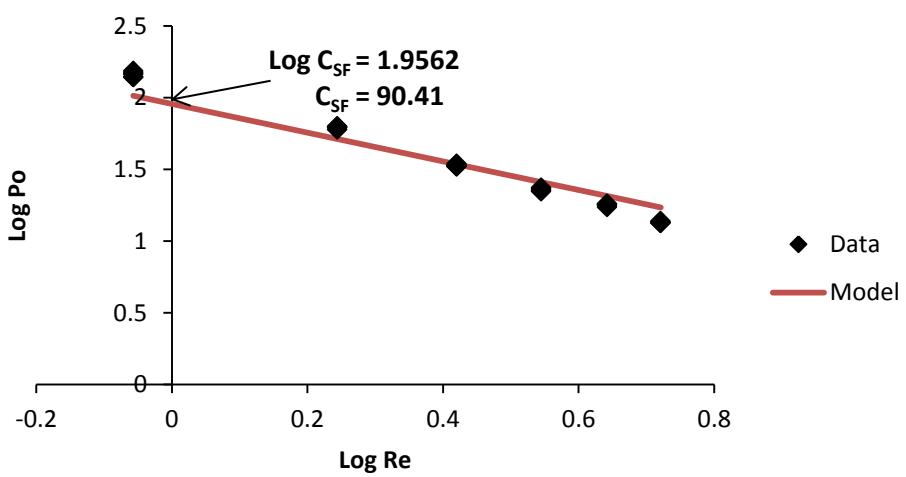
Log C_{SF} = 1.9562
C_{SF} = 90.41
Log Po
Log Re
Data
Model

c)

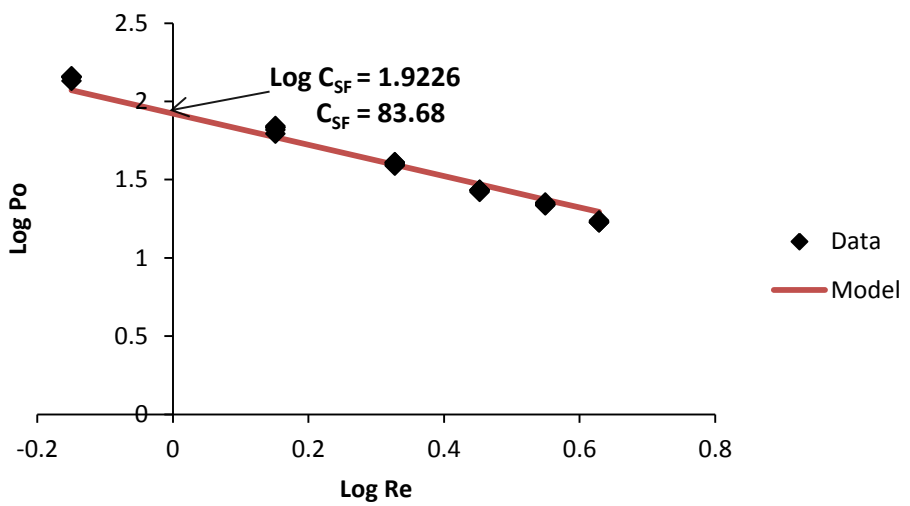
Log C_{SF} = 1.9226
C_{SF} = 83.68
Log Po
Log Re
Data
Model

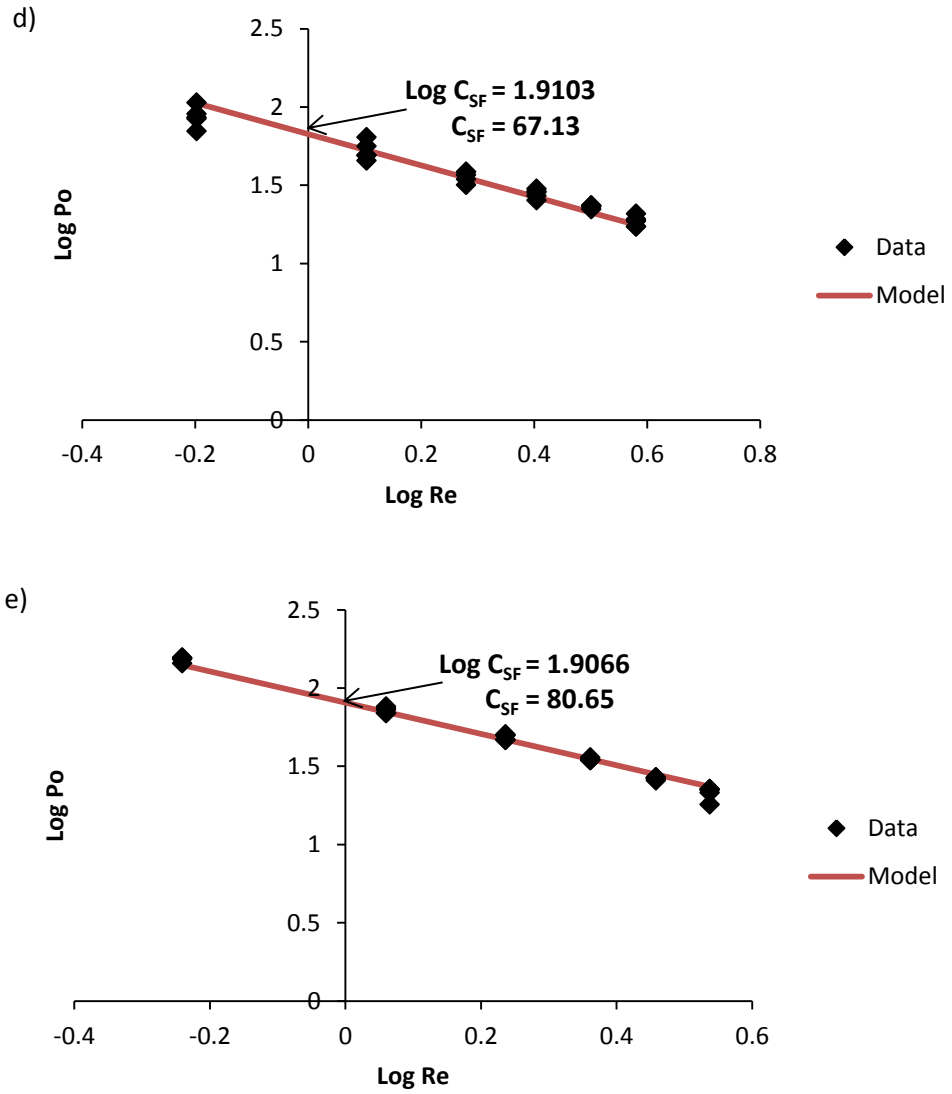

Figure 5.30: Power curves for Newtonian calibration fluids (silicone oils) of different viscosities- (a) 4.9 Pas at 35 ^{o}C, (b) 5.9 Pas at 25 ^{o}C, (c) 7.3 Pas at 25 ^{o}C, (d) 8.2 Pas at 20 ^{o}C and (e) 9.1 Pas at 15 ^{o}C

Given the foregoing result, C_{SF} consequently was recalculated using a master power curve by combining Re and Po data extracted from each of the silicone oils used for calibration as shown Figure 5.31 below.

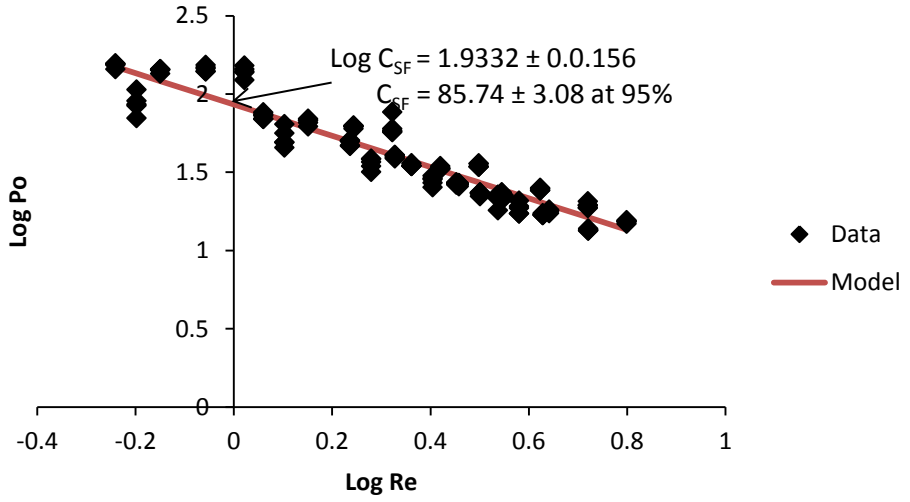

Figure 5.31: Master power curve using combined data from Newtonian calibration fluids (silicone oils 4.9 Pas at 35 ^{o}C, 5.9 Pas and 7.3 Pas at 25 ^{o}C, 8.2 Pas at 20 ^{o}C and 9.1 Pas at 15 ^{o}C)

The apparent dependency of C_{SF} on viscosity of the Newtonian calibration fluids is being attributed to extraneous torque readings due to interferences from mechanical seals and stability issues. As may be observed in equations 2.26 – 2.28, the torque component of Po counteracts the viscosity component of Re, both of which determine the constant C_{SF}. Equation 5.6 below, a simplified form of equation 2.26, clearly illustrates this relationship between viscosity and torque on one hand, and C_{SF} on the other hand.

$$C_{SF} = \frac{2\pi M}{ND^3\mu} \qquad 5.6$$

With the exception of torque, all other components or parameters of C_{SF}, a function of the impeller rotational speed, are constants or machine independent. The torque effect on C_{SF} is further manifested in Figure 5.32 and Figure 5.33. Figure 5.32 clearly shows that Log

Re, which contains the viscosity parameter, has no effect on Log C_{SF}. This was validated by subjecting the experimental data to F-statistics test under a null hypothesis that the observed C_{SF} values did not show any linear dependency on Reynolds number and thus a random scatter. This hypothesis is accepted if the F-statistic (F_{stat}) for the data is less than the F-critical (F_{crit}) value that corresponds to the degrees of freedom (df) for the same data

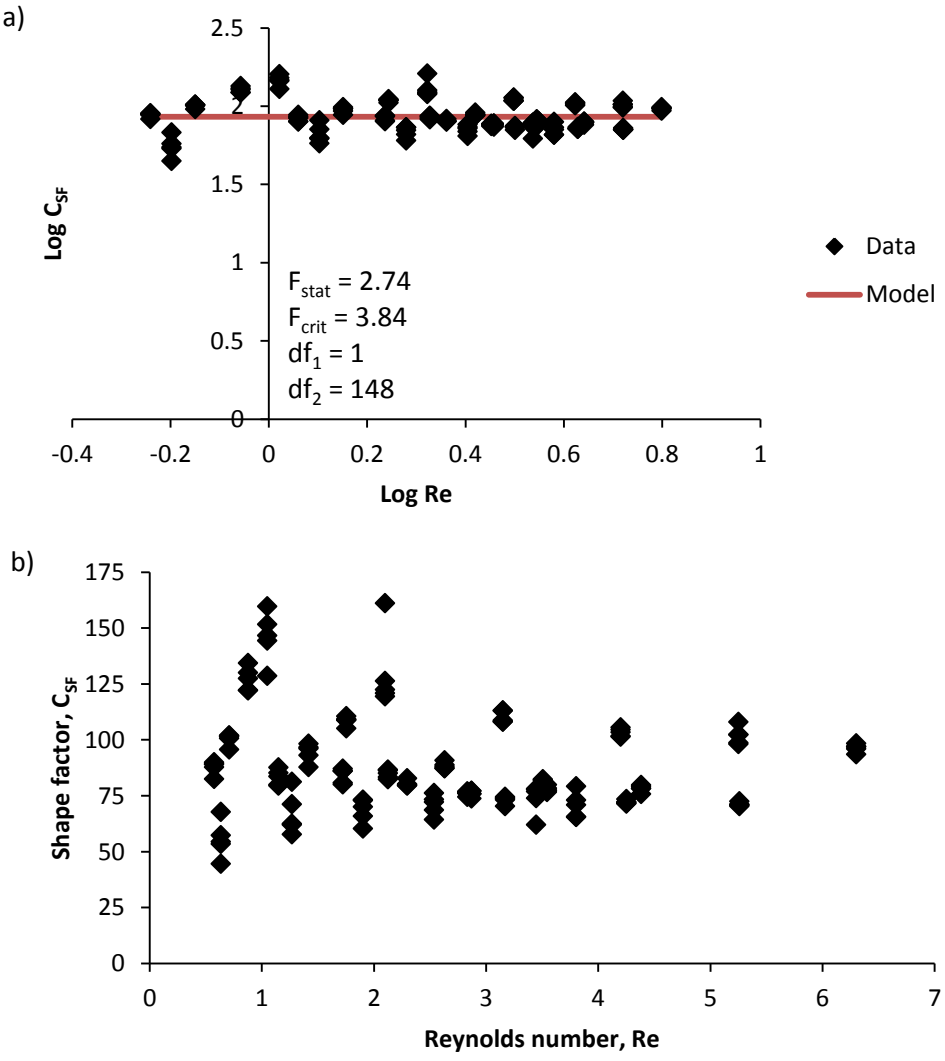

Figure 5.32: Effect of (a) Log Re on Log C_{SF} and (b) Re on C_{SF}

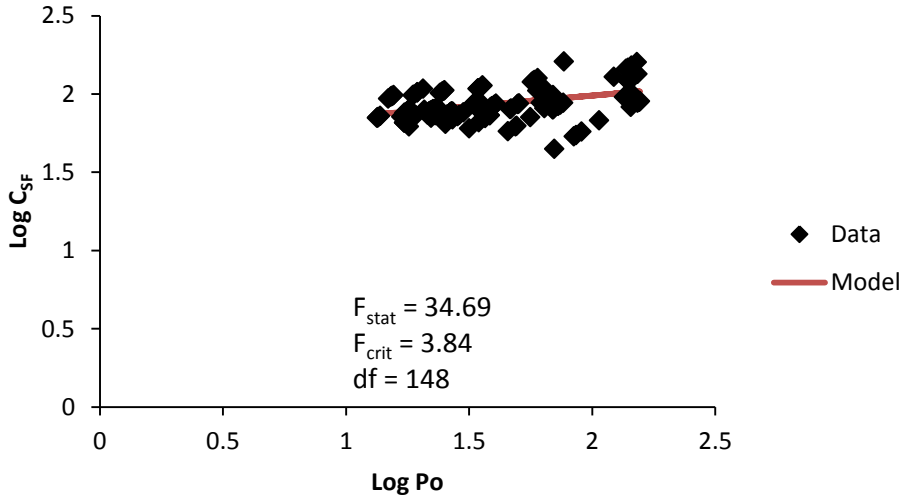

Figure 5.33: Effect of Log Po on Log C_{SF}

set at 95% confidence interval and vice versa if F_{stat} is greater than F_{crit}. In the case of Figure 5.33a, the hypothesis was accepted as F_{stat} was less than F_{crit} and as a result C_{SF} was taken as the mean of the data points. Figure 5.32b shows the scatter of C_{SF} values at each Reynolds number reduces as Reynolds number increases. Reynolds number increases as the impeller rotational speed increases and/or viscosity reduces. Since the viscosity of each Newtonian calibration fluid is a machine independent parameter, the rotational speed, independent variable, produced low torque values at low rotational speeds which contained substantial blank calibration torque values (35 - 70% at 0.8 rps as opposed to 10 - 22% at 5 rps). Thus torque values produced at low rotational speeds were more susceptible to errors that may be contained in the blank calibration torque compared to the higher torque values at higher rotational speed.

By way of validating the C_{SF} value from the master curve determined to be 85.74 ± 3.08 at 95% level of confidence, the mean value of the C_{SF} distribution in Figure 5.32b, derived using equation 2.26 from each data point generated with the silicone oils at different

temperatures and corresponding viscosities (Table 5.11), was taken. This method yielded a C_{SF} value of 87.97 ± 3.38 at a confidence level of 95%, but was seen to have been taken from a non-normal data as revealed in Figure 5.34. Figure 5.34 displays the result of the Anderson-Darling normality test, among other descriptive statistics results, conducted using MINITAB® statistical software. The Anderson-Darling normality test tests the data against a null hypothesis that the data is sampled from a normally distributed population at a given significance level (α), the probability that the data is not normal (0.05 or 5% in this case) (Minitab., 2012). The test returns a p-value, which indicates the probability that the data conforms to the null hypothesis, and an Anderson-Darling statistic, A^2, a measure of the difference between the empirical cumulative distribution function of an observed data with that of normally distributed data (Minitab., 2012). The p-value is compared with the significance level (α) and is used to accept the hypothesis of normality, when the p-value is greater than the chosen significance level, or reject it, if the p-value is less than or equal to the significance. The Anderson-Darling statistic on the other hand is used to compare how well a sample data fits various parametric distributions and data transformation models.

Probability plots of the data were created and a goodness of fit test conducted using MINITAB® comparing the distribution of the data to 14 parametric distributions and 2 data transformation models as shown in Table 5.12. Going by the p-values of the results, corroborated by the A^2 values, the null hypothesis of normality was rejected for all 14 distributions and the Box-Cox transformation model with the exception of the Johnson transformation model at a significance level of 0.05. Hence, the C_{SF} data distribution was

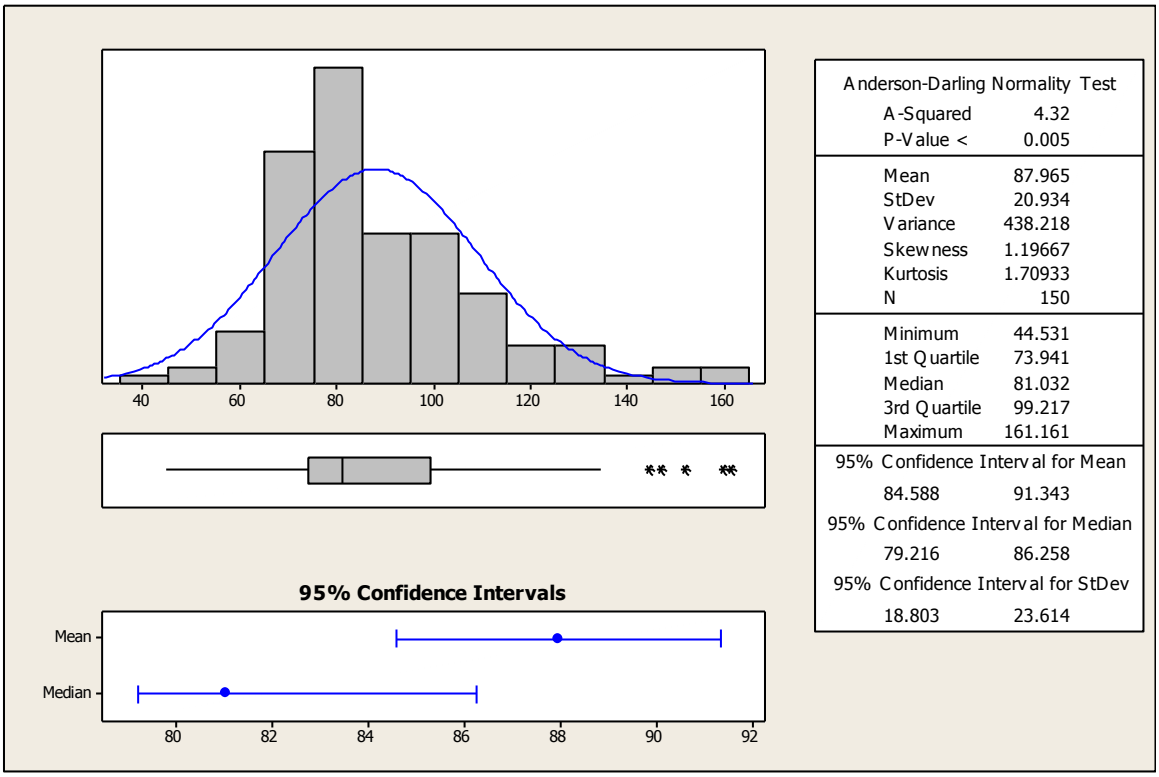

Figure 5.34: Descriptive statistics summary of C_{SF} data

Table 5.12: MINITAB goodness of fit test results

Distribution	AD (A^2)	P
Normal	4.317	<0.005
Box-Cox Transformation	1.267	<0.005
Lognormal	1.933	<0.005
3-Parameter Lognormal	1.384	*
Exponential	42.921	<0.003
2-Parameter Exponential	22.075	<0.010
Weibull	5.728	<0.010
3-Parameter Weibull	2.953	<0.005
Smallest Extreme Value	10.127	<0.010
Largest Extreme Value	1.182	<0.010
Gamma	2.584	<0.005
3-Parameter Gamma	1.737	*
Logistic	3.051	<0.005
Loglogistic	1.621	<0.005
3-Parameter Loglogistic	1.030	*
Johnson Transformation	0.549	0.155

transformed using the Johnson transformation model equation (equation 5.7) to produce a transformed C_{SF} distribution (C_{SF}'). Despite the Johnson transformation passing the null hypothesis of normality, C_{SF}' still exhibited a non-normal distribution as indicated by the result of its descriptive statistics vis-a-vis the skew and the divergence of the median from the mean of the data as shown in Figure 5.35. After back transformation, a mean C_{SF} of 82.16 with lower and upper critical limits of 79.89 and 84.72, and a median of 81.03 with

$$C'_{SF} = -1.13174 + 1.05083 \times \text{Asinh}\left(\frac{C_{SF}-69.9855}{9.83482}\right) \quad 5.7$$

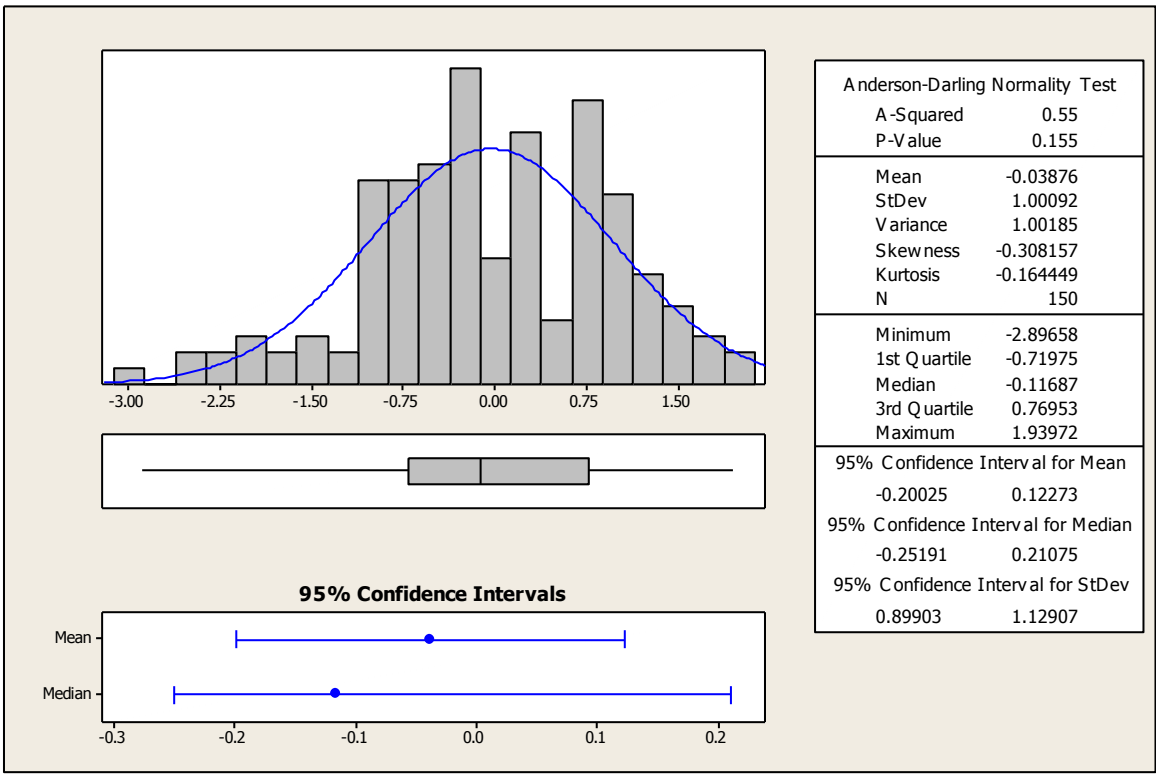

Figure 5.35: Descriptive statistics summary of Johnson transform C_{SF} data

lower and upper critical limits of 79.21 and 86.26 were obtained, both at 95% confidence level. Consequently the median C_{SF} value from the original skewed data distribution,

which remained unchanged after the Johnson transformation was performed, was chosen as the true C_{SF} value. Moreover, it was observed that the divergence between the mean and median C_{SF} value of the transformed data distribution was reduced compared with the divergence in the original data, thus approaching the median.

The shear rate conversion factor, k', for the sealed impeller viscometer was determined with the aid of the 2% and 2.25% CMC non-Newtonian calibration fluids (Table 5.10) according to according to steps 3 – 6 of the Metzner and Otto (1957) calibration procedure on page 92. As with the Newtonian calibration fluids, residual torque values were also extracted from the sealed-vessel impeller viscometer, charged with Carboxymethylcellulose (CMC), from which Power number values were derived. Reynolds numbers corresponding to the Power numbers were derived using equation 2.27 using the C_{SF} and its lower and upper critical limits at 95% confidence levels, with apparent viscosities and shear rates subsequently calculated using equations 2.21 and 2.4b, respectively, as shown in Table 5.13. Table 5.13 also shows the shear rate conversion factors, k', derived using equation 2.29 for each of the CMC calibration fluids at derived the C_{SF} value and its lower and upper critical limits. Given the similarities between the pairs of k' values obtained, average conversion factor values, at the C_{SF} value and its lower and upper critical limits, for the sealed-vessel impeller viscometer were derived as shown in Figure 5.36 using the combined data from both CMC calibration fluids.

Please note that a row of data was removed from Table 5.13, for each impeller speed to prevent the table spilling over into the next page. Removed data can be found in Table A.11 in appendices.

Table 5.13: Average shear rate (k') determination with non-Newtonian calibration fluids

N (rps)	2% CMC										2.25% CMC									
	Po	Lower C_{SF} (79.22)			C_{SF} (81.03)			Upper C_{SF} (82.26)			Po	Lower C_{SF} (79.22)			C_{SF} (81.03)			Upper C_{SF} (82.26)		
		Re	n	$\dot{Y}$	Re	n	$\dot{Y}$	Re	n	$\dot{Y}$		Re	n	$\dot{Y}$	Re	n	$\dot{Y}$	Re	n	$\dot{Y}$
0.8	63.1741	1.2540	4.3	32	1.2826	4.2	33	1.3654	3.9	36	180.2374	0.4395	12.2	18	0.4496	12.0	18	0.4786	11.2	20
0.8	82.1251	0.9646	5.6	23	0.9867	5.4	23	1.0503	5.1	25	192.5609	0.4114	13.1	16	0.4208	12.8	17	0.4480	12.0	18
0.8	96.5133	0.8208	6.5	18	0.8396	6.4	19	0.8938	6.0	21	196.2345	0.4037	13.3	16	0.4129	13.0	16	0.4396	12.2	18
0.8	99.1242	0.7992	6.7	18	0.8175	6.6	18	0.8702	6.2	20	190.6821	0.4155	12.9	17	0.4249	12.7	17	0.4524	11.9	18
1.7	25.6561	3.0878	3.5	43	3.1583	3.4	44	3.3622	3.2	48	47.0520	1.6837	6.4	41	1.7221	6.2	42	1.8333	5.9	46
1.7	34.9392	2.2674	4.7	28	2.3192	4.6	29	2.4689	4.4	32	50.9954	1.5535	6.9	37	1.5890	6.8	38	1.6915	6.4	42
1.7	31.8884	2.4843	4.3	32	2.5410	4.2	33	2.7051	4.0	36	49.2374	1.6089	6.7	39	1.6457	6.5	40	1.7519	6.1	44
1.7	32.0769	2.4697	4.3	32	2.5261	4.3	33	2.6892	4.0	35	48.6308	1.6290	6.6	40	1.6662	6.5	41	1.7738	6.1	44
2.5	14.2597	5.5555	2.9	54	5.6824	2.8	56	6.0492	2.7	61	24.3628	3.2517	5.0	57	3.3260	4.8	59	3.5406	4.6	64
2.5	11.6098	6.8235	2.4	71	6.9794	2.3	74	7.4299	2.2	80	26.1936	3.0244	5.3	52	3.0935	5.2	54	3.2932	4.9	58
2.5	11.8514	6.6844	2.4	69	6.8372	2.4	72	7.2785	2.2	78	22.8785	3.4626	4.7	62	3.5417	4.6	64	3.7703	4.3	70
2.5	12.0743	6.5611	2.5	68	6.7110	2.4	70	7.1441	2.3	76	22.5221	3.5174	4.6	64	3.5978	4.5	65	3.8300	4.2	71
3.3	8.8115	8.9905	2.4	70	9.1960	2.3	72	9.7895	2.2	79	15.0521	5.2631	4.1	74	5.3833	4.0	76	5.7308	3.7	82
3.3	8.2859	9.5608	2.2	76	9.7792	2.2	79	10.4104	2.1	85	15.7412	5.0327	4.3	70	5.1476	4.2	72	5.4799	3.9	78
3.3	8.2210	9.6363	2.2	77	9.8565	2.2	79	10.4926	2.0	86	15.4950	5.1126	4.2	71	5.2294	4.1	73	5.5670	3.9	79
3.3	8.3110	9.5320	2.3	76	9.7498	2.2	78	10.3791	2.1	85	15.6459	5.0633	4.2	70	5.1790	4.2	72	5.5133	3.9	78
4.2	5.0189	15.7844	1.7	111	16.1451	1.7	114	17.1871	1.6	124	9.6905	8.1750	3.3	98	8.3618	3.2	101	8.9015	3.0	109
4.2	5.3625	14.7729	1.8	101	15.1104	1.8	104	16.0857	1.7	113	12.2406	6.4719	4.1	72	6.6198	4.1	74	7.0470	3.8	81
4.2	5.9241	13.3724	2.0	89	13.6779	2.0	91	14.5608	1.8	99	10.9031	7.2658	3.7	84	7.4318	3.6	86	7.9115	3.4	94
4.2	5.7773	13.7124	2.0	92	14.0257	1.9	94	14.9309	1.8	103	10.7019	7.4024	3.6	86	7.5716	3.6	88	8.0603	3.3	96
4.2	5.7593	13.7551	2.0	92	14.0694	1.9	95	14.9775	1.8	103	10.7829	7.3468	3.7	85	7.5147	3.6	88	7.9997	3.4	95
5.0	4.3003	18.4220	1.7	107	18.8429	1.7	110	20.0591	1.6	119	7.1194	11.1274	2.9	115	11.3816	2.8	119	12.1162	2.7	129
5.0	4.3737	18.1129	1.8	104	18.5267	1.7	107	19.7225	1.6	117	7.4958	10.5687	3.0	108	10.8101	3.0	111	11.5079	2.8	120
5.0	5.0596	15.6574	2.1	86	16.0152	2.0	88	17.0489	1.9	96	7.8873	10.0439	3.2	101	10.2734	3.1	104	10.9365	2.9	113
5.0	4.8027	16.4950	2.0	92	16.8718	1.9	95	17.9608	1.8	103	7.6043	10.4178	3.1	106	10.6558	3.0	109	11.3436	2.8	118
5.0	4.9533	15.9935	2.0	88	16.3589	2.0	91	17.4148	1.9	99	7.7763	10.1874	3.2	103	10.4202	3.1	106	11.0927	2.9	115
	k'	**21.5**			**22.2**			**24.1**			k'	**21.3**			**21.9**			**23.8**		

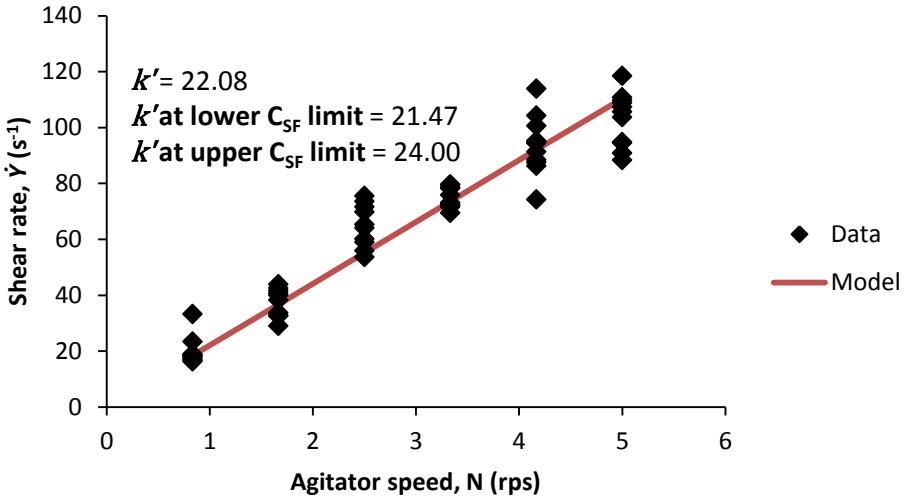

Figure 5.36: Average shear rate conversion factor (k')

5.4 VISCOSITY MEASUREMENT USING THE SEALED-VESSEL IMPELLER VISCOMETER

Based on the results of the DSC and TGA on the products of the HDPE solvent treatment performed under reflux with the 12-station carousel, pentadecane, which appeared to have the best reducing effect on HDPE melting (Figure 5.10 and Figure 5.11) and decomposition (Figure 5.19 and Figure 5.21) temperatures after treatment, was chosen as the treatment solvent.

334 grammes of HDPE pellets was mixed with 501 grammes pentadecane solvent to create a 40:60 PE-nC15 mixture in the sealed-vessel impeller viscometer. Temperature was controlled electrically via a heating mantle but was difficult to regulate. The viscometer was started at an impeller rotational speed of 3.3 rps (200 rpm) which corresponds to a shear rate of between $71s^{-1}$ and $80s^{-1}$ at 95% confidence level, and an initial temperature of

24.8 ^{o}C and run for about 21 hours. Residual torque readings were generated at the defined impeller rotational speed from which viscosity values were derived using equation 5.6 and the shape factor constant at its 95% confidence interval limits as shown in Table 5.14. A blank torque value and its 95% confidence limits were generated by combining the data points from the blank calibration runs done at 15, 20, 25 and 35 ^{o}C and taking the median of the torque distribution across the impeller rotational speed.

Table 5.14: Agitation and viscosity estimation of a 40:60 PE-nC15 mixture using the sealed-vessel viscometer

		Torque (Nm)				η (CSF = 79.22)			η (CSF = 81.03)			η (CSF = 82.26)		
t (hr)	T ^{o}C	M_A	M_R	M_{LCL}	M_{UCL}	(M_R)	(M_{LCL})	(M_{UCL})	(M_R)	(M_{LCL})	(M_{UCL})	(M_R)	(M_{LCL})	(M_{UCL})
0	24.8	0.258	0.224	0.227	0.217	10.4	10.5	10.1	10.2	10.3	9.9	10.4	10.5	10.1
1.67	200.0	0.217	0.183	0.186	0.176	8.5	8.6	8.2	8.3	8.5	8.0	8.5	8.6	8.2
4.25	219.0	0.214	0.180	0.183	0.173	8.4	8.5	8.0	8.2	8.3	7.9	8.4	8.5	8.0
8.00	202.0	0.215	0.181	0.184	0.174	8.4	8.6	8.1	8.2	8.4	7.9	8.4	8.6	8.1
8.40	206.0	0.213	0.179	0.182	0.172	8.3	8.5	8.0	8.1	8.3	7.8	8.3	8.5	8.0
9.01	228.0	0.198	0.164	0.167	0.157	7.6	7.8	7.3	7.5	7.6	7.1	7.6	7.8	7.3
9.41	231.0	0.195	0.161	0.164	0.154	7.5	7.6	7.2	7.3	7.5	7.0	7.5	7.6	7.2
10.00	237.0	0.190	0.156	0.159	0.149	7.2	7.4	6.9	7.1	7.2	6.8	7.2	7.4	6.9
10.60	243.0	0.190	0.156	0.159	0.149	7.2	7.4	6.9	7.1	7.2	6.8	7.2	7.4	6.9
11.01	248.0	0.186	0.152	0.155	0.145	7.1	7.2	6.7	6.9	7.0	6.6	7.1	7.2	6.7
11.45	251.0	0.187	0.153	0.156	0.146	7.1	7.2	6.8	7.0	7.1	6.6	7.1	7.2	6.8
19.40	223.0	0.189	0.155	0.158	0.148	7.2	7.3	6.9	7.0	7.2	6.7	7.2	7.3	6.9
20.85	209.0	0.194	0.160	0.163	0.153	7.4	7.6	7.1	7.3	7.4	7.0	7.4	7.6	7.1

Where: M_A = actual torque; M_R = residual torque; M_{LCL} = lower critical limit torque; M_{uCL} = upper critical limit torque.

It can be seen from Table 5.14 that the viscosity of the mixture, initially a suspension of pellets in the pentadecane solvent, dropped from between 9.9 - 10.5 Pas at ambient temperature, to around 7 Pas at around 250^{o}C. This shows a significant drop in viscosity from the 1400 - 1300 Pas obtained using the Rosand RH7 twin-bore rheometer at similar shear rates i.e. 71s^{-1} and 80s^{-1}.

DSC measurements of the extrapolated onset and peak temperatures of melting were also undertaken on the product of 40:60 PE-nC15 mixture carried out in the sealed-vessel impeller viscometer in comparison to the pure HDPE sample as was done in the preliminary experiments in the 12-station carousel. TGA measurements were also undertaken of the extrapolated onset and peak maximum temperatures of decomposition likewise. As was observed then, the extrapolated onset and peak temperatures of melting of the PE-nC15 (40:60) samples all experienced significant reduction from corresponding values obtained from pure HDPE samples summarised in Table 5.15 below (see Figure A.8 and A.9 appendices for endotherms). Decomposition onset temperatures as well as peak maximum temperatures were also observed to have reduced likewise but only marginally as shown in Table 5.16 (See Figures A.16 and A.17 of the appendices for TGA curves Run 1 for both HDPE and PE-nC15).

Table 5.15: Effect of pentadecane solvent-treatment on HDPE melting temperatures.

Samples	Run	Melting temperatures(°C)	
		Onset	Peak
HDPE	1	120.9	125.3
	2	120.6	127.4
	3	120.8	129.7
PE-nC15	1	106.1	112.3
	2	108.6	111.0
	3	107.1	112.5

Table 5.16: Effect of pentadecane solvent-treatment on HDPE decomposition temperatures

Samples	Run	Decomposition temperatures(°C)	
		Onset	Peak
HDPE	1	443.9	462.8
	2	443.1	462.4
	3	443.5	462.5
PE-nC15	1	438.8	459.6
	2	437.0	458.1
	3	437.5	458.6

6 CONCLUSION AND RECOMMENDATIONS

6.1 CONCLUSION

To assess the viability of hydrocracking mixed plastic waste from a rheological standpoint, rheological characterisation of five main polymers was undertaken having highlighted high viscosity as a major heat and mass transfer impediment in the chemical recycling of plastics in the course of the literature review. For operations in the petroleum industry, such as hydrocracking, a viscosity specification of not more than 0.5 Pas is demanded of feedstock at 200^{o}C. Solvent treatment was carried out on HDPE in customised sealed-vessel impeller viscometer, which was calibrated to extract viscosity measurements, by refluxing sacrificial volatile saturated hydrocarbon solvents at around their respective boiling temperatures.

At the end of the research, the following key inferences have been made

- Polymers are very viscous materials, the order of which was confirmed by characterising the five main polymer types namely HDPE, LLDPE, PP, PS and PET; viscosities at 200^{o}C being 400 – 1200 times the feedstock viscosity specification in the petrochemical industry (not more than 0.5 Pas) at shear rate of 500 s^{-1} (typical shear rate for pumping and atomisation operations). See Table 5.1.

- They were also found to be still extremely laminar over the range of shear rate and temperatures subjected to and observed to have a plug-like velocity profile which suggests the existence of a yield or critical stress that would have to be overcome for flow to commence.
- Boundary layer thicknesses were calculated and observed to diminish with shear rate in the transition phase between the shear-thinning and the Newtonian, zero shear-rate regions but were unaffected in the shear-thinning region.
- Temperature increase was observed to increase the boundary layer thickness in the shear-thinning region and appeared to induce the transitioning into the zero-shear-rate viscosity region in PS and PET melts at 250^{o}C and 300^{o}C respectively.
- DSC results of the solvent treated HDPE revealed that the melting temperatures, i.e. the extrapolated peak onset and the peak temperatures, both showed a reducing linear dependency with increasing solvent concentration for nC14, nC15 and nC16 while iC8 and nC10 had no discernible effect. Thus, the more volatile, shorter chain, hydrocarbon solvents with boiling points not significantly higher than the melting point of the polymer were ineffective while the less volatile, longer chain, hydrocarbon solvents interact with HDPE lowering its melting temperatures.
- Results of the TGA conducted on the solvent-treated HDPE using nC14, nC15 and nC16 revealed 2 weight loss regions consistent with vaporisation of the treatment solvents and pyrolysis of a HDPE residue, suggesting the formation of a clathrate, unlike the iC8 and nC10 treated HDPE
- The clathrates of each solvent-treated HDPE, i.e. PE-nC14, PE-nC15 and PE-nC16 (formed from initial solvent concentration of 20, 30, 40, 50, 60, 70 and 80% in PE-

solvent mixtures), were identified as ideal solutions obeying Raoult's law as opposed to a porous media undergoing drying. This was determined by first estimating vapour pressures of the volatising treatment solvent (first weight loss region of the TGA curve) from each clathrate using the modified Langmuir equation (equation 4.4) revealing a suppression of vapour pressure compared to that of the pure solvent. As there did appear to be a period of high constant vapour pressure between the initial high vapour pressure of the pure solvents and a declining vapour pressure phase synonymous with drying (or evaporation) from a saturated porous media, a model simulating the drying theory was tested against a Raoult's law model. Then the Antoine A coefficients for vapour pressures at the solvent concentration for each set of clathrates were fit to the drying theory model (equation 5.3) and the Raoult's law model (equation 5.4), and their respective standard error of estimate (S_ε) compared (Figure 5.27). In the case of nC16-treated HDPE, the Antoine A coefficients for vapour pressures at the solvent concentration fit the model for drying in porous media better, according the lower S_ε returned, although the difference between both models appear to be marginal

- The pyrolysis onset temperature of the HDPE residue of the solvent-treated HDPE product did not reveal any significant change with increasing solvent concentration with the exception of nC15 which had a decreasing effect
- Calibration of the sealed-vessel impeller was very tedious and time consuming especially as regards attaining calibration temperatures in the calibration fluids, and working with the non-Newtonian calibration fluids which exhibited thixotropy and had to be allowed to recover

- C_{SF} ,the shape factor for the sealed-vessel impeller viscometer was observed to exhibit an apparent inverse linear dependency on the viscosity of the Newtonian calibration fluids which has been attributed to extraneous torque readings, especially at low impeller rotational speeds, caused by interferences from mechanical seals and stability issues of the apparatus
- The true C_{SF} value for the sealed-vessel impeller viscometer was determined to be 81.03, the median of a distribution of C_{SF} values generated from individual variable impeller speed and corresponding torque reading for each calibration fluid, with 95% confidence interval limits of 79.21 and 86.26
- Corresponding shear rate conversion factors were (k', k'_{LCL} and k'_{UCL}) derived as 22.08, 21.47 and 24, respectively.
- Viscosity measurement of a 40:60 PE-nC15 mixture in the sealed-vessel impeller viscometer at a shear rate of between $71s^{-1}$ and $80s^{-1}$ at 95% confidence level and 250^{o}C was 7 Pas representing approximately 200 fold reduction from the virgin HDPE measured in the conventional Rosand RH7 twin-bore rheometer

6.2 RECOMMENDATIONS

Results of the solvent treatment using hydrocarbon solvents have revealed longer chain saturated hydrocarbon solvents nC14 – nC16 to be more effective sacrificial solvents than their more volatile, shorter chain counterparts which are more valuable. Longer chain hydrocarbons are however more susceptible to cracking but this can be reduced by shortening contact time. Despite the apparent positive result achieved with the calibration

of the sealed-vessel impeller viscometer the authenticity of the viscosity results needs to be validated through more testing using non-Newtonian calibration fluids of specifications different from those used for calibration. A more rigid design is needed to eliminate extraneous torque originating from mechanical seals and glands, as well as stability and alignment issues which affected the authenticity of the calibration results

REFERENCES

Achilias, D. S., Andriotis, L., Koutsidis, I. A., Louka, D. A., Nianias, N. P., Siafaka, P., Tsagkalias, I. & Tsintzou, G., 2012. Recent advances in the chemical recycling of polymers (PP, PS, LDPE, HDPE, PVC, PC, NYLON, PMMA). *In:* Achilias, D. S., ed. *Material recycling – trends and perspectives.* Rijeka: Intech.

Agassant, J. F., 1991. *Polymer processing: principles and modeling,* Munich: Hanser

Aguado, J. & Serrano, D. P., 1999. *Feedstock recycling of plastic wastes,* Cambridge: Royal Society Of Chemistry.

Aguado, J., Serrano, D. P. & Escola, J. M., 2006a. Catalytic upgrading of plastic. *In:* Scheirs, J. & Kaminsky, W., eds. *Feedstock recycling and pyrolysis of waste plastics: converting waste plastics into diesel and other fuels.* Chichester: Wiley.

Aguado, J., Serrano, D. P. & Escola, J. M., 2008. Fuels from waste plastics by thermal and catalytic processes: a review. *Industrial and engineering chemistry research,* 47**,** 7982-7992.

Aguado, J., Serrano, D. P., Escola, J. M. & Garagorri, E., 2002. Catalytic conversion of low-density polyethylene using a continuous screw kiln reactor. *Catalysis today,* 75**,** 257-262.

Aguado, J., Serrano, D. P. & San Miguel, G., 2007. European trends in the feedstock recycling of plastic wastes. *Global nest journal,* 9**,** 12-19.

Aguado, J., Serrano, D. P., Vicente, G. & Sánchez, N., 2006b. Effect of decalin solvent on the thermal degradation of hdpe. *Journal of polymers and the environment,* 14**,** 375-384.

Aguado, R., Olazar, M., Gaisán, B., Prieto, R. & Bilbao, J., 2003. Kinetics of polystyrene pyrolysis in a conical spouted bed reactor. *Chemical engineering journal,* 92 91–99

Al-Salem, S. M., 2009. Establishing an integrated databank for plastic manufacturers and converters in kuwait. *Waste management,* 29**,** 479-484.

Al-Salem, S. M., Lettieri, P. & Baeyens, J., 2009. Recycling and recovery routes of plastic solid waste (PSW): a review. *Waste management,* 29**,** 2625-2643.

REFERENCES

Al-Salem, S. M., Lettieri, P. & Baeyens, J., 2010. The valorization of plastic solid waste (PSW) by primary to quaternary routes: from re-use to energy and chemicals. *Progress in energy and combustion science,* 36**,** 103-129.

Ali, M. F., Ahmed, S. & Qureshi, M. S., 2011. Catalytic coprocessing of coal and petroleum residues with waste plastics to produce transportation fuels. *Fuel processing technology,* 92**,** 1109-1120.

Ali, M. F. & Siddiqui, M. N., 2005. Thermal and catalytic decomposition behavior of PVC mixed plastic waste with petroleum residue. *Journal of analytical and applied pyrolysis,* 74**,** 282-289.

Ali, M. F. & Siddiqui, M. N., 2006. The conversion of waste plastics/petroleum residue mixtures to transportation fuels. *In:* Scheirs, J. & Kaminsky, W., eds. *Feedstock recycling and pyrolysis of waste plastics : converting waste plastics into diesel and other fuels.* Chichester: Wiley.

Ali, M. F., Siddiqui, M. N. & Redhwi, S. H. H., 2004. Study on the conversion of waste plastics/petroleum resid mixtures to transportation fuels. *J mater cycles waste manage,* 6**,** 27-34.

Aminu, M. O., Elliott, J. A. W., Mccaffrey, W. C. & Gray, M. R., 2004. Fluid properties at coking process conditions. *Industrial and engineering chemistry research,* 43**,** 2929-2935.

Ancheyta, J. & Speight, J. G., 2007. *Hydroprocessing of heavy oils and residua,* Boca Raton: CRC Press.

Andrady, A. L., 2003a. Common plastics materials. *In:* andrady, a. L. (ed.) *Plastics and the environment.* Hoboken: Wiley-Interscience.

Andrady, A. L., 2003b. An Environmental Primer. *In:* Andrady, A. L. (ed.) *Plastics and the environment*. Hoboken: Wiley-Interscience.

Andrady, A. L., 2011. Microplastics in the marine environment. *Marine pollution bulletin,* 62**,** 1596-1605.

Andrady, A. L. & Neal, M. A., 2009. Applications and societal benefits of plastics. *Philosophical transactions of the royal society b-biological sciences,* 364**,** 1977-1984.

REFERENCES

Arandes, J. M., Abajo, I., López-Valerio, D., Fernández, I., Azkoiti, M. J., Olazar, M. & Bilbao, J., 1997. Transformation of several plastic wastes into fuels by catalytic cracking. *Industrial and engineering chemistry research,* 36**,** 4523-4529.

Arandes, J. M., Ereña, J., Azkoiti, M. J., López-Valerio, D. & Bilbao, J., 2003a. Valorization by thermal cracking over silica of polyolefins dissolved in LCO. *Fuel processing technology,* 85**,** 125-140.

Arandes, J. M., Ereña, J., Azkoiti, M. J., Olazar, M. & Bilbao, J., 2003b. Thermal recycling of polystyrene and polystyrene-butadiene dissolved in a light cycle oil. *Journal of analytical and applied pyrolysis,* 70**,** 747-760.

Arena, U. & Mastellone, M. L., 2006. Fluidized bed pyrolysis of plastic wastes. *In:* Scheirs, J. & Kaminsky, W., eds. *Feedstock recycling and pyrolysis of waste plastics: converting waste plastics into diesel and other fuels.* Chichester: Wiley.

Aznar, M. P., Caballero, M. A., Sancho, J. A. & Frances, E., 2006. Plastic waste elimination by co-gasification with coal and biomass in fluidized bed with air in pilot plant. *Fuel processing technology,* 87**,** 409-420.

Bagley, E. B., Cabott, I. M. & West, D. C., 1958. Discontinuity in the flow curve of polyethylene. *Journal of applied physics,* 29**,** 109-110.

Bagri, R. & Williams, P. T., 2002. Catalytic Pyrolysis Of Polyethylene. *Journal Of Analytical And Applied Pyrolysis,* 63**,** 29 - 44.

Barnes, D. K. A., Galgani, F., Thompson, R. C. & Barlaz, M., 2009. Accumulation and fragmentation of plastic debris in global environments. *Philosophical transactions of the royal society b-biological sciences,* 364**,** 1985-1998.

Barnes, H. A., 1997. Thixotropy - a review. *Journal of non-newtonian fluid mechanics,* 70**,** 1-33.

Barnes, H. A., 2000. *Handbook of elementary rheology,* aberystwyth, university of wales, institute of non-newtonian fluid mechanics.

Barnes, H. A. & Carnali, J. O., 1990. The vane-in-cup as a novel rheometer geometry for shear thinning and thixotropic materials. *Journal of rheology,* 34**,** 841-866.

Bauer, G., 1996. Solvolysis of polyurethanes. *In:* Brandrup, J., Bittner, M., Michaeli, W. & Menges, G., eds. *Recycling and recovery of plastics.* Munich: Hanser.

REFERENCES

Bazyleva, A. B., Hasan, M. D. A., Fulem, M., Becerra, M. & Shaw, J. M., 2010. Bitumen And heavy oil rheological properties: reconciliation with viscosity measurements. *Journal of chemical & engineering data,* 55**,** 1389-1397.

Bentley, R. W., 2002. Global oil & gas depletion: an overview. *Energy policy,* 30**,** 189-205.

Bhaskar, T., Matsui, T., Kaneko, J., Uddin, M. A., Muto, A. & Sakata, Y., 2002. Novel calcium based sorbent (Ca-C) for the dehalogenation (Br, Cl) process during halogenated mixed plastic (PP/PE/PS/PVC and HIPS-Br) pyrolysis. *Green chemistry,* 4**,** 372-375.

Bhaskar, T., Uddin, M. A., Kaneko, J., Kusaba, T., Matsui, T., Muto, A., Sakata, Y. & Murata, K., 2003. Liquefaction of mixed plastics containing PVC and dechlorination by calcium-based sorbent. *Energy and fuels,* 17**,** 75-80.

Bird, R. B., Stewart, W. E. & Lightfoot, E. N., 2007. *Transport phenomena,* New York: J. Wiley.

Birol, F., 2004. Transportation and global emissions to 2030. Available from: http://www.ipieca.org/activities/climate_change/downloads/workshops/oct_04/Birol_presentation274.00.ppt [Accessed 11 September 2009].

Biron, M., 2007. Thermoplastics and thermoplastics composites. Amstadam: Elsevier.

Blyler, L. L. & Hart, A. C., 1970. capillary flow instability of ethylene polymer melts. *polymer engineering and science,* 10**,** 193-203.

Bockhorn, H., Hornung, A. & Hornung, U., 1998. Stepwise pyrolysis for raw material recovery from plastic waste. *Journal of analytical and applied pyrolysis,* 46**,** 1 – 13.

Bohlin Instruments., 1994. A basic introduction to rheolgy. Part No Man0334 Issue 2

Bontoux, L., 1996. Survey of current projects for plastics recycling by chemolysis. Servilla: institute for perspective technological studies, european commission joint research centre.

Borgianni, C., De Filippis, P., Pochetti, F. & Paolucci, M., 2002. Gasification process of wastes containing PVC. *Fuel,* 81**,** 1827-1833.

REFERENCES

BP 2009., BP statistical review of world energy 2009.

Brandrup, J., 1996. Preparation of feedstock for petrochemical recycling- requirements imposed on plastics wasted. *In:* Brandrup, J., Bittner, M., Michaeli, W. & Menges, G., eds. *Recycling and recovery of plastics.* Munich: Hanser.

Brauch, R., Fainberg, V., Kalchouck, H. & Hetsroni, G., 1996. Correlations between properties of various feedstocks and products of visbreaking. *Fuel science and technology international,* 14**,** 753-765.

Bremner, T., Rudin, A. & Cook, D. G., 1990. Melt flow index values and molecular weight distributions of commercial thermoplastics. *Journal of applied polymer science,* 41**,** 1617-1627.

British Plastics Federation., ca 2010. *Plastics recycling* [online]. London: British Plastics Federation. Available from: http://www.bpf.co.uk/Sustainability/Plastics_Recycling.aspx [Accessed 5 June 2012].

British Plastics Federation., ca 2011. *A history of plastics* [online]. London: British Plastics Federation. Available from: http://bpf.co.uk/Plastipedia/Plastics_History/Default.aspx [Accessed 20 June 2011].

Brochard, F. & Degennes, P. G., 1992. Shear-dependent slippage at a polymer solid interface. *Langmuir,* 8**,** 3033-3037.

Brydson, J. A. 1981., *Flow properties of polymer melts,* London: George Godwin Ltd.

Brydson, J. A., 1999. *Plastics materials,* Oxford: Elsevier.

Buekens, A., G. 2006. Introduction to feedstock recycling of plastics. *In:* Scheirs, J. & Kaminsky, W. (eds.) *Feedstock recycling and pyrolysis of waste plastics: converting waste plastics into diesel and other fuels.* Chichester: Wiley.

Buekens, A. G. & Huang, H., 1998. Catalytic plastics cracking for recovery of gasoline-range hydrocarbons from municipal plastic wastes. *Resources, conservation and recycling,* 23**,** 163 - 181.

Butler, E., Devlin, G. & Mcdonnell, K., 2011. Waste polyolefins to liquid fuels via pyrolysis: review of commercial state-of-the-art and recent laboratory research. *Waste and biomass valorization,* 2**,** 227-255.

REFERENCES

Callister, W. D. & Rethwisch, D. G., 2011. *Materials science and engineering,* Hoboken: John Wiley & sons.

Casper, J. K., 2010. *Changing ecosystems: effects of global warming,* New York: Facts on file.

Chatterjee, K., Hazra, A., Dollimore, D. & Alexander, K. S., 2002. Estimating vapor pressure curves by thermogravimetry: a rapid and convenient method for characterization of pharmaceuticals. *European journal of pharmaceutics and biopharmaceutics,* 54**,** 171-180.

Chhabra, R. P. & Richardson, J. F., 1999. *Non-newtonian flow in the process industries [electronic resource]: fundamentals and engineering applications,* Oxford: Butterworth-Heinemann.

Christmann, W., Kasiske, D., Kloppel, K. D., Partscht, H. & Rotard, W., 1989. Combustion of polyvinylchloride- an important source for the formation of PCDD/PCDF. *Chemosphere,* 19**,** 387-392.

Cogwell, F. N., 1981. *Polymer melt rheology.* London: George Goodwin Limited.

Collyer, A. A., 1973a. Demonstrations with viscoelastic liquids. *Physics education,* 8**,** 111-116.

Collyer, A. A., 1973b. Time independent fluids. *Physics education,* 8**,** 333-338.

Coulson, J. M., Richardson, J. F., Backhurst, J. R. & Harker, J. H., 1999. *Coulson and Richardson's chemical engineering,* Amsterdam: Elsevier Butterworth-Heinemann.

Council Directive 1994. On packaging and packaging waste. Oj Ed.

Council Directive 1999. On the landfill of waste.

Council Directive 2008. On waste and repealing certain directives. Oj Ed.

Council Directive 2012. On waste electrical and electronic equipment (Weee) (Recast). Oj Ed.

Coussot, P., 2000. Scaling approach of the convective drying of a porous medium. *The european physical journal b,* 15, 557-566.

REFERENCES

Cowie, J. M. G. & Arrighi, V., 2008. *Polymers: chemistry and physics of modern materials.* 3rd ed. New York: CRC Press.

Crompton, T. R., 1993. *Practical polymer analysis.* New York: Plenum Press.

Cross, M. M., 1970. Viscosity, molecular weight and chain entanglement. *Polymer,* 11**,** 238-244.

Daintith, J. & Martin, E., 2010. Dictionary of science. 5th ed. Oxford: Oxford University Press.

De La Puente, G. & Sedran, U., 1998. Recycling polystyrene into fuels by means of fcc: performance of various acidic catalysts. *Applied catalysis b: Environmental,* 19**,** 305-311.

De, P. P., 2010. Instrumental techniques used for thermal analysis of rubbers and rubbery materials *In:* Choudhury, N. R., De, P. P. & Dutta, N. K., eds. *Thermal analysis of rubbers and rubbery materials.* Shrewsbury: Ismithers.

DEFRA, 2007. Waste strategy for england 2007 annexes. London, UK: Department For Environment, Food And Rural Affairs.

Demirbas, A., 2004. Pyrolysis of municipal plastic wastes for recovery of gasoline-range hydrocarbons. *Journal of analytical and applied pyrolysis,* 72**,** 97-102.

DFT., 2008. Tsgb 2008: energy and the environment - data tables.

Di Blasi, C., 1997. Linear pyrolysis of cellulosic and plastic waste. *Journal of analytical and applied pyrolysis,* 40-41**,** 463-479.

Ding, W., Liang, J. & Anderson, L. L., 1997a. Hydrocracking of waste plastics to clean liquid fuels. *Acs division of fuel chemistry, preprints,* 42**,** 1008-1010.

Ding, W. B., Liang, J. & Anderson, L. L., 1997b. Hydrocracking and hydroisomerization of high-density polyethylene and waste plastic over zeolite and silica-alumina-supported ni and ni-mo sulfides. *Energy & fuels,* 11**,** 1219-1224.

Ding, W. B., Tuntawiroon, W., Liang, J. & Anderson, L. L., 1996. Depolymerization of waste plastics with coal over metal-loaded silica-alumina catalysts. *Fuel processing technology,* 49**,** 49-63.

REFERENCES

DIRECTGOV., 2012. *Key facts about the united kingdom* [Online]. Available from: http://www.direct.gov.uk/en/Governmentcitizensandrights/LivingintheUK/DG_10012517 [Accessed 30 September 2012].

Douglas, J. F., Gasiorek, J. M., Swaffield, J. A. & Jack, L. B., 2005. *Fluid mechanics.* Harlow: Pearson/Prentice Hall.

Drda, P. P. & Wang, S. Q., 1995. Stick-slip transition at polymer melt/solid interfaces. *Physical review letters,* 75**,** 2698-2701.

Dusseault, M. B., 2001. Comparing venezuelan and canadian heavy oil and tar sands. *Petrol society,* 61**,** 1-19.

Earnest, C. M. ed., 1988. *Compositional analysis by thermogravimetry : symposium : Papers,* Philadelphia: ASTM.

EIA, 2009. annual energy review (Table 1.3 And 2.1e). Available from: http://www.eia.doe.gov/emeu/aer/pdf/aer.pdf [Accessed 11 September 2009]

EIA, 2009. Reference case projections by end-use sector and country grouping data tables (2006-2030). DOE/EIA-0484(2009). Available from: http://www.eia.doe.gov/oiaf/ieo/pdf/ieoenduse.pdf [Accessed 11 September 2009]

Elder, J. P., 1997. Sublimation measurements of pharmaceutical compounds by isothermal thermogravimetry. *Journal of thermal analysis,* 49**,** 897-905.

EPIC, 2004a. The gasification of residual plastics derived from municipal recycling facilities. Onatorio: Canadian Plastics Industry Association. Available from: http://www.plastics.ca/_files/file.php?fileid=filegXOOqaldWF&filename=file_files_Gasification2_Pop._Science_7_Aug._03.pdf [Accessed 20 August 2012].

EPIC, 2004b. A review of the options for the thermal treatment of plastics. Onatorio: Canadian Plastics Industry Association. Available from: http://www.plastics.ca/_files/file.php?fileid=0&filename=file_files_Review_of_options_for_the_thermal_treatment_of_plastics_full_paper_14_Oct._04.pdf [Accessed 11 September 2012].

Everaert, K. & Baeyens, J., 2004. Removal of PCDD/F from flue gases in fixed or moving bed adsorbers. *Waste management (New York, N.Y.),* 24**,** 37-42.

Fahim, M., Al-Sahhaf, T & Amal, E., 2010. Fundamentals of petroleum refining. Oxford: Elsevier.

Fainberg, V., Podorozhansky, M., Hetsroni, G., Brauch, R. & Kalchouck, H., 1996. Changes in the composition and properties of the vacuum residues as a result of visbreaking. *Fuel science and technology international,* 14**,** 839-866.

Fan, L. S., 1989. *Gas-liquid-solid fluidization engineering,* Stoneham: Butterworth-Heinemann.

Faravelli, T., Pinciroli, M., Pisano, F., Bozzano, G., Dente, M. & Ranzi, E., 2001. Thermal degradation of polystyrene. *Journal of analytical and applied pyrolysis,* 60**,** 103-121.

Feng, Z., Zhao, J. M., Rockwell, J., Bailey, D. & Huffman, G., 1996. Direct liquefaction of waste plastics and coliquefaction of coal-plastic mixtures. *Fuel processing technology,* 49**,** 17-30.

Ferry, J. D., 1980. *Viscoelastic properties of polymers,* New York: John Wiley And Sons.

Fink, M. & Fink, J. K., 1997. Plastics recycling coupled with enhanced oil recovery. A critical survey of the concept. *Journal of analytical and applied pyrolysis,* 40-41**,** 187-200.

Fisher, D. T., Clayton, S. A., Boger, D. V. & Scales, P. J., 2007. The bucket rheometer for shear stress-shear rate measurement of industrial suspensions. *Journal of rheology,* 51**,** 821-831.

Franklin Associates., 1990. A comparison of energy consumption by the plastic industry to total consumption in the united states. Kansas: Franklin Associates.

Garforth, A. A., Ali, S., Hernandez-Martinez, J. & Akah, A., 2004. Feedstock recycling of polymer wastes. *Current opinion in solid state & materials science,* 8**,** 419-425.

Garforth, A. A., Lin, Y. H., Sharratt, P. N. & Dwyer, J., 1998. Production of hydrocarbons by catalytic degradation of high density polyethylene in a laboratory fluidised-bed reactor. *Applied catalysis a: general,* 169**,** 331-342.

Gebauer, M. & Stannard, D., 1996. Gasification of plastics waste. *In:* Bandrup, J., Bittner, M., Michaeli, W. & Menges, G., eds. *Recycling and recovery of plastics.* Munich: Hanser.

Giles, H. F., Wagner, J. R. & Mount, E. M., 2005. *Extrusion: the definitive processing guide and handbook,* Norwich: William Andrew.

REFERENCES

Grause, G., Buekens, A., Sakata, Y., Okuwaki, A. & Yoshioka, T., 2011. Feedstock recycling of waste polymeric material. *Journal of material cycles and waste management,* 13**,** 265-282.

Hauke, G., 2008. *An introduction to fluid mechanics and transport phenomena.* New York: Springer.

Heal, G. R., 2002. Thermogravimetry and derivative thermogravimetry. *In:* Haines, P. J., ed. *Principles of thermal analysis and calorimetry.* Cambridge: Royal Society of Chemistry.

Heidolph UK., 2010. General Catalog 2010. Schwabach: Heidolph Instruments Gmbh & Co. Kg.

Heo, N. H., Baek, C. Y. & Yim, C. H., 2000a. Analysis of furnace conditions with waste plastics injection into blast furnace. *Journal of korean institute of resources recycling,* 9**,** 23-30.

Heo, N. H., Baek, C. Y. & Yim, C. H., 2000b. Thermal decomposition and combustion behaviour of plastic into blast furnaceno title. *Journal of korean institute of resources recycling,* 9**,** 15-22.

Heo, N. H. & Yim, C. H., 1998. Effect of plastic injection on the blast furnace operation under one-tuyere test. *Journal of korean institute of resources recycling,* 7**,** 16-22.

Hill, M. K., 2010. *Understanding environmental pollution.* 3rd ed. Cambridge: Cambridge University Press.

Hinkle, A. & Batzle, M., 2006. Heavy oils: a worldwide overview. *Leading edge* , 25 (6), 742-749.

Hoffert, M., 2009. Global warming. *In:* Cleveland, C. J. & Morris, C. eds. *Dictionary of energy.* Expanded ed. Amsterdam:Elsevier.

Hohne, G., Hemminger, W. & Flammersheim, H. J., 2003. *Differential scanning calorimetry,* Berlin: Springer.

Holland, F. A. & Bragg, R., 1995. Fluid flow for chemical engineers. 2nd ed. London: Arnold.

REFERENCES

Holland, F. A. & Chapman, F. S., 1966. *Liquid mixing and process in stirred tanks.* New York: Reinhold.

Hopewell, J., Dvorak, R. & Kosior, E., 2009. Plastics recycling: challenges and opportunities. *Philosophical transactions of the royal society b-biological sciences,* 364**,** 2115-2126.

Huang, Y., Bird, R. N. & Heidrich, O., 2007. A review of the use of recycled solid waste materials in asphalt pavements. *Resources conservation and recycling,* 52**,** 58-73.

Huffman, G. P., Feng, Z., Bailey, D., Rockwell, J., Zhao, J. & Huggins, F. E., 1996. Liquefaction of commingled waste plastics containing PVC. *ACS division of fuel chemistry, preprints,* 41**,** 1043-1045.

Huffman, G. P., Feng, Z., Hggins, F. E. & Mahajan, V., 1995. Direct liquefaction of plastics and coliquefaction of waste plastic with coal. *Coal science and technology,* 24**,** 1519-1522.

Ibrahim, M. M. & Seehra, M. S., 1997. Sulfur-promoted degradation of polyethylene/polypropylene detected by electron spin resonance spectroscopy. *Energy and fuels,* 11**,** 926-930.

ICPE, 2006. Use of plastics waste in blast furnace. *Management of plastics, polymer wastes and bio-polymers and impact of plastics on the eco-system,* 4 (2)**,** 1 - 8.

Iida, T., Nakanishi, M. & Goto, K., 1974. Investigations on poly(vinyl chloride) - 1. Evolution of aromatics on pyrolysis of poly(vinyl chloride) and its mechanism. *J polym sci part a-1 polym chem,* 12**,** 737-749.

Indermuhle, A., Stocker, T. F., Joos, F., Fischer, H., Smith, H. J., Wahlen, M., Deck, B., Mastroianni, D., Tschumi, J., Blunier, T., Meyer, R. & Stauffer, B., 1999. Holocene carbon-cycle dynamics based on CO_2 trapped in ice at taylor dome, antarctica. *Nature,* 398**,** 121-126.

ISOPA, 2001. Chemolysis. Available from: http://www.isopa.org/isopa/uploads/Documents/documents/chemolysis.pdf [Accessed 4 August 2012].

Jansen, R., Koster, M. & Strijtveen, B., 1992. Environmentally-friendly packaging in the future. *In:* Lox, F., ed. *Packaging and ecology.* Surrey: Pira International.

Joo, H. K. & Curtis, C. W., 1996. Catalytic coprocessing of plastics with coal and petroleum resid using $NiMo/Al_2O_3$. *Energy & fuels,* 10**,** 603-611.

Joo, H. K. & Curtis, C. W., 1998. Catalytic coprocessing of ldpe with coal and petroleum resid using different catalysts. *Fuel processing technology,* 53**,** 197-214.

Joo, H. S. & Guin, J. A., 1997. Hydrocracking of a plastics pyrolysis gas oil to naphtha. *Energy and fuels,* 11**,** 586-590.

Jung, C. G. & Fontana, A. 2006. Production of gaseous and liquid fuels by pyrolysis and gasification of plastics: technological approach. *In:* Scheirs, J. & Kaminsky, W., eds. *Feedstock recycling and pyrolysis of waste plastics: converting waste plastics into diesel and other fuels.* Chichester: Wiley.

Kakuta, Y., Hirano, K., Sugano, M. & Mashimo, K. 2006. Influence of iron chloride on hydrocracking of waste plastics using coal tar. *Journal- japan institute of energy,* 85**,** 876-881.

Kaminsky, W. & And Sinn, H. 1995. Petrochemical processes for recycling plastics: pyrolytic techniques. *In:* Bandrup, J., Bittner, M., Michaeli, W. & Menges, G., eds. *Recycling and recovery of plastics.* Munich: Hanser.

Kaminsky, W. & Franck, J. 1991. Monomer recovery by pyrolysis of poly(methyl methacrylate) (PMMA). *Journal of analytical and applied pyrolysis,* 19**,** 311-318.

Kaminsky, W. & Sinn, H. 1995. Pyrolytic techniques. *In:* Bandrup, J., Bittner, M., Michaeli, W. & Menges, G., eds. *Recycling and recovery of plastics.* Munich: Hanser.

Kamo, T. 2013. Thermal decomposition of poly(vinyl chloride) in organic solvents under high pressure. *Polymer degradation and stability,* 98**,** 502-507.

Karaduman, A., Imşek, E. H., Çiçek, B. & Bilgesü, A. Y. 2002. Thermal degradation of polystyrene wastes in various solvents. *Journal of analytical and applied pyrolysis,* 62**,** 273-280.

Karagoz, S., Karayildirim, T., Ucar, S., Yuksel, M. & Yanik, J. 2003a. Liquefaction of municipal waste plastics in VGO over acidic and non-acidic catalysts. *Fuel,* 82**,** 415-423.

Karagoz, S., Yanik, J., Ucar, S., Saglam, M. & Song, C. 2003b. Catalytic and thermal degradation of high-density polyethylene in vacuum gas oil over non-acidic and acidic catalysts. *Applied catalysis a-general,* 242**,** 51-62.

Karayildirim, T., Yanik, J., Uçar, S., Saglam, M. & Yüksel, M. 2001. Conversion of plastics/HVGO mixtures to fuels by two-step processing. *Fuel processing technology,* 73**,** 23-35.

Kartalis, C. N., Papaspyrides, C. D., Pfaendner, R., Hoffmann, K. & Herbst, H. 2000. Mechanical recycling of post-used HDPE crates using the restabilization technique. Ii: influence of artificial weathering. *Journal of applied polymer science,* 77**,** 1118-1127.

Kataoka, T. & Ueda, S., 1971. Flow instability of high molecular weight linear polyethylene. *Rheologica acta,* 10**,** 446-447.

Kaushish, J. P., 2010. *Manufacturing processes.* New Delhi: Phi Learning Pvt. Ltd.

Kaviany, M. & Mittal, M., 1987. Funicular state in drying of a porous slab. *International journal of heat and mass transfer,* 30.

Keane, M. A. 2007., catalytic conversion of waste plastics: focus on waste pvc. *Journal of chemical technology and biotechnology,* 82**,** 787-795.

Keey, R. B. 1972. *Drying principles and practice*. Oxford: Pergamon Press.

Kim, D., Shin, S., Sohn, S., Choi, J. & Ban, B., 2002. Waste plastics as supplemental fuel in the blast furnace process: improving combustion efficiencies. *Journal of hazardous materials,* 94**,** 213-22.

Kim, J. S., Kaminsky, W. & Schlesselmann, B., 1997. Pyrolysis of a fraction of mixed plastic wastes depleted in PVC. *Journal of analytical and applied pyrolysis,* 40-41**,** 365-372.

Kim, S. D. & Laurent, A., 1991. State of knowledge on heat transfer in three-phase fluidized beds. *International chemical engineering,* 31**,** 284-302.

Kiran, N., Ekinci, E. & Snape, C. E., 2000. Recyling of plastic wastes via pyrolysis. *Resources, conservation and recycling,* 29**,** 273-283.

Klein, P., 1996. Solvolysis of polyethylene terephthalate. *In:* Brandrup, J., Bittner, M., Michaeli, W. & Menges, G., eds. *Recycling and recovery of plastics.* Munich: Hanser.

Kopietz, M. & Seeliger, U., 1996. Depolymerization of polyamides. *In:* Brandrup, J., Bittner, M., Michaeli, W. & Menges, G., eds. *Recycling and recovery of plastics.* Munich: Hanser.

Krieger, I. M. & Maron, S. H., 1952. Direct determination of the flow curves of non-newtonian fluids. *Journal of applied physics,* 23**,** 147-149.

Laye, P. G., 2002. Differential thermal analysis and differential scanning calorimetry. *In:* Haines, P. J., ed. *Principles of thermal analysis and calorimetry.* Cambridge: Royal Society of Chemistry.

Lee, D.-H., Kim, J.-O. & Kim, S. D., 1993. Mass transfer and phase holdup characteristics in three-phase fluidized beds. *Chemical engineering communications,* 119**,** 179-196.

Lehmann, P., Assouline, S. & Or, D., 2008. Characteristic lengths affecting evaporative drying of porous media. *Physical review. E, statistical, nonlinear, and soft matter physics,* 77**,** 56309.

Leidner, J., 1981. *Plastics waste: recovery of economic value.* New York: Marcel Dekkel.

Lettieri, P. & Al-Salem, S. M., 2011. Thermomechanical treatment of plastic solid waste. *In:* Letcher, T. M. & Vallero, D. A., eds. *Waste: a handbook for management.* London: Academic.

Levec, J. & Goto, S., 1986. Mass transfer and kinetics in three-phase reactors. *In:* Cheremisinoff, N. P, ed. *Handbook of heat and mass transfer.* Houston: Gulf.

Lingaiah, N., Uddin, M. A., Morikawa, K., Muto, A., Murata, K. & Sakata, Y., 2001. Catalytic dehydrochlorination of chloro-organic compounds from pvc containing waste plastics derived fuel oil over $FeCl_2/SiO_2$ catalyst. *Green Chemistry,* 3**,** 74-75.

Liu, K. & Meuzelaar, H. L. C., 1996. Catalytic reactions in waste plastics, HDPE and coal studied by high-pressure thermogravimetry with on-line GC/MS. *Fuel processing technology,* 49**,** 1-15.

Lopez-Urionabarrenechea, A., De Marco, I., Caballero, B. M., Laresgoiti, M. F. & Adrados, A., 2011. Dechlorination of fuels in pyrolysis of PVC containing plastic wastes. *Fuel processing technology,* 92**,** 253-260.

Lopez-Urionabarrenechea, A., De Marco, I., Caballero, B. M., Laresgoiti, M. F. & Adrados, A., 2012. Catalytic stepwise pyrolysis of packaging plastic waste. *Journal of analytical and applied pyrolysis,* 96**,** 54-62.

Lovett, S., Berruti, F. & Behie, L. A., 1997. Ultrapyrolytic upgrading of plastic wastes and plastics/heavy oil mixtures to valuable light gas products. *Industrial and engineering chemistry research,* 36**,** 4436-4444.

Luo, M. S. & Curtis, C. W., 1996. Effect of reaction parameters and catalyst type on waste plastics liquefaction and coprocessing with coal. *Fuel processing technology,* 49**,** 177-196.

Macleay, I., Harris, K. & Annut, A., 2009. Digest of united kingdom energy statistics 2009. London: National Statistics.

Macleay, I., Harris, K. & Annut, A., 2012. Digest of united kingdom energy statistics (Dukes). London: National Statistics

Macosko, C. W., 1994. *Rheology: principles, measurements, and applications.* New York: Wiley-VCH.

Malvern Instruments, 2006. Rosand Rh7/Rh10 User Manual.

Marcilla, A., García, Á. N. & Del Remedio Hernández, M., 2007. Thermal degradation of ldpe - vacuum gas oil mixtures for plastic wastes valorization. *Energy and fuels,* 21**,** 870-880.

Marcilla, A., Odjo, A. O., García-Quesada, J. C., Gómez, A., Martínez, R. N. & Berenguer, D., 2008. Flow properties of vacuum gas oil-low density polyethylene blends. *Fuel processing technology,* 89**,** 83-89.

Marcilla, A., Gómez-Siurana, A., Odjo, A. O.,Navarro, R. & Berenguer, D., 2008. Characterization of vacuum gas oil-low density polyethylene blends by thermogravimetric analysis. *Polymer degration and stability,* 93**,** 723-730.

Marine Conservation Society, Ca. 2008. *Marine conservation society beachwatch* [Online]. Available from:

http://kb.keepbritaintidy.org/litterv5/FactsandFigures/beachwatch.pdf [Accessed 25 June 2012].

Marklund, S., Rappe, C., Tysklind, M. & Egeback, K. E., 1987. Identification of polychlorinated dibenzofurans and dioxins in exhausts from cars run on leaded gasoline. *Chemosphere,* 16**,** 29 – 36.

Marland, G., 2009. Greenhouse gas. *In:* Cleveland, C. J. & Morris, C., eds. *Dictionary of energy*. Expanded ed. Amsterdam: Elsevier.

Mastellone, M. L., 1999. *Thermal treatments of plastic wastes by means of fluidized bed reactors.* Phd thesis, Second University Of Naples, Italy.

Matsumoto, Y., 2001. Cracking styrene derivative polymers in decalin solvent with metal-supported carbon catalysts. *Journal of material cycles and waste management,* 3**,** 82-87.

Menczel, J. D., Judovits, L., Prime, R. B., Bair, H., Reading, M. & Swier, S., 2009. Differential scanning calorimetry (DSC). *In:* Menczel, J. D. & Prime, R. B., eds. *Thermal analysis of polymers.* Oxford: Wiley.

Menges, G. & Lackner, V., 1996. Degaradative extrusion of plastics scraps. *In:* Brandrup, J., Bittner, M., Michaeli, W. & Menges, G., eds. *Recycling and recovery of plastics.* Munich: Hanser.

Meszaros, M. W., 1996. Advanced recycling technologies for plastics *In:* Khan, M. R., ed. *Conversion and utilization of waste materials.* Washington D.C.: Taylor And Francis.

Metzger, A. P., Hamilton, C. W. & Merz, E. H., 1963. Anomalous flow behavior of high density polyethylene melts. *SPE transactions,* 3**,** 21-26.

Metzner, A. B. & Otto, R. E., 1957. Agitation of non-newtonian fluids. *AIChE journal,* 3**,** 3-10.

Miadonye, A., Singh, B. & Puttagunta, V. R., 1994. Modelling the viscosity-temperature relationship of alberta bitumen. *Fuel science and technology international,* 12**,** 335-350.

Michaeli, W. & Breyer, K., 1998. Polymer recycling- status and perspectives. *Macromolecular symposia,* 135**,** 83-96.

Michaeli, W. & Lackner, V., 1995. Degradative extrusion as a pretreating process for chemical recycling of plastics waste. *Die angewandte makromolekulave chemie,* 232**,** 167-285.

Minitab, 2012. Minitab 16 statistical software [Computer Software]. State college, Pa: Minitab, Inc.

Mudgal, S., Lyons, L., Bain, J., Dias, D., Faninger, T., Johansson, L., Dolley, P., Shields, L. & Bowyer, C., 2011. Plastic waste in the environment. European commission.

Murakata, T., Saito, Y., Yosikawa, T., Suzuki, T. & Sato, S., 1993. Solvent effect on thermal degradation of polystyrene and poly-α-methylstyrene. *Polymer,* 34**,** 1436-1439.

Ng, S. H., 1995. Conversion of polyethylene blended with VGO to transportation fuels by catalytic cracking. *Energy & fuels,* 9**,** 216-224.

Niemann, K., 1996. Hydrogenation. *In:* Bandrup, J., Bittner, M., Michaeli, W. & Menges, G., eds. *Recycling and recovery of plastics.* Munich: Hanser.

Niemoller, B., 1996. Reduction in blast furnaces. *In:* Bandrup, J., Bittner, M., Michaeli, W. & Menges, G., eds. *Recycling and recovery of plastics.* Munich: Hanser.

Nikles, D. E. & Farahat, M. S., 2005. New motivation for the depolymerization products derived from poly(ethylene terephthalate) (PET) waste: a review. *Macromolecular materials and engineering,* 290**,** 13-30.

Ochoa, R., Van Woert, H., Lee, W. H., Subramanian, R., Kugler, E. & Eklund, P. C., 1996. Catalytic degradation of medium density polyethylene over silica - alumina supports. *Fuel processing technology,* 49**,** 119-136.

Oehlmann, J., Schulte-Oehlmann, U., Kloas, W., Jagnytsch, O., Lutz, I., Kusk, K. O., Wollenberger, L., Santos, E. M., Paull, G. C., Van Look, K. J. W. & Tyler, C. R., 2009. A critical analysis of the biological impacts of plasticizers on wildlife. *Philosophical transactions of the royal society b-biological sciences,* 364**,** 2047-2062.

Okuwaki, A., Yoshioka, T., Asai, M., Tachibana, H., Wakai, K. & Tada, K., 2006. The liquefaction of plastic containers and packaging in japan. *In:* Scheirs, J. & Kaminsky, W., eds. *Feedstock recycling and pyrolysis of waste plastics: converting waste plastics into diesel and other fuels.* Chichester: Wiley.

REFERENCES

Osswald, T. A., Baur, E., Brinkmann, S., Oberbach, K. & Schmanachtenberg, E., 2006. *International plastics handbook: the resource for plastics engineers.* Cincinnati: Hanser.

Panda, A. K., Singh, R. K. & Mishra, D. K., 2010. Thermolysis of waste plastics to liquid fuel a suitable method for plastic waste management and manufacture of value added products-a world prospective. *Renewable & sustainable energy reviews,* 14**,** 233-248.

Peacock, A. J. & Calhoun, A. R., 2006. *Polymer chemistry : properties and applications,* Munich: Hanser Gardner.

Peishi, C. & Pei, D. C. T., 1989. A mathematical model of drying processes. *International journal of heat and mass transfer,* 32 (2), 297-310.

Perry, R. H. & Green, D. W., 2008. *Perry's chemical engineers' handbook.* New York: Mcgraw-Hill.

Phang, P. & Dollimore, D. 2001. The calculation of the vapor pressures of antioxidants over a range of temperatures using thermogravimetry. *Thermochimica acta,* 367**,** 263-271.

Pichtel, J. 2005. *Waste management practices : municipal, hazardous, and industrial,* Boca Raton: CRC Press.

Pielichowski, K. & Njuguna, J., 2005. *Thermal degradation of polymeric materials.* Shawbury: Rapra Technology.

Pinto, L. C. & Salgado, A. F., 2004. Raising awareness of environmental risks: a case study in portugal. *Management of environmental quality,* 15**,** 438 – 442.

Plastics Europe, 2008a. The compelling facts about plastics 2006- an analysis of european plastics production, demand and recovery for 2006. Brussels.

Plastics Europe, 2008b. The compelling facts about plastics 2007- an analysis of european plastics production, demand and recovery for 2007. Brussels.

Plastics Europe, 2009a. The compelling facts about plastics 2009- an analysis of european plastics production, demand and recovery for 2008. Brussels.

Plastics Europe, 2009b. Plastics convert iron ore to steel- feedstock recycling in blast furnaces. Brussels.

Plastics Europe, 2010. Plastics– the facts 2010. An analysis of european plastics production, demand and recovery for 2009. Brussels.

Plastics Europe, 2011. Plastics- the facts 2011. An analysis of european plastics production, demand and recovery for 2010. Brussels.

Plastics europe, 2013. Plastics- the facts 2013. An analysis of european latest plastics production, demand and waste data for 2012. Brussels.

Plastics News Global Group, 2010. *Fyi Charts* [Online]. Available from: http://plasticsnews.com/fyi-charts/index.html?id=18024 [Accessed 21 June 2012].

Plastics Waste Management Institute, 2009. An introduction to plastic recycling 2009. Tokyo.

Price, D. M., 2001. Vapor pressure determination by thermogravimetry. *Thermochimica acta,* 367**,** 253-262.

Price, D. M. & Hawkins, M., 1998. Calorimetry of two disperse dyes using thermogravimetry. *Thermochimica acta,* 315**,** 19-24.

Prime, R. B., Bair, H., Vyazovkin, S., Gallagher, P. K. & Riga, A., 2009. Thermogravimetric Analysis (TGA). *In:* Menczel, J. D. & Prime, R. B., eds. *Thermal Analysis Of Polymers.* Oxford: Wiley.

Probert, S. D., Kerr, K. & Brown, J., 1987. Harnessing energy from domestic, municipal and industrial refuse. *Applied energy,* 27**,** 89-168.

Rada, E. C., Istrate, I. A. & Ragazzi, M., 2009. Trends in the management of residual municipal solid waste. *Environmental technology,* 30**,** 651 – 661.

Ranade, V. V., Chaudhari, R. V., & Gunjal, P. R., 2011. *Trickle bed reactors: reactor engineering & applications.* Amsterdam: Elsevier.

Rao, M. N. & Rao, H. V. N., 1989. *Air pollution.* New Delhi: Tata Mcgraw-Hill.

Recoup, ca. 2002. Factsheet- how plastic bottles are turned into clothes. Available from: http://www.recoup.org/shop/product_documents/99.pdf [Accessed April 17 2008].

Rheology School, No Date. *Making use of models: the cross model* [Online]. Available from: http://www.rheologyschool.com/cross_model.html [Accessed 18 October 2012].

Rigo, H. G. & Chandler, A. J., 1998. Is there a strong dioxin: chlorine link in commercial scale systems? *Chemosphere,* 37**,** 2031-2046.

Rosato, D. V., Rosato, D. V., Rosato, M. G. & Schott, N. R., 2001. Plastics institute of america plastics engineering manufacturing and data handbook. Boston: Kluwer Academic.

Rothenberger, K. S., Cugini, A. V., Thompson, R. L. & Ciocco, M. V., 1997. Investigation of first-stage liquefaction of coal with model plastic waste mixtures. *Energy & fuels,* 11**,** 849-855.

Royco, ca. 2013. *Faqs* [Online]. Available from: http://www.roycobeijing.com/faqsvb.php [Accessed 6 September 2013.

Rudin, A. & Chang, R. J., 1978. Study of melt density of flowing linear polyethylene. *Journal of applied polymer science,* 22**,** 781-799.

Salvucci, G. D., 1997. Soil and moisture independent estimation of stage-two evaporation from potential evaporation and albedo or surface temperature. *Water resources research,* 33, 111-122.

Sato, S., Murakata, T., Baba, S., Saito, Y. & Watanabe, S., 1990. Solvent effect on thermal degradation of polystyrene. *Journal of applied polymer science,* 40**,** 2065-2071.

Scheirs, J., 2006. Overview of commercial pyrolysis processes for waste plastics. *In:* Scheirs, J. & Kaminsky, W., eds. *Feedstock recycling and pyrolysis of waste plastics: converting waste plastics into diesel and other fuels.* Chichester: Wiley.

Scherer, G. W., 1990. Theory of drying. *Journal of the american ceramic society,* 73, 3-14.

Scherzer, J. & Gruia, A. J., 1996. *Hydrocracking science and technology.* New York: Marcel Dekker.

Schiermerier, Q., 2012. Kyoto protocol: hot air. *Nature,* 491, 656-658.

Schramm, G., 2000. *A practical approach to rheology and rheometry.* 2nd ed. Karlsruhe: Haake.

Schultz, P., 1991. On the falling-rate period. *Chemical engineering & technology,* 14 (4), 234-239.

Serrano, D. P., Aguado, J., Escola, J. M. & Garagorri, E., 2001. Conversion of low density polyethylene into petrochemical feedstocks using a continuous screw kiln reactor. *Journal of analytical and applied pyrolysis,* 58**,** 789-801.

Serrano, D. P., Aguado, J., Escola, J. M. & Garagorri, E., 2003. Performance of a continuous screw kiln reactor for the thermal and catalytic conversion of polyethylene-lubricating oil base mixtures. *Applied catalysis b-environmental,* 44**,** 95-105.

Serrano, D. P., Aguado, J., Vicente, G. & Sánchez, N., 2007. Effects of hydrogen-donating solvents on the thermal degradation of hdpe. *Journal of analytical and applied pyrolysis,* 78**,** 194-199.

Shabtai, J., Xiao, X. & Zmierczak, W., 1997. Depolymerization-liquefaction of plastics and rubbers. 1. Polyethylene, polypropylene, and polybutadiene. *Energy and fuels,* 11**,** 76-87.

Shah, N., Rockwell, J. & Huffman, G. P., 1999. Conversion of waste plastic to oil: direct liquefaction versus pyrolysis and hydroprocessing. *Energy & fuels,* 13**,** 832-838.

Shah, Y. T., 1991. Design parameters for mechanically agitated reactors. *Advances in chemical engineering,* 17**,** 1-206.

Shimasaki, C., Watanabe, N., Fukushima, K., Rengakuji, S., Nakamura, Y., Ono, S., Yoshimura, T., Morita, H., Takakura, M. & Shiroishi, A., 1997. Effect of the fire-retardant, melamine, on the combustion and the thermal decomposition of polyamide-6, polypropylene and low-density polyethylene. *Polymer degradation and stability,* 58**,** 171-180.

Shokri, N., Lehmann, P. & Or, D., 2009. Characteristics of evaporation from partially wettable porous media. *Water resources research,* 45 (2), 1-12.

Shokri, N. & Or, D., 2013. Drying patterns of porous media containing wettability contrasts. *Journal of colloid and interface science,* 391**,** 135-141.

Shyichuk, A. V., 1996. How to measure the degradation index by viscometry. *Journal of applied polymer science,* 62**,** 1735-1738.

Siddique, R., Khatib, J. & Kaur, I., 2008. Use of recycled plastic in concrete: a review. *Waste management,* 28**,** 1835-1852.

Siddiqui, M. N., Ali, M. F. & Redhwi, S. H. H., 2002. Catalytic conversion of waste plastics/petroleum resid mixtures into transportation fuels. 47, 374-377.

Siddiqui, M. N. & Redhwi, H. H., 2009. Catalytic coprocessing of waste plastics and petroleum residue into liquid fuel oils. *Journal of analytical and applied pyrolysis,* 86**,** 141-147.

Sinha, V., Patel, M. R. & Patel, J. V., 2010. PET waste management by chemical recycling: a review. *Journal of polymers and the environment,* 18**,** 8-25.

Smolders, K. & Baeyens, J., 2004. Thermal degradation of pmma in fluidised beds. *Waste management,* 24**,** 849-857.

Sperling, L. H., 2006. *Introduction to physical polymer science.* New York: Wiley.

Steffe, J. F., 1996. *Rheological methods in food process engineering.* East Lansing: Freeman Press.

Stein, R. S. & Wilcox, V., 1996. The national plastics center and museum. *Trends in polymer science,* 4 358 – 360.

Stelmachowski, M., 2010. Thermal conversion of waste polyolefins to the mixture of hydrocarbons in the reactor with molten metal bed. *Energy conversion and management,* 51**,** 2016-2024.

Taghiei, M. M., Feng, Z., Huggins, F. E. & Huffman, G. P., 1994. Coliquefaction of waste plastics with coal. *Energy & fuels,* 8**,** 1228-1232.

Tavoularis, G. & Keane, M. A., 1999. Gas phase catalytic dehydrochlorination and hydrodechlorination of aliphatic and aromatic systems. *Journal of molecular catalysis a: chemical,* 142**,** 187-199.

REFERENCES

Teuten, E. L., Saquing, J. M., Knappe, D. R. U., Barlaz, M. A., Jonsson, S., Bjorn, A., Rowland, S. J., Thompson, R. C., Galloway, T. S., Yamashita, R., Ochi, D., Watanuki, Y., Moore, C., Pham, H. V., Tana, T. S., Prudente, M., Boonyatumanond, R., Zakaria, M. P., Akkhavong, K., Ogata, Y., Hirai, H., Iwasa, S., Mizukawa, K., Hagino, Y., Imamura, A., Saha, M. & Takada, H., 2009. Transport and release of chemicals from plastics to the environment and to wildlife. *Philosophical transactions of the royal society b-biological sciences,* 364**,** 2027-2045.

The Volatile Organic Compounds in Paints, Varnishes and Vehicle Refinishing Products Regulations 2012. SI 2012/1715. London: The Stationery Office.

Themelis, N. J., Castaldi, M. J., Bhatti, J. & Arsova, L., 2011. Energy and economic value of non-recycled plastics (NRP) and municipal solid wastes (MSW) that are currently landfilled in the fifty states. Columbia: Earth Engineering Centre.

Thoenes, D., 1994. *Chemical reactor development: from laboratory synthesis to industrial pollution.* Dordrecht: Kluwer Academic.

Thompson, R. C., Swan, S. H., Moore, C. J. & Vom Saal, F. S., 2009. Our plastic age. *Philosophical transactions of the royal society b-biological sciences,* 364**,** 1973-1976.

Tukker, A., 2002. *Plastics waste- feedstock recycling, chemical recycling and incineration*. Shropshire: RAPRA Technology. Report number: 148.

Ube Industries Ltd, 2010. *Ube withdraws from ebara-ube process recycling business* [Online]. Available from: http://www.ube-ind.co.jp/english/news/2010/2010_03.htm [Accessed 20 August 2012].

Uçar, S., Karagöz, S., Karayildirim, T. & Yanik, J., 2002. Conversion of polymers to fuels in a refinery stream. *Polymer degradation and stability,* 75**,** 161-171.

UNEP, 1999. Dioxin and furan inventories. National and regional emissions of PCDD/PCDF. Geneva: UNEP Chemicals.

UNFCCC, 1998. Kyoto protocol to the united nations framework convention on climate change. Available from: http://unfccc.int/resource/docs/convkp/kpeng.pdf [Accessed 20 July 2013]

UNFCCC, 2013. Doha amendment to the kyoto protocol. Available from: http://unfccc.int/files/kyoto_protocol/application/pdf/kp_doha_amendment_english.pdf [Accessed 20 July 2013]

USEPA, 1989. Characterization of products containing lead and cadmium in municipal **s**olid waste in the U.S. EPA/530-SW-89-015C

USEPA, 1990. Plastics: the facts about production, use, and disposal. EPA/530-SW-90-017A

USEPA, 2009. *About air toxics* [Online]. Available from: http://www.epa.gov/ttn/atw/allabout.html [Accessed 6 September 2009].

Van Brakel, J., 1980. Mass transfer in convective drying. *Advances in drying,* 1**,** 217-267.

Vasile, C., Pakdel, H., Mihai, B., Onu, P., Darie, H. & Ciocâlteu, S. 2001. Thermal and catalytic decomposition of mixed plastics. *Journal of analytical and applied pyrolysis,* 57**,** 287-303.

Venkatesh, K. R., Hu, J., Wang, W., Holder, G. D., Tierney, J. W. & Wender, I., 1996. Hydrocracking and hydroisomerization of long-chain alkanes and polyolefins over metal-promoted anion-modified zirconium oxides. *Energy and fuels,* 10**,** 1163-1170.

Walendziewski, J., 2006. Conversion of polyolefins. *In:* Scheirs, J. & Kaminsky, W., eds. *Feedstock recycling and pyrolysis of waste plastics : converting waste plastics into diesel and other fuels.* Chichester: Wiley.

Walendziewski, J., & Steininger, M. 2001. Thermal and catalytic conversion of waste polyolefines. *Catalysis today,* 65**,** 323-330.

Wang, S. Q. & Drda, P. A., 1996a. Stick-slip transition in capillary flow of polyethylene .2. Molecular weight dependence and low-temperature anomaly. *Macromolecules,* 29**,** 4115-4119.

Wang, S. Q. & Drda, P. A., 1996b. Superfluid-like stick-slip transition in capillary flow of linear polyethylene melts .1. General features. *Macromolecules,* 29**,** 2627-2632.

Waste Watch, 2006. Plastics recycling information sheet. Available from: http://www.wasteonline.org.uk/resources/InformationSheets/Plastics.htm [Accessed 14 April 2009].

Waste Watch & Recoup, 2003. Plastics in the UK economy: a guide to polymer use and the opportunities for recycling.

Webber, G. V., 2009. *The origin of multiple dsc melting peaks of fischer-tropsch hard waxes.* Thesis, (Phd), University of Cape Town.

White, R. L., 2006. Acid-catalyzed cracking of polyolefins: primary reaction mechanisms. *In:* Scheirs, J. & Kaminsky, W., eds. *Feedstock recycling and pyrolysis of waste plastics: converting waste plastics into diesel and other fuels.* Chichester: Wiley.

Williams, E. A. & Williams, P. T., 1997. The pyrolysis of individual plastics and a plastic mixture in a fixed bed reactor. *Journal of chemical technology and biotechnology,* 70**,** 9-20.

Williams, P. T., 2005. *Waste treatment and disposal.* Chichester: John Wiley & Sons.

WMO, 2013. Greenhouse gas bulletin. No 9. Available from: http://www.wmo.int/pages/prog/arep/gaw/ghg/documents/GHG_Bulletin_No.9_en.pdf [Accessed 14 November 2013].

Yanik, J. & Karayildirim, T., 2006. Liquefaction of municipal waste plastics over acidic and nonacidic catalysts. *In:* Scheirs, J. & Kaminsky, W., eds. *Feedstock recycling and pyrolysis of waste plastics: converting waste plastics into diesel and other fuels.* Chichester: Wiley.

Yanik, J., Uddin, M. A., Ikeuchi, K. & Sakata, Y., 2001. The catalytic effect of red mud on the degradation of poly (vinyl chloride) containing polymer mixture into fuel oil. *Polymer degradation and stability,* 73**,** 335-346.

Yiotis, A., Tsimpanogiannis, I., Stubos, A. & Yortsos, Y., 2006. Pore-network study of the characteristic periods in the drying of porous materials. *Journal of colloid and interface science,* 297**,** 738-748.

Yoshioka, T. & Grause, G., 2006. Feedstock recycling of pet. *In:* Scheirs, J. & Kaminsky, W., eds. *Feedstock recycling and pyrolysis of waste plastics: converting waste plastics into diesel and other fuels.* Chichester: Wiley.

Zhang, Z. B., Hirose, T., Nishio, S., Morioka, Y., Azuma, N., Ueno, A., Ohkita, H. & Okada, M., 1995. Chemical recycling of waste polystyrene into styrene ever solid acids and bases. *Industrial & engineering chemistry research,* 34**,** 4514-4519.

REFERENCES

Zhou, Q., Tang, C., Wang, Y. Z. & Zheng, L., 2004. Catalytic degradation and dechlorination of PVC-containing mixed plastics via Al-Mg composite oxide catalysts. *Fuel,* 83**,** 1727-1732.

Zia, K. M., Bhatti, H. N. & Bhatti, I. A., 2007. Methods for polyurethane and polyurethane composites, recycling and recovery: a review. *Reactive & functional polymers,* 67**,** 675-692.

Zmierczak, W., Xiao, X. & Shabtai, J., 1996. Depolymerization-liquefaction of plastics and rubbers. 2. Polystyrenes and styrene-butadiene copolymers. *Fuel processing technology,* 49**,** 31-48.

APPENDICES

a)

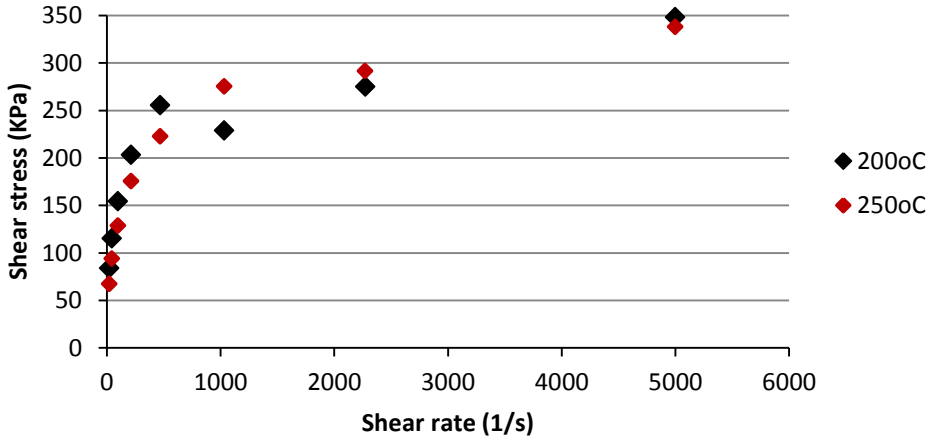

b)

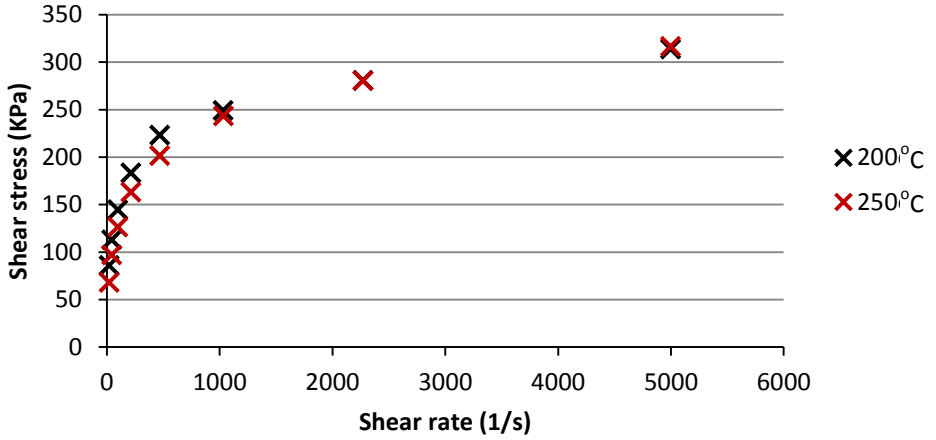

c)

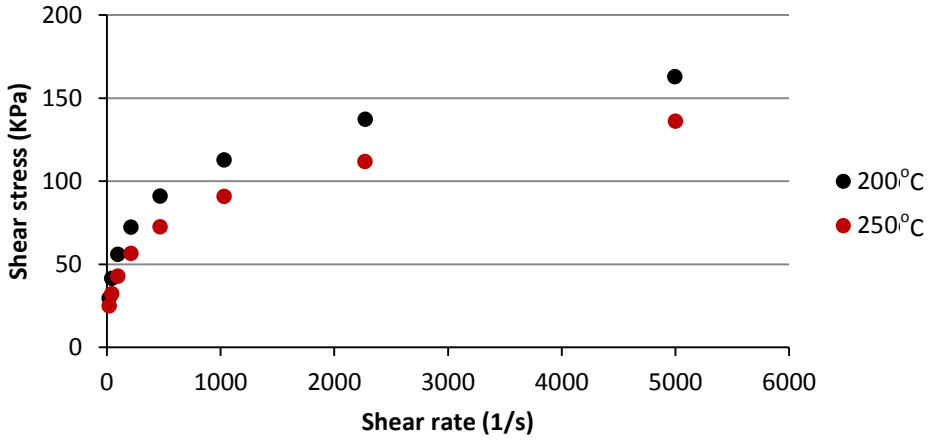

d)

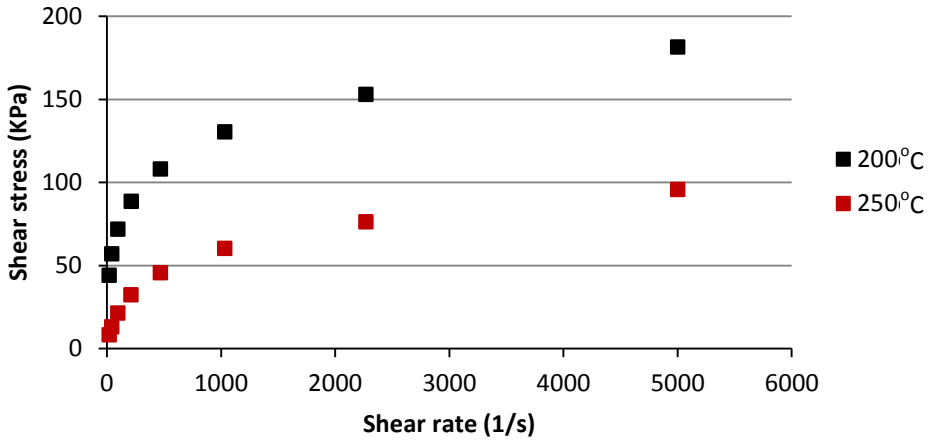

Figure A.1: Effect of temperature on flow curves for: a) HDPE; b) LLDPE; c) PP and d) PS

Table A.1: Shear stress and viscosity data for HDPE at 200°C

	Run 1			Run 2			Run 3		
Shear rate (s^{-1})	**Shear stress (Pa)**	**Shear viscosity (Pa.s)**	**n**	**Shear stress (Pa)**	**Shear viscosity (Pa.s)**	**n**	**Shear stress (Pa)**	**Shear viscosity (Pa.s)**	**n**
20	71940	3600	0.45	91850	4590	0.40	88270	4410	0.40
40	101690	2540	0.40	124900	3120	0.35	118930	2970	0.35
100	137010	1370	0.35	166840	1670	0.30	159250	1590	0.30
210	181540	860	0.29	219340	1040	0.25	208880	990	0.25
470	236130	500	0.24	267770	570	0.20	262890	560	0.21
1030	233260	230	0.18	227230	220	0.15	225770	220	0.16
2270	268180	120	0.13	279870	120	0.09	276950	120	0.11
5000	335160	70	0.07	354520	70	0.04	354610	70	0.06

Table A.2: Shear stress and viscosity data for HDPE at 250°C

	Run 1			Run 2			Run 3		
Shear rate (s^{-1})	**Shear stress (Pa)**	**Shear viscosity (Pa.s)**	**n**	**Shear stress (Pa)**	**Shear viscosity (Pa.s)**	**n**	**Shear stress (Pa)**	**Shear viscosity (Pa.s)**	**n**
20	53830	2690	0.55	76840	3840	0.51	69660	3480	0.46
40	79090	1980	0.49	106830	2670	0.44	94260	2360	0.41
100	112190	1120	0.42	146800	1470	0.37	127180	1270	0.37
210	153700	730	0.36	203320	970	0.30	168760	800	0.32
470	204470	440	0.30	245390	520	0.23	221030	470	0.27
1030	263720	260	0.23	289760	280	0.16	273230	270	0.23
2270	273370	120	0.17	287600	130	0.08	304720	130	0.18
5000	328280	70	0.10	331210	70	0.01	346170	70	0.13

Table A.2 continued (Run 4)

Shear rate (s^{-1})	Shear stress (Pa)	Shear viscosity (Pa.s)	n
20	69590	3480	0.47
40	95870	2400	0.42
100	129270	1290	0.37
210	176420	840	0.32
470	220260	470	0.27
1030	274650	270	0.22
2270	301090	130	0.17
5000	347010	70	0.12

Table A.3: Shear stress and viscosity data for LLDPE at 200^{o}C

Shear rate (s^{-1})	Run 1			Run 2			Run 3		
	Shear stress (Pa)	Shear viscosity (Pa.s)	n	Shear stress (Pa)	Shear viscosity (Pa.s)	n	Shear stress (Pa)	Shear viscosity (Pa.s)	n
20	78280	3910	0.40	85890	4294.7	0.38	93510	4680	0.36
40	105740	2640	0.36	112810	2563.0	0.34	119880	3000	0.32
100	137310	1370	0.31	144630	1493.2	0.30	151960	1520	0.28
210	174330	830	0.27	183400	860.3	0.25	192480	920	0.24
470	214950	460	0.22	223170	476.2	0.21	231390	490	0.21
1030	239990	230	0.17	249220	241.3	0.17	258450	250	0.17
2270	269990	120	0.13	280690	123.5	0.13	291380	130	0.13
5000	304830	60	0.08	313890	62.8	0.09	322960	60	0.09

Table A.4: Shear stress and viscosity data for LLDPE at 250^{o}C

Shear rate (s^{-1})	Run 1			Run 2			Run 3		
	Shear stress (Pa)	Shear viscosity (Pa.s)	n	Shear stress (Pa)	Shear viscosity (Pa.s)	n	Shear stress (Pa)	Shear viscosity (Pa.s)	n
20	59310	2970	0.45	81210	4060	0.38	63150	3160	0.46
40	83410	2090	0.41	105210	2630	0.34	89560	2990	0.43
100	112060	1120	0.36	135370	1350	0.31	102100	2550	0.41
210	146050	700	0.32	176140	840	0.27	131850	1320	0.35
470	185790	400	0.27	210440	450	0.23	166950	800	0.30
1030	227750	220	0.23	251950	240	0.20	208750	440	0.25
2270	267530	120	0.19	286110	130	0.16	250040	240	0.20
5000	303050	60	0.14	321280	60	0.12	287340	130	0.15

Table A.5: Shear stress and viscosity data for PP at 200°C

Shear rate (s^{-1})	Run 1			Run 2			Run 3		
	Shear stress (Pa)	Shear viscosity (Pa.s)	n	Shear stress (Pa)	Shear viscosity (Pa.s)	n	Shear stress (Pa)	Shear viscosity (Pa.s)	n
20	22420	1120	0.52	36620	1830	0.35	29520	1480	0.42
40	35180	880	0.47	47760	1190	0.33	41470	1040	0.39
100	49820	500	0.42	61740	620	0.31	55780	560	0.36
210	66120	310	0.37	78190	370	0.29	72160	340	0.32
470	85190	180	0.32	96450	210	0.26	90820	190	0.29
1030	107950	100	0.27	117470	110	0.24	112710	110	0.26
2270	133470	60	0.22	140650	60	0.22	137060	60	0.22
5000	158420	30	0.17	166870	30	0.20	162650	30	0.19

Table A.6: Shear stress and viscosity data for PP at 250°C

Shear rate (s^{-1})	Run 1			Run 2			Run 3		
	Shear stress (Pa)	Shear viscosity (Pa.s)	n	Shear stress (Pa)	Shear viscosity (Pa.s)	n	Shear stress (Pa)	Shear viscosity (Pa.s)	n
20	24420	1220	0.39	25050	1250	0.38	24890	1240	0.38
40	32210	810	0.37	31910	800	0.36	31990	800	0.36
100	43120	430	0.35	42540	430	0.34	42690	430	0.34
210	56660	270	0.32	56240	270	0.32	56340	270	0.32
470	72660	150	0.30	72330	150	0.30	72420	150	0.30
1030	91110	90	0.28	90520	90	0.28	90670	90	0.28
2270	112380	50	0.26	111170	50	0.26	111470	50	0.26
5000	136720	30	0.24	135420	30	0.24	135750	30	0.24

Table A.7: Shear stress and viscosity data for PS at 200°C

Shear rate (s^{-1})	Run 1			Run 2			Run 3		
	Shear stress (Pa)	Shear viscosity (Pa.s)	n	Shear stress (Pa)	Shear viscosity (Pa.s)	n	Shear stress (Pa)	Shear viscosity (Pa.s)	n
20	44010	2200	0.32	46210	2310	0.32	41810	2090	0.32
40	57040	1430	0.30	59890	1500	0.30	54190	1350	0.30
100	71870	720	0.28	75460	750	0.28	68280	680	0.28
210	88640	420	0.26	93070	440	0.26	84210	400	0.26
470	108120	230	0.24	113530	240	0.24	102710	220	0.24
1030	130440	130	0.22	136960	130	0.22	123920	120	0.22
2270	152920	70	0.20	160560	70	0.20	145270	60	0.20
5000	181330	40	0.18	190400	40	0.19	172260	30	0.18

Table A.8: Shear stress and viscosity data for PS at 250^{o}C

Shear rate (s^{-1})	Run 1			Run 2			Run 3		
	Shear stress (Pa)	Shear viscosity (Pa.s)	n	Shear stress (Pa)	Shear viscosity (Pa.s)	n	Shear stress (Pa)	Shear viscosity (Pa.s)	n
20	8110	410	0.68	8440	420	0.67	8310	420	0.67
40	12840	320	0.61	13170	330	0.60	13040	330	0.61
100	21140	210	0.55	21470	210	0.54	21340	210	0.54
210	32160	150	0.48	32490	150	0.47	32360	150	0.48
470	45410	100	0.41	45740	100	0.41	45600	100	0.41
1030	60100	60	0.35	60430	60	0.34	60290	60	0.35
2270	76040	30	0.28	76370	30	0.28	76230	30	0.28
5000	95460	20	0.21	95790	20	0.22	95660	20	0.22

Table A.9: Shear stress and viscosity data for PET at 300^{o}C

Shear rate (s^{-1})	Shear stress (Pa)	Shear viscosity (Pa.s)	n
20	1450	70	1.03
40	3170	80	0.99
100	6800	70	0.94
210	14490	70	0.90
470	27650	60	0.85
1030	53260	50	0.81
2270	105440	50	0.76
5000	177000	40	0.71

Table A.10: Spillover data from Table 5.11

N (rps)	Residual Torque					Re					Po				
	9.1 Pas (15°C)	8.2 Pas (20°C)	5.9 Pas (25°C)	7.3 Pas (25°C)	4.9 Pas (35°C)	9.1 Pas (15°C)	8.2 Pas (20°C)	5.9 Pas (25°C)	7.3 Pas (25°C)	4.9 Pas (35°C)	9.1 Pas (15°C)	8.2 Pas (20°C)	5.9 Pas (25°C)	7.3 Pas (25°C)	4.9 Pas (35°C)
0.8	0.055	0.038	0.054	0.051	0.048	0.5744	0.6341	0.8768	0.7087	1.0503	155.1939	106.7697	153.1609	143.8344	137.4778
1.7	0.108	0.091	0.087	0.097	0.107	1.1487	1.2683	1.7537	1.4174	2.1007	76.3806	64.0790	62.0503	69.3232	76.7186
2.5	0.149	0.122	0.106	0.127	0.108	1.7231	1.9024	2.6305	2.1260	3.1510	46.4999	38.3443	33.4974	40.0485	34.3198
3.3	0.197	0.163	0.132	0.153	0.135	2.2974	2.5366	3.5073	2.8347	4.2014	34.7481	28.8955	23.5050	27.1417	24.1288
4.2	0.238	0.205	0.157	0.192	0.170	2.8718	3.1707	4.3842	3.5434	5.2517	26.8509	23.2717	17.8818	21.8733	19.4709
5.0	0.274	0.237	0.171	0.219	0.192	3.4462	3.8049	5.2610	4.2521	6.3020	21.4648	18.6224	13.5350	17.2956	15.2209

Table A.11: Spillover data from Table 5.13

N (rps)	2% CMC										2.25% CMC									
	Po	Lower C_{SF} (79.22)			C_{SF} (81.03)			Upper C_{SF} (82.26)			Po	Lower C_{SF} (79.22)			C_{SF} (81.03)			Upper C_{SF} (82.26)		
		Re	η	$\dot{Y}$	Re	η	$\dot{Y}$	Re	η	$\dot{Y}$		Re	η	$\dot{Y}$	Re	η	$\dot{Y}$	Re	η	$\dot{Y}$
0.8	98.6751	0.8028	6.7	18	0.8212	6.5	18	0.8742	6.1	20	185.9903	0.4259	12.6	17	0.4357	12.3	18	0.4638	11.6	19
1.7	31.2403	2.5358	4.2	33	2.5938	4.1	34	2.7612	3.9	37	47.8003	1.6573	6.5	40	1.6952	6.3	42	1.8046	6.0	45
2.5	11.3917	6.9542	2.3	73	7.1131	2.3	75	7.5722	2.1	82	23.9882	3.3025	4.9	59	3.3779	4.8	60	3.5959	4.5	65
3.3	8.2045	9.6557	2.2	77	9.8763	2.2	80	10.5138	2.0	87	16.1093	4.9177	4.4	68	5.0300	4.3	69	5.3547	4.0	75
4.2	5.7433	13.7935	1.9	92	14.1086	1.9	95	15.0193	1.8	103										
5.0	4.8109	16.4668	2.0	92	16.8431	1.9	95	17.9302	1.8	103										

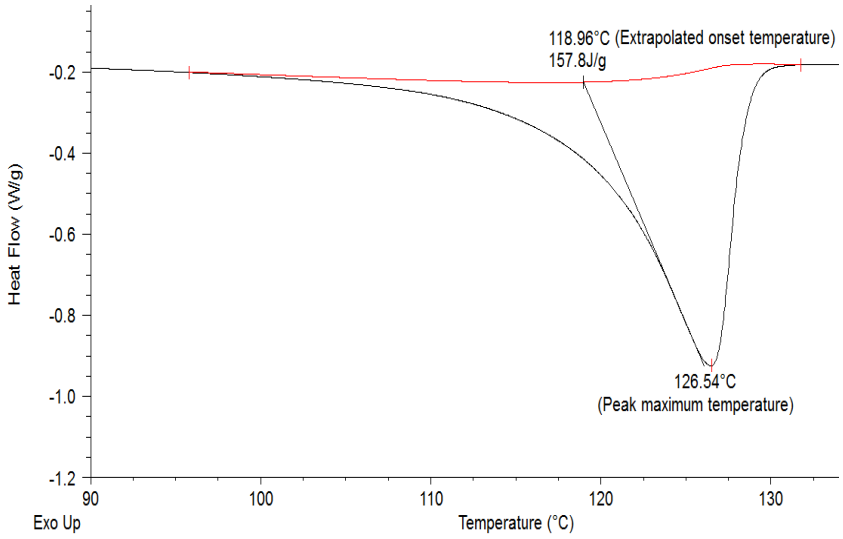

Figure A.2: HDPE melting endotherm

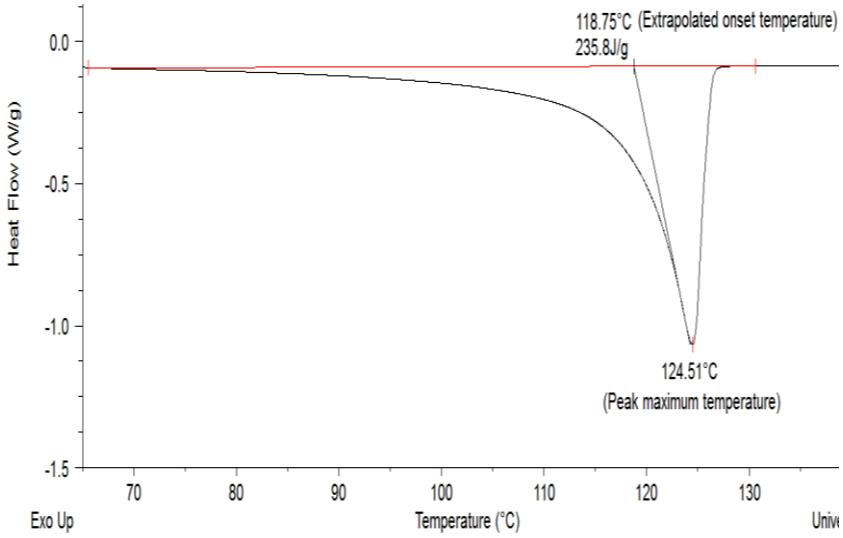

Figure A.3: PE-iC8 (50:50) melting endotherm

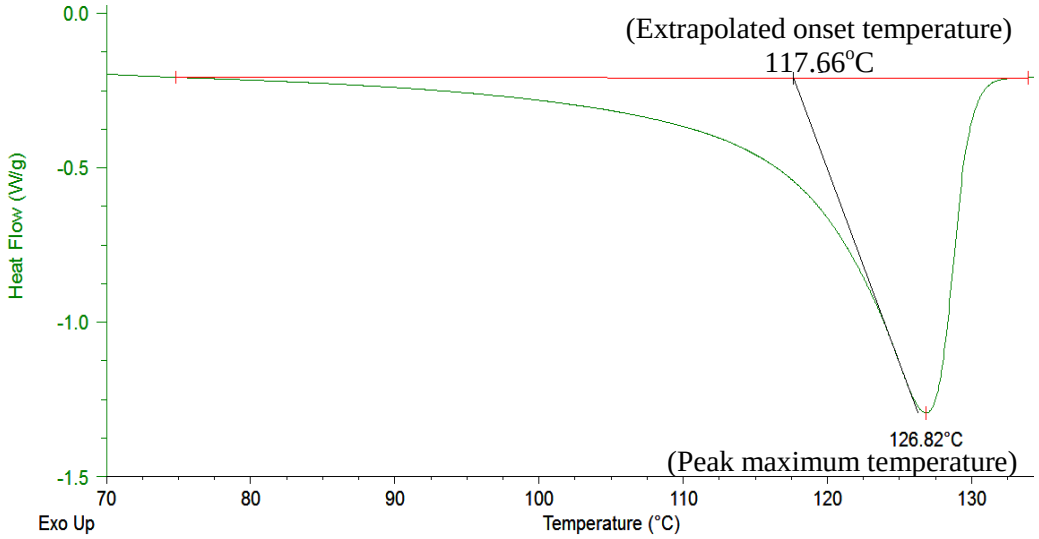

Figure A.4: PE-nC10 (50:50) melting endotherm

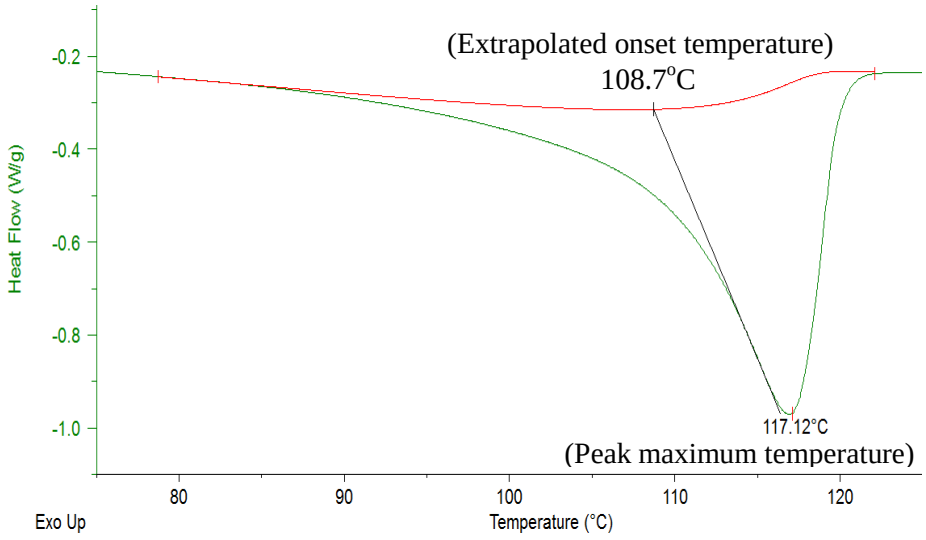

Figure A.5: PE-nC14 (50:50) melting endotherm

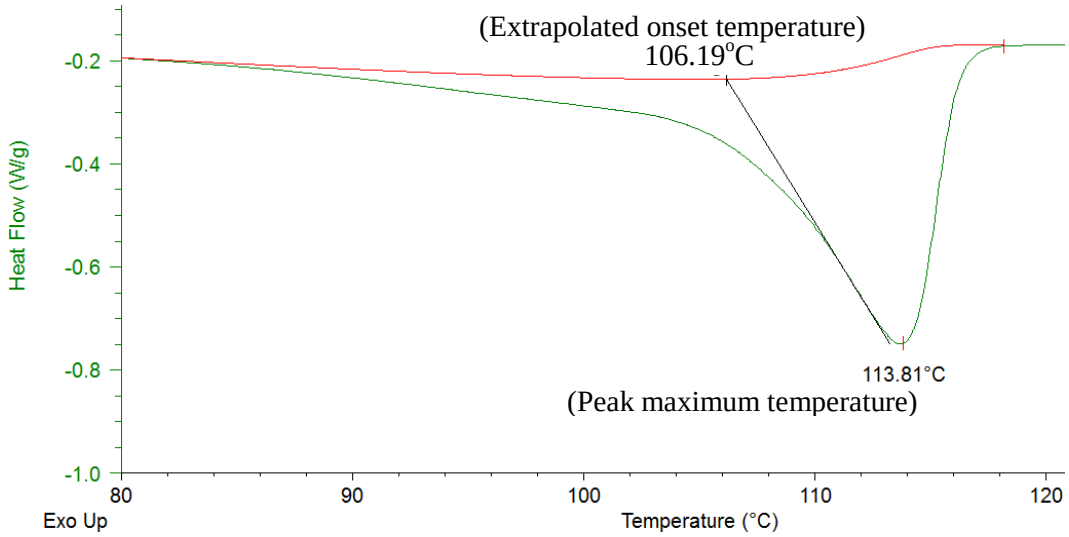

Figure A.6: PE-nC15 (50:50) melting endotherm

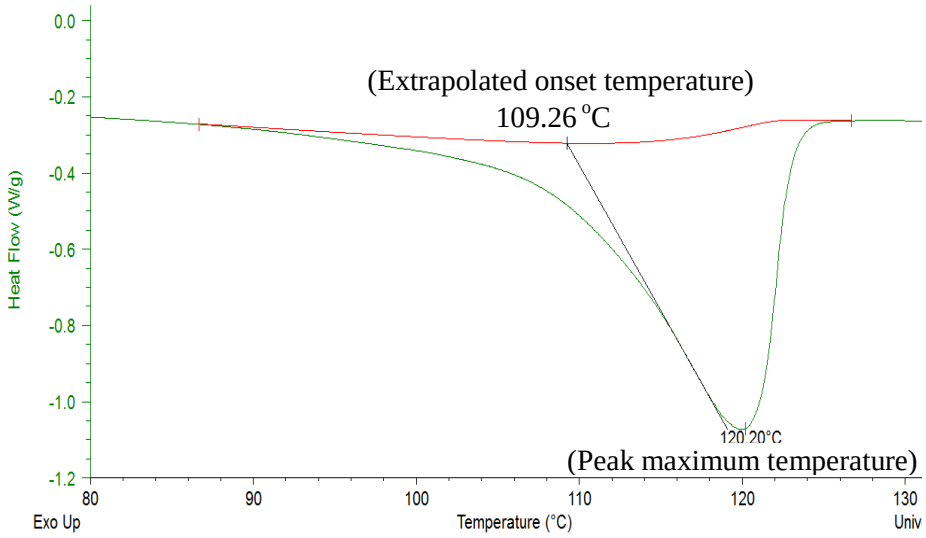

Figure A.7: PE-nC16 (50:50) melting endotherm

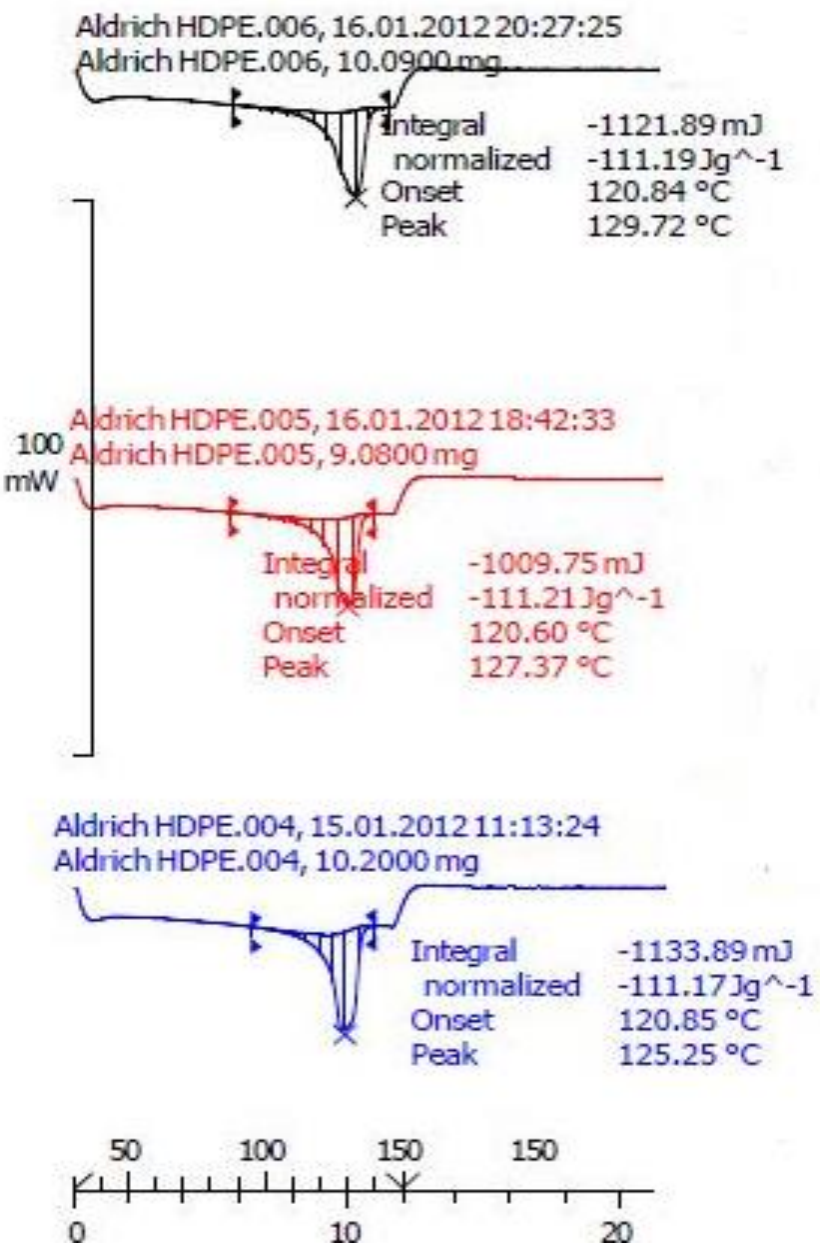

Figure A.8: Melting endotherms for pure HDPE (Aldrich) before solvent treatment in pentadecane using the sealed-impeller viscometer

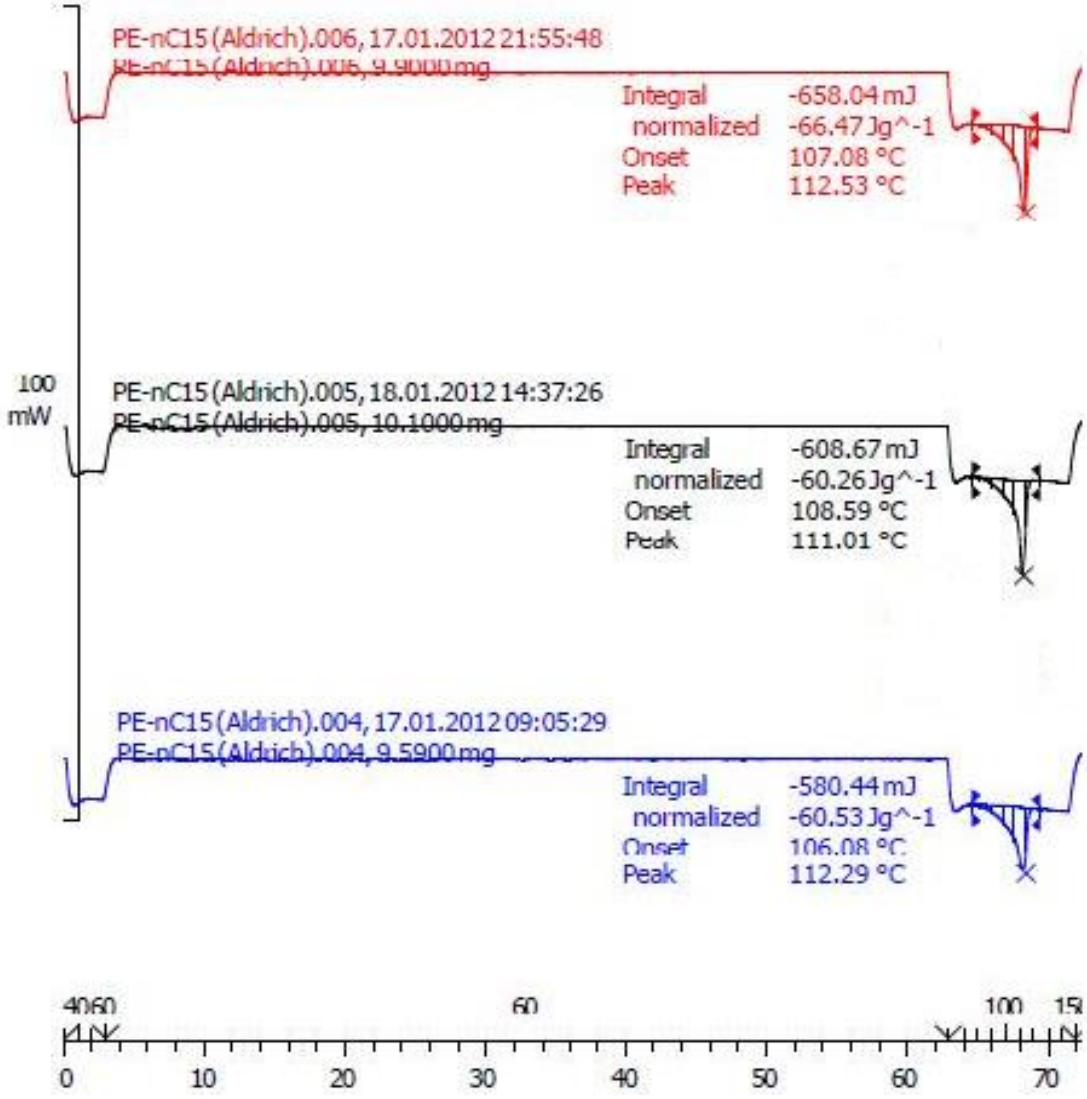

Figure A.9: Melting endotherms for the solvent (pentadecane) treated HDPE (Aldrich) using the sealed-impeller viscometer

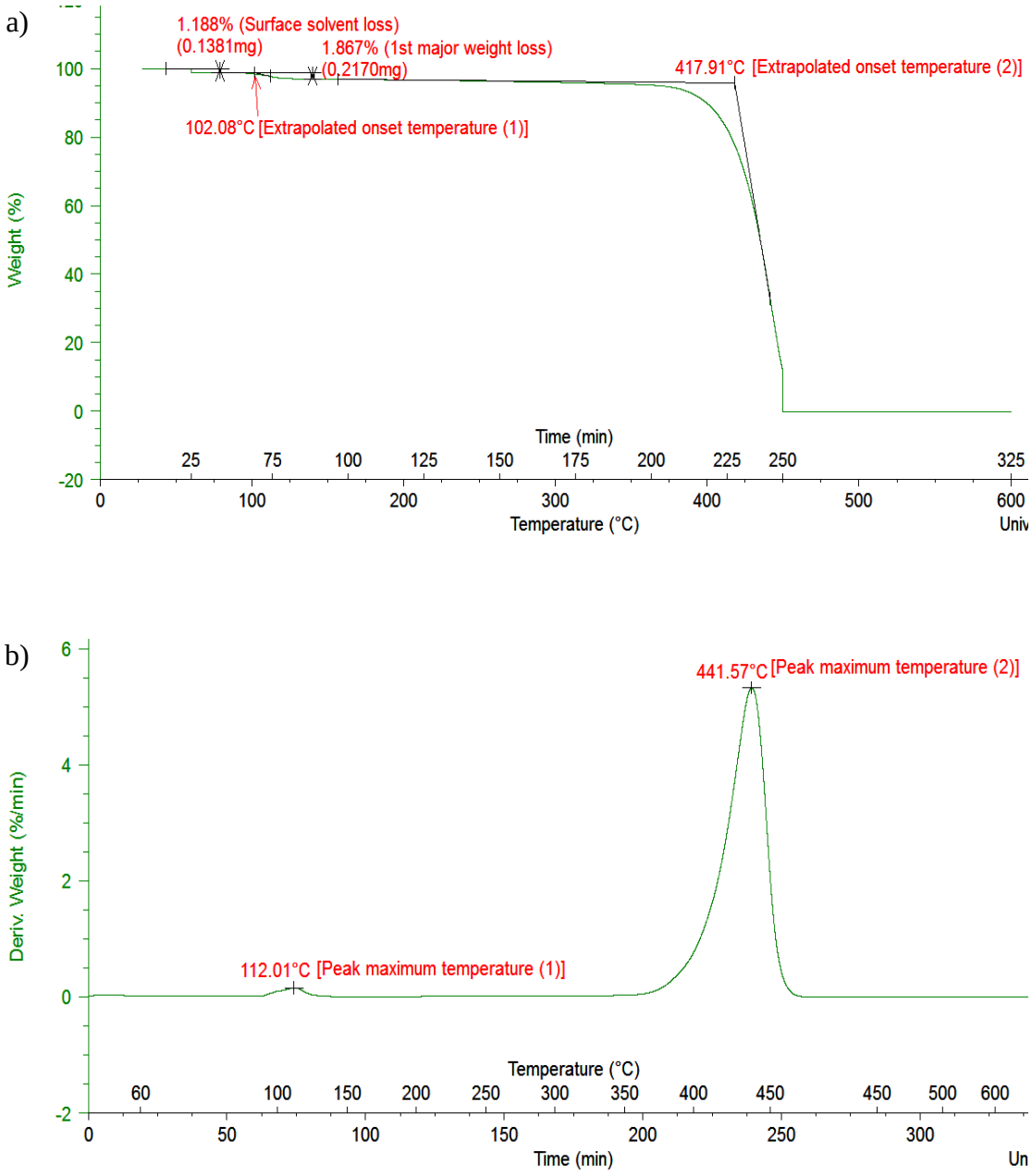

Figure A.10: PE:iC8 (50:50)- a) TGA; b) DTG

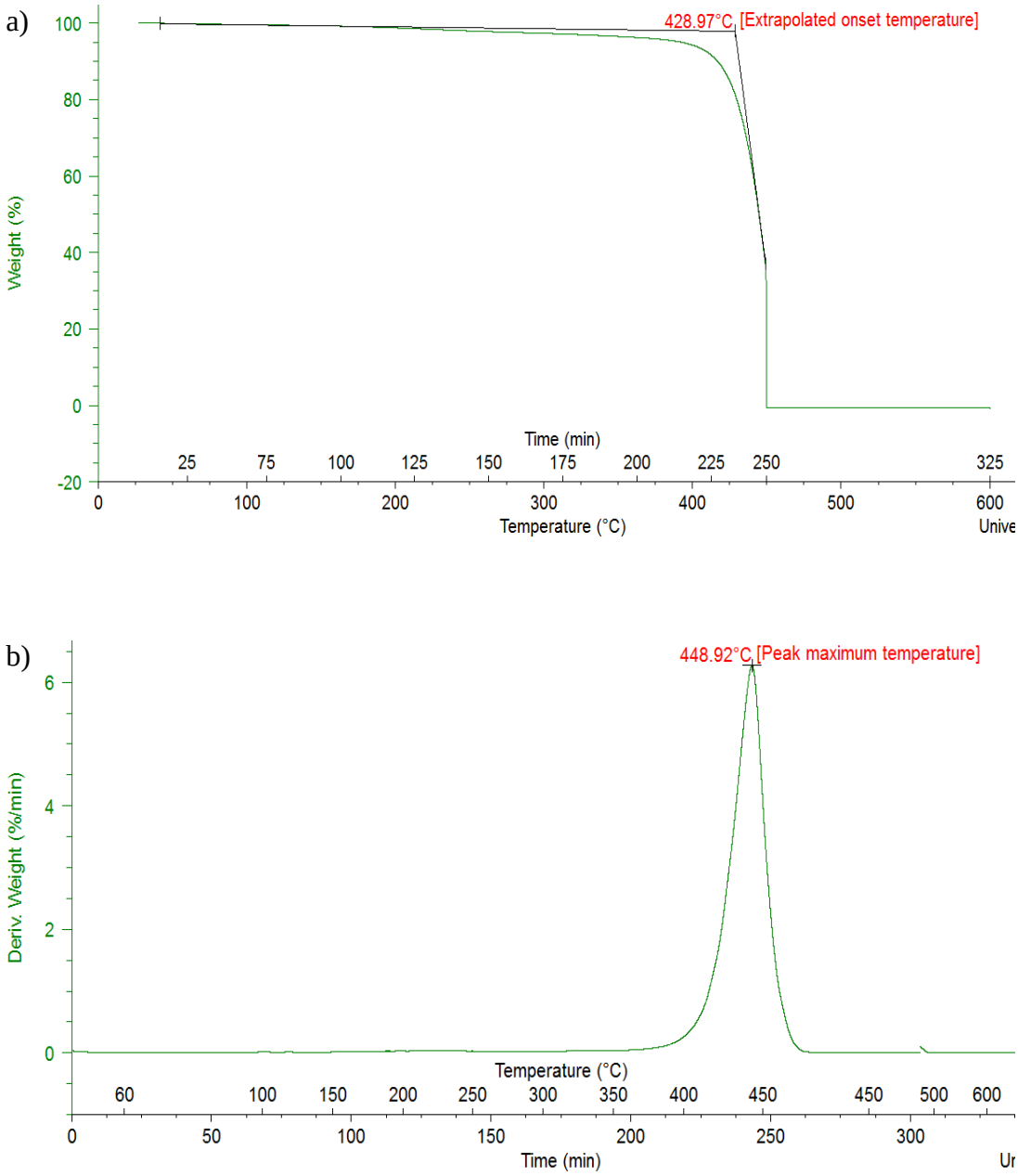

Figure A.11: PE:nC10 (50:50)- a) TGA; b) DTG

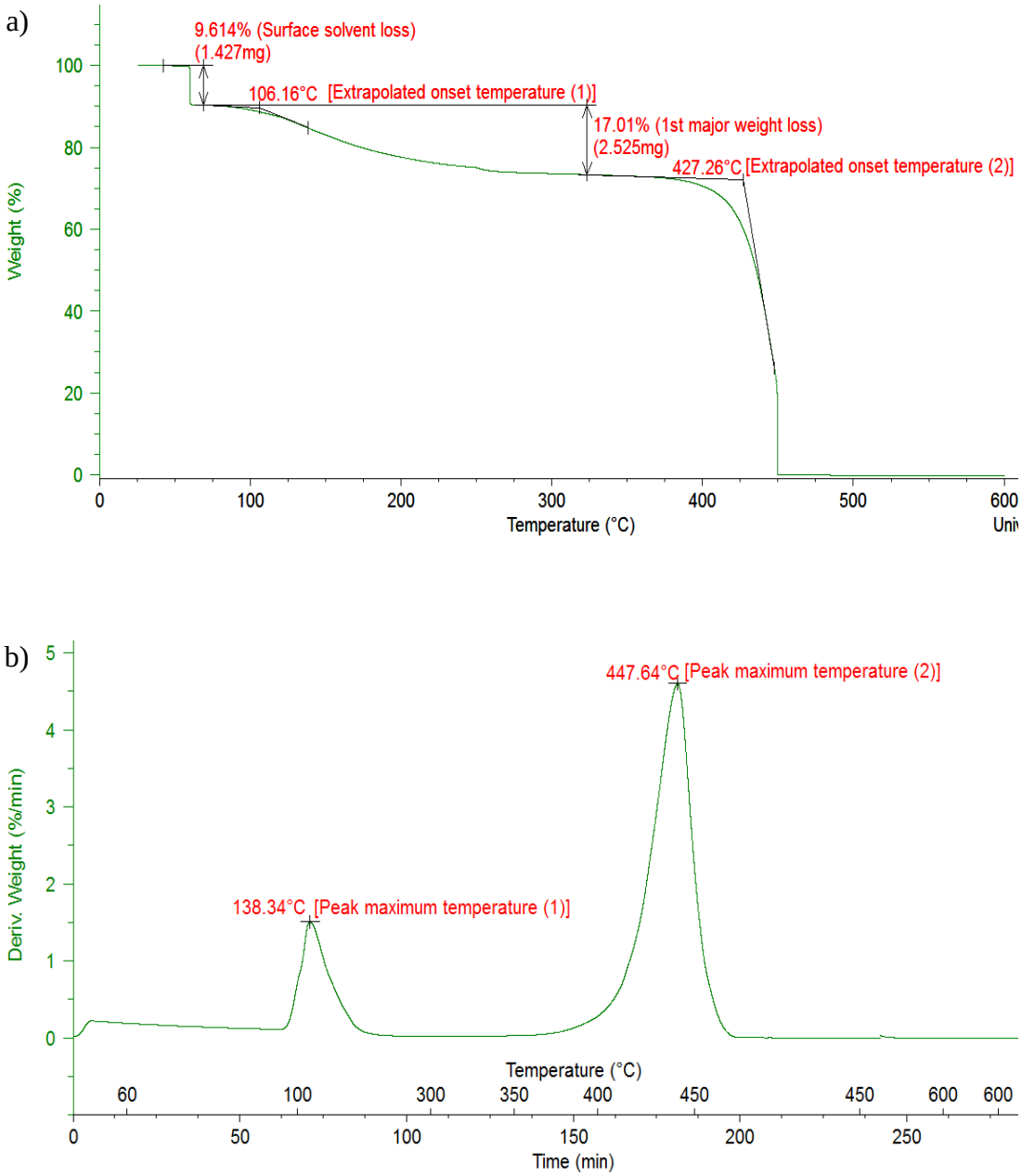

Figure A.12: PE:nC14 (50:50)- a) TGA; b) DTG

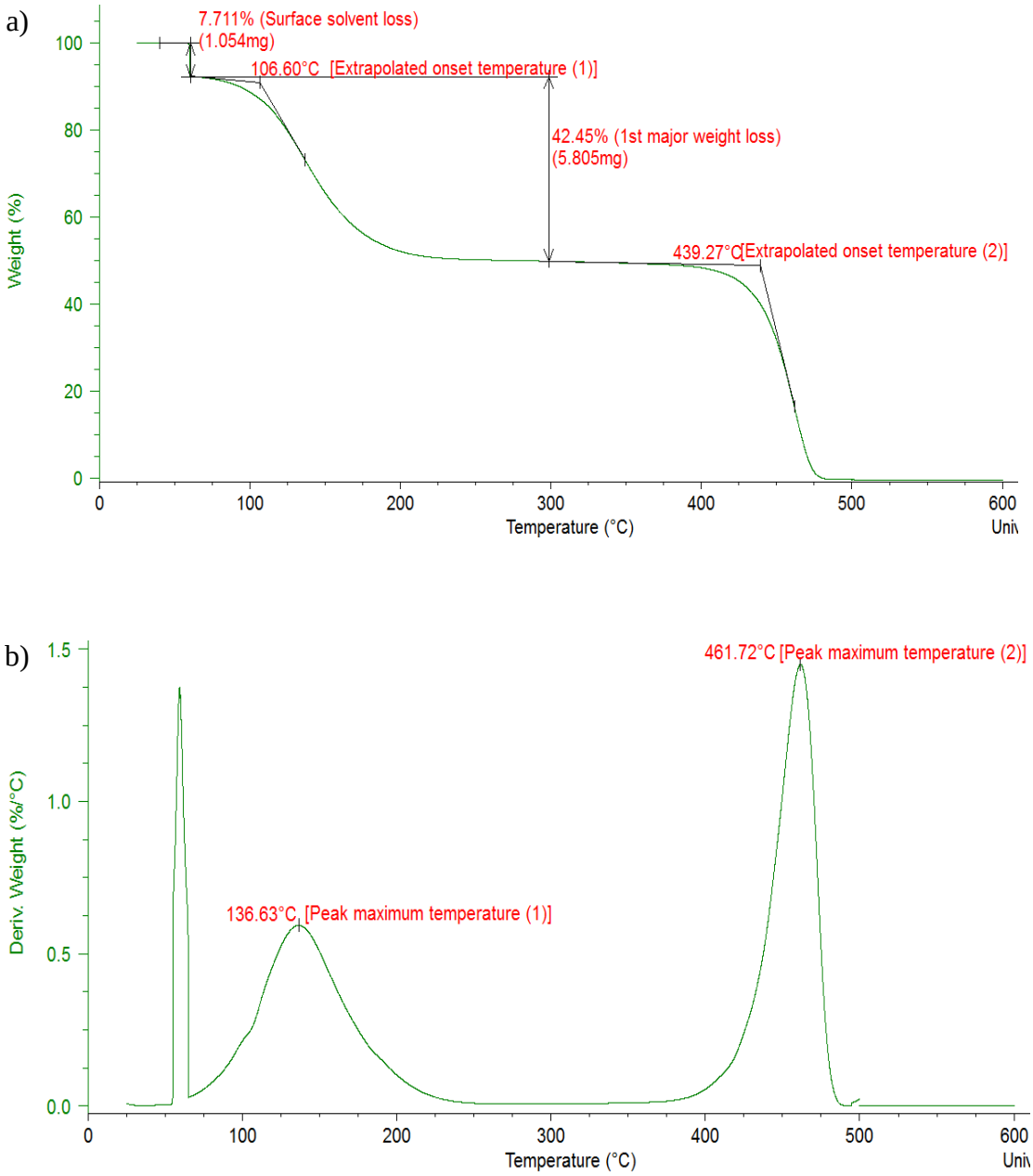

Figure A.13: PE:nC15 (50:50)- a) TGA; b) DTG

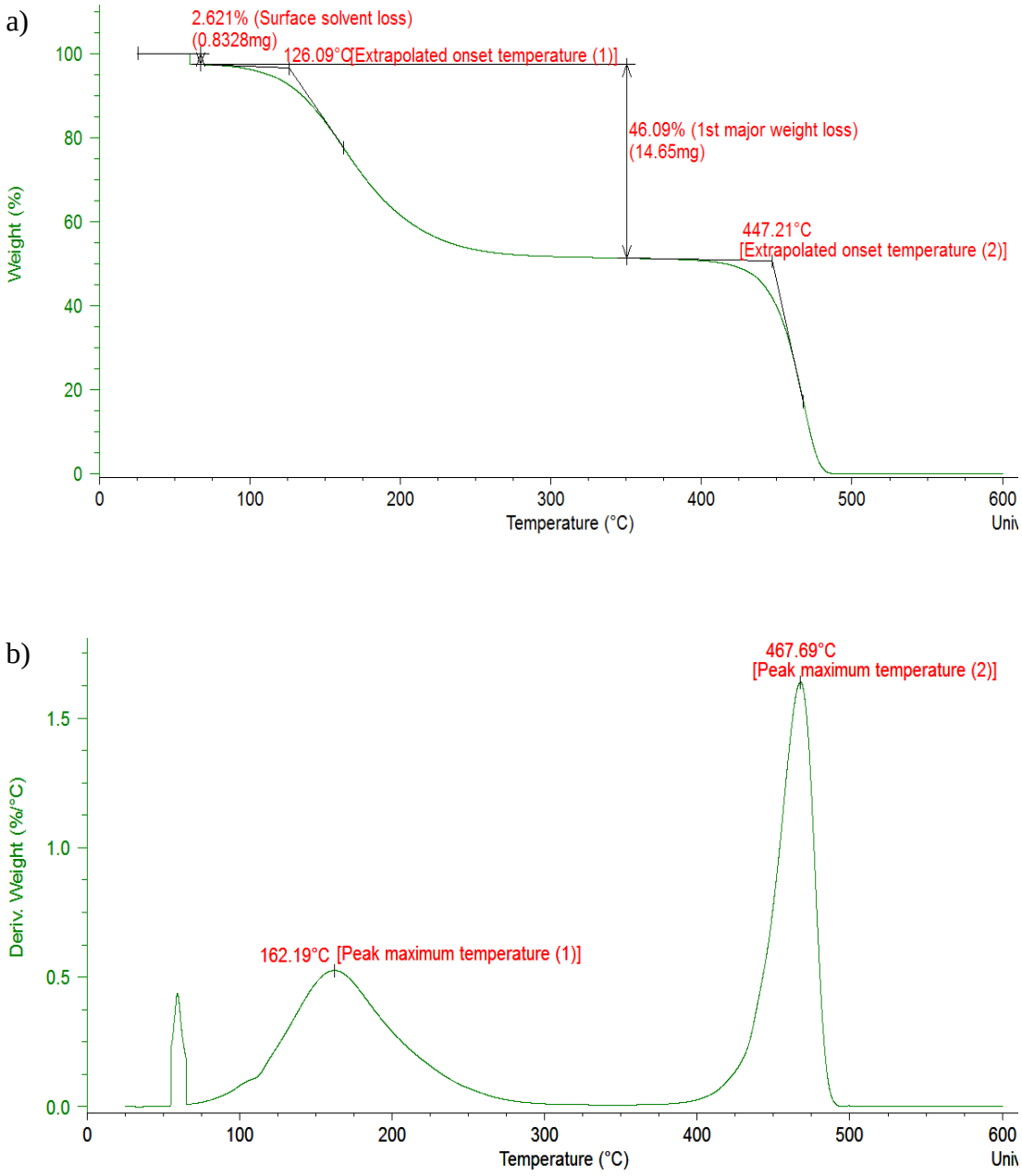

Figure A.14: PE:nC16 (50:50)- a) TGA; b) DTG

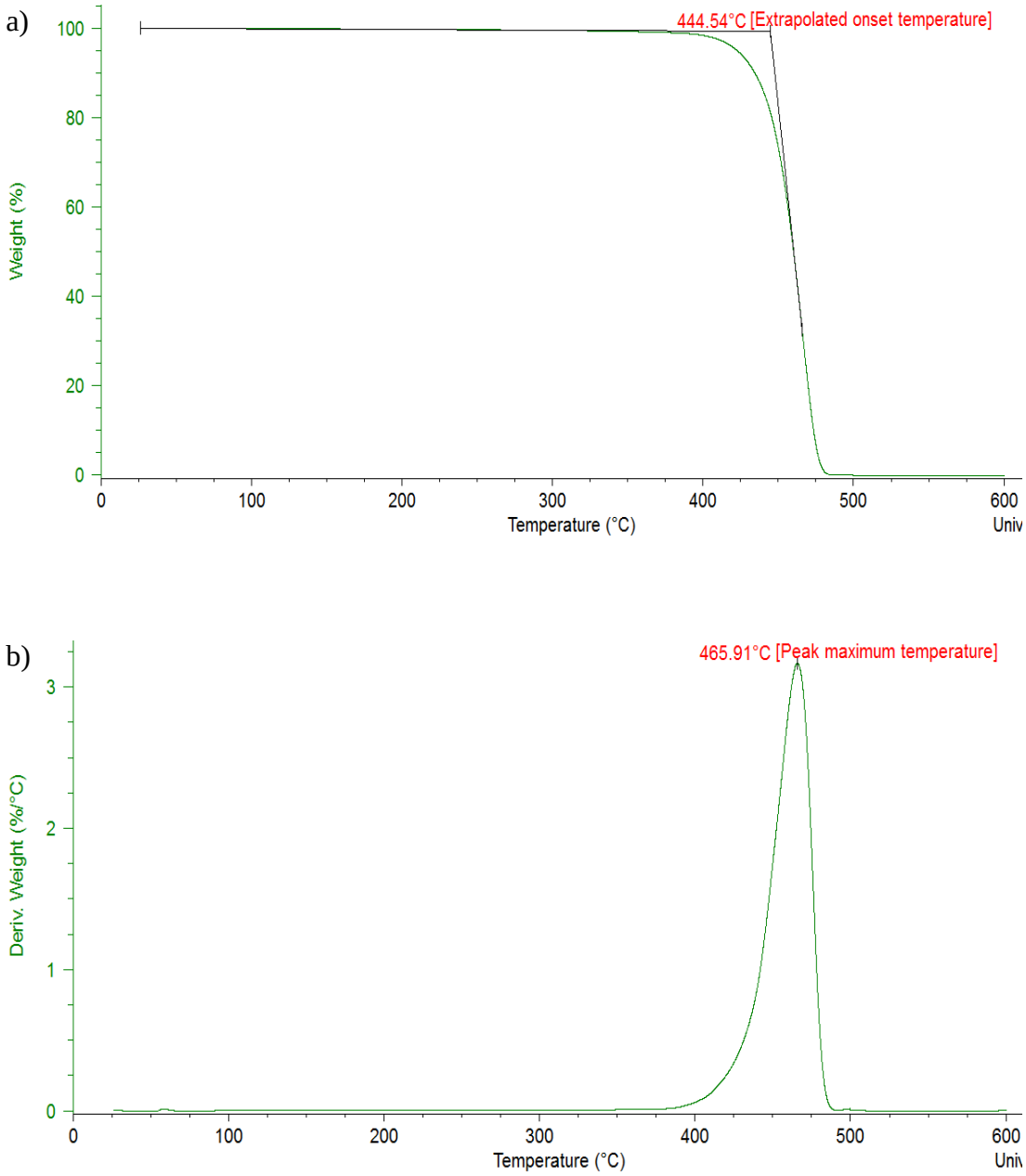

Figure A.15: HDPE (Borealis)- a) TGA; b) DTG

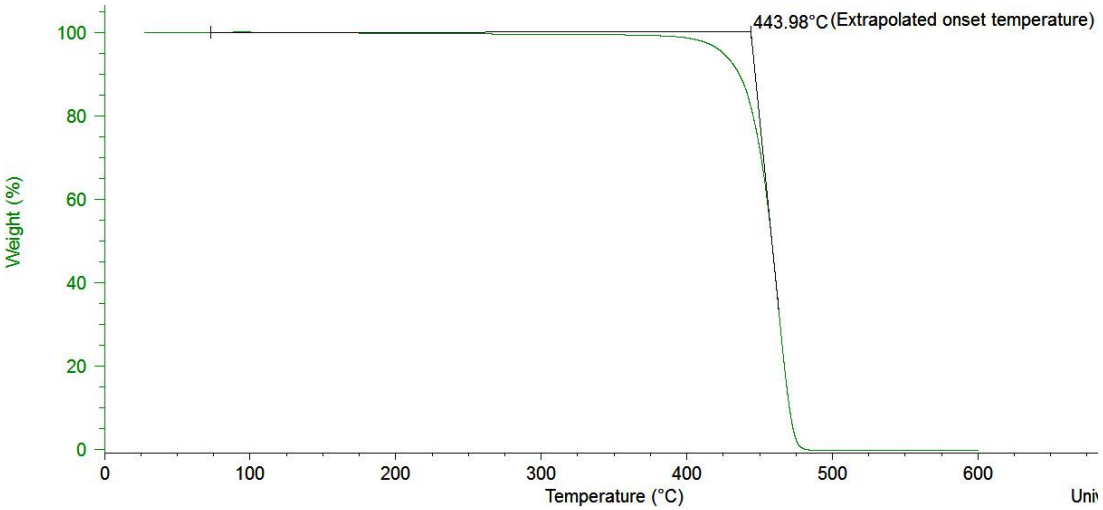

Figure A.16: TGA curve (Run 1) for HDPE (Aldrich) used for solvent treatment in sealed-impeller viscometer

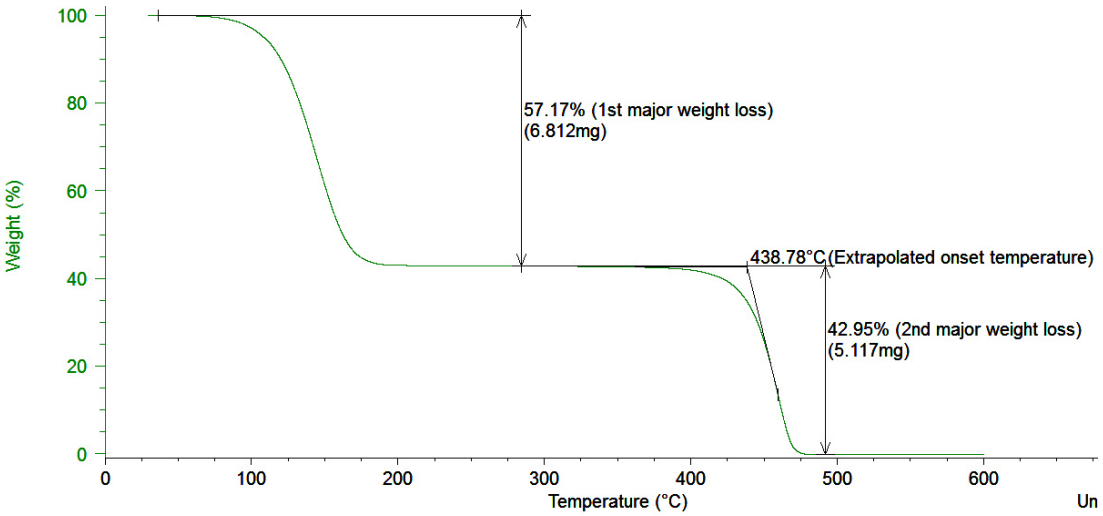

Figure A.17: TGA curve (Run 1) for HDPE-nC15 product in the sealed-impeller viscometer